Poznań University of Life Sciences
Faculty of Environmental and Mechanical Engineering

Michal Antala

Assessment of peatland vegetation physiology under manipulated environmental conditions by leaf and canopy level chlorophyll fluorescence measurements

Ocena fizjologii roślinności torfowiskowej w manipulowanych warunkach środowiskowych z użyciem pomiarów fluorescencji chlorofilu na poziomie liści i pokrywy roślinnej

Doctoral dissertation in the field of engineering and technology
in the discipline of environmental engineering, mining and energy

Scientific supervisor:
Prof. UPP dr hab. Anshu Rastogi
Laboratory of Bioclimatology
Poznan University of Life Sciences

Auxiliary supervisor:
Dr inż. Marcin Stróżecki
Laboratory of Bioclimatology
Poznan University of Life Sciences

Poznań, 2024

Acknowledgments

I would like to thank my supervisor prof. UPP dr hab. Anshu Rastogi, my auxiliary supervisor dr inż. Marcin Stróżecki, and to prof. Radosław Juszczak for their guidance, supervision and scholarly input.

I would also like to thank all members of the Laboratory of Bioclimatology for their support during the measurements and discussions of various lengths.

I am thankful to all co-authors of publications included in this thesis for their help and insights.

A special thanks belong to my family for their support throughout my life and academic endeavours.

The research conducted during the doctoral dissertation was financially supported by the National Science Centre of Poland (NCN) funded project grant no. 2020/37/B/ST10/01213. The 3rd publication of the cycle was financed within the framework of the Polish Ministry of Science and Higher Education's Program: "Regional Excellence Initiative" in the years 2019-2023 with grant No. 005/RID/2018/19.

List of scientific papers included in the cycle

1. **Antala, M.**, Juszczak, R., van der Tol, Ch., Rastogi, A. (2022). Impact of climate change-induced alterations in peatland vegetation phenology and composition on carbon balance. *Science of the Total Environment*. 827, 154294. https://doi.org/10.1016/j.scitotenv.2022.154294

   200 points; IF = 9.8

2. **Antala, M.**, Juszczak, R., Rastogi, A., (2024). Nonphotochemical quenching does not alter the relationship between sun-induced fluorescence and gross primary production under heatwave. *New Phytologist*. 20312. https://doi.org/10.1111/nph.20312

   140 points; IF = 8.3

3. **Antala, M.**, Rastogi, A., Cogliati, S., Stróżecki, M., Colombo, R., Juszczak, R. (2024). Sun-induced fluorescence spectrum as a tool for assessing peatland vegetation productivity in the framework of warming and reduced precipitation experiment. *Remote Sensing of Environment*. 301, 113921. https://doi.org/10.1016/j.rse.2023.113921

   200 points; IF = 11.1

4. **Antala, M.**, Abdelmajeed, A.Y.A., Stróżecki, M., Krzesiński, W., Juszczak, R., Rastogi, A. (2024). Photosynthetic Responses of Peat Moss (*Sphagnum* spp.) and Bog Cranberry (*Vaccinium oxycoccos* L.) to Spring Warming. *Plants* 13 (22), 3246. https://doi.org/10.3390/plants13223246

   70 points; IF = 4.0

The sum of points for publications in the presented cycle, as per the Communication from the Minister of Science dated January 5, 2024, regarding the list of scientific journals and peer-reviewed proceedings of international conferences, is 610, and the sum of impact factors (IFs) in the year of publication is 33.2.

Table of Contents

List of scientific papers included in the cycle 5

List of used abbreviations 8

Streszczenie 9

Abstract 10

1. Introduction 11

2. Aim and hypotheses of the dissertation 14

3. Materials and methods 15

    3.1 Literature review 15

    3.2 Site description 15

    3.3 Methods of conducting experiments 16

    3.3.1 Canopy-level data collection and processing 16

    3.3.2 Leaf-level measurements and processing 18

    3.4 Statistical analysis 18

4. Characteristics of the obtained results 19

    4.1 Impact of climate change-induced alterations in peatland vegetation phenology and composition on carbon balance 19

    4.2 Nonphotochemical quenching does not alter the relationship between sun-induced fluorescence and gross primary production under heatwave 19

    4.3 Sun-induced fluorescence spectrum as a tool for assessing peatland vegetation productivity in the framework of warming and reduced precipitation experiment 20

    4.4 Photosynthetic Responses of Peat Moss (*Sphagnum* spp.) and Bog Cranberry (*Vaccinium oxycoccos* L.) to Spring Warming 21

5. Discussion 22

6. Conclusions 25

References 27

Attachments of published articles 37

    Impact of climate change-induced alterations in peatland vegetation phenology and composition on carbon balance 37

    Nonphotochemical quenching does not alter the relationship between sun-induced fluorescence and gross primary production under heatwave 55

    Sun-induced fluorescence spectrum as a tool for assessing peatland vegetation productivity in the framework of warming and reduced precipitation experiment 61

    Photosynthetic Responses of Peat Moss (*Sphagnum* spp.) and Bog Cranberry (*Vaccinium oxycoccos* L.) to Spring Warming 83

Declarations of co-authors, supervisors and author 101

List of used abbreviations

APAR – Absorbed Photosynthetically Active Radiation
C - Control
EVI – Enhanced Vegetation Index
FWHM – Full-Width Half Maximum
GPP – Gross Primary Production
MTCI – MERRIS Terrestrial Chlorophyll Index
NDVI – Normalised Difference Vegetation Index
NIRv – Near-Infrared Vegetation Index
NPQ – NonPhotochemical Quenching of maximal fluorescence
φNPQ – quantum yield of light intensity-dependent heat dissipation
PAR – Photosynthetically Active Radiation
PFG – Plant Functional Group
PRI – Photochemical Reflectance Index
PSII – Photosystem II
RC – reaction centre
reNDVI – red-edge Normalised Difference Vegetation Index
SIF – Sun-Induced chlorophyll Fluorescence
W – Warming
WP – Warming and reduced Precipitation

Streszczenie

Dokładne prognozowanie przyszłego klimatu jest możliwe jedynie przy uwzględnieniu sprzężeń zwrotnych wywoływanych w głównych ekosystemach przez zmiany przeszłe, obecne i przyszłe. Jednymi z najważniejszych ekosystemów w lądowym cyklu węglowym są torfowiska. Pomimo ich znaczenia, zmiany w funkcjach roślinności torfowisk spowodowane zmieniającymi się warunkami środowiskowymi nie są wystarczająco dobrze zrozumiane, co utrudnia ich uwzględnienie w modelach klimatycznych. Jednym z możliwych sposobów monitorowania fizjologii roślinności torfowisk jest teledetekcja, szczególnie fluorescencja indukowana promieniowaniem słonecznym (SIF). Jednak zmiany w składzie roślinności i fenologii, fizjologia roślin na poziomie liścia oraz związek między stanem fizjologicznym a właściwościami spektralnymi roślinności torfowisk muszą zostać zbadane przed przeprowadzeniem wiarygodnego monitorowania na dużą skalę. Dlatego niniejsza dysertacja bada wpływ symulowanego ocieplenia oraz zredukowanych opadów na fizjologię roślinności torfowisk, mierząc fluorescencję na poziomie liścia i pokrywy roślinnew połączeniu z pomiarami pomocniczymi. Metody oparte na pełnym spektrum fluorescencji SIF z pomiarów na poziomie pokrywy roślinnej okazały się wiarygodnie przewidywać fotosyntezę roślinności torfowisk w obecnych, i cieplejszych i suchszych warunkach. Jednak występowanie ekstremalnych stresów cieplnych, które prawdopodobnie wpłyną na torfowiska w przyszłości, utrudnia wykorzystanie SIF w monitorowaniu fizjologii roślinności. Pomiary fluorescencji na poziomie liścia wykazały, że aktywność fizjologiczna żurawiny błotnej (*Vaccinium oxycoccos* L.) w cieplejszej przyszłości rozpocznie się wcześniej z powodu szybszego relaksowania nieuregulowanego rozpraszania ciepła, związanego z reaktywacją centrów reakcji fotosyntetycznej. Jednak torfowiec (Sphagnum spp.) odnosi stosunkowo mniejsze korzyści z ocieplenia, ponieważ pozostaje fizjologicznie aktywny nawet zimą, pod warunkiem że rośliny nie są zamarznięte.Wyniki te ułatwiają lepsze zrozumienie modyfikacji funkcji roślinności torfowisk wywołanych zmianami klimatycznymi i sposobów ich oceny. Przyszłe modele roślinności i obiegu węgla powinny uwzględnić te informacje, aby dokładnie przewidzieć funkcje torfowisk w zmieniającym się klimacie.

Abstract

Accurate predictions of the future climate are possible only when accounting for the feedback loops induced in the major ecosystems by past, ongoing and future changes. One of the most important ecosystems in terrestrial carbon cycling are peatlands. Despite peatlands' importance, changes in the peatland vegetation functions caused by the changing environmental conditions are not as well understood as desirable, which hampers their inclusion in the climate models. One of the possible ways to monitor peatland vegetation physiology is remote sensing, especially sun-induced fluorescence (SIF). However, the changes in the vegetation composition and phenology, leaf-level plant physiology and the connection between the physiological status and the spectral properties of the peatland vegetation must be examined before reliable large-scale monitoring can be performed. Therefore, this dissertation studied the impacts of simulated warming and reduced precipitation on peatland vegetation physiology, measuring leaf and canopy level fluorescence measurements in combination with ancillary measurements. Methods based on the full SIF spectrum retrieval from the top-of-canopy measurements were found to reliably predict the peatland vegetation photosynthesis under current and warmer and dryer conditions. However, the occurrence of extreme heat stress that will probably affect the peatlands in the future hampers the use of SIF in vegetation physiology monitoring. The leaf-level fluorescence measurements have shown that the physiological activity of bog cranberry (*Vaccinium oxycoccos* L.) in the warmer future will start sooner because of faster relaxation of non-regulated heat dissipation connected with the reactivation of photosynthetic reaction centres. However, peat moss (*Sphagnum* spp.) benefits relatively less from the warming, as it remains physiologically active even during winter, provided the plants are not frozen. These findings facilitate a better understanding of climate change-induced modifications in peatland vegetation functions and the means of their assessment. The future vegetation and carbon cycle models should take this information into account to accurately predict the peatland functions under a changing climate.

1. Introduction

Changing climate is one of the major issues that the human population of the 21st century must face. The rate of temperature rise is not only the highest ever recorded but also the highest that humankind could ever experience (NOAA., 2024; Tripati et al., 2009). As the occurrence of climate-related natural catastrophes is increasing around the globe, it is difficult to ignore the rising global temperature and changes in weather patterns. The warming and increasing occurrence and severity of droughts influence human activities as well as natural ecosystems. Negative and positive changes in ecosystems, in turn, affect the speed of climate change by feedback loops. Understanding and predicting the rate of change is possible only if the climate models include those feedback loops for at least the most important ecosystems (Calvin et al., 2023; Cox et al., 2000).

Peatlands belong to the most important terrestrial ecosystems in the carbon cycle, as they store 30-50% of all soil carbon (Amesbury et al., 2019; Gorham, 1991). According to recent estimates, the amount of carbon stored in the peatlands may be as much as two times higher than carbon in all terrestrial vegetation (Amesbury et al., 2019; Erb et al., 2018). This vast amount of carbon is stored in the form of partially decomposed organic matter, peat. Peat accumulation is possible due to acidic, waterlogged, low nutrient and oxygen conditions, and the vegetation adapted to these conditions (van Breemen, 1995). Most of the northern peatlands are covered by several plant functional groups (PFGs), the most abundant of which are mosses, graminoids, and creeping or low shrubs (Wiedermann et al., 2017). The peatland's functions and peat accumulation rate depend on the physiological status and photosynthetic activity of plants and on the proportions of PFGs in the vegetation cover (Kuiper et al., 2014; Mao et al., 2018).

Mosses, and especially peat moss (*Sphagnum* spp.), are considered peatland engineers, due to their high water-holding capacity and environment acidification to such a degree which is unfavourable for a majority of vascular plants. Moreover, the litter of peat moss decomposes slowly due to the high carbon-to-nitrogen ratio and the presence of polyphenols (Lyons et al., 2020; Pacheco-Cancino et al., 2024; van Breemen, 1995). Peat moss and peatland vascular plants constantly compete for light and scarce nutrients. Vascular plants may suppress peat moss by limiting the light availability, while peat moss limits the nutrient availability for vascular plants, especially in oligotrophic peatlands (Dorrepaal et al., 2006; Malmer et al., 1994). However, changing climate may disturb this fine mutual control and cause abrupt shifts in vegetation composition, phenology and physiology when the tipping point is crossed

(Lamentowicz et al., 2019). As the northern peatlands are located in the high latitudes of the northern hemisphere, which are characterised by the highest rate of temperature growth, the changes in the environment and vegetation bring the risk that the vast amount of accumulated carbon will contribute to the acceleration of warming by a positive feedback loop in the future (Calvin et al., 2023; Robinson et al., 2023; Waddington et al., 2015; Xu et al., 2018).

Despite their significant ecological role, peatlands remain relatively understudied and underrepresented in models which is partially due to their remote locations and difficult terrain, which limit direct observation and data collection. Satellite remote sensing offers a promising solution for monitoring peatland vegetation. However, to effectively utilize satellite data, it is essential to establish a connection between spectral properties and physiological functions, particularly carbon assimilation, commonly referred to as gross primary production (GPP; Bandopadhyay et al., 2019; McPartland et al., 2019). The link between ground-based remote sensing signals and GPP have been studied across various vegetation types and environmental conditions (Martini et al., 2022; Migliavacca et al., 2017; Pierrat et al., 2022; Yang et al., 2015), but has not been examined for peatland vegetation before.

The most widely used remote sensing metrics for vegetation monitoring are reflectance-based vegetation indices. They make use of the fact that various plant components such as pigments, cellulose, and water, absorb, reflect and scatter the light at certain wavelengths more than others. Therefore, vegetation indices allow for the assessment of green biomass, changes in pigment quantity and quality and the estimation of absorbed photosynthetically active radiation (APAR) by vegetation (Zeng et al., 2022). While the reflectance-based metrics can be used for carbon assimilation assessment, sun-induced chlorophyll fluorescence (SIF) yields more exact estimates as it is not impacted by soil background, is more sensitive to vegetation stress and is directly linked to the leaf physiology (Damm et al., 2022; Porcar-Castell et al., 2021).

Chlorophyll fluorescence is one of the four major paths in which the light absorbed by plants can be used. Photochemistry, light intensity-dependent, and light intensity-independent heat dissipation are the other three. As the sum of their respective quantum yields equals unity, they are competing paths for the absorbed energy use. Around 80% of the energy is generally utilized for photochemistry and light intensity-dependent heat dissipation, while only 1-2% is emitted as fluorescence (Lazár, 2015). Nevertheless, the fluorescence intensity and the photochemistry rate correlate in normal conditions due to the fact that they both originate from reaction centres (RCs) of photosystems and the main protective, energy dissipation mechanism, light intensity-dependent heat dissipation, acts before the energy reaches RCs (Magney et al., 2020; Van Der Tol et al., 2014). Due to this covariation, SIF can be used for global monitoring of ecosystems' productivity and the assessment of changes caused by extreme weather events and climate change (Li et al., 2018; Martini et al., 2022). However, before the use of satellite-derived SIF for global photosynthesis assessment, the relationship between photosynthesis and SIF must be investigated for different ecosystems, including peatlands and information provided by SIF has to be understood in the broader context of plant physiology.

Passive chlorophyll fluorescence measurements (i.e. SIF) is a relatively new technique, but so-called active chlorophyll fluorescence measurements have been used for the analysis of plant physiology for several decades (Govindjee, 2007; Mohammed et al., 2019). Active measurements of fluorescence use the artificial source of light for chlorophyll excitation and translate the changes in chlorophyll fluorescence over time, ranging from milliseconds to minutes, into information about the status of photosynthetic apparatus (Kalaji et al., 2014). One of the widely used active methods is chlorophyll transient kinetics, which provides detailed information about the structure and functions of photosynthetic apparatus. This technique is commonly used to study the effect of different stressors on plants' physiology and to understand their reactions (Kalaji et al., 2017; Strasser et al., 2000).

In this doctoral dissertation, active and passive fluorescence measurement methods were used to reveal the impact of simulated climate change on peatland vegetation physiology.

2. Aim and hypotheses of the dissertation

The overall aim of this thesis is to assess the changes in peatland vegetation functioning caused by warmer and drier conditions projected for the near future. The work focuses specifically on the physiological changes in peatland species at the leaf and canopy levels measured by means of active and passive chlorophyll fluorescence techniques.

The **specific aims** of the dissertation are:

1. Describe the changes in peatland vegetation composition and phenology under future climatic conditions and derive their implications for the carbon balance of peatlands, based on the currently available literature.
2. Examine the potential of remote sensing in assessing the vegetation's physiological status and photosynthetic activity with a particular focus on SIF and peatland vegetation.
3. Assess the impact of warming alone and in combination with reduced precipitation on peatland vegetation physiology by remote sensing while taking into account vegetation communities of different compositions.
4. Investigate the influence of elevated temperature on different peatland vegetation plant species, focusing on their photosynthetic apparatus activity assessed by chlorophyll a fluorescence measurements.

The **hypotheses** of research included in this thesis are:

- Climate change will induce a shift in the peatland vegetation towards a higher abundance of vascular plants, which will have a longer vegetation season due to warming. These changes will enhance the vegetation's photosynthetic rate, but due to increased respiration rate, peatlands will become weaker carbon sinks or even carbon sources.
- Remote sensing metrics such as vegetation indices and SIF are robust proxies for peatland vegetation photosynthesis and can be used to track the physiological changes of vegetation in current and future warmer conditions.
- Warming and reduced precipitation induce changes in peatland vegetation structure, phenology and physiology that are traceable as changes in greenness related vegetation indices or SIF.
- Increased temperature impacts individual peatland PFGs differently, with vascular plants being impacted positively and mosses negatively.

3. Materials and methods

3.1 Literature review

A thorough published literature search was conducted in the second quartile of 2021 to identify the current knowledge on the topic of climate change impacts on peatland vegetation phenology and composition. The search was done using Scopus and Web of Science databases with keywords: peatland; bog; fen; mire; *Sphagnum*; climate change; warming; heating; drying; precipitation; water table level; phenology; vegetation composition; change; shift. The found literature was critically evaluated for the contained information and used for summary tables preparation of the literature review and/or for the review's main body text writing. Next search of literature using keywords: peatland; bog; fen; mire; *Sphagnum*; climate change; warming; heating; drying; precipitation; water table level; carbon balance; photosynthesis; primary production; primary productivity; respiration; methane, was done to discuss the impact of changes in peatland vegetation phenology and composition on carbon balance.

3.2 Site description

The experiments conducted within this dissertation were carried out in Rzecin peatland localised in western Poland (52° 45'41" N, 16°18'35" E, 54 m a.s.l.). The area covered by peatland is 86 ha, including a shallowing and overgrowing lake of around 16 ha (Barabach, 2013; Juszczak et al., 2012). The vegetation of peatland follows its rich-poor nutrient gradient with nutrient-rich edges of peat connected to mineral bedrock and nutrient-poor centre in the form of a floating mat. In total, 127 species of vascular plants and 34 taxa of mosses are present, including 26 rare and endangered species and 20 locally endangered species (Lamentowicz et al., 2015; Milecka et al., 2017). The average annual precipitation at the site is 600 mm, while the average temperature is 9.0°C.

In 2017 two research sites aimed at assessment of the warming and reduced precipitation impacts on two peatland vegetation communities were established in Rzecin peatland and named after dominant graminoids CL (after *Carex lasiocarpa* Ehrh.) and CR (after C*arex rostrata* Stokes). Vegetation of the CL site is dominated by bog cranberry (*Vaccinium oxycoccos* L.), peat moss (*Sphagnum* spp.), *Carex lasiocarpa* Ehrh., *Equisetum fluviatile* L., *Menianthes trifoliata* L., and *Comarum palustre* L. and the site is located at the transition between the part underlaid by sediment and the floating mat. CR site is situated on the floating mat, and its vegetation is dominated by bog cranberry, peat moss, *Carex rostrata* Stokes, and *Equisetum fluviatile* L. The pH at the CL site is around 5.2, while at the CR site, it is around 4.4 (Górecki et al., 2021).

Each of the sites consists of nine experimental plots divided into three treatments in triplicates: control (C), warming (W), and warming and reduced precipitations (WP). All plots are marked by squared collars with an inside length of 70 cm. C plots are exposed to the ambient conditions, while W and WP plots are enclosed by prototyped openable hexagonal open-top chambers (OTCs) with 2.1 m × 1.6 m base-width, 1.4 m × 1.1 m top-width, and 0.65 m height, made of transparent polycarbonate on the aluminium frame for passive warming during the daytime. During the nighttime, warming is induced actively by 100 W infrared mounted above the centre of the plots. Additionally, WP plots are equipped with curtains made of water-resistant fabric to reduce precipitation. The curtains open automatically during the nighttime rain events when the wind speed is <3.0 $m \cdot s^{-1}$ and the air temperature is above 5.0°C (Górecki et al., 2021).

Radiation-shielded thermohygrometers HygroVue5 (Campbell Sci., Logan, UT, USA) were installed next to the collar marking plots, 30 cm above the surface to measure the air temperature and humidity. They were installed inside the OTCs in the case of W and WP plots and all thermohygrometers were connected to datalogger CR1000 (Campbell Sci., Logan, UT, USA). Air temperature and humidity were recorded every 30 min during the whole day. Heated rain gauges TPG-124-H-24 (A-STER sp. z o.o., Krakow, Poland) were installed at each site to record precipitation and to facilitate the rain curtain closure above WP plots when the conditions were fulfilled. On each site, three TD-divers (Eijkelkamp Soil & Water, the Netherlands) were installed in the PVC piezometers that were permanently fixed to the construction of the wooden platforms reaching the solid bottom of the peatland for water table depth measurements. The measured values of water table depth were corrected by surface movement measured every 2-3 weeks and interpolated to daily values. BF5 Sunshine Sensor (Delta-T, UK) installed on a 3-meter-tall tower was used for measurements of photosynthetically active radiation (PAR) every 30 s.

3.3 Methods of conducting experiments

3.3.1 Canopy-level data collection and processing

Spectrally resolved irradiance and radiance were obtained from measurements by the Piccolo Doppio system (MacArthur et al., 2014). The system has a dual field of view with hemispherical irradiance fore optics and conical, 25° field of view radiance fore optics. The fore optics are connected to spectroradiometers placed in a cooled box by double bifurcated fibre optics that ensure that each spectroradiometer receives radiance from the same surface. Piccolo Doppio consists of two spectroradiometers: 1) FLAME-T-VIS_NIR (Ocean Insight

Inc., Dunedin, FL, USA), with a full-width half maximum (FWHM) of 1.3 nm, a sampling interval of approximately 0.33 nm, and a spectral range of 350-1000 nm; and 2) QEPro-FL (Ocean Insight Inc., Dunedin, FL, USA) with the FWHM of 0.31 nm, a sampling interval of approximately 0.16 nm, and a spectral range of 640-780 nm (Xu et al., 2021).

The measurements were taken from around the centre of experimental plots on a clear sky day from 1.4 m above the peatland surface, which resulted in a field of view with a diameter of 0.62 m. The measurements were performed every 2-5 weeks in the period between February and December and only the data for 2021 were used for this thesis. The measured digital numbers were converted to radiance and irradiance, accounting for periodically optimised integration time and instrumental noise and using the calibration coefficient obtained from the National Institute for Laser, Plasma, and Radiation Physics, Magurele, Romania. Reflectance was calculated from data acquired by FLAME-T-VIS_NIR as a ratio of radiance and irradiance and Normalised Difference VI (NDVI; Rouse et al., 1974), red-edge NDVI (reNDVI; Gitelson et al., 1994), Photochemical Reflectance Index (PRI; Gamon et al., 1992), Near-Infrared Reflectance of vegetation (NIRv; Badgley et al., 2017) and MERRIS Terrestrial Chlorophyll Index (MTCI; Dash et al., 2004) were subsequently calculated.

The SIF spectrum in the spectral range of 670-780 nm was retrieved from QEPro-FL radiance and irradiance using the Spectrum Fitting (SpecFit) algorithm (Cogliati et al., 2019). Several parameters, including the maximal SIF value in the red and far-red regions, the SIF values in O_2-A and O_2B absorption bands, the position of the red and far-red maximums and the integrated SIF values, were subsequently retrieved.

Fluxes of carbon dioxide from the experimental plots were measured with the closed dynamic portable system (Acosta et al., 2017; Juszczak et al., 2018). The measurements were taken in the same period and mostly on the same days as spectral measurements and started early morning and continued till late afternoon for both experimental sites on the same day. Net ecosystem exchange fluxes measured by a transparent chamber, and ecosystem respiration fluxes measured by an opaque chamber were calculated based on the CO_2 concentration change in the chamber’s headspace. These fluxes were used for GPP calculation and subsequent GPP modelling by rectangular hyperbolic light response Michaelis-Menten kinetic model (Hoffmann et al., 2015; Sakowska et al., 2018).

3.3.2 Leaf-level measurements and processing

Pulse–amplitude modulated and fluorescence kinetics measurements were performed by FluorPen FP 110/D (Photon System Instruments, Drasov, Czech Republic) with detachable dark adaptation clips. The measurements were performed under cloudy conditions in the spring of 2024 on bog cranberry and peat moss. The fluorescence of bog cranberry was measured on the adaxial side of the leaves of different plants in the plot. Measurements of peat moss fluorescence were derived from the freshly detached capitula’s top surface. 5 samples from each PFG in every plot were measured after 25 minutes of dark adaptation by the OJIP and NPQ3 protocols provided by the manufacturer. The OJIP protocol is a 2-s-lasting fast chlorophyll a fluorescence kinetics measurement, while NPQ3 is pulse–amplitude modulated fluorescence measurement under artificial actinic light that takes 200 s and comprises 10 pulses. The measurement light was set to 85%, while the actinic light for the NPQ3 protocol was 300 μmol m^{-2} s^{-1}. The blue light of 455 nm was used as actinic and measurement light.

3.4 Statistical analysis

Statistical analysis for canopy-level data was performed using RStudio version 2022.02.0+ 443, while the leaf-level data was analysed with version 2023.12.1+402 (RStudio Inc., Boston, MA, USA). The canopy-level data was tested for the normality of distribution and variance equality. The data that fulfilled the assumption of one-way analysis of variance (ANOVA) were tested for the significance of differences by ANOVA and Tukey’s range test. In the cases when the assumptions of ANOVA were not fulfilled, Kruskal-Wallis one-way analysis of variance and Dunn’s test were used. Simple and bidirectional stepwise linear regressions were used for GPP prediction from remote sensing data. A multiple linear regression model was built and cross-validated with k-fold cross-validation. Coefficients of determination (r^2) for the relationship of GPP and remote sensing parameters were determined by Pearson’s correlation. Normalized root mean square error was calculated as the ratio of root mean square error and the mean of the corresponding parameter. The significance of the difference for the leaf-level data was tested using Student’s t-test

4. Characteristics of the obtained results

4.1 Impact of climate change-induced alterations in peatland vegetation phenology and composition on carbon balance

The literature review published as Antala, M., Juszczak, R., van der Tol, Ch., Rastogi, A. (2022). Impact of climate change-induced alterations in peatland vegetation phenology and composition on carbon balance. *Science of the Total Environment*. 827, 154294. https://doi.org/10.1016/j.scitotenv.2022.154294, has shown that:

- increasing temperature causes shifts in peatland vegetation, including the earlier onset of shrubs and graminoids flowering, increased number of shrubs' flowers and earlier start of vegetative growth of graminoids while associated drying prolongs the vegetation season of graminoids;
- warmer and drier conditions cause the increasing abundance of shrubs in bogs, and warming favours graminoids in fens, both at the expense of *Sphagnum* spp.;
- the prolonged vegetation season and higher abundance of vascular plants will result in higher GPP of peatlands in the future;
- warming and drying of bogs, together with the shifts in vegetation composition, will result in a faster decomposition rate and higher release of CO_2;
- warming and a higher abundance of graminoids in fens will increase the production and release of methane;
- despite the increased carbon assimilation by peatland vegetation, peatlands will most probably become weaker sinks or even sources of carbon as the climate warms up.

4.2 Nonphotochemical quenching does not alter the relationship between sun-induced fluorescence and gross primary production under heatwave

The study and analysis of published data on the canopy and leaf-level fluorescence resulted in the correspondence publication: Antala, M., Juszczak, R., Rastogi, A., (2024). Nonphotochemical quenching does not alter the relationship between sun-induced fluorescence and gross primary production under heatwave. *New Phytologist*. 20312. https://doi.org/10.1111/nph.20312, reacting on the previously published article by Martini et al., (2022), and arguing that:

- the heatwave, as identified by the authors of the original article, in fact, did not break the linear relationship between SIF and GPP, as there was no linear relationship to begin with, in the period prior to the heatwave;
- nonphotochemical quenching of maximal fluorescence (NPQ), or quantum yield of light intensity-dependent heat dissipation (φNPQ), did not saturate during the heatwave, as their correlations with GPP in the case of NPQ and photochemistry in the case of φNPQ stayed linear and their trends remained unchanged during the heatwave compared to the pre-heatwave period;
- considering that stomata closure is one of the most common reactions of plants to heat and drought stress and observing that SIF mostly followed the diurnal changes of PAR while GPP was found vapour pressure deficit-dependent, closing stomata was most probably the cause of the broken linear correlation between SIF and GPP observed in the original article;
- SIF decreased during the extreme heat disproportionally more than GPP, which could be caused by temperature dependency of the fluorescence emission.

4.3 Sun-induced fluorescence spectrum as a tool for assessing peatland vegetation productivity in the framework of warming and reduced precipitation experiment

The results obtained from the canopy-level measurement and published as Antala, M., Rastogi, A., Cogliati, S., Stróżecki, M., Colombo, R., Juszczak, R. (2024). Sun-induced fluorescence spectrum as a tool for assessing peatland vegetation productivity in the framework of warming and reduced precipitation experiment. *Remote Sensing of Environment*. 301, 113921. https://doi.org/10.1016/j.rse.2023.113921, revealed that:

- unlike in the case of the annual crops, the spectrum of top-of-canopy peatland vegetation SIF is characterized by a higher far-red peak than the red peak for the whole season;
- far-red SIF was found to be the best-performing tested remote sensing metrics for statistical prediction of GPP by simple linear regression;
- the use of multiple wavelength regression trained on the full SIF spectrum yielded more accurate and more stable predictions of GPP, especially for more challenging CR vegetation, where changes in biomass over the season are less pronounced;
- the predictions using multiple wavelength regression are stable across the microclimate conditions (C, W, WP) and the vegetation communities (CL and CR), which was not the case for simple SIF parameters or studied VIs;

- W and WP significantly increased the near-infrared reflectance and SIF intensity in CR vegetation for the majority of the summer, while they caused significant changes in CL vegetation's remote sensing signals only at the beginning of summer;
- the vegetation with a higher share of vascular plants, like CL vegetation or CR vegetation under W and WP conditions, exhibits stronger seasonality of SIF intensity.

4.4 Photosynthetic Responses of Peat Moss (*Sphagnum* spp.) and Bog Cranberry (*Vaccinium oxycoccos* L.) to Spring Warming

Leaf-level measurements results published as Antala, M., Abdelmajeed, A.Y.A., Stróżecki, M., Krzesiński, W., Juszczak, R., Rastogi, A. (2024). Photosynthetic Responses of Peat Moss (*Sphagnum* spp.) and Bog Cranberry (*Vaccinium oxycoccos* L.) to Spring Warming. *Plants* 13 (22), 3246. https://doi.org/10.3390/plants13223246, suggest that:

- peat mosses are able to quickly react on even shorter periods of favourable conditions by increased rates of photochemistry because they regulate their heat dissipation during winter;
- bog cranberries utilize the strategy of more constant protection in the form of light intensity-independent heat dissipation that relaxes comparatively slower and needs a period of warmer temperature to reach full activity;
- the activation of bog cranberry's photosynthetic activity in spring is faster, when the temperature is higher, whereas peat moss benefits from the warming relatively less;
- the process of photosynthesis activation in bog cranberries is accompanied by the activation of RCs, decreased heat dissipation, and increased overall efficiency of photosysntem II (PSII), all of which were found to be temperature-dependent;
- the experimental W further enhanced the performance of bog cranberry's photosynthesis, indicated by a significant increase in the PSII performance index on an absorption basis.

5. Discussion

Accurate predictions of the future climate are possible only when accounting for the feedback loops induced by past, ongoing and future changes. Modifications in peatland vegetation functioning belong to the important, but uncertain parts of these predictions (Cox et al., 2000; Hoegh-Guldberg, O. et al., 2018; Ripple et al., 2023). As the climate warms up, the vegetation of Earth's ecosystems needs to adapt in order to survive in the new conditions. As some plants are better adapted to warmer conditions and can sustain more pronounced extremes, the vegetation composition is changing (Corlett, 2016). An increasing abundance of shrubs, and especially ericaceous shrubs, belongs to the main observed warming-induced changes in the peatland vegetation (Bragazza et al., 2016; Gunnarsson et al., 2002; Jassey et al., 2018). The small leaves with thicker cuticle and increased growth of roots in the warmer conditions allow the shrubs to take advantage of increasing temperature (Buttler et al., 2015; Malhotra et al., 2020). The mineralisation and the growth of mycorrhizal fungi increase in warmer peat, which makes more of the essential nutrients, such as nitrogen and phosphorus, available to the faster-growing roots of shrubs and favours their growth even more (Asemaninejad et al., 2018; Malmer et al., 2003). Moreover, the work within this thesis has shown, that ericaceous shrubs, such as bog cranberry, benefit from spring warming by faster onset of photosynthetic activity. As the PSII structure of evergreen plants in temperate and boreal regions changes during the winter for protection from high light intensity during low temperatures, its efficiency is decreased. This decrease in PSII efficiency is accompanied by increased non-regulated heat dissipation (Gilmore et al., 2000; Lehner et al., 2003; Lundell et al., 2008). As the presented results of leaf-level measurements have shown, the rate of spring reactivation of RCs and PSII photochemistry is temperature-dependent, and increases with experimental W despite the measurements were taken in the warmest spring ever recorded, yet (NOAA., 2024). However, peat moss stays photosynthetically active even under the snow cover, if it is not frozen and continues to grow over wintertime (Campbell et al., 2019; Küttim et al., 2020). The presented results showing the constantly low reliance on non-regulated and high reliance on regulated heat dissipation are in concordance with those previous findings. Because peat mosses do not require longer period of warmer weather for their photosynthetic activity, they benefit from warming relatively less compared to shrubs. These results show that the efficient utilization of photosynthetic potential by shrubs may contribute to the observed shrub encroachment in peatlands.

Increased green biomass of vegetation increases the intensity of SIF (Cogliati et al., 2019). The increased SIF of CR vegetation in W and WP can be, therefore, interpreted as an increase in the cover of vascular plants. Indeed, previous studies have shown, that the leaf area index and the cover of graminoids in Rzecin peatland increase with warmer conditions (Łuców et al., 2017; Rastogi et al., 2022). As the results of this dissertation suggest, warming has a stronger effect on peatland vegetation communities that had previously sparser cover of vascular plants. However, the dominance of the far-red peak in the SIF spectrum all around the year suggests that a significant part of the surface is covered by evergreen shrubs in both studied vegetations in C, W and WP plots (Porcar-Castell et al., 2021).

Vegetation phenology represents the onset of the phenophases that are accompanied or preceded by the physiological changes (Chen et al., 2022; Collins et al., 2021). More pronounced shifts in peatland vegetation reproductive phenology than in vegetative phenology found by reviewing literature are in agreement with the results found for tundra plants by Collins et al. (2021). However, the physiological changes in peatland vegetation at the leaf and canopy levels were observed in this doctoral research. As previously mentioned, W caused an earlier onset of photosynthetic activity of bog cranberry. Moreover, in the spring, the SIF of both studied vegetations exposed to W and WP increased more rapidly than in C plots. This suggests not only the physiological but also structural changes in the vegetation caused by warmer and drier conditions (Rascher et al., 2021).

Results of this dissertation acquired from the analysis of different research work along with performing the experiments at canopy and leaf level, which suggested that shifts in the peatland vegetation composition and phenology are the results of plants' physiology, and they further affect vegetation photosynthesis. The higher values of GPP in CR vegetation during summer caused by W and WP are the most direct proof of these changes. As found before, more vascular plants in the vegetation cause stronger assimilation by peatland vegetation at the peak of the season (Laine et al., 2012). The prolonged vegetation season found in this work suggests a further increase in the annual GPP of peatland vegetation in warmer conditions (Lund et al., 2010).

The results of canopy-level measurements showed a good relationship between greenness VIs like NDVI, reNDVI, MTCI and GPP for CL vegetation. Which experiences larger changes in standing green biomass during the season than CR vegetation. The correlation of the mentioned VIs and GPP for CR vegetation was weaker due to less prominent changes in its green biomass. Relatively newer index NIRv showed a good correlation with GPP and SIF for both vegetation as it did for other ecosystems in previous research (Badgley et al., 2017; Dechant et al., 2020). However, the use of SIF instead of reflectance-based indices for the prediction of GPP in the evergreen ecosystem was found to bring more consistent results (Pierrat et al., 2022). Indeed, a very strong relationship between SIF and GPP over the growing season was found in the research included in this dissertation. Far-red SIF was the best-correlated traditional remote sensing parameter among those examined. As far-red SIF is a good proxy for APAR, which also drives GPP, this did not come as a surprise (Magney et al., 2019; Wieneke et al., 2018). Because of the fact that far-red SIF dominates the SIF spectrum over the whole season, integrated SIF did not outperform the commonly used far-red SIF. However, using the multiple-wavelength regression trained based on the band chosen by bidirectional stepwise linear regression yielded superior accuracy and transferability compared to the traditional metrics. The use of multiple wavelengths of SIF from different portions of the SIF spectrum was found to be a robust method for GPP estimation in deciduous forests and using the simulated dataset in past (Liu et al., 2019; Verrelst et al., 2016). In concordance with those previous results, this work showed that a novel multiple-wavelength regression approach is the best statistical approach also for peatland. Nevertheless, the integrated full SIF spectrum may be used in future for mechanistic calculation of photochemistry and GPP by the approach suggested by Gu et al. (2019), Sun, Gu, et al. (2023), and Sun, Wen, et al. (2023)

Although the SIF metrics were positively linearly correlated with GPP under C, W and WP conditions in this dissertation, the SIF and GPP relationship may break down in extreme conditions, such as prolonged severe heat (Martini et al., 2022). When that happens, it is important to examine the causes of the broken relationship not only statistically but also mechanistically. Correspondence that is part of this thesis suggests that the main cause of the disruption of the SIF and GPP correlation during the heat and drought stress conditions in the stomata closure, which prevents the gas exchange between the leaf interior and atmosphere but does not impact the light phase of photosynthesis to the same degree (Farquhar et al., 1980; Marrs et al., 2020). When severe heat that may damage the structure of proteins occurs, SIF intensity drops similarly to the chlorophyll fluorescence intensity measured at the leaf level when their physiological threshold was crossed (Kouřil et al., 2004). Therefore, thermal remote sensing might be an optimal additional approach to monitor the plants' physiology under stress conditions (Chakhvashvili et al., 2024). These are important considerations to make once the SIF is applied for large-scale monitoring of peatlands and assessment of climate change on the physiology of their vegetation.

6. Conclusions

The work done within this thesis brought more clarity to the changes that peatland vegetation functions are undergoing and will undergo when the temperature rises even more.

The published work included in this dissertation has shown that:

- Warming and drying induce significant changes in the peatland vegetation, including the lowering of peat moss abundance and increase in shrubs share in the bogs and graminoids in fens. Moreover, generative and vegetative phenophases of peatland inhabiting species are starting sooner with warmer springs. Shifts towards vascular plants' dominance and the vegetation season prolongation enhance the carbon assimilation by plants, but the warming and drying, together with changes in vegetation composition speed up also carbon release in the form of CO_2 and methane. Taking into account the reviewed research, based on up-to-date knowledge, the result of climate-induced changes in peatland vegetation phenology and composition will be lower carbon accumulation by peatlands in the short term with possible becoming of carbon source in the long term (Paper no. 1).
- Greenness-related VIs relate well with GPP if the change of GPP is driven by biomass growth. If the peatland vegetation is highly dominated, the best parameter for modelling of GPP by simple regression is SIF in the far-red region. However, for more accurate and robust predictions of GPP, multiple wavelength regression utilising information from the full SIF spectrum is required. Such an approach yields stable high correlations and low NRMSE across studied vegetation communities and temperature and precipitation regimes (Paper no. 3). However, when weather anomalies, such as drought and heat waves, become more extreme in the future, SIF alone may not be enough for vegetation photosynthesis monitoring (Paper no. 2).
- A higher proportion of shrubs and graminoids in the plots under W and WP conditions for the vegetation previously dominated by peat moss resulted in significant changes in the vegetation spectral properties detectable as an increase in near-infrared reflectance and far-red and total SIF. Moreover, the increased seasonal amplitude and earlier increase of SIF were detected by hyperspectral measurements at the canopy level. W and WP had an overall positive effect on CR vegetation physiology and a rather insignificant impact on CL vegetation. However, only GPP was assessed in this thesis and for the full carbon balance assessment, the ecosystem respiration must be studied in the future (Paper no. 3).

- The observed changes in the peatland vegetation stem from the differences in the individual PFGs' physiology and their reactions to the changing environmental conditions. Ericaceous shrubs, such as bog cranberry benefit from the warmer conditions and start their photosynthetic activity sooner. However, warming has little positive impact on peat moss, which is adapted for the start of its physiological activity in colder conditions (Paper no. 4).

References

1. Acosta, M., Juszczak, R., Chojnicki, B., Pavelka, M., Havránková, K., Lesny, J., Krupková, L., Urbaniak, M., Machačová, K., & Olejnik, J. (2017). CO2 Fluxes from Different Vegetation Communities on a Peatland Ecosystem. *Wetlands, 37*(3), 423–435. doi: 10.1007/s13157-017-0878-4
2. Amesbury, M. J., Gallego-Sala, A., & Loisel, J. (2019). Peatlands as prolific carbon sinks. *Nature Geoscience*, *12*(11), 880–881. doi: 10.1038/s41561-019-0455-y
3. Asemaninejad, A., Thorn, R. G., Branfireun, B. A., & Lindo, Z. (2018). Climate change favours specific fungal communities in boreal peatlands. *Soil Biology and Biochemistry*, *120*(July 2017), 28–36. doi: 10.1016/j.soilbio.2018.01.029
4. Badgley, G., Field, C. B., & Berry, J. A. (2017). Canopy near-infrared reflectance and terrestrial photosynthesis. *Science Advances*, *3*(3), 1–6. doi: 10.1126/sciadv.1602244
5. Bandopadhyay, S., Rastogi, A., Rascher, U., Rademske, P., Schickling, A., Cogliati, S., Julitta, T., Arthur, A. Mac, Hueni, A., Tomelleri, E., Celesti, M., Burkart, A., Strózecki, M., Sakowska, K., Gabka, M., Rosadziński, S., Sojka, M., Iordache, M. D., Reusen, I., … Juszczak, R. (2019). Hyplant-derived Sun-Induced Fluorescence-A new opportunity to disentangle complex vegetation signals from diverse vegetation types. *Remote Sensing*, *11*(14). doi: 10.3390/rs11141691
6. Barabach, J. (2013). The history of Lake Rzecin and its surroundings drawn on maps as a background to palaeoecological reconstruction. *Limnological Review*, *12*(3), 103–114. doi: 10.2478/v10194-011-0050-0
7. Bragazza, L., Buttler, A., & Robroek, B. J. M. (2016). Persistent high temperature and low precipitation reduce peat carbon accumulation. *Global Change Biology*, *22*, 4114–4123. doi: https://doi.org/10.1111/gcb.13319
8. Buttler, A., Robroek, B. J. M., Laggoun-Défarge, F., Jassey, V. E. J., Pochelon, C., Bernard, G., Delarue, F., Gogo, S., Mariotte, P., Mitchell, E. A. D., & Bragazza, L. (2015). Experimental warming interacts with soil moisture to discriminate plant responses in an ombrotrophic peatland. *Journal of Vegetation Science*, *26*(5), 964–974. doi: 10.1111/jvs.12296
9. Calvin, K., Dasgupta, D., Krinner, G., Mukherji, A., Thorne, P. W., Trisos, C., Romero, J., Aldunce, P., Barrett, K., Blanco, G., Cheung, W. W. L., Connors, S., Denton, F., Diongue-Niang, A., Dodman, D., Garschagen, M., Geden, O., Hayward, B., Jones, C., … Ha, M. (2023). *Climate Change 2023: Synthesis Report. Contribution of Working Groups I, II and III to the Sixth Assessment Report of the Intergovernmental Panel on Climate Change* (P. Arias, M. Bustamante, I. Elgizouli, G. Flato, M. Howden, C. Méndez-Vallejo, J. J. Pereira, R. Pichs-Madruga, S. K. Rose, Y. Saheb, R. Sánchez Rodríguez, D. Ürge-Vorsatz, C. Xiao, N. Yassaa, J. Romero, J. Kim, E. F. Haites, Y. Jung, R. Stavins, … C. Péan, Eds.). doi: 10.59327/IPCC/AR6-9789291691647
10. Campbell, C., & Rydin, H. (2019). The effects of winter stress on Sphagnum species with contrasting macro- and microdistributions. *Journal of Bryology*, *41*(3), 205–217. doi: 10.1080/03736687.2019.1626167
11. Chakhvashvili, E., Machwitz, M., Antala, M., Rozenstein, O., Prikaziuk, E., Schlerf, M., Naethe, P., Wan, Q., Komárek, J., Klouek, T., Wieneke, S., Siegmann, B., Kefauver, S., Kycko, M., Balde, H., Paz, V. S., Jimenez-Berni, J. A., Buddenbaum, H., Hänchen, L., … Rascher, U. (2024). Crop stress detection

from UAVs: best practices and lessons learned for exploiting sensor synergies. *Precision Agriculture*. doi: 10.1007/s11119-024-10168-3

12. Chen, S., Fu, Y. H., Hao, F., Li, X., Zhou, S., Liu, C., & Tang, J. (2022). Vegetation phenology and its ecohydrological implications from individual to global scales. *Geography and Sustainability*, *3*(4), 334–338. doi: 10.1016/j.geosus.2022.10.002
13. Cogliati, S., Celesti, M., Cesana, I., Miglietta, F., Genesio, L., Julitta, T., Schuettemeyer, D., Drusch, M., Rascher, U., Jurado, P., & Colombo, R. (2019). A spectral fitting algorithm to retrieve the fluorescence spectrum from canopy radiance. *Remote Sensing*, *11*(16). doi: 10.3390/rs11161840
14. Collins, C. G., Elmendorf, S. C., Hollister, R. D., Henry, G. H. R., Clark, K., Bjorkman, A. D., Myers-Smith, I. H., Prevéy, J. S., Ashton, I. W., Assmann, J. J., Alatalo, J. M., Carbognani, M., Chisholm, C., Cooper, E. J., Forrester, C., Jónsdóttir, I. S., Klanderud, K., Kopp, C. W., Livensperger, C., … Suding, K. N. (2021). Experimental warming differentially affects vegetative and reproductive phenology of tundra plants. *Nature Communications*, *12*(1). doi: 10.1038/s41467-021-23841-2
15. Corlett, R. T. (2016). Plant diversity in a changing world: Status, trends, and conservation needs. *Plant Diversity*, *38*(1), 10–16. doi: 10.1016/j.pld.2016.01.001
16. Cox, P. M., Betts, R. A., Jones, C. D., Spall, S. A., & Totterdell, I. J. (2000). Acceleration of global warming due to carbon-cycle feedbacks in a coupled climate model. *Nature*, *408*(6809), 184–187. doi: 10.1038/35041539
17. Damm, A., Cogliati, S., Colombo, R., Fritsche, L., Genangeli, A., Genesio, L., Hanus, J., Peressotti, A., Rademske, P., Rascher, U., Schuettemeyer, D., Siegmann, B., Sturm, J., & Miglietta, F. (2022). Response times of remote sensing measured sun-induced chlorophyll fluorescence, surface temperature and vegetation indices to evolving soil water limitation in a crop canopy. *Remote Sensing of Environment*, *273*(January), 112957. doi: 10.1016/j.rse.2022.112957
18. Dash, J., & Curran, P. J. (2004). The MERIS terrestrial chlorophyll index. *International Journal of Remote Sensing*, *25*(23), 5403–5413. doi: 10.1080/0143116042000274015
19. Dechant, B., Ryu, Y., Badgley, G., Zeng, Y., Berry, J. A., Zhang, Y., Goulas, Y., Li, Z., Zhang, Q., Kang, M., Li, J., & Moya, I. (2020). Canopy structure explains the relationship between photosynthesis and sun-induced chlorophyll fluorescence in crops. *Remote Sensing of Environment*, *241*(June 2019). doi: 10.1016/j.rse.2020.111733
20. Dorrepaal, E., Aerts, R., Cornelissen, J. H. C., Van Logtestijn, R. S. P., & Callaghan, T. V. (2006). Sphagnum modifies climate-change impacts on subarctic vascular bog plants. *Functional Ecology*, *20*(1), 31–41. doi: 10.1111/j.1365-2435.2006.01076.x
21. Erb, K. H., Kastner, T., Plutzar, C., Bais, A. L. S., Carvalhais, N., Fetzel, T., Gingrich, S., Haberl, H., Lauk, C., Niedertscheider, M., Pongratz, J., Thurner, M., & Luyssaert, S. (2018). Unexpectedly large impact of forest management and grazing on global vegetation biomass. *Nature*, *553*(7686), 73–76. doi: 10.1038/nature25138
22. Farquhar, G. D., Von Caemmerer, S., & Berry, J. A. (1980). A Biochemical Model of Photosynthetic CO 2 Assimilation in Leaves of C 3 Species. *Planta*, *149*, 78–90.

23. Gamon, J. A., Peñuelas, J., & Field, C. B. (1992). A narrow-waveband spectral index that tracks diurnal changes in photosynthetic efficiency. *Remote Sensing of Environment*, *41*(1), 35–44. doi: 10.1016/0034-4257(92)90059-S
24. Gilmore, A. M., & Ball, M. C. (2000). Protection and storage of chlorophyll in overwintering evergreens. *Proceedings of the National Academy of Sciences*, *97*(20), 11098–11101. doi: 10.1073/pnas.150237697
25. Gitelson, A., & Merzlyak, M. N. (1994). Quantitative estimation of chlorophyll-a using reflectance spectra: Experiments with autumn chestnut and maple leaves. *Journal of Photochemistry and Photobiology, B: Biology*, *22*(3), 247–252. doi: 10.1016/1011-1344(93)06963-4
26. Górecki, K., Rastogi, A., Stróżecki, M., Gąbka, M., Lamentowicz, M., Łuców, D., Kayzer, D., & Juszczak, R. (2021). Water table depth, experimental warming, and reduced precipitation impact on litter decomposition in a temperate Sphagnum-peatland. *Science of the Total Environment*, *771*. doi: 10.1016/j.scitotenv.2021.145452
27. Gorham, E. (1991). Northern peatlands: role in the carbon cycle and probable responses to climatic warming. *Ecological Applications*, *1*(2), 182–195. doi: 10.2307/1941811
28. Govindjee. (2007). Chlorophyll a Fluorescence: A Bit of Basics and History. In Chlorophyll a Fluorescence (pp. 1–41). Springer Netherlands. doi: 10.1007/978-1-4020-3218-9_1
29. Gu, L., Han, J., Wood, J. D., Chang, C. Y. Y., & Sun, Y. (2019). Sun-induced Chl fluorescence and its importance for biophysical modeling of photosynthesis based on light reactions. *New Phytologist*, *223*(3), 1179–1191. doi: 10.1111/nph.15796
30. Gunnarsson, U., Maimer, N., & Rydin, H. (2002). Dynamics or constancy in Sphagnum dominated mire ecosystems? A 40-year study. *Ecography*, *25*(6), 685–704. doi: 10.1034/j.1600-0587.2002.250605.x
31. Hoegh-Guldberg, O., D., Jacob, M., Taylor, M., Bindi, S., Brown, I., Camilloni, A., Diedhiou, R., Djalante, K. L., Ebi, F., Engelbrecht, J., Guiot, Y., Hijioka, S., Mehrotra, A., Payne, S. I., Seneviratne, A., Thomas, R., Warren, G., & Zhou. (2018). Impacts of 1.5°C of Global Warming on Natural and Human Systems. In and T. W. Masson-Delmotte, V., P. Zhai, H.-O. Pörtner, D. Roberts, J. Skea, P.R. Shukla, A. Pirani, W. Moufouma-Okia, C. Péan, R. Pidcock, S. Connors, J.B.R. Matthews, Y. Chen, X. Zhou, M.I. Gomis, E. Lonnoy, T. Maycock, M. Tignor (Ed.), Global Warming of 1.5°C. An IPCC Special Report on the impacts of global warming of 1.5°C above pre-industrial levels and related global greenhouse gas emission pathways, in the context of strengthening the global response to the threat of climate change,.
32. Hoffmann, M., Jurisch, N., Albiac Borraz, E., Hagemann, U., Drösler, M., Sommer, M., & Augustin, J. (2015). Automated modeling of ecosystem CO2 fluxes based on periodic closed chamber measurements: A standardized conceptual and practical approach. *Agricultural and Forest Meteorology*, *200*, 30–45. doi: 10.1016/j.agrformet.2014.09.005
33. Jassey, V. E. J., Reczuga, M. K., Zielińska, M., Słowińska, S., Robroek, B. J. M., Mariotte, P., Seppey, C. V. W., Lara, E., Barabach, J., Słowiński, M., Bragazza, L., Chojnicki, B. H., Lamentowicz, M., Mitchell, E. A. D., & Buttler, A. (2018). Tipping point in plant–fungal interactions under severe drought causes abrupt rise in peatland ecosystem respiration. *Global Change Biology*, *24*(3), 972–986. doi: 10.1111/gcb.13928

34. Juszczak, Radoslaw, Acosta, M., & Olejnik, J. (2012). Comparison of daytime and nighttime ecosystem respiration measured by the closed chamber technique on a temperate mire in Poland. *Polish Journal of Environmental Studies*, *21*(3), 643–658.
35. Juszczak, Radosław, Uździcka, B., Stróżecki, M., & Sakowska, K. (2018). Improving remote estimation of winter crops gross ecosystem production by inclusion of leaf area index in a spectral model. *PeerJ*, *2018*(9). doi: 10.7717/peerj.5613
36. Kalaji, H. M., Goltsev, V. N., Zuk-Golaszewska, K., Zivcak, M., & Brestic, M. (2017). *Chlorophyll Fluorescence - Basics and Applicatrions*. Boca Raton, FL, USA: CRC Press.
37. Kalaji, H. M., Schansker, G., Ladle, R. J., Goltsev, V., Bosa, K., Allakhverdiev, S. I., Brestic, M., Bussotti, F., Calatayud, A., Dąbrowski, P., Elsheery, N. I., Ferroni, L., Guidi, L., Hogewoning, S. W., Jajoo, A., Misra, A. N., Nebauer, S. G., Pancaldi, S., Penella, C., … Zivcak, M. (2014). Frequently asked questions about in vivo chlorophyll fluorescence: Practical issues. *Photosynthesis Research*, *122*(2), 121–158. doi: 10.1007/s11120-014-0024-6
38. Kouřil, R., Lazár, D., Ilík, P., Skotnica, J., Krchňák, P., & Nauš, J. (2004). High-temperature induced chlorophyll fluorescence rise in plants at 40–50°C: experimental and theoretical approach. *Photosynthesis Research*, *81*, 49–66.
39. Kuiper, J., Mooji, W., Bragazza, L., & Robroek, B. J. M. (2014). Plant functional types define magnitude of drought response in peatland CO2 exchange. *Ecology*. doi: 10.1890/13-0270.1
40. Küttim, M., Küttim, L., Ilomets, M., & Laine, A. M. (2020). Controls of Sphagnum growth and the role of winter. *Ecological Research*, *35*(1), 219–234. doi: 10.1111/1440-1703.12074
41. Laine, A. M., Bubier, J., Riutta, T., Nilsson, M. B., Moore, T. R., Vasander, H., & Tuittila, E. S. (2012). Abundance and composition of plant biomass as potential controls for mire net ecosytem CO 2 exchange. *Botany*, *90*(1), 63–74. doi: 10.1139/B11-068
42. Lamentowicz, M., Mueller, M., Gałka, M., Barabach, J., Milecka, K., Goslar, T., & Binkowski, M. (2015). Reconstructing human impact on peatland development during the past 200 years in CE Europe through biotic proxies and X-ray tomography. *Quaternary International*, *357*, 282–294. doi: 10.1016/j.quaint.2014.07.045
43. Lamentowicz, Mariusz, Gałka, M., Marcisz, K., Słowinski, M., Kajukało-Drygalska, K., Dayras, M. D., & Jassey, V. E. J. (2019). Unveiling tipping points in long-term ecological records from Sphagnum-dominated peatlands. *Biology Letters*, *15*(4). doi: 10.1098/rsbl.2019.0043
44. Lazár, D. (2015). Parameters of photosynthetic energy partitioning. *Journal of Plant Physiology*, *175*, 131–147. doi: 10.1016/j.jplph.2014.10.021
45. Lehner, G., & Lütz, C. (2003). Photosynthetic functions of cembran pines and dwarf pines during winter at timberline as regulated by different temperatures, snowcover and light. *J. Plant Physiol*, *160*, 153–166. Retrieved from http://www.urbanfischer.de/journals/jpp
46. Li, X., Xiao, J., He, B., Altaf Arain, M., Beringer, J., Desai, A. R., Emmel, C., Hollinger, D. Y., Krasnova, A., Mammarella, I., Noe, S. M., Ortiz, P. S., Rey-Sanchez, A. C., Rocha, A. V., & Varlagin, A. (2018). Solar-induced chlorophyll fluorescence is strongly correlated with terrestrial photosynthesis for a wide variety of biomes: First global analysis based on OCO-2 and flux tower observations. *Global Change Biology*, *24*(9), 3990–4008. doi: 10.1111/gcb.14297

47. Liu, Z., Lu, X., An, S., Heskel, M., Yang, H., & Tang, J. (2019). Advantage of multi-band solar-induced chlorophyll fluorescence to derive canopy photosynthesis in a temperate forest. *Agricultural and Forest Meteorology*, *279*(August), 107691. doi: 10.1016/j.agrformet.2019.107691
48. Łuców, D., Basinska, A., Chojnicki, B., Józefczyk, D., Juszczak, R., Lesny, J., Olejnik, J., Reczuga, M., Samson, M., Silvennoinen, H., Strózecki, M., Urbaniak, M., Zielińska, M., & Lamentowicz, M. (2017). The response of vegetation structure to active warming and precipitation reduction of the Sphagnum peatland. *Geophysical Research Abstracts*, *19*(April), 2017–8001. Retrieved from www.wetman.pl
49. Lund, M., Lafleur, P. M., Roulet, N. T., Lindroth, A., Christensen, T. R., Aurela, M., Chojnicki, B. H., Flanagan, L. B., Humphreys, E. R., Laurila, T., Oechel, W. C., Olejnik, J., Rinne, J., Schubert, P., & Nilsson, M. B. (2010). Variability in exchange of CO2 across 12 northern peatland and tundra sites. *Global Change Biology*, *16*(9), 2436–2448. doi: 10.1111/j.1365-2486.2009.02104.x
50. Lundell, R., Saarinen, T., Åström, H., & Hänninen, H. (2008). The boreal dwarf shrub Vaccinium vitis-idaea retains its capacity for photosynthesis through the winter. *Botany*, *86*(5), 491–500. doi: 10.1139/B08-022
51. Lyons, C. L., & Lindo, Z. (2020). Above- and belowground community linkages in boreal peatlands. *Plant Ecology*, *221*(7), 615–632. doi: 10.1007/s11258-020-01037-w
52. MacArthur, A., Robinson, I., Rossini, M., Davis, N., & MacDonald, K. (2014). Edinburgh Research Explorer A dual-field-of-view spectrometer system for reflectance and fluorescence measurements (Piccolo Doppio) and correction of etaloning Citation for published version: A DUAL-FIELD-OF-VIEW SPECTROMETER SYSTEM FOR REFLECTANCE AND FL. *Proceedings of the Fifth International Workshop on Remote Sensing of Vegetation Fluorescence, 22-24 APRIL 2014, PARIS (FRANCE)*, 1–8. Retrieved from https://www.research.ed.ac.uk/portal/files/17385047/A_DFOV_spectrometer_system_for_reflectance_and_fluorescence_Piccolo_.pdf
53. Magney, T. S., Barnes, M. L., & Yang, X. (2020). On the Covariation of Chlorophyll Fluorescence and Photosynthesis Across Scales. *Geophysical Research Letters*, *47*(23). doi: 10.1029/2020GL091098
54. Magney, T. S., Frankenberg, C., Köhler, P., North, G., Davis, T. S., Dold, C., Dutta, D., Fisher, J. B., Grossmann, K., Harrington, A., Hatfield, J., Stutz, J., Sun, Y., & Porcar-Castell, A. (2019). Disentangling Changes in the Spectral Shape of Chlorophyll Fluorescence: Implications for Remote Sensing of Photosynthesis. *Journal of Geophysical Research: Biogeosciences*, *124*(6), 1491–1507. doi: 10.1029/2019JG005029
55. Malhotra, A., Brice, D. J., Childs, J., Graham, J. D., Hobbie, E. A., Vander Stel, H., Feron, S. C., Hanson, P. J., & Iversen, C. M. (2020). Peatland warming strongly increases fine-root growth. *Proceedings of the National Academy of Sciences of the United States of America*, *117*(30), 17627–17634. doi: 10.1073/pnas.2003361117
56. Malmer, N., Albinsson, C., Svensson, B. M., & Wallén, B. (2003). Interferences between Sphagnum and vascular plants: Effects on plant community structure and peat formation. *Oikos*, *100*(3), 469–482. doi: 10.1034/j.1600-0706.2003.12170.x

57. Malmer, N., Svensson, B. M., & Wallén, B. (1994). Interactions between Sphagnum mosses and field layer vascular plants in the development of peat-forming systems. *Folia Geobotanica et Phytotaxonomica*, *29*(4), 483–496. doi: 10.1007/BF02883146
58. Mao, R., Zhang, X., Song, C., Wang, X., & Finnegan, P. M. (2018). Plant functional group controls litter decomposition rate and its temperature sensitivity: An incubation experiment on litters from a boreal peatland in northeast China. *Science of the Total Environment*, *626*, 678–683. doi: 10.1016/j.scitotenv.2018.01.162
59. Marrs, J. K., Reblin, J. S., Logan, B. A., Allen, D. W., Reinmann, A. B., Bombard, D. M., Tabachnik, D., & Hutyra, L. R. (2020). Solar-Induced Fluorescence Does Not Track Photosynthetic Carbon Assimilation Following Induced Stomatal Closure. *Geophysical Research Letters*, *47*(15). doi: 10.1029/2020GL087956
60. Martini, D., Sakowska, K., Wohlfahrt, G., Pacheco-Labrador, J., van der Tol, C., Porcar-Castell, A., Magney, T. S., Carrara, A., Colombo, R., El-Madany, T. S., Gonzalez-Cascon, R., Martín, M. P., Julitta, T., Moreno, G., Rascher, U., Reichstein, M., Rossini, M., & Migliavacca, M. (2022). Heatwave breaks down the linearity between sun-induced fluorescence and gross primary production. *New Phytologist*, *233*(6), 2415–2428. doi: 10.1111/nph.17920
61. McPartland, M. Y., Falkowski, M. J., Reinhardt, J. R., Kane, E. S., Kolka, R., Turetsky, M. R., Douglas, T. A., Anderson, J., Edwards, J. D., Palik, B., & Montgomery, R. A. (2019). Characterizing boreal peatland plant composition and species diversity with hyperspectral remote sensing. *Remote Sensing*, *11*(14). doi: 10.3390/rs11141685
62. Migliavacca, M., Perez-Priego, O., Rossini, M., El-Madany, T. S., Moreno, G., van der Tol, C., Rascher, U., Berninger, A., Bessenbacher, V., Burkart, A., Carrara, A., Fava, F., Guan, J. H., Hammer, T. W., Henkel, K., Juarez-Alcalde, E., Julitta, T., Kolle, O., Martín, M. P., … Reichstein, M. (2017). Plant functional traits and canopy structure control the relationship between photosynthetic CO2 uptake and far-red sun-induced fluorescence in a Mediterranean grassland under different nutrient availability. *New Phytologist*, *214*(3), 1078–1091. doi: 10.1111/nph.14437
63. Milecka, K., Kowalewski, G., Fiałkiewicz-Kozieł, B., Gałka, M., Lamentowicz, M., Chojnicki, B. H., Goslar, T., & Barabach, J. (2017). Hydrological changes in the Rzecin peatland (Puszcza Notecka, Poland) induced by anthropogenic factors: Implications for mire development and carbon sequestration. *Holocene, 27*(5), 651–664. doi: 10.1177/0959683616670468
64. Mohammed, G. H., Colombo, R., Middleton, E. M., Rascher, U., van der Tol, C., Nedbal, L., Goulas, Y., Pérez-Priego, O., Damm, A., Meroni, M., Joiner, J., Cogliati, S., Verhoef, W., Malenovský, Z., Gastellu-Etchegorry, J. P., Miller, J. R., Guanter, L., Moreno, J., Moya, I., … Zarco-Tejada, P. J. (2019). Remote sensing of solar-induced chlorophyll fluorescence (SIF) in vegetation: 50 years of progress. *Remote Sensing of Environment*, *231*(April), 111177. doi: 10.1016/j.rse.2019.04.030
65. NOAA. (2024). National Centers for Environmental Information, Monthly Global Climate Report for May 2024. *Retrieved on September 1, 2024 from Https://Www.Ncei.Noaa.Gov/Access/Monitoring/Monthly-Report/Global/202405., published online June 2024*.

66. Pacheco-Cancino, P. A., Carrillo-López, R. F., Sepulveda-Jauregui, A., & Somos-Valenzuela, M. A. (2024). Sphagnum mosses, the impact of disturbances and anthropogenic management actions on their ecological role in CO2 fluxes generated in peatland ecosystems. *Global Change Biology*, *30*(1). doi: 10.1111/gcb.16972
67. Pierrat, Z., Magney, T., Parazoo, N. C., Grossmann, K., Bowling, D. R., Seibt, U., Johnson, B., Helgason, W., Barr, A., Bortnik, J., Norton, A., Maguire, A., Frankenberg, C., & Stutz, J. (2022). Diurnal and Seasonal Dynamics of Solar-Induced Chlorophyll Fluorescence, Vegetation Indices, and Gross Primary Productivity in the Boreal Forest. *Journal of Geophysical Research: Biogeosciences*, *127*(2). doi: 10.1029/2021JG006588
68. Porcar-Castell, A., Malenovský, Z., Magney, T., Van Wittenberghe, S., Fernández-Marín, B., Maignan, F., Zhang, Y., Maseyk, K., Atherton, J., Albert, L. P., Robson, T. M., Zhao, F., Garcia-Plazaola, J. I., Ensminger, I., Rajewicz, P. A., Grebe, S., Tikkanen, M., Kellner, J. R., Ihalainen, J. A., … Logan, B. (2021). Chlorophyll a fluorescence illuminates a path connecting plant molecular biology to Earth-system science. *Nature Plants*, *7*(8), 998–1009. doi: 10.1038/s41477-021-00980-4
69. Rascher, U., Acebron, K., Bendig, J., Krämer, J., Krieger, V., Quiros-Vargas, J., Siegmann, B., & Muller, O. (2021). Measuring and Understanding the Dynamics of Solar-Induced Fluorescence (Sif) and Its Relation To Photochemical and Non-Photochemical Energy Dissipation – Scaling Leaf Level Regulation To Canopy and Ecosystem Remote Sensing. *International Geoscience and Remote Sensing Symposium (IGARSS)*, 203–206. doi: 10.1109/IGARSS47720.2021.9554870
70. Rastogi, A., Antala, M., Prikaziuk, E., Yang, P., van der Tol, C., & Juszczak, R. (2022). Exploring the Potential of SCOPE Model for Detection of Leaf Area Index and Sun-Induced Fluorescence of Peatland Canopy. *Remote Sensing*, *14*(16), 4010. doi: 10.3390/rs14164010
71. Ripple, W. J., Wolf, C., Lenton, T. M., Gregg, J. W., Natali, S. M., Duffy, P. B., Rockström, J., & Schellnhuber, H. J. (2023). Many risky feedback loops amplify the need for climate action. In One Earth (Vol. 6, Issue 2, pp. 86–91). Cell Press. doi: 10.1016/j.oneear.2023.01.004
72. Robinson, C. H., Ritson, J. P., Alderson, D. M., Malik, A. A., Griffiths, R. I., Heinemeyer, A., Gallego-Sala, A. V., Quillet, A., Robroek, B. J. M., Evans, C., Chandler, D. M., Elliott, D. R., Shutttleworth, E. L., Lilleskov, E. A., Kitson, E., Cox, F., Worrall, F., Clay, G. D., Crosher, I., … Evans, M. G. (2023). Aspects of microbial communities in peatland carbon cycling under changing climate and land use pressures. *Mires and Peat*, *29*. doi: 10.19189/MaP.2022.OMB.StA.2404
73. Rouse, J. W., Haas, R. H., Schell, J. A., & Deering, D. W. (1974). Monitoring vegetation systems in the great plains with ERTS. S. C. Freden, E. P. Mercanti, & M. Becker (Eds.), Third Earth Resources Technology Satellite–1 Symposium. Volume I: Technical Presentations (pp. 309–317). Washington D.C.: NASA. doi: 10.1021/jf60203a024
74. Sakowska, K., Alberti, G., Genesio, L., Peressotti, A., Delle Vedove, G., Gianelle, D., Colombo, R., Rodeghiero, M., Panigada, C., Juszczak, R., Celesti, M., Rossini, M., Haworth, M., Campbell, B. W., Mevy, J. P., Vescovo, L., Cendrero-Mateo, M. P., Rascher, U., & Miglietta, F. (2018). Leaf and canopy photosynthesis of a chlorophyll deficient soybean mutant. *Plant Cell and Environment*, *41*(6), 1427–1437. doi: 10.1111/pce.13180

75. Strasser, R. J., Srivastava, A., & Tsimilli-Michael, M. (2000). The fluorescence transient as a tool to characterize and screen photosynthetic samples. In M. Yunus, U. Pathre, & P. Mohanty (Eds.), Probing Photosynthesis: Mechanism, Regulation and Adaptation (pp. 445–483). CRC Press.
76. Sun, Y., Gu, L., Wen, J., van der Tol, C., Porcar-Castell, A., Joiner, J., Chang, C. Y., Magney, T., Wang, L., Hu, L., Rascher, U., Zarco-Tejada, P., Barrett, C. B., Lai, J., Han, J., & Luo, Z. (2023). From remotely sensed solar-induced chlorophyll fluorescence to ecosystem structure, function, and service: Part I—Harnessing theory. *Global Change Biology*, *29*(11), 2926–2952. doi: 10.1111/gcb.16634
77. Sun, Y., Wen, J., Gu, L., Joiner, J., Chang, C. Y., van der Tol, C., Porcar-Castell, A., Magney, T., Wang, L., Hu, L., Rascher, U., Zarco-Tejada, P., Barrett, C. B., Lai, J., Han, J., & Luo, Z. (2023). From remotely-sensed solar-induced chlorophyll fluorescence to ecosystem structure, function, and service: Part II—Harnessing data. In Global Change Biology (Vol. 29, Issue 11, pp. 2893–2925). John Wiley and Sons Inc. doi: 10.1111/gcb.16646
78. Tripati, A. K., Roberts, C. D., & Eagle, R. A. (2009). Coupling of CO2 and Ice sheet stability over major climate transitions of the last 20 million years. *Science*, *326*(5958), 1394–1397. doi: 10.1126/science.1178296
79. van Breemen, N. (1995). How Sphagnum bogs down other plants. *Trends in Ecology & Evolution*, *10*(7), 270–275. doi: 10.1016/0169-5347(95)90007-1
80. Van Der Tol, C., Berry, J. A., Campbell, P. K. E., & Rascher, U. (2014). Models of fluorescence and photosynthesis for interpreting measurements of solar-induced chlorophyll fluorescence. *Journal of Geophysical Research: Biogeosciences*, *119*(12), 2312–2327. doi: 10.1002/2014JG002713
81. Verrelst, J., Rivera, J. P., Gitelson, A., Delegido, J., Moreno, J., & Camps-Valls, G. (2016). Spectral band selection for vegetation properties retrieval using Gaussian processes regression. *International Journal of Applied Earth Observation and Geoinformation*, *52*, 554–567. doi: 10.1016/j.jag.2016.07.016
82. Waddington, J. M., Morris, P. J., Kettridge, N., Granath, G., Thompson, D. K., & Moore, P. A. (2015). Hydrological feedbacks in northern peatlands. *Ecohydrology*, *8*(1), 113–127. doi: 10.1002/eco.1493
83. Wiedermann, M. M., Kane, E. S., Potvin, L. R., & Lilleskov, E. A. (2017). Interactive plant functional group and water table effects on decomposition and extracellular enzyme activity in Sphagnum peatlands. *Soil Biology and Biochemistry*, *108*, 1–8. doi: 10.1016/j.soilbio.2017.01.008
84. Wieneke, S., Burkart, A., Cendrero-Mateo, M. P., Julitta, T., Rossini, M., Schickling, A., Schmidt, M., & Rascher, U. (2018). Linking photosynthesis and sun-induced fluorescence at sub-daily to seasonal scales. *Remote Sensing of Environment*, *219*(October), 247–258. doi: 10.1016/j.rse.2018.10.019
85. Xu, J., Morris, P. J., Liu, J., & Holden, J. (2018). PEATMAP: Refining estimates of global peatland distribution based on a meta-analysis. *Catena*, *160*(January), 134–140. doi: 10.1016/j.catena.2017.09.010
86. Xu, S., Atherton, J., Riikonen, A., Zhang, C., Oivukkamäki, J., MacArthur, A., Honkavaara, E., Hakala, T., Koivumäki, N., Liu, Z., & Porcar-Castell, A. (2021). Structural and photosynthetic dynamics mediate the response of SIF to water stress in a potato crop. *Remote Sensing of Environment*, *263*(November 2020). doi: 10.1016/j.rse.2021.112555
87. Yang, X., Tang, J., Mustard, J. F., Lee, J. E., Rossini, M., Joiner, J., Munger, J. W., Kornfeld, A., & Richardson, A. D. (2015). Solar-induced chlorophyll fluorescence that correlates with canopy

photosynthesis on diurnal and seasonal scales in a temperate deciduous forest. *Geophysical Research Letters*, *42*(8), 2977–2987. doi: 10.1002/2015GL063201

88. Zeng, Y., Hao, D., Huete, A., Dechant, B., Berry, J., Chen, J. M., Joiner, J., Frankenberg, C., Bond-Lamberty, B., Ryu, Y., Xiao, J., Asrar, G. R., & Chen, M. (2022). Optical vegetation indices for monitoring terrestrial ecosystems globally. *Nature Reviews Earth and Environment*, *3*(7), 477–493. doi: 10.1038/s43017-022-00298-5

Attachments of published articles

Impact of climate change-induced alterations in peatland vegetation phenology and composition on carbon balance

Publication No. 1

Antala, M., Juszczak, R., van der Tol, Ch., Rastogi, A. (2022). Impact of climate change-induced alterations in peatland vegetation phenology and composition on carbon balance. *Science of the Total Environment*. 827, 154294. https://doi.org/10.1016/j.scitotenv.2022.154294

Science of the Total Environment 827 (2022) 154294

Contents lists available at ScienceDirect

Science of the Total Environment

journal homepage: www.elsevier.com/locate/scitotenv

Review

Impact of climate change-induced alterations in peatland vegetation phenology and composition on carbon balance

Michal Antala [a], Radoslaw Juszczak [a], Christiaan van der Tol [b], Anshu Rastogi [a,b,]*

[a] Laboratory of Bioclimatology, Department of Ecology and Environmental Protection, Faculty of Environmental Engineering and Mechanical Engineering, Poznan University of Life Sciences, Piątkowska 94, 60-649 Poznań, Poland
[b] Faculty of Geo-Information Science and Earth Observation (ITC), University of Twente, 7500 AE Enschede, the Netherlands

HIGHLIGHTS

- Climate change induces changes in peatland vegetation phenology and composition.
- Shrubs produce more flowers and phenophases of vascular plants start sooner.
- Peat mosses are becoming less abundant and vascular plants cover is increasing.
- Changing peatland vegetation modifies the carbon balance.

GRAPHICAL ABSTRACT

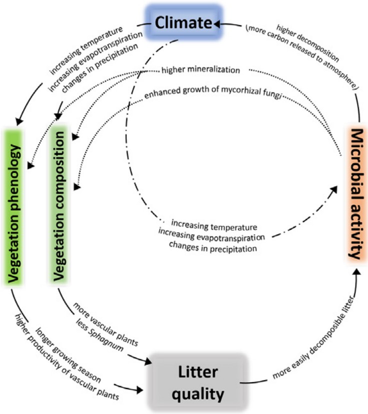

ARTICLE INFO

Article history:
Received 1 November 2021
Received in revised form 3 February 2022
Accepted 28 February 2022
Available online 2 March 2022

Editor: Jan Vymazal

Keywords:
Peatland
Climate change
Plant phenology
Vegetation composition
Carbon balance

ABSTRACT

Global climate is changing faster than humankind has ever experienced. Model-based predictions of future climate are becoming more complex and precise, but they still lack crucial information about the reaction of some important ecosystems, such as peatlands. Peatlands belong to one of the largest carbon stores on the Earth. They are mostly distributed in high latitudes, where the temperature rises faster than in the other parts of the planet. Warmer climate and changes in precipitation patterns cause changes in the composition and phenology of peatland vegetation. Peat mosses are becoming less abundant, vascular plants cover is increasing, and the vegetation season and phenophases of vascular plants start sooner. The alterations in vegetation cause changes in the carbon assimilation and release of greenhouse gases. Therefore, this article reviews the impact of climate change-induced alterations in peatland vegetation phenology and composition on future climate and the uncertainties that need to be addressed for more accurate climate prediction.

---

* Corresponding author at: Faculty of Geo-Information Science and Earth Observation (ITC), University of Twente, 7500 AE Enschede, the Netherlands.
E-mail address: a.rastogi-1@utwente.nl (A. Rastogi).

http://dx.doi.org/10.1016/j.scitotenv.2022.154294

Contents

1. Introduction . . . 2
2. Changes in peatland vegetation phenology . . . 3
   2.1. Use of remote sensing in peatland vegetation phenology detection . . . 4
3. Changes in peatland vegetation composition . . . 5
   3.1. Common techniques used for peatland climate manipulation . . . 6
4. Impact of changes in peatland vegetation on carbon balance . . . 7
   4.1. Carbon fixation . . . 8
   4.2. Respiration . . . 9
   4.3. Methane release . . . 9
5. Conclusions and future perspectives . . . 10

CRediT authorship contribution statement . . . 11
Declaration of competing interest . . . 11
Acknowledgment . . . 11
References . . . 11

1. Introduction

The latest report of the Intergovernmental Panel on Climate Change (IPCC) reported that the climate is changing faster than expected (IPCC, 2021). Every decade is warmer than the previous one, and temperature over land has already increased by 1.5 °C compared to the preindustrial era. The changes in global climate are undoubtedly caused by anthropogenic activities and impact a plethora of processes on Earth. The temperature will certainly continue to increase in the next decades, and extreme weather events, such as hot and drought waves and extreme precipitation events, will become more frequent (IPCC, 2021). The impact of climate change at high latitudes and altitudes is projected to be more pronounced than in other regions of the globe (Hoegh-Guldberg et al., 2018; IPCC, 2021). These regions are typical for boreal forests, tundra, and peatlands, all of which are undergoing and will experience dramatic changes due to global warming (Bjorkman et al., 2018; Boulanger et al., 2017; Dise, 2009).

Northern peatlands belong to the most important ecosystems of the Earth. Despite the fact that peatlands cover only around 3% of the terrestrial surface or 1% of the total Earth surface, they are the ecosystem with one of the highest concentrations of stored carbon. It is estimated that about 30% of all carbon stored in the world's soils is stored in peatlands (Gorham, 1991). The high carbon accumulation potential of peatlands is due to very specific conditions, namely low pH, low nutrient and oxygen availability created by waterlogged conditions, and specific vegetation of the peatlands (van Breemen, 1995). Due to their high water holding capacity, specific morphology and physiology, and chemical composition, *Sphagnum* spp. are able to modify the environment in their favor and create adverse conditions for most of the vascular plants; thus, the *Sphagnum* spp. are considered as ecosystem engineers (Malmer et al., 2003; Rochefort, 2000; van Breemen, 1995). Only very specific vascular plants are able to co-inhabit the peatlands along with mosses (Chapin et al., 1996; Turetsky et al., 2012). The peatland's functions and peat accumulation rate depend on the physiological status and photosynthetic activity of plants and on proportions of plant functional groups in the vegetation cover (Kuiper et al., 2014; Mao et al., 2018).

Generally, plants growing in the peatlands can be divided into five plant functional groups: a) mosses, b) graminoids – grasses (Poaceae), sedges (Cyperaceae) and rushes (Juncaceae), c) forbs – annual broadleaf herbs and pteridophytes, d) shrubs – subdivided to evergreen and deciduous, and e) trees (Moore et al., 2002; Rupp et al., 2019; Walker et al., 2015). Denser cover of the taller shrubs and trees in peatlands are normally prevented by high water saturation and low nutrient availability, and if it occurs, it is a sign of climate change (Holmgren et al., 2015). Most of the peatlands are covered by mosses, graminoids, and creeping or low shrubs (Wiedermann et al., 2017).

Mosses and especially *Sphagnum* spp. play a crucial role in peatlands' carbon accumulation (Buttler et al., 2015). They belong to evolutionary primitive plants without roots, conducting tissues, or cuticula protecting their surface from water loss (Chiapusio et al., 2021). Peat mosses acquire nutrients through the whole surface, mostly from atmospheric deposition, and water supply to the physiologically active part is provided by precipitation and capillary action (Hájek and Beckett, 2008; Hyyryläinen et al., 2018; Weston et al., 2015). Unlike the majority of vascular plants, *Sphagnum* spp. growth continues as long as the mosses are not frozen (Malmer et al., 2003).

Graminoids growing in waterlogged conditions of peatlands must have a root system adapted to low oxygen conditions. Their roots contain aerenchyma, the sponge-like tissue with air channels, which allows proper aeration of root tissues, but also gas exchange between the atmosphere and peat (Noyce et al., 2014; Visser et al., 2000). The foliage of graminoids dies in the autumn and typically stays in the canopy for at least one year (Chapin et al., 1996). Plants mostly overwinter as rhizomes, and new leaves appear in spring when the temperature is suitable (Bernard and Hankinson, 1979; Wein, 1973).

Peatland shrubs had to evolve different strategies to cope with the continuous growth of mosses, which would otherwise overgrow and deprive them of light. Their shoots need to either constantly grow, or new shoots must develop from buds of subterranean runners. Roots of shrubs are mostly shallow, and adventitious roots are formed once the shoot gets overgrown by mosses (Buttler et al., 2015; Malmer et al., 1994). Mycorrhizal fungi help shrubs with shallow roots with nutrient acquisition and also water supply (Cullings, 1996). Leaf of many evergreen shrubs found in peatlands have traits connected with lowering water losses, such as a thick layer of waxes, stomata only on the abaxial side, or revolute margins (Buttler et al., 2015). Deciduous shrubs usually have thinner leaves and a shorter photosynthetically activity season because, unlike evergreen shrubs, they first need to develop leaves at the beginning of the vegetation season (Chapin et al., 1996).

Many different plant communities may exist in the same peatland (Bandopadhyay et al., 2021), but based on the hydrology, nutrient availability, pH, calcium content, and vegetation composition, peatlands are divided into two major groups: bogs and fens (Hájek et al., 2006). Bogs are the type of peatlands where the surface is due to accumulated peat so high above the groundwater level that it does not receive any minerogenic water. The water regime of bogs and the plant water supply depends on atmospheric precipitation, evapotranspiration, and water holding capacity (Aaby, 1976; Mauquoy et al., 2002b). The vegetation of bogs is dominated by *Sphagnum* spp. and shrubs with the lower cover of graminoids, forbs, and trees (Hájek et al., 2006). On the other hand, fens are fed with water and nutrients from ground or surface water, along with precipitation. This causes higher basic cations content and higher pH. Fens are generally dominated by *Sphagnum* spp. and gramminoids with the considerable cover of forbs and lower abundance of shrubs and trees (Hájek et al., 2006; Weltzin et al., 2003).

The majority of today's peatlands started to form between 8 and 6 thousand years ago, and there are hardly peatlands older than twenty thousand years (Gorham et al., 2007). The current rate of climate change is fastest than in the last twenty million years, implicating that the ongoing climate change is faster than existing peatlands have ever experienced (Tripati et al., 2009). The information regarding the peatland is still limited; thus, the peatlands are still not fully included in climate models, which brings uncertainties to predictions about future climate (IPCC, 2021). Therefore, the objectives of this review are to (1) summarize the existing knowledge about the impact of climate change on peatland vegetation phenology and composition, (2) improve the understanding of impact of these changes on carbon balance and 3) provide a future direction to peatland research for the purpose to understand the basic mechanism of peatland vegetation interaction with climate.

2. Changes in peatland vegetation phenology

Changes in plant phenology are one of the consequences of climate change; therefore, a shift in plant phenology may be considered an indicator of the changing climate and the adaptation of species to new environmental conditions (Parmesan and Yohe, 2003; Visser and Both, 2005). The intensity of change in plant life cycle varies for different species, but the general trend is an earlier onset of phenophases observed in the warmer and still warming world (Menzel et al., 2006; Peñuelas and Filella, 2001). This is caused by the fact that temperature is one of the most important factors controlling the plant's developmental process (Hatfield and Prueger, 2015). However, the warming at high latitudes is not connected just with the positive effect of higher temperatures on plant development. The higher occurrence of extremely warm periods during winter causes snow to thaw and exposes the plants' flower buds to freezing temperatures during the night or subsequent low-temperature period, which causes the delay and reduction of fruit production (Bokhorst et al., 2008; Callaghan et al., 2004). Bryophytes exposed to freezing temperatures without snow cover suffer from stress which then negatively impacts the beginning of the vegetation season (Küttim et al., 2019). In some regions, climate warming causes less frost days in a year, but increases their number during the growing season. That increases the days in a season plants are exposed to freezing temperature (Liu et al., 2018). Despite the effect of changing climate on plants is not only straightforward, it is clear that changes in plant phenology caused due to environmental factors will have a wide range of consequences for the ecosystem, agriculture, forestry, world economy, and human health (Peñuelas et al., 2002). Therefore, there is a need for close examination of the impact of global warming on the ecosystems to predict at least the reaction of dominant species and either prepare for the changes or take measures to avoid the changes, which may be destructive to the whole ecosystem.

Several experiments studying the phenological response of peatland vegetation to different climate change scenarios have been performed (Table 1). Flowering is one of the most important stages in a plant's life as the next generation of the species depends on it. Therefore, plants evolved various mechanisms to control the time of flowering and the number of flowers produced (Gaudinier and Blackman, 2020). Ambient temperature is one of the most important factors regulating flowering (Cho et al., 2017). A study on peatland shrubs *Andromeda polifolia* and *Rubus chamaemorus* has revealed that increased temperature in various seasons impacts the flowering to a different extent. While warmer summer or winter do not alter the number of produced flowers, the total number of flowers increases when spring temperature was significantly higher than average (Aerts et al., 2004). Based on current predictions of changes in climate, the flower production of these shrubs will very likely increase in the next decades (IPCC, 2021). However, an increased number of flowers accompanied by higher production of fruits does not necessarily mean a better chance for generative reproduction, especially in the case of *Rubus chamaemorus*, which is also known as cloudberry. The fruits are harvested

Table 1
Changes in the phenology of peatland inhabiting plants caused by climate change.

Climate factor (change)	Time period	The method used for manipulation	Observation related to phenology		References
			Parameter	Change	
Temperature (increase)	Spring of two years	Open-top chambers	Total flower production of *Andromeda polifolia*	+	(Aerts et al., 2004)
			Total flower production of *Rubus chamaemorus*	+	
			Median flowering date of *Andromeda polifolia*	−	
			Median flowering date of *Rubus chamaemorus*	−	
Temperature (increase)	Summer of two years	Open-top chambers	Total flower production of *Andromeda polifolia*	0	(Aerts et al., 2004)
			Total flower production of *Rubus chamaemorus*	0	
			Median flowering date of *Andromeda polifolia*	−	
			Median flowering date of *Rubus chamaemorus*	0	
Temperature (increase)	Winter of two years	Snow addition	Total flower production of *Andromeda polifolia*	0	(Aerts et al., 2004)
			Total flower production of *Rubus chamaemorus*	0	
			Median flowering date of *Andromeda polifolia*	−	
			Median flowering date of *Rubus chamaemorus*	−	
Temperature (increase)	Fourth and fifth seasons after the beginning of the manipulation	Open-top chambers	Timing of total maximum leaf area of forbs in the southern fen (62°N)	−	(Mäkiranta et al., 2018)
			Timing of total maximum leaf area of forbs in the northern fen (68°N)	+	
			Timing of total maximum leaf area of shrubs and sedges in the southern (62°N) and northern (68°N) fens	0	
			The length of growing period of forbs in the southern fen (62°N)	+	
			The length of growing period of forbs in the northern fen (68°N) and shrubs and sedges in the southern (62°N) and northern (68°N) fens	0	
Temperature (increase)	Second season after the beginning of the manipulation	Open-top chambers	Length of female and male spikes of *Carex bigelowii*	+	(Stenström and Jónsdóttir, 1997)
			Flowering time of *Carex bigelowii*	0	
			Prefloration period of *Carex bigelowii*	−	
	Second to the fifth season after the beginning of the manipulation		Beginning and end of stigma receptivity to the pollen of *Carex bigelowii*	−	(Stenström and Jónsdóttir, 1997, 2004)
			Beginning and end of pollen release of *Carex bigelowii*	−	
			Gender phase overlap of *Carex bigelowii*	+	
Temperature (increase)	Three seasons	Open-top chambers	Time of maximal leaf biomass occurrence of *Eriophorum vaginatum*	−	(Sullivan and Welker, 2005)
	Second season		Beginning of root growth of *Eriophorum vaginatum*	−	
Water table level (decrease)	Fourth and fifth seasons after the beginning of the manipulation	A ditch dug around the plot	Timing of total maximum leaf area of forbs, shrubs, and sedges in the southern (62°N) and northern (68°N) fens	0	(Mäkiranta et al., 2018)
			The length of growing period of sedges in the southern (62°N) and northern (68°N) fens	+	
			The length of growing period of forbs and shrubs in the southern (62°N) and northern (68°N) fens	0	

Change: no change 0, decrease (sooner) −, increase (later) +.

by people and eaten by birds. Therefore, people and animals may benefit from higher fruit production more than the plant itself, which shows how complex the relationships in nature are (Leišová-Svobodová et al., 2018). The impact of climatic conditions on flowering is also very intricate as many species create the flower buds in the previous year, and the environmental conditions of the present year influence flowering in the following year more than the flowering of the observed year (Lyngstad et al., 2017).

Not only the number of flowers is an important variable, but also the time of flowering, which is generally more dependent on the ambient temperature (Cho et al., 2017). *Andromeda polifolia* and *Rubus chamaemorus* bloom sooner when winter and spring are warmer. Higher summer temperature promotes the beginning of *Andromeda polifolia* flowering (Aerts et al., 2004). Unlike shrubs, the emergence of sedge *Carex bigelowii* flowers is not changed by increased temperature. However, once the flowers appear, pollen release and stigma receptivity start faster in warmer conditions (Stenström and Jónsdóttir, 1997, 2004). Earlier stigma receptivity and pollen release result in earlier pollination and grain establishment, which positively affect the grain weight and possibly viability of grains. Hence, the warmer conditions may increase the chance of healthy progeny establishment and spread of the species (Stenström, 1999). Despite *Carex bigelowii* being, to some extent, self-pollinated, cross-pollination is the dominant pollination strategy of species. Therefore, the prolonged gender phase overlap resulting from increased temperature will not have any significant impact on grain viability (Stenström et al., 2001; Stenström and Jónsdóttir, 2004). Although the flowering is an essential phenophase for generative reproduction, studies of flowering responses of peatland plants are just one piece in the reproduction response puzzle, as all of the studied species are known for strong vegetative reproduction (Filippova and Thormann, 2015; Leišová-Svobodová et al., 2018; Stenström, 1999).

The formation of generative organs like flowers and fruits with seeds is a nutrient-demanding process, which must be preceded by long enough period of above and belowground vegetative organs growth and development (Sletvold and Ågren, 2015). Sedges occurring in peatlands like *Eriophorum vaginatum* are perennial plants, which overwinter in the form of rhizomes and start to form roots and leaves once the conditions are favorable (Wein, 1973). Leaves of *Eriophorum vaginatum* start to grow earlier, and the maximal leaf biomass is developed sooner when the ambient temperature is higher. The root growth also begins earlier in warmer conditions (Sullivan and Welker, 2005). Earlier establishment on site, root development, and shading of the ground by maximally developed leaf mass may give the plant a competitive advantage in such nutrient-poor environments like peatland (Damgaard and Weiner, 2017).

The growing season of plants in high latitudes is usually prolonged by warming more than those in mid and low latitudes (Ruosteenoja et al., 2016). However, a multifactorial study conducted in two peatlands in different latitudes found that only forbs in mid-latitude fen took advantage of warmer air and the growing period of sedges or shrubs in mid-latitudes and none of the plant functional groups in the fen above the arctic circle were influenced by higher temperature (Mäkiranta et al., 2018). The mean daily temperature is not the only factor influencing the length of the growing season. The length of the day is a very important factor sensed by buds, which is not changing with climate change. Therefore, annual plants are more likely to take advantage of earlier onset of higher temperature if their seeds are not photoblastic (Galvão and Fankhauser, 2015). The variations among the responses of plants in different latitudes may be ascribed to the different degrees of seed dormancy, which may not always be broken by the right temperature (Penfield, 2017). Plants in the harsher environment of the arctic region had to evolve better protection from germinating in suboptimal conditions, which would mean loss of progeny (Jurado and Flores, 2005).

Changes in precipitation patterns and higher evapotranspiration are expected results of climate change, which may cause a lowering of the water table in peatlands. The growing period of sedges was prolonged regardless of latitude in the study of Mäkiranta et al. (2018) when water table level was deeper, but shrubs and forbs were not affected by the drop in water table. Leaf biomass development of peatland plants is typically fast, and it declines more gradually until the end of vegetation season. Therefore, earlier reaching of maximum leaf area implies a longer period of photosynthetic activity and accumulation of carbohydrates (Wilson et al., 2007). Timing of maximum leaf area occurrence was not observed to change by higher temperature, but the maximal leaf area developed sooner in the mid-latitude fen, while later in an arctic fen in response to warmer ambient air (Mäkiranta et al., 2018).

The studies of peatland vegetation phenological responses are performed for a rather short period of time. Such studies may not provide the full insight into changes coming with climate change, as short-term and long-term phenological responses of plants in the boreal region may differ. Although drawing general conclusions based on one site experiment is almost impossible, as plants of different latitudes may utilize diverse strategies in reaction to altered environmental conditions (Arft et al., 1999), conducted studies provide a clue about the direction of changes, which can be expected in the warmer future world. However, when making predictions about the plants' developments in the future, it is necessary to remember that the magnitude of actual changes in phenological events may be greater than the changes observed in the climate change experiments (Wolkovich et al., 2012).

2.1. Use of remote sensing in peatland vegetation phenology detection

Studying plant phenology by classical, personal observation-based approach in the remote areas with almost impenetrable terrain of peatlands is a very complicated task. Digital repeat photography overcomes the need for the daily personal presence of the researcher on-site and provides information about the greening, peak of the green biomass occurrence, and senescence of vegetation. If the camera's field of view is synchronized with the eddy covariance flux tower, information about the biomass can be linked with vegetation photosynthetic activity (Koebsch et al., 2020; Peichl et al., 2015). However, due to involvement of several environmental factors, the obtained data with controlled climate change scenarios is insufficient to provide clear idea of phenological changes under changing climate. Therefore, information about the timing of main phenological events in different temperatures must be obtained by comparing different years. This approach was used to reveal that the growing period of mosses and vascular plants in mid-latitude peatland starts sooner when the spring temperature is higher (Peichl et al., 2015).

Some areas of peatland occurrence are so remote that the only way of monitoring is remote sensing through satellites. Vegetation indices such as Normalized Difference Vegetation Index (NDVI) are a useful tool to obtain information about the beginning or the peak of a vegetation season. They may be used not only for satellite remote sensing but also for ground measurements in climate change experiments (May et al., 2020). Despite the wide availability of satellite products for NDVI calculation with fair spatial and temporal resolution (Cao et al., 2018), one must be careful when monitoring peatland vegetation. Changes in NDVI are well-correlated with the phenology of vascular plants but poorly correlated with mosses (Buttler et al., 2015). Therefore, vegetation composition must be taken into account while interpreting signals to prevent the overestimation of carbon fixation by peatlands (Yuan et al., 2014). Areas covered by *Sphagnum* spp. and vascular plants can be distinguished using satellite remote sensing products of green, near-infra-red, and short-wave infra-red regions (Schaepman-strub et al., 2008).

The boreal region, where most northern peatlands occur, is covered by snow for a considerably long period of the year. Monitoring of plant phenology, especially phenology of evergreen species, by NDVI might be less reliable due to differences in values at the beginning of vegetation season caused rather by snow-melt than by green-up of plants. Plant phenology index (PPI) was developed and tested for tracking the phenology of boreal region vegetation and was observed to perform better than NDVI (Jin and Eklundh, 2014; Karkauskaite et al., 2017). Therefore, PPI may be a good option for remote sensing of peatland vegetation phenology.

Backscattering of different waves is a general phenomenon used by meteorologist and environmental scientist to predict the status of Earth vegetation. Different measurements including the satellite remote sensing techniques are used to compare the vegetation status between years and prediction of future change based on past variations in climate and the reactions of plants to them (Jones et al., 2011). Passive microwave remote sensing can be more precisely applied to predict the phenological cycles of short vegetation like the one in peatlands (Jones et al., 2011). Peatland is also inhabited by evergreen shrubs and mosses, which at the beginning and end of vegetation season may be difficult to assess by reflectance-based vegetation indices only. Sun-induced chlorophyll fluorescence (SIF) is a remote sensing technique utilizing the properties of the photosynthetic apparatus of plants. SIF was proven to be useful for peatland plant communities distinguishing, but thanks to its direct link to photosynthesis and possibility to use from ground through drone and airplane to satellite level, it has high potential to be used for phenological studies in peatlands (Bandopadhyay et al., 2019, 2020).

3. Changes in peatland vegetation composition

The prevailing climatic conditions are the main driver of the vegetation composition of ecosystems (Sonesson et al., 2002). Vegetation composition is a major characteristic of any ecosystem, and functions of the ecosystem are linked to it (Carrick and Forsythe, 2020). The ecosystem can support the important functions only as long as it possesses sufficient species richness and diversity of functional traits (Robroek et al., 2017b). Biodiversity is a key to the resistance and resilience of ecosystems and to fulfilling ecosystem services in altered climatic conditions (Cardinale et al., 2012; Isbell et al., 2015). Land-use and climate change are the most important drivers of changes in vegetation composition and biodiversity (Sala et al., 2000). If species fail to acclimate or adapt to altered climatic conditions, they need to either move to more favorable conditions to survive. Plants as sessile organisms relocating by reproductive organs may fail to keep pace with the speed of environmental changes. Moreover, the fragmented nature of mid-latitude peatlands and the fact that boreal peatlands span to the edge of the terrestrial surface makes it impossible for plants of these ecosystems to relocate to a more suitable place once the climate changes in their actual location. Therefore, they are left only with two options: adjust to new conditions or go extinct (Corlett, 2016; Xu et al., 2018). Losing one species generally does not pose a threat to the ecosystem, but losing a plant functional group may mean the total change of ecosystem type (Hooper et al., 2012). The species with distinct traits are more valuable to the ecosystem than species possessing the traits common to several species (Robroek et al., 2017b). Peatlands are globally the most homogenous natural ecosystems with very similar vegetation composition among various wetlands in different parts of the globe (Carrick and Forsythe, 2020). Northern peatlands consist of a relatively small number of species with complex relationships and contrasting responses to climate change (Walker et al., 2015). Because of the strong role of the vegetation itself in sustaining a favorable environment, the substantial changes in vegetation are the result of crossing the tipping points in abiotic parameters, for example the depth of water table level (Lamentowicz et al., 2019). Based on responses of species to climate change the majority of northern peatlands plants can be divided into two groups with strongly correlated responses between species within the group. However, some of the major species, such as *Eriophorum vaginatum* or *Sphagnum magellanicum*, have distinct reactions to climate change non-correlated to other species (Robroek et al., 2017b).

Species of genus *Sphagnum* are recognized as creators of conditions inevitable for peatland formation; hence this genus is essential for peatland formation initiation and to keep the environment with high carbon storage potential (van Breemen, 1995). *Sphagnum* spp. are also the main engineers of distinct hummock-lawn-hollow (patches of the elevated, flat, and lowered surface) topography of peatlands. Different *Sphagnum* spp. inhabit different elevations above the water table (Bragazza, 2006; Yang et al., 2019). The ability of *Sphagnum* spp. to fulfill the abovementioned functions in the future is endangered as the studies report decreasing abundance of different *Sphagnum* spp. with increasing temperature (Bragazza et al., 2016; Dieleman et al., 2015; Łuców et al., 2017; Lyons et al., 2020; Norby et al., 2019; Weltzin et al., 2003) and decreasing water table (Jassey et al., 2018), which are the consequences of climate change (IPCC, 2021). The increasing temperature does not always result in a negative effect on peat mosses. The moderately higher temperature in the arctic region enhances the length growth and biomass production of widespread *S. fuscum* (Dorrepaal et al., 2004). Moreover, the trend in precipitation amount is impossible to generalize. Some regions of the world will experience a higher amount of precipitation (IPCC, 2021). When the water availability increases, the abundance of *Sphagnum* spp. is also higher (Jassey et al., 2018) because their length growth is enhanced (Sonesson et al., 2002).

Peatlands are usually inhabited by more than one *Sphagnum* spp. at each topographical position; therefore, the decreasing abundance of one species may not endanger the ecosystem balance if other species with similar traits colonize the niche (Robroek et al., 2017b). Despite *Sphagnum* spp. are generally considered as desiccation-avoiding species, the water management strategy of hummock and hollow species differs. Due to their growth in compact clusters, the hummock species are able to conduct water from the deeper water table and may take advantage of warmer weather usually connected with dry periods, which occur in the summer months. Therefore, despite their lower overall growth rates, hummock species are especially important during drier months, when the productivity of hollow species is hampered by lower water tables (Asada et al., 2003; Bengtsson et al., 2021). However, the biomass production of *Sphagnum* spp. or *Polytrichum strictum* is normally negatively correlated to the distance from the water table (Weltzin et al., 2001). Although the peatland ecosystem is surprisingly stable and developmentally older peatlands are very resilient (Backéus, 1972; Oke and Hager, 2020; Turetsky et al., 2012), the occurrence of climate extremes like heat waves may lead to irreversible damage and die-off of hummock *Sphagnum* spp., which are not well adapted to drying. This impacts the carbon uptake of peatland as death zones, which cannot be colonized due to unfavorable elevation above water table by hollow or lawn *Sphagnum* spp. appear in carpet and persist for years after heatwave occurrence (Bragazza, 2008).

The dependence of different *Sphagnum* spp. on specific climate, especially water availability, is so pronounced that changes in *Sphagnum* spp. abundance in peat can be used to reconstruct the local or global climate (Jassey et al., 2018). Whenever in history, the conditions in peatlands shifted towards wetter *Sphagnum cuspidatum* became more abundant. On the other hand, *Sphagnum papillosum* and *Sphagnum imbricatum* are associated with dry conditions (Mauquoy et al., 2002a; Van Geel et al., 1996). These findings are in accordance with the modern climate manipulation experiments, which found decreasing abundance of *Sphagnum cuspidatum* and increasing abundance of *Sphagnum papillosum* in drier conditions (Breeuwer et al., 2009; Robroek et al., 2007a).

Not only changes in abiotic conditions present a challenge for *Sphagnum* spp., changes in biotic conditions, especially competition by vascular plants, are at least an equal threat. Although, the relationship between peat mosses and vascular plants is very complex. *Sphagnum* development from diaspores and subsequent growth is increased by vascular plants cover, which provides a more stable microclimate in water deficit conditions (Buttler et al., 1998). Sparse cover of vascular plants decreases the wind speed directly above the *Sphagnum* surface, hence decreasing the evapotranspiration and improving the water use efficiency by mosses (Heijmans et al., 2001). However, denser vascular plant canopy deprives underlying *Sphagnum* spp. of necessary light and causes their death (Bragazza et al., 2015; Chong et al., 2012). *Sphagnum* spp. can, to some extent, control the growth of vascular plants by limiting the nutrient availability, as the atmospheric deposition goes firstly through the moss layer and only then reaches the roots of vascular plants. Nevertheless, increasing temperature enhances mineralization and nutrient availability in the zone of vascular plants roots, out of reach of *Sphagnum* spp. (Dorrepaal et al., 2006; Malmer et al., 1994; van Breemen, 1995). Hence, a higher mineralization rate gives a competitive advantage to vascular plants and makes it difficult for mosses to control the environmental conditions (Malmer et al., 1994, 2003). The growth of shrubs' fine roots is also increased in warmer and drier conditions, enabling shrubs to acquire more available nutrients (Malhotra et al., 2020). In addition, a warmer climate enhances the growth of mycorrhizal fungi, which makes more nutrients available to ericaceous shrubs, giving them another advantage over mosses (Asemaninejad et al., 2018; Bragazza et al., 2013). The increasing temperature has also a direct effect on the *Sphagnum*-vascular plants' relationship. While low, creeping shrubs may be overgrown in warmer conditions by *Sphagnum*, the growth of higher shrubs will be enhanced enough to compete with peat mosses (Dorrepaal et al., 2006).

The vascular plants are not the sole competitors of mosses. One species of *Sphagnum* may suppress the other *Sphagnum* spp. as well. Although the increase in temperature improves the growth of various species, hummock species can outcompete the hollow ones and become more abundant in moss carpets. The *Sphagnum* spp. occurring in the mid-latitude peatlands will in warmer world replace the species occurring in more northern peatlands (Breeuwer et al., 2008; Gunnarsson et al., 2004; Robroek et al., 2009). The studies of Gunnarsson et al. (2004) and Breeuwer et al. (2008) are a good example of the importance of biotic components when evaluating abiotic factors as *S. balticum* competitive strength was found to be enough for outcompeting *S. fuscum* and *S. magellanicum*, but the species was suppressed by *S. papillosum*, in higher temperature conditions. The changes in vegetation composition do not depend on the reaction of one species. Despite *S. magellanicum* was found to grow faster in warmer and slower in drier conditions (Robroek et al., 2007b), outperforming other species in drier and being outperformed in warmer conditions was reported (Breeuwer et al., 2008; Robroek et al., 2007a). *Sphagnum* spp. react to fluctuating water table levels in the same manner as to its constant drop (Breeuwer et al., 2009). Nevertheless, the species growing in higher topographic positions, e.g., lawn and hummock species, generally possess stronger competitive capacity even in high water table level conditions. The competition is stronger when the water table drops, which causes the increased abundance of lawn species in hollows and typical hummock species in low hummocks (Robroek et al., 2007a). Although the competition among species is considerable, the survival of individual plants of the peatland mosses depends on being surrounded by other mosses. Some *Sphagnum* spp. may grow faster when they are surrounded by other than their own moss species, like in the case of *S. fuscum* growing among *Dicranum elongatum* (Sonesson et al., 2002).

Different vegetation composition of bogs and fens causes different reactions to climate change, but the hampered growth of mosses and improved growth of vascular plants in dryer conditions is a common feature. Warming causes higher biomass increment of shrubs and slower growth of sedges in bogs, but in fens, sedges grow better when the temperature is higher (Weltzin et al., 2000). Sedges of genus *Carex* are together with *Eriophorum vaginatum,* the most widespread graminoids in northern peatlands (Bedford et al., 1988; Bernard and Hankinson, 1979; Robroek et al., 2017b). With increasing temperature, *Carex* spp. are becoming more abundant in fens at the expense of *Sphagnum* spp. (Dieleman et al., 2015; Łuców et al., 2017). Other sedges, like *Eriophorum vaginatum* and *Scheuchzeria palustris*, also thrive in warmer fens and increase their range (Weltzin et al., 2003). Sedges in fens are able to take advantage of different changes in water availability. While *Trichophorum cespitosum* thrives in dryer conditions, *Carex lasiocarpa* and *Carex livida* take advantage of a wetter environment (Mäkiranta et al., 2018; Weltzin et al., 2003). Moreover, *Eriophorum vaginatum* does spread to niches previously occupied by shrubs when the water table level increases (Jassey et al., 2018). However, sedges inhabiting bogs cede the space to shrubs when a longer period of drought causes water table level fluctuation (Breeuwer et al., 2009). The reactions of *Carex lasiocarpa* to drought depend on the severity or length of the drought period. If plants of this sedge are subjected to longer drought, their growth is hampered, and vegetative reproduction is reduced. Plants start to focus more on the production of aboveground biomass, leaves get thicker, and physiological changes occur (Yuan et al., 2017). When the precipitation-evapotranspiration relationship changes in prospect to evapotranspiration, causing the drop of the water table for more than a decade, all peatland plants struggle and start to diminish, while the bare litter patches become more abundant (McPartland et al., 2019b).

Forbs are the plant functional group, which is the most prone to diminish from peatlands under changed climatic conditions. Studies report that increasing temperature (McPartland et al., 2019a) and rising as well as falling water table (McPartland et al., 2019b) cause a lower abundance of different forbs. One of the reasons for their disappearance from warmer peatlands is probably the damage on photosynthetic apparatus and subsequent substantially lower photosynthetic activity of forbs than other plant functional groups (Rastogi et al., 2019).

The most morphologically, physiologically, and systematically variable group of peatland vegetation are shrubs. Thanks to their relatively high variability, some species can take advantage of increasing temperature while others are impacted negatively. Species of the *Andromeda* genus may become more abundant in the future warmer world, but *Kalma polifolia* will become rarer (Buttler et al., 2015; Weltzin et al., 2003). The temperature-related changes in abundance of *Vaccinium* spp. depend on the developmental stage of peatland and the current climatic conditions. Warming of mid-latitude bog without tree cover or near-arctic fen results in a higher abundance of *Vaccinium* spp. (Bragazza et al., 2016; Wiedermann et al., 2007). However, decreasing abundance with increasing temperature was found in mid-latitude bog dominated by trees and in mid-latitude fen (Buttler et al., 2015; McPartland et al., 2020). Peatlands inhabiting shrubs, in general, expand in drier conditions (Table 2), which is proven by the negative effect of higher water table level on the abundance of *Vaccinium oxycoccos* (Jassey et al., 2018). The ongoing climate change favors most of the shrubs of peatlands, and they are becoming more abundant (Gunnarsson et al., 2002). Additionally, the denser cover of shrubs, together with warmer and drier conditions, provide suitable conditions for tree seedling establishment. Subsequently, tree cover further increases the density of the shrub canopy. Such positive feedback slowly changes *Sphagnum*-dominated peatland to the forest (Holmgren et al., 2015). Afforestation of peatlands will be triggered rather by increasing temperature than by decreasing precipitation or longer and more often occurring drought events (Heijmans et al., 2013).

The climate change manipulation experiments provide useful information about the most probable changes in peatland vegetation in a future changed climate. However, the experiments are done just over small patches of peatland and observe only the vegetation already existing in the peatland. Global climate change will create in peatland suitable conditions for species that are not yet present. These new plants will probably be the most significant factor shaping future peatlands and the reactions of plants to climate change (Alexander et al., 2015; Bragazza et al., 2016). When the change in vegetation occurs, it will not be a slow process taking centuries but rather a rapid shift of vegetation types or ecosystems (Loisel and Yu, 2013; Pellerin and Lavoie, 2003).

3.1. Common techniques used for peatland climate manipulation

Over the years, several different techniques have been used to simulate the possible future climatic conditions in peatlands. The increase in temperature was reached by either passive methods, like open-top chambers or warming chambers, or by active methods such as infrared heaters, heating in glasshouses, or propane-fueled heaters (Table 2). Passive warming is a cost-effective way of increasing the air temperature. However, warming is higher during the day than at night, and unwanted cooling of the peat may occur due to increased evapotranspiration caused by warming up the air (Dabros et al., 2010; Górecki et al., 2021). Therefore, passive warming simulates future climate change only partially. Active methods, especially a combination of active and passive heating, allow for more precise and stable manipulation but come with higher running costs and more laborious maintenance (Aronson and Mcnulty, 2009). A unique method was used by Bragazza et al. (2016) when whole blocks of vegetation with the peat below were transplanted from higher latitude to lower latitude bog, changing the temperature and precipitation regimes. However, the vegetation

Table 2

Changes in abundance of peatland plant species caused by simulated climate change.

Climate factor (change)	Time period	The method used for manipulation	Type of peatland	Changes in species abundance		References
				Increased abundance	Decreased abundance	
Temperature (increase)	1 year	Increased temperature in the greenhouse	Fen	*Carex disperma* ♦ *Carex magellanica* ♦	*Sphagnum* spp. ●	(Dieleman et al., 2015)
Temperature (increase)	4 years	Open-top chambers	Bog	*Andromeda polifolia* ■	*Vaccinium oxycoccos* ■	(Buttler et al., 2015)
Temperature (increase)	9 years	Warming chambers	Fen	*Vaccinium oxycoccos* ■ *Eriophorum vaginatum* ♦		(Wiedermann et al., 2007)
Temperature (increase)	3 years	Warming chambers	Fen	*Sphagnum papillosum* ●	*Sphagnum balticum* ●	(Gunnarsson et al., 2004)
Temperature (increase)	4 years	Infrared heat lamps	Bog	*Andromeda glaucophylla* ■	*Sphagnum* sect. *Acutifolia* ● *Kalmia polifolia* ■	(Weltzin et al., 2003)
			Fen	*Scheuchzeria palustris* ♦		
Temperature (increase)	1 year	Open-top chambers	Fen		*Sphagnum angustifolium* ●	(Lyons et al., 2020)
Temperature (increase)	154 days	Increased temperature in the greenhouse	Unspecified	*Sphagnum balticum* ●	*Sphagnum fuscum* ● *Sphagnum magellanicum* ●	(Breeuwer et al., 2008)
Temperature (increase)	2 years	Propane-fired heat exchangers for air and low-wattage heaters for peat	Bog	Shrubs ■	Forbs □	(McPartland et al., 2019a)
Temperature (increase)	3 years	Propane-fired heat exchangers for air and low-wattage heaters for peat	Bog		*Sphagnum angustifolium* ● *Sphagnum fallax* ● *Sphagnum magellanicum* ●	(Norby et al., 2019)
Temperature (increase)	4 years	Propane-fired heat exchangers for air and low-wattage heaters for peat	Bog		*Vaccinium oxycoccos* ■ *Menyanthes trifoliata* □	(McPartland et al., 2020)
Temperature (increase)	1 year	Infrared heaters	Fen	*Carex limosa* ♦ *Carex rostrata* ♦	*Sphagnum angustifolium* ● *Sphagnum teres* ●	(Łuców et al., 2017)
Temperature (increase) and precipitation (decrease)	3 years	Transplanting of mesocosms from higher to lower altitude	Bog	*Vaccinium uliginosum* ■	*Sphagnum fallax* ● *Eriophorum vaginatum* ♦	(Bragazza et al., 2016)
Water table level (decrease)	1 year	Regulated in mesocosm	Fen	*Kalma polifolia* ■ *Ledum groenlandicum* ■		(Dieleman et al., 2015)
Water table level (decrease)	4 years	Regulated in mesocosm	Bog	*Andromeda glaucophylla* ■ *Chamaedaphne calyculata* ■		(Weltzin et al., 2003)
Water table level (decrease)	3 years	A ditch dug around the plot	Fen	*Betula nana* ■ *Vaccinium oxycoccos* ■ *Trichophorum cespitosum* ♦ *Sphagnum subnitens* ●	*Menyanthes trifoliata* □ *Equisetum fluviatile* □	(Mäkiranta et al., 2018)
Water table level (decrease)	12 years	A ditch dug around the plot	Fen	No vegetation points	Mosses ● Graminoids ♦ Shrubs ■ Forbs □	(McPartland et al., 2019b)
Water table level (decrease)	27 months	Addition of 10 cm of peat under vegetation	Fen	Vascular plants ■♦	*Sphagnum* spp. ●	(Jassey et al., 2018)
Water table level (decrease)	16 months	Regulated in mesocosm	Bog	*Sphagnum papillosum* ● *Sphagnum magellanicum* ● *Sphagnum austinii* ●	*Sphagnum cuspidatum* ● *Sphagnum cuspidatum* ● *Sphagnum rubellum* ●	(Robroek et al., 2007a)
Water table level (fluctuation)	2 years	Regulated in mesocosm	Bog	*Sphagnum magellanicum* ● Shrubs ■	*Sphagnum cuspidatum* ● Graminoids ♦	(Breeuwer et al., 2009)
Water table level (increased)	12 years	Water pumped into the plot	Fen		Mosses ● Shrubs ■ Forbs □	(McPartland et al., 2019b)
Water table level (increased)	27 months	Removal of 10 cm of peat below vegetation	Fen	*Sphagnum* spp. ● *Eriophorum vaginatum* ♦	*Vaccinium oxycoccos* ■	(Jassey et al., 2018)
Water table level (increase)	4 years	Regulated in mesocosm	Fen	*Carex lasiocarpa* ♦ *Carex livida* ♦		(Weltzin et al., 2003)

Graminoid ♦ shrub ■ forb □ moss ●.

Note: Only significant increase or decrease in species or plant functional group caused by climate factors are shown in the table.

was suddenly exposed to different climatic conditions and new vegetation community, which is not the precise simulation of climate change.

Water table depth was manipulated either in the controlled conditions with relatively precisely defined depth or in natural conditions, by digging ditches or removing the underlying layer of peat to decrease the water table level or adding peat under vegetation or pumping water into the plot of vegetation to increase the level of the water table (Table 2). The manipulation in mesocosms permit for more precisely defined and stable water table level, but is possible only with small patches of vegetation, and the water is mostly added in the form of artificial solution (Breeuwer et al., 2008, 2009; Dieleman et al., 2015; Robroek et al., 2007a). The addition of water from ditch dug in the original peatland is more laborious but expose the vegetation to more natural conditions (Weltzin et al., 2003). Water table level manipulations in situ allow for altering the water regime for larger patches of vegetation and ensure the natural supply of the water. Nonetheless, the water table level by in situ manipulation is less controlled by scientists and more dependent on the natural conditions of the site (Mäkiranta et al., 2018; McPartland et al., 2019b).

Different climate and water table depth manipulation methods have their advantages and disadvantages. The exact simulation of the future is impossible due to its uncertain scale and the complicated relationships of ecosystem components with climate. However, the combination of temperature and water regime manipulation provides a more truthful perspective than the change of only one climate variable and in situ manipulation better considers the complexity of nature. A combination of active and passive methods, like in McPartland et al. (2019a), may be necessary to achieve realistic manipulation of the climate.

4. Impact of changes in peatland vegetation on carbon balance

Northern peatlands belong to ecosystems with the highest potential to enhance the pace of climate change by positive feedback due to their large carbon stock and location in the most rapidly warming region of the globe (Gorham, 1991; Hoegh-Guldberg et al., 2018). Whether the ecosystem is a sink or source of carbon in relation to the atmosphere depends on rates of carbon uptake and release. Carbon is taken up through photosynthesis and released by respiration and methane release. Ecosystem photosynthesis, known as gross primary production, is influenced by the vegetation composition, physiological status of its components, and the length of photosynthetic activity (Laine et al., 2012; Lund et al., 2010). Ecosystem respiration also depends on vegetation composition and the physiological status of plants. Additionally, the respiration of peatlands depends on hydrology, composition, amount, and activity of microorganisms, and the quality of litter (Juszczak et al., 2013; Acosta et al., 2017; Górecki et al., 2021; Laiho, 2006). Methane release is determined by rates of methanogenesis and methanotrophy, which both depend on microbial activity, litter quality, water table depth, temperature and vegetation composition (Riutta et al., 2007; Whalen, 2005; Juszczak and Augustin, 2013). All of the abovementioned factors will change with climate change, and all of them will shape the future climate. Climate change-induced changes in vegetation and their impact on the carbon balance of peatland must be included in climatic models; otherwise, models underestimate the scale and pace of changes (Cox et al., 2000; Müller and Joos, 2021).

4.1. Carbon fixation

Length of vegetation season belongs to the most important parameters influencing gross primary production of peatlands (Lund et al., 2010). Temperature is a major factor influencing carbon assimilation in northern peatlands. Enhanced carbon fixation with increasing temperature is predicted in mid- and high latitude peatlands as a result of longer vegetation season (Gallego-Sala et al., 2018; Peñuelas et al., 2004). However, the increasing temperature cannot prolong the vegetation season of high latitudes infinitely. Photosynthetically active radiation is a critical factor for carbon assimilation. The availability of light in high latitudes is not constrained only by shading or clouds but also by the length of days during the winter half of the year, which are not predicted to change (Gallego-Sala et al., 2018). Cloud shading and aerosol thickness are also significant factors decreasing the carbon uptake by peatlands, but it is difficult to predict what changes in cloud cover and aerosol presence climate change will bring (Harenda et al., 2021; Nijp et al., 2015). Although phenology is closely linked to climatic conditions, it is better correlated with the rate of carbon uptake than any of the climatic variables itself (Järveoja et al., 2018). The effect of climate warming on peatland gross primary production is mediated through vegetation phenology, especially sooner green-up during spring and later senescence in autumn (Koebsch et al., 2020). Plant phenology is influenced by the compound effect of abiotic factors; therefore, it is the most significant factor controlling the maximal rate of gross primary production of peatland (Peichl et al., 2018).

The beginning of vascular plants' vegetation season is an important event impacting carbon uptake and net ecosystem exchange of carbon (Peichl et al., 2015). Increased temperature triggers sooner spring growth of graminoids and earlier full leaf biomass establishment, which prolongs the period of photosynthetic activity (Sullivan and Welker, 2005). The decreased water table level also prolongs the vegetation period of graminoids, probably by enhancing warm-up of the top layer of peat and by improved aeration (Mäkiranta et al., 2018). Graminoids play a crucial role in fens' gross primary production (Robroek et al., 2017a). Increasing temperature favors the growth and expansion of graminoids of fens as long as the water table is high enough (Table 2). Therefore, fens can, in the future, potentially fix more carbon during the vegetation season in the areas where precipitation will not become lower than evapotranspiration (Li et al., 2021; Robroek et al., 2017a). However, *Sphagnum*-dominated fens are a significantly stronger sink of carbon than graminoids-dominated fens due to a longer period of photosynthetic activity and a higher ratio of assimilation to respiration (Glenn et al., 2006). Peat mosses start the photosynthetic activity as the first plants of peatland vegetation because of their “evergreen” nature and low temperature requirements for physiological activity. Evergreen shrubs begin vegetation season shortly after mosses when the top layer of peat warms up. The vegetation season of graminoids and forbs starts later after they produce leaves. The contribution of plant functional groups to peatland carbon assimilation follows the pattern of the beginning of their photosynthetic activity (Korrensalo et al., 2016; Moore et al., 2006). The changes caused by climate change will likely have opposite effects on carbon assimilation by peatland vegetation in spring. Decreasing cover of *Sphagnum* spp. will decrease the carbon uptake, but the sooner start of the physiological activity of vascular plants may erase this decrease and possibly increase the carbon assimilation during the spring green-up (Tables 1, 2).

Mosses of genus *Sphagnum* are an important contributor to overall gross primary production. Despite their relatively low level of photosynthetic apparatus light saturation, they are responsible for a substantial part of maximal gross primary production (Peichl et al., 2018). *Sphagnum* spp. are also the most important component of the peatland vegetation for resistance and resilience of carbon accumulation to drought (Kuiper et al., 2014). However, some species of *Sphagnum* cope with climate change better than others. While carbon assimilation of hummock species *S. medium* continues at the same rate under warmer and drier conditions, carbon assimilation of hollow species *S. fallax* drops rapidly (Jassey and Signarbieux, 2019). Growth of *S. fallax* is then hampered, and species can be overgrown by better performing *Sphagnum* spp. (Rastogi et al., 2020). Increasing cover of vascular plants reported by climate manipulation studies (Dieleman et al., 2015; Jassey et al., 2018; Weltzin et al., 2003; Wiedermann et al., 2007) reduces the productivity of *Sphagnum* spp. (Bragazza et al., 2013). The production reduction by vascular plants cover is even higher than the reduction caused by water level drop (Bengtsson et al., 2021). Shrubs are the plant functional group of peatland vegetation, which is the most responsible for the reduction of photosynthesis. Hence, the increasing cover of shrubs in bogs due to climate changes will decrease the rate of assimilated carbon. However, the presence of shrubs decreases not only the carbon assimilation but the overall carbon turnover, and the net ecosystem exchange is not significantly impacted (Ward et al., 2009). In addition to mosses photosynthesis reduction, shrubs cause the lowering of peatland carbon exchange by their slow photosynthesis and respiration relative to mosses or graminoids. Higher carbon assimilation and accumulation by shrubs can be expected in the future, as shrubs' gross primary production is higher when precipitation events are less frequent. Longer periods between rains lower the photosynthesis of mosses and graminoids (Adkinson and Humphreys, 2011; Radu and Duval, 2018). In general, the photosynthetic activity of vascular plants increases with warmer and drier conditions, but the photosynthetic activity of *Sphagnum* spp. dramatically decreases (Bragazza et al., 2016). The beginning, end, and length of the growing season are significant factors for the amount of assimilated carbon per year, but the leaf area index of vascular plants is even stronger correlated with gross primary production than abiotic or phenological variables. Therefore, changes in vegetation composition towards more vascular plants abundance will probably lead to higher assimilation of carbon from the atmosphere to plant biomass (Gavazov et al., 2018; Lund et al., 2010; Ward et al., 2013).

Some of the northern peatlands lay in the locations where the soil is permanently frozen for years with the minimal physiological activity of plants. Permafrost peatlands, which contain a large amount of carbon, are thawing, which makes the stored carbon available for decomposers, but also creates the conditions for colonization by plants. The carbon accumulation of newly thawed peatlands rapidly increases, and carbon dioxide uptake exceeds its release, but such peatlands are a substantial source of methane, which may make them a net contributor to global warming for decades (Swindles et al., 2015; Turetsky et al., 2007).

In addition to plant photosynthesis, microbial photosynthesis is an important contributor to peatland carbon fixation. Although the presence of specific phototrophic microorganisms depends on vegetation composition, the carbon fixation rate by microbes remains similar for different communities and climatic conditions. However, microbial photosynthesis is related to the presence of *Sphagnum* spp. and will probably decline with the diminishing of peat mosses and increasing temperature (Basińska et al., 2020; Hamard et al., 2021).

4.2. Respiration

Peatland microbiota is strongly connected to the plants occurring in the peatland. Occurrence and ratios between fungi and bacteria or different groups of bacteria depend on the litter properties, which ultimately depend on the vegetation composition (Bragazza et al., 2015). The impact of changes in abiotic conditions on litter quality is mainly mediated via changes in vegetation composition (Straková et al., 2010). The litter of *Sphagnum* spp. is decomposed significantly slower than the litter of other plant functional groups of peatland vegetation (Dorrepaal et al., 2005). Slower *Sphagnum* spp. litter decomposition is caused by the lower enzymatic activity of microorganisms in it, especially carbon-acquiring enzymes (Strakova et al., 2011). On the contrary, the residuals of forbs are decomposed the fastest of all plant functional groups of peatlands. The decomposition rate of vascular plants litter is increasing in a warmer climate (Dorrepaal et al., 2005). Higher carbon release from vascular plants litter compared to *Sphagnum* spp. litter is caused by both higher aerobic and anaerobic decomposition, which increase with higher temperature (Duval and Radu, 2018). However, not all *Sphagnum* spp. decompose at the same speed. Hummock species with their higher cellulose: hemicellulose and structural: metabolic carbohydrates decompose slower than hollow species (Straková et al., 2010).

Phenolic compounds belong to one of the most important groups of compounds related to peat properties. The role of phenolic compounds in peatland carbon balance is very complex. *Sphagnum* spp. polyphenols are part of cell walls and persist as a part of litter instead of leaching to the pore water. Contrastingly, vascular plants produce easily leachable polyphenols or exude polyphenolic compounds by roots, which persist in pore water (Dieleman et al., 2016; Dorrepaal et al., 2005). While relatively simple phenolic compounds produced by the roots of vascular plants lower the microbial carbon use efficiency resulting in higher carbon dioxide release, polyphenols present in *Sphagnum* spp. or shrub leaves decrease the population of microbes and carbon release by reducing nitrogen availability (Bragazza et al., 2013; Dieleman et al., 2015; Frey et al., 2013). Low pH created by *Sphagnum* spp. protects phenolic compounds from degradation by lowering phenol oxidase activity in wet as well as dry conditions. Graminoid peat provides conditions for higher phenol oxidase activity, which increases in drier conditions. With less peat moss litter and more graminoid peat, phenolic compounds will degrade faster, and peat will be more prone to decomposition (Williams and Yavitt, 2000).

Emission of carbon dioxide from *Carex* spp. dominated peatlands is significantly higher than from *Sphagnum*-dominated peatlands because *Carex* spp. provide litter of higher quality with narrower carbon: nitrogen ratio (Lyons and Lindo, 2020). Higher ecosystem respiration of graminoid-dominated peatlands is also driven by the higher amount of dissolved organic carbon compared to *Sphagnum* spp. dominated peatlands. Dissolved organic carbon stimulates the activity of microbiota and the decay of litter. Increasing the abundance of graminoids at the expense of peat mosses will very likely stimulate the decomposition and enhance the carbon release from fens (Dieleman et al., 2015). When vascular plants become more abundant and peat mosses less abundant in a future warmer climate, ecosystem respiration may increase because the litter of vascular plants decomposes faster than *Sphagnum* spp. litter due to higher carbon lability (Bell et al., 2018; Bragazza et al., 2016; Del Giudice and Lindo, 2017; Mao et al., 2018). Warming enhances decomposition and respiration also through the reduction of predators like testate amoebae, which in turn cause an increase in the number of bacterial decomposers (Jassey et al., 2013; Basińska et al., 2020).

A plant removal experiment suggests that graminoids are mostly responsible for respiration increase, and dwarf shrubs like *Caluna vulgaris* may decrease ecosystem respiration of bogs (Ward et al., 2009). Although litter of some graminoids like *Eriophorum vaginatum* has high nitrogen and phosphorus content, which makes it ideal for fast decomposition, plants have high nutrient recycling capacity causing fast depletion of macronutrients from peat and hampering microbial activity. Shrubs of *Vaccinium* spp. provide lower quality litter than graminoids, but because of their lower resorption of nutrients, shrub litter increase the macronutrient content of peat and enhance the microbial activity (Kaštovská et al., 2018). Litter of different species does not exist separately in the peatlands but is present in mixtures. Litter of some species like deciduous shrubs *Betula* spp. enhance the decomposition of other plants' residuals. On the contrary, *Sphagnum* spp. litter slows down the decomposition of shrubs and graminoids litter (Zhang et al., 2019). With increasing temperature and abundance of shrubs, fungi and gram-negative bacteria become more abundant. Fungi enriched communities possess more carbon degrading enzymes, which speed up peat degradation (Bragazza et al., 2015). Long-term observation from boreal peatland confirms that climate-induced vegetation changes cause decreasing carbon accumulation (Malmer et al., 2005).

4.3. Methane release

Vegetation composition is an important determinant of methane flux from peatland. The largest effect on methane release from all plant functional groups has graminoids. Graminoids influence methane flux in two ways. They produce a high amount of dissolved organic carbon molecules, which are an easy source of energy for microorganisms and their roots contain aerenchymal tissue, which conduces methane produced in catothelm directly to the atmosphere without passing through acrothelm, where methane could be oxidized to carbon dioxide (Chanton, 2005; Goud et al., 2017; Moore et al., 2011; Rooney-Varga et al., 2007). The increasing abundance of graminoids in warmer fens will likely increase the methane released by their aerenchymal tissues (Dieleman et al., 2017; Noyce et al., 2014; Ward et al., 2013). Forbs with high belowground biomass may also play an important role in increasing methane emissions (Moore et al., 2011). The vegetation type also influences methane production by the litter quality. High lignin to cellulose ratio decreases the relative amount of produced methane and increases the production of carbon dioxide by microbiota (Duval and Radu, 2018). Therefore, shrub encroaching of bogs in warmer and drier future may change the ratio of produced greenhouse gasses in the prospect of carbon dioxide (Dieleman et al., 2015; McPartland et al., 2019a; Weltzin et al., 2003). The effect of abiotic factors on methane production is also modulated by vegetation. Decreased precipitation frequency together with increased rainfall per event cause higher methane release from *Sphagnum* spp. or graminoid-dominated parts of fen, but methane release of the shrub-dominated part is unaffected (Radu and Duval, 2018). Increased vascular plant cover as a result of, and together with higher temperature, cause an increase in the methane flux from the peatland (Zhang et al., 2022). The presence of graminoids increases methanogenesis, and the presence of vascular plants decreases methanotrophy. Considering the projected increasing abundance of vascular plants, methane release from peatlands will increase due to higher production and lower oxidation (Robroek et al., 2015; Table 2).

The methanogenic archaea community is closely related to peatland vegetation. Communities living in peatland dominated by *Sphagnum* spp. accumulate acetate, but graminoid-dominated peatlands are inhabited by acetoclastic methanogens (Rooney-Varga et al., 2007). In optimal conditions, *Sphagnum* spp. provide methane-oxidizing conditions and are related to lower methane release (Goud et al., 2017). However, the relationship between graminoids and methane release from peatlands is not simple and straightforward. Results from Alaskan rich fen suggest that sedges, thanks to their aerenchyma, create oxidizing conditions and support methanotrophy, which in turn lower the amount of methane present in the porewater and probably also methane release (Rupp et al., 2019). The oxidation of graminoids rhizosphere and methane release are species or genus dependent. *Carex rostrata* dominated vegetation provides less oxidizing conditions and subsequently supports higher methane release than *Eriophorum vaginatum* dominated vegetation. Even lower methane release was found from vegetation dominated by *Juncus effusus* (Strom et al., 2005).

The phenology of graminoids also influences methane release from peatlands. The earlier beginning of graminoids vegetation season, together with its prolonging in warmer conditions, will increase the methane release (Moore et al., 2011; Sullivan and Welker, 2005).

5. Conclusions and future perspectives

Our climate is subjected to rapid changes, and ecosystems all over the world need to adapt to these changes. However, it is not only climate that is changing the ecosystems, but the changes in ecosystems also modulate the climate through positive and negative feedbacks. From a climate change point of view, the northern peatlands are one of the most important ecosystems due to their large carbon stock. Many experiments in peatlands in different countries were performed to assess the impact of future climate change on peatland vegetation and the fate of stored carbon. Those experiments were reviewed in this article and summarized in Fig. 1. Results of studies suggest that the rising temperature and altered water availability will change the vegetation phenology and composition.

As discussed in Section 2 (Changes in peatland vegetation phenology), climate warming will result in the earlier onset of shrubs and graminoids flowering. Shrubs will also increase the number of flowers, which may result in more seeds and improve their possibility for spreading. The roots of graminoids will start to grow sooner in the spring, and the leaves will develop sooner in future warmer peatlands. Drop of water table level caused by higher evapotranspiration and changed precipitation regime will prolong the vegetation season of graminoids. The short-term reaction of forbs will depend on present climatic conditions. While their vegetation season will start sooner and last longer in warmer mid-latitude peatlands, the vegetation season will start later in the colder arctic, and its length will most probably not change.

The short-term reaction of peatland vegetation to changes in climate depends on the peatland developmental stage, biodiversity, and the current climatic conditions of the site. Co-existing species may often have a more decisive impact on climate change-induced shifts in peatland vegetation than climate change itself. Bog and fen vegetation will react differently to increased temperature and changes in water availability. It seems that the common feature for both major groups of peatlands is the spreading of vascular plants at the expense of *Sphagnum* spp. With the changing climate, graminoids are becoming more abundant in fens and shrubs in bogs (more elaborated in Section 3 Changes in peatland vegetation composition; Fig. 1). Despite that, peatland plant communities are in general resilient and can adapt to steady changes in climate. However, climate extremes like heat and drought waves, with the projected increasing occurrence, present a considerable danger to biodiversity and ecosystem functions of northern bogs and fens.

The changes in peatland vegetation phenology and composition will ultimately impact climate change through altered carbon dioxide and methane fluxes (Fig. 1). The decreasing abundance of *Sphagnum* spp. together with increased shading by larger vascular plant cover will result in lower carbon fixation by peat mosses and probably also by associated phototropic microorganisms. However, this decrease will be lower than the increasing carbon fixation by spreading vascular plants and their longer vegetation period, and the climate change will very likely result in higher carbon fixation by plants (Section 4.1 Carbon fixation).

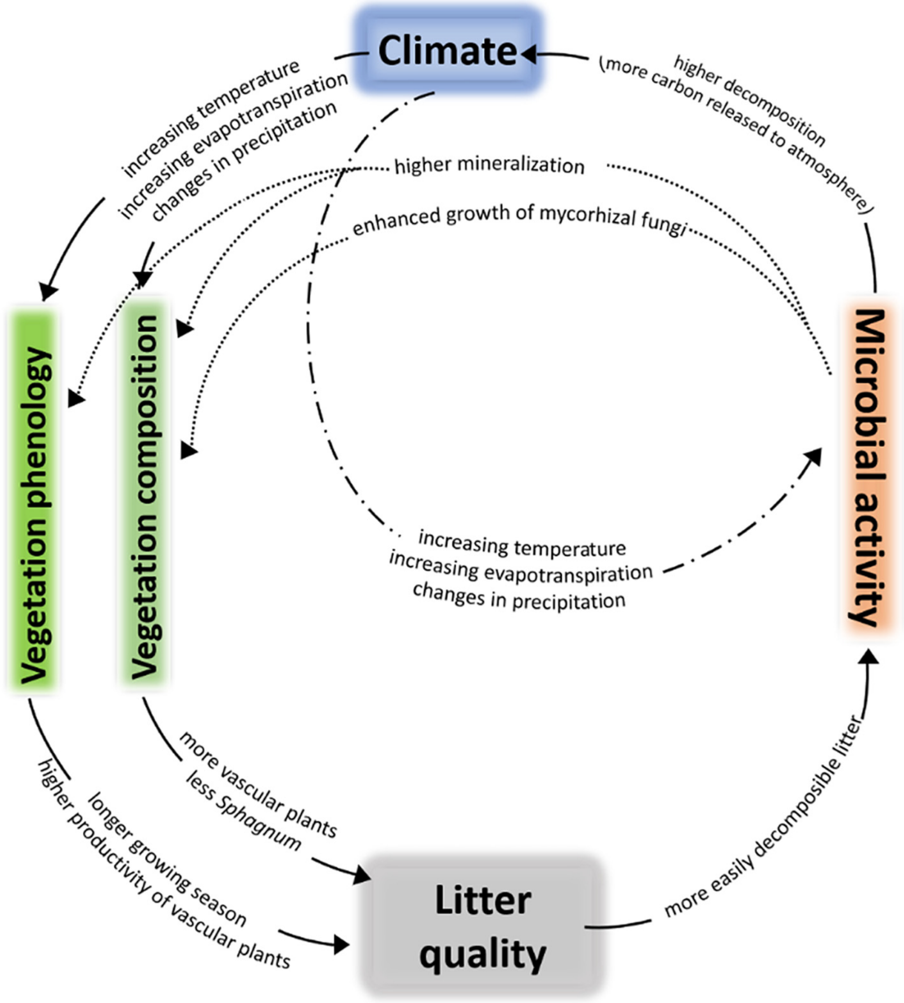

Fig. 1. Climate change-induced changes in peatland vegetation phenology and composition alter climate change.

Peatlands accumulated a vast amount of carbon because of anoxic conditions and litter of poor quality for microbial decomposition. However, the quality of litter input will change together with changes in vegetation composition. Higher decomposition is expected in fens than in bog. An increase in graminoid litter input will create peat with lower polyphenols content together with more suitable carbon: nitrogen and cellulose: lignin ratios for faster microbial decomposition. Shrubs' encroachment of bogs will also alter the litter quality to easier-decomposable, but the presence of woody elements will lower the decomposition rate. The increasing carbon release from bogs will also be caused by increasing colonization by mycorrhizal fungi associated with shrubs. Increased input of simple carbon molecules via root exudates of vascular plants will further increase the number and activity of microorganisms in future peatlands (Section 4.2 Respiration; Fig. 1).

Wetlands, including peatlands, are one of the largest emitters of methane. It is very likely that there will not be significant changes in methane release from bogs in the future. However, due to decreasing water table level and increasing oxidation of the upper layer of peat by shrub roots, methane release from bogs may decrease. Future methane emissions from fens will depend on the water regime. Methane release will increase from fens with an increasing or stable level of the water table due to litter of higher quality, more easily decomposable carbon from root exudates, and more aerenchyma present with a higher abundance of graminoids, which will provide the direct way for methane to escape from deeper layers without being exposed to the oxidative environment of upper layers of peat. Changes in methane release from drier fens are not completely clear, but it is possible that drier fens will release less methane due to thicker acrothelm inhabited by methanotrophic bacteria. The amount of produced and released methane will depend on dominant graminoid species of fens or peatlands in general (Section 4.3 Methane release; Fig. 1).

A special case are peatlands lying at the edge of the permafrost region. Such peatlands are expected to experience dramatic changes once the temperature increases enough to thaw the ice. The plants will start to fix more carbon via photosynthesis, but higher microbial activity will cause higher greenhouse gases, especially methane, release (discussed in Section 4.1 Carbon fixation).

Despite higher carbon uptake from the atmosphere by plants, based on up-to-date knowledge, the result of climate-induced changes in peatland vegetation phenology and composition will be lower carbon accumulation by peatlands in the short term with possible becoming of carbon source in the long term (Section 4 Impact of changes in peatland vegetation on carbon balance).

Although decades of research on climate change impact on peatlands and the possible feedback were conducted, some important information is still missing, which brings uncertainties to predictions about the future climate:

- only the impact of climate change on generative propagation, root, and leaf development was assessed, but the information about the impact of climate change on vegetative reproduction has not been directly studied. The increasing abundance of vascular plants has been reported, but the way of their spreading has not been studied.
- there is no study directly assessing the impact of climate change on *Sphagnum* spp. phenology such as length of growing period or length of photosynthetic activity in natural conditions. Considering the large role of *Sphagnum* spp. in environmental conditions creation and maintenance and carbon storage, this knowledge gap should be addressed. The use of automatization and remote sensing may be necessary to collect frequent enough data for such purpose.
- the biggest threat for peatland plants is not a gradual climate change but the increasing occurrence of climate extremes. There is still relatively little information about the effect of drought and heat waves or extreme precipitation events, especially about their long-term and cumulative effect. There is a need for more information about the mid-term (5–10 years) effect of such events and the resilience of peatland vegetation.

The general trends, which can be expected in this century, are outlined thanks to the decades of work of researchers from many countries cited in this review. However, as humankind, we need more information to make more precise predictions about the future climate and the point in carbon concentration or temperature increase, which cannot be exceeded to not start unstoppable loops of positive feedback.

CRediT authorship contribution statement

Michal Antala: Conceptualization, Formal analysis, Investigation, preparation of the first draft; **Radosław Juszczak:** Review and editing, Funding acquisition; **Christiaan Van der Tol:** Review and editing; **Anshu Rastogi:** Conceptualization, Formal analysis, Investigation, Funding acquisition, editing, Supervision.

Declaration of competing interest

The authors declare that they have no known competing financial interests or personal relationships that could have appeared to influence the work reported in this paper.

Acknowledgment

This work was supported by the projects funded by Polish National Agency for Academic Exchange (NAWA) within the Bekker Programme grant No. PPN/BEK/2019/1/00090 and National Science Centre of Poland (NCN) within grants No. 2016/21/B/ST10/02271 and 2020/37/B/ST10/01213.

References

Aaby, B., 1976. Cyclic climatic variations in climate over the past 5,500 yr reflected in raised bogs. Nature 263, 281–284. https://doi.org/10.1038/263281a0.

Acosta, M., Juszczak, R., Chojnicki, B., Pavelka, M., Havránková, K., Lesny, J., Krupková, L., Urbaniak, M., Machačová, K., Olejnik, J., 2017. CO2 fluxes from different vegetation communities on a peatland ecosystem. Wetlands 37, 423–435. https://doi.org/10.1007/s13157-017-0878-4.

Adkinson, A.C., Humphreys, E.R., 2011. The response of carbon dioxide exchange to manipulations of sphagnum water content in an ombrotrophic bog. Ecohydrology 743, 733–743. https://doi.org/10.1002/eco.

Aerts, R., Cornelissen, J.H.C., Dorrepaal, E., Van Logtestijn, R.S.P., Callaghan, T.V., 2004. Effects of experimentally imposed climate scenarios on flowering phenology and flower production of subarctic bog species. Glob. Chang. Biol. 10, 1599–1609. https://doi.org/10.1111/j.1365-2486.2004.00815.x.

Alexander, J.M., Diez, J.M., Levine, J.M., 2015. Novel competitors shape species' responses to climate change. Nature https://doi.org/10.1038/nature14952.

Arft, A.M., Walker, M.D., Gurevitch, J., Alatalo, J.M., Bret-Harte, M.S., Dale, M., Diemer, M., Gugerli, F., Henry, G.H.R., Jones, M.H., Hollister, R.D., Jónsdóttir, I.S., Laine, K., Lévesque, E., Marion, G.M., Molau, U., MØlgaard, P., Nordenhäll, U., Raszhivin, V., Robinson, C.H., Starr, G., Stenström, A., Stenström, M., Totland, Walker, L.J., Webber, P.J., Welker, J.M., Wookey, P.A., Turner, P.L., 1999. Responses of Tundra plants to experimental warming: meta-analysis of the International Tundra Experiment. Ecol. Monogr. 69, 491–511. https://doi.org/10.1890/0012-9615(1999)069[0491:ROTPTE]2.0.CO;2.

Aronson, E.L., Mcnulty, S.G., 2009. Appropriate experimental ecosystem warming methods by ecosystem, objective, and practicality. Agric. For. Meteorol. 149, 1791–1799. https://doi.org/10.1016/j.agrformet.2009.06.007.

Asada, T., Warner, B.G., Banner, A., 2003. Growth of mosses in relation to climate factors in a hypermaritime coastal peatland in British Columbia, Canada. Bryologist 106, 516–527. https://doi.org/10.1639/0007-2745(2003)106[516:GOMIRT]2.0.CO;2.

Asemaninejad, A., Thorn, R.G., Branfireun, B.A., Lindo, Z., 2018. Climate change favours specific fungal communities in boreal peatlands. Soil Biol. Biochem. 120, 28–36. https://doi.org/10.1016/j.soilbio.2018.01.029.

Backéus, I., 1972. Bog vegetation re-mapped after sixty years. Oikos 23, 384–393.

Bandopadhyay, S., Rastogi, A., Rascher, U., Rademske, P., Schickling, A., Cogliati, S., Julitta, T., Arthur, A.Mac, Hueni, A., Tomelleri, E., Celesti, M., Burkart, A., Strózecki, M., Sakowska, K., Gabka, M., Rosadziński, S., Sojka, M., Iordache, M.D., Reusen, I., Van Der Tol, C., Damm, A., Schuettemeyer, D., Juszczak, R., 2019. Hyplant-derived sun-induced fluorescence-a new opportunity to disentangle complex vegetation signals from diverse vegetation types. Remote Sens. 11, 1691. https://doi.org/10.3390/rs11141691.

Bandopadhyay, S., Rastogi, A., Juszczak, R., 2020. Review of top-of-canopy sun-induced fluorescence (SIF) studies from ground, UAV, airborne to spaceborne observations. Sensors (Switzerland) 20, 1144. https://doi.org/10.3390/s20041144.

Bandopadhyay, S., Rastogi, A., Cogliati, S., Rascher, U., Gąbka, M., Juszczak, R., 2021. Can vegetation indices serve as proxies for potential sun-induced fluorescence (SIF)? A fuzzy simulation approach on airborne imaging spectroscopy data. Remote Sens. 13, 2545. https://doi.org/10.3390/rs13132545.

Basińska, A.M., Reczuga, M.K., Gąbka, M., Stróżecki, M., Łuców, D., Samson, M., Urbaniak, M., Leśny, J., Chojnicki, B.H., Gilbert, D., Sobczyński, T., Olejnik, J., Silvennoinen, H., Juszczak, R., Lamentowicz, M., 2020. Experimental warming and precipitation reduction affect the biomass of microbial communities in a Sphagnum peatland. Ecol. Indic. 112, 106059. https://doi.org/10.1016/j.ecolind.2019.106059.

Bedford, B.L., Rappaport, N.R., Bernard, J.M., 1988. A life history of Carex lasiocarpa Ehrh. ramets. Aquat. Bot. 30, 63–80. https://doi.org/10.1016/0304-3770(88)90007-1.

Bell, M.C., Ritson, J.P., Verhoef, A., Brazier, R.E., Templeton, M.R., Graham, N.J.D., Freeman, C., Clark, J.M., 2018. Sensitivity of peatland litter decomposition to changes in temperature and rainfall. Geoderma 331, 29–37. https://doi.org/10.1016/j.geoderma.2018.06.002.

Bengtsson, F., Rydin, H., Baltzer, J.L., Bragazza, L., Bu, Z.J., Caporn, S.J.M., Dorrepaal, E., Flatberg, K.I., Galanina, O., Gałka, M., Ganeva, A., Goia, I., Goncharova, N., Hájek, M., Haraguchi, A., Harris, L.I., Humphreys, E., Jiroušek, M., Kajukało, K., Karofeld, E., Koronatova, N.G., Kosykh, N.P., Laine, A.M., Lamentowicz, M., Lapshina, E., Limpens, J., Linkosalmi, M., Ma, J.Z., Mauritz, M., Mitchell, E.A.D., Munir, T.M., Natali, S.M., Natcheva, R., Payne, R.J., Philippov, D.A., Rice, S.K., Robinson, S., Robroek, B.J.M., Rochefort, L., Singer, D., Stenøien, H.K., Tuittila, E.S., Vellak, K., Waddington, J.M., Granath, G., 2021. Environmental drivers of sphagnum growth in peatlands across the Holarctic region. J. Ecol. 109, 417–431. https://doi.org/10.1111/1365-2745.13499.

Bernard, J.M., Hankinson, G., 1979. Seasonal changes in standing crop, primary production, and nutrient levels in a Carex rostrata wetland. Oikos 32, 328–336.

Bjorkman, A.D., Myers-Smith, I.H., Elmendorf, S.C., Normand, S., Rüger, N., Beck, P.S.A., Anne Blach-Overgaard, D.B., Cornelissen, J.H.C., Forbes, B.C., Georges, D., Goetz, S.J., Guay, K.C., Gregory, H.R., Henry, J.S., Weiher, SergeEvan, 2018. Plant functional trait change across a warming tundra biome. Nature 562. https://doi.org/10.1038/s41586-018-0563-7.

Bokhorst, S., Bjerke, J.W., Bowles, F.W., Melillo, J., Callaghan, T.V., Phoenix, G.K., 2008. Impacts of extreme winter warming in the sub-Arctic: growing season responses of dwarf shrub heathland. Glob. Chang. Biol. 14, 2603–2612. https://doi.org/10.1111/j.1365-2486.2008.01689.x.

Boulanger, Y., Taylor, A.R., Price, D.T., Cyr, D., McGarrigle, E., Rammer, W., Sainte-Marie, G., Beaudoin, A., Guindon, L., Mansuy, N., 2017. Climate change impacts on forest landscapes along the Canadian southern boreal forest transition zone. Landsc. Ecol. 32, 1415–1431. https://doi.org/10.1007/s10980-016-0421-7.

Bragazza, L., 2006. A decade of plant species changes on a mire in the Italian alps: vegetation-controlled or climate-driven mechanisms? Clim.Change 77, 415–429. https://doi.org/10.1007/s10584-005-9034-x.

Bragazza, L., 2008. A climatic threshold triggers the die-off of peat mosses during an extreme heat wave. Glob. Chang. Biol. 14, 2688–2695. https://doi.org/10.1111/j.1365-2486.2008.01699.x.

Bragazza, L., Parisod, J., Buttler, A., Bardgett, R.D., 2013. Biogeochemical plant-soil microbe feedback in response to climate warming in peatlands. Nat. Clim. Chang. 3, 273–277. https://doi.org/10.1038/nclimate1781.

Bragazza, L., Bardgett, R.D., Mitchell, E.A.D., Buttler, A., 2015. Linking soil microbial communities to vascular plant abundance along a climate gradient. New Phytol. 205, 1175–1182. https://doi.org/10.1111/nph.13116.

Bragazza, L., Buttler, A., Robroek, B.J.M., 2016. Persistent high temperature and low precipitation reduce peat carbon accumulation. Glob. Chang. Biol. 22, 4114–4123. https://doi.org/10.1111/gcb.13319.

Breeuwer, A., Heijmans, M.M.P.D., Robroek, B.J.M., Berendse, F., 2008. The effect of temperature on growth and competition between Sphagnum species. Oecologia 156, 155–167. https://doi.org/10.1007/s00442-008-0963-8.

Breeuwer, A., Robroek, B.J.M., Limpens, J., Heijmans, M.M.P.D., Schouten, M.G.C., Berendse, F., 2009. Decreased summer water table depth affects peatland vegetation. Basic Appl. Ecol. 10, 330–339. https://doi.org/10.1016/j.baae.2008.05.005.

Buttler, A., Grosvernier, P., Matthey, Y., 1998. Development of *Sphagnum fallax* diaspores on bare peat with implications for the restoration of cut-over bogs. J. Appl. Ecol. 35, 800–810. https://doi.org/10.1046/j.1365-2664.1998.355351.x.

Buttler, A., Robroek, B.J.M., Laggoun-Défarge, F., Jassey, V.E.J., Pochelon, C., Bernard, G., Delarue, F., Gogo, S., Mariotte, P., Mitchell, E.A.D., Bragazza, L., 2015. Experimental warming interacts with soil moisture to discriminate plant responses in an ombrotrophic peatland. J. Veg. Sci. 26, 964–974. https://doi.org/10.1111/jvs.12296.

Callaghan, T.V., Björn, L.O., Chernov, Y., Chapin, T., Christensen, T.R., Huntley, B., Ims, R.A., Johansson, M., Jolly, D., Jonasson, S., Matveyeva, N., Panikov, N., Oechel, W., Shaver, G., Elster, J., Jónsdóttir, I.S., Laine, K., Taulavuori, K., Taulavuori, E., Zöckler, C., 2004. Responses to projected changes in climate and UV-B at the species level. Ambio 33, 418–435. https://doi.org/10.1579/0044-7447-33.7.418.

Cao, R., Chen, Y., Shen, M., Chen, J., Zhou, J., Wang, C., Yang, W., 2018. A simple method to improve the quality of NDVI time-series data by integrating spatiotemporal information with the Savitzky-Golay filter. Remote Sens. Environ. 217, 244–257. https://doi.org/10.1016/j.rse.2018.08.022.

Cardinale, B.J., Duffy, J.E., Gonzalez, A., Hooper, D.U., Perrings, C., Venail, P., Narwani, A., MacE, G.M., Tilman, D., Wardle, D.A., Kinzig, A.P., Daily, G.C., Loreau, M., Grace, J.B., Larigauderie, A., Srivastava, D.S., Naeem, S., 2012. Biodiversity loss and its impact on humanity. Nature 486, 59–67. https://doi.org/10.1038/nature11148.

Carrick, P.J., Forsythe, K.J., 2020. The species composition-ecosystem function relationship: a global meta-analysis using data from intact and recovering ecosystems. PLoS One 15, 1–23. https://doi.org/10.1371/journal.pone.0236550.

Chanton, J.P., 2005. The effect of gas transport on the isotope signature of methane in wetlands. Org. Geochem. 36, 753–768. https://doi.org/10.1016/j.orggeochem.2004.10.007.

Chapin, F.S., Bret-Harte, M.S., Hobbie, S.E., Zhong, H., 1996. Plant functional types as predictors of transient responses of arctic vegetation to global change. J. Veg. Sci. 7, 347–358. https://doi.org/10.2307/3236278.

Chiapusio, G., Binet, P., Bertheau, C., Priault, P., 2021. Sphagnum physiological responses to elevated temperature, nitrogen, CO 2 and low moisture in laboratory and in situ microhabitats: a review. Aquat. Ecol. 8. https://doi.org/10.1007/s10452-021-09924-8.

Cho, L.H., Yoon, J., An, G., 2017. The control of flowering time by environmental factors. Plant J. 90, 708–719. https://doi.org/10.1111/tpj.13461.

Chong, M., Humphreys, E., Moore, T.R., 2012. Microclimatic response to increasing shrub cover and its effect on sphagnum CO2 exchange in a bog. Ecoscience 19, 89–97. https://doi.org/10.2980/19-1-3489.

Corlett, R.T., 2016. Plant diversity in a changing world: status, trends, and conservation needs. Plant Divers. 38, 10–16. https://doi.org/10.1016/j.pld.2016.01.001.

Cox, P.M., Betts, R.A., Jones, C.D., Spall, S.A., Totterdell, I.J., 2000. Acceleration of global warming due to carbon-cycle feedbacks in a coupled climate model. Nature 408, 184–187. https://doi.org/10.1038/35041539.

Cullings, K.W., 1996. Single phylogenetic origin of ericoid mycorrhizae within the Ericaceae. Can. J. Bot. 74, 1896–1909. https://doi.org/10.1139/b96-227.

Dabros, A., Fyles, J.W., Strachan, I.B., 2010. Effects of open-top chambers on physical properties of air and soil at post- disturbance sites in northwestern Quebec. Plant Soil 333, 203–218. https://doi.org/10.1007/s11104-010-0336-z.

Damgaard, C., Weiner, J., 2017. It's about time: a critique of macroecological inferences concerning plant competition. Trends Ecol. Evol. 32, 86–87. https://doi.org/10.1016/j.tree.2016.12.001.

Del Giudice, R., Lindo, Z., 2017. Short-term leaching dynamics of three peatland plant species reveals how shifts in plant communities may affect decomposition processes. Geoderma 285, 110–116. https://doi.org/10.1016/j.geoderma.2016.09.028.

Dieleman, C.M., Branfireun, B.A., Mclaughlin, J.W., Lindo, Z., 2015. Climate change drives a shift in peatland ecosystem plant community: implications for ecosystem function and stability. Glob. Chang. Biol. 21, 388–395. https://doi.org/10.1111/gcb.12643.

Dieleman, C.M., Branfireun, B.A., McLaughlin, J.W., Lindo, Z., 2016. Enhanced carbon release under future climate conditions in a peatland mesocosm experiment: the role of phenolic compounds. Plant Soil 400, 81–91. https://doi.org/10.1007/s11104-015-2713-0.

Dieleman, C.M., Branfireun, B.A., Lindo, Z., 2017. Northern peatland carbon dynamics driven by plant growth form — the role of graminoids. Plant Soil 415, 25–35. https://doi.org/10.1007/s11104-016-3099-3.

Dise, N.B., 2009. Peatland response to global change. Science 326, 810–811. https://doi.org/10.1126/science.1174268.

Dorrepaal, E., Aerts, R., Cornelissen, J.H.C., Callaghan, T.V., Van Logtestijn, R.S.P., 2004. Summer warming and increased winter snow cover affect Sphagnum fuscum growth, structure and production in a sub-arctic bog. Glob. Chang. Biol. 10, 93–104. https://doi.org/10.1111/j.1365-2486.2003.00718.x.

Dorrepaal, E., Cornelissen, J.H.C., Aerts, R., Wallén, B., Van Logtestijn, R.S.P., 2005. Are growth forms consistent predictors of leaf litter quality and decomposability across peatlands along a latitudinal gradient? J. Ecol. 93, 817–828. https://doi.org/10.1111/j.1365-2745.2005.01024.x.

Dorrepaal, E., Aerts, R., Cornelissen, J.H.C., Van Logtestijn, R.S.P., Callaghan, T.V., 2006. Sphagnum modifies climate-change impacts on subarctic vascular bog plants. Funct. Ecol. 20, 31–41. https://doi.org/10.1111/j.1365-2435.2006.01076.x.

Duval, T.P., Radu, D.D., 2018. Effect of temperature and soil organic matter quality on greenhouse-gas production from temperate poor and rich fen soils. Ecol. Eng. 114, 66–75. https://doi.org/10.1016/j.ecoleng.2017.05.011.

Filippova, N.V., Thormann, M.N., 2015. The fungal consortium of Andromeda polifolia in bog habitats. Mires Peat 16, 1–29.

Frey, S.D., Lee, J., Melillo, J.M., Six, J., 2013. The temperature response of soil microbial efficiency and its feedback to climate. Nat. Clim. Chang. 3, 395–398. https://doi.org/10.1038/nclimate1796.

Gallego-Sala, A.V., Charman, D.J., Brewer, S., Page, S.E., Prentice, I.C., Friedlingstein, P., Moreton, S., Amesbury, M.J., Beilman, D.W., Björck, S., Blyakharchuk, T., Bochicchio, C., Booth, R.K., Bunbury, J., Camill, P., Carless, D., Chimner, R.A., Clifford, M., Cressey, E., Courtney-Mustaphi, C., De Vleeschouwer, F., de Jong, R., Fialkiewicz-Koziel, B., Finkelstein, S.A., Garneau, M., Githumbi, E., Hribjlan, J., Holmquist, J., Hughes, P.D.M., Jones, C., Jones, M.C., Karofeld, E., Klein, E.S., Kokfelt, U., Korhola, A., Lacourse, T., Le Roux, G., Lamentowicz, M., Large, D., Lavoie, M., Loisel, J., Mackay, H., MacDonald, G.M., Makila, M., Magnan, G., Marchant, R., Marcisz, K., Martínez Cortizas, A., Massa, C., Mathijssen, P., Mauquoy, D., Mighall, T., Mitchell, F.J.G., Moss, P., Nichols, J., Oksanen, P.O., Orme, L., Packalen, M.S., Robinson, S., Roland, T.P., Sanderson, N.K., Sannel, A.B.K., Silva-Sánchez, N., Steinberg, N., Swindles, G.T., Turner, T.E., Uglow, J., Väliranta, M., van Bellen, S., van der Linden, M., van Geel, B., Wang, G., Yu, Z., Zaragoza-Castells, J., Zhao, Y., 2018. Latitudinal limits to the predicted increase of the peatland carbon sink with warming. Nat. Clim. Chang. 8, 907–913. https://doi.org/10.1038/s41558-018-0271-1.

Galvão, V.C., Fankhauser, C., 2015. Sensing the light environment in plants: photoreceptors and early signaling steps. Curr. Opin. Neurobiol. 34, 46–53. https://doi.org/10.1016/j.conb.2015.01.013.

Gaudinier, A., Blackman, B.K., 2020. Evolutionary processes from the perspective of flowering time diversity. New Phytol. https://doi.org/10.1111/nph.16205.

Gavazov, K., Albrecht, R., Buttler, A., Dorrepaal, E., Mark, H., Gogo, S., Hagedorn, F., Mills, R.T.E., Bjorn, J.M., Bragazza, L., Impacts, C., Science, E., 2018. Vascular plant-mediated controls on atmospheric carbon assimilation and peat carbon decomposition under climate change. Glob. Chang. Biol., 0–2 https://doi.org/10.1111/gcb.14140.

Glenn, A.J., Flanagan, L.B., Syed, K.H., Carlson, P.J., 2006. Comparison of net ecosystem CO2 exchange in two peatlands in western Canada with contrasting dominant vegetation, Sphagnum and Carex. Agric. For. Meteorol. 140, 115–135. https://doi.org/10.1016/j.agrformet.2006.03.020.

Górecki, K., Rastogi, A., Stróżecki, M., Gąbka, M., Lamentowicz, M., Łuców, D., Kayzer, D., Juszczak, R., 2021. Water table depth, experimental warming, and reduced precipitation impact on litter decomposition in a temperate Sphagnum-peatland. Sci. Total Environ. 771, 145452. https://doi.org/10.1016/j.scitotenv.2021.145452.

Gorham, E., 1991. Northern peatlands: role in the carbon cycle and probable responses to climatic warming. Ecol. Appl. 1, 182–195. https://doi.org/10.2307/1941811.

Gorham, E., Lehman, C., Dyke, A., Janssens, J., Dyke, L., 2007. Temporal and spatial aspects of peatland initiation following deglaciation in North America. Quat. Sci. Rev. 26, 300–311. https://doi.org/10.1016/j.quascirev.2006.08.008.

Goud, E.M., Moore, T.R., Roulet, N.T., 2017. Predicting peatland carbon fluxes from non-destructive plant traits. Funct. Ecol. https://doi.org/10.1111/1365-2435.12891.

Gunnarsson, U., Maimer, N., Rydin, H., 2002. Dynamics or constancy in Sphagnum dominated mire ecosystems? A 40-year study. Ecography 25, 685–704. https://doi.org/10.1034/j.1600-0587.2002.250605.x.

Gunnarsson, U., Granberg, G., Nilsson, M., 2004. Growth, production and interspecific competition in Sphagnum: effects of temperature, nitrogen and sulphur treatments on a boreal mire. New Phytol. 163, 349–359. https://doi.org/10.1111/j.1469-8137.2004.01108.x.

Hájek, T., Beckett, R.P., 2008. Effect of water content components on desiccation and recovery in sphagnum mosses. Ann. Bot., 165–173 https://doi.org/10.1093/aob/mcm287.

Hájek, M., Horsák, M., Hájková, P., Dítě, D., 2006. Habitat diversity of central European fens in relation to environmental gradients and an effort to standardise fen terminology in ecological studies. Perspect. Plant Ecol. 8, 97–114. https://doi.org/10.1016/j.ppees.2006.08.002.

Hamard, S., Céréghino, R., Barret, M., Sytiuk, A., Lara, E., Dorrepaal, E., Kardol, P., Küttim, M., Lamentowicz, M., Leflaive, J., Le Roux, G., Tuittila, E.S., Jassey, V.E.J., 2021. Contribution of microbial photosynthesis to peatland carbon uptake along a latitudinal gradient. J. Ecol., 1–18 https://doi.org/10.1111/1365-2745.13732.

Harenda, K.M., Samson, M., Juszczak, R., Markowicz, K.M., Stachlewska, I.S., Kleniewska, M., Macarthur, A., Schüttemeyer, D., Chojnicki, B.H., 2021. Impact of atmospheric optical properties on net ecosystem productivity of peatland in Poland. Remote Sens. 13, 1–22, 2124. https://doi.org/10.3390/rs13112124.

Hatfield, J.L., Prueger, J.H., 2015. Temperature extremes: effect on plant growth and development. Weather Clim. Extrem. 10, 4–10. https://doi.org/10.1016/j.wace.2015.08.001.

Heijmans, M.M.P.D., Arp, W.J., Berendse, F., 2001. Effects of elevated CO2 and vascular plants on evapotranspiration in bog vegetation. Glob. Chang. Biol. 7, 817–827. https://doi.org/10.1046/j.1354-1013.2001.00440.x.

Heijmans, M.M.P.D., Van der Knaap, Y.A.M., Holmgren, M., Limpens, J., 2013. Persistent versus transient tree encroachment of temperate peat bogs: effects of climate warming and drought events. Glob. Chang. Biol. 19, 2240–2250. https://doi.org/10.1111/gcb.12202.

Hoegh-Guldberg, O.D., Jacob, M., Taylor, M., Bindi, S., Brown, I., Camilloni, A., Diedhiou, R., Djalante, K.L., Ebi, F., Engelbrecht, J., Guiot, Y., Hijioka, S., Mehrotra, A., Payne, S.I., Seneviratne, A., Thomas, R., Warren, G., Zhou, 2018. Impacts of 1.5°C of global warming on natural and human systems. In: Masson-Delmotte, V., Zhai, P., Pörtner, H.-O., Roberts, D., Skea, J., Shukla, P.R., Pirani, A., Moufouma-Okia, W., Péan, C., Pidcock, R., Connors, S., Matthews, J.B.R., Chen, Y., Zhou, X., Gomis, M.I., Lonnoy, E., Maycock, T., Tignor, M., T.W. (Eds.), Global Warming of 1.5°C. An IPCC Special Report on the Impacts of Global Warming of 1.5°C Above Pre-Industrial Levels and Related Global Greenhouse Gas Emission Pathways, in the Context of Strengthening the Global Response to the Threat of Climate Change.

Holmgren, M., Lin, C.Y., Murillo, J.E., Nieuwenhuis, A., Penninkhof, J., Sanders, N., van Bart, T., van Veen, H., Vasander, H., Vollebregt, M.E., Limpens, J., 2015. Positive shrub-tree interactions facilitate woody encroachment in boreal peatlands. J. Ecol. 103, 58–66. https://doi.org/10.1111/1365-2745.12331.

Hooper, D.U., Adair, E.C., Cardinale, B.J., Byrnes, J.E.K., Hungate, B.A., Matulich, K.L., Gonzalez, A., Duffy, J.E., Gamfeldt, L., Connor, M.I., 2012. A global synthesis reveals biodiversity loss as a major driver of ecosystem change. Nature 486, 105–108. https://doi.org/10.1038/nature11118.

Hyyryläinen, A., Turunen, M., Rautio, P., Huttunen, S., 2018. Perspectives in plant ecology, evolution and systematics Sphagnum mosses in a changing UV-B environment: a review. Perspect. Plant Ecol. Evol. Syst. 33, 1–8. https://doi.org/10.1016/j.ppees.2018.04.001.

IPCC, 2021. Climate Change 2021: The Physical Science Basis. Contribution of Working Group I to the Sixth Assessment Report of the Intergovernmental Panel on Climate Change. https://doi.org/10.1260/095830507781076194.

Isbell, F., Craven, D., Connolly, J., Loreau, M., Schmid, B., Beierkuhnlein, C., Bezemer, T.M., Bonin, C., Bruelheide, H., De Luca, E., Ebeling, A., Griffin, J.N., Guo, Q., Hautier, Y., Hector, A., Jentsch, A., Kreyling, J., Lanta, V., Manning, P., Meyer, S.T., Mori, A.S., Naeem, S., Niklaus, P.A., Polley, H.W., Reich, P.B., Roscher, C., Seabloom, E.W., Smith, M.D., Thakur, M.P., Tilman, D., Tracy, B.F., Van Der Putten, W.H., Van Ruijven, J., Weigelt, A., Weisser, W.W., Wilsey, B., Eisenhauer, N., 2015. Biodiversity increases the resistance of ecosystem productivity to climate extremes. Nature 526, 574–577. https://doi.org/10.1038/nature15374.

Järveoja, J., Nilsson, M.B., Gažovič, M., Crill, P.M., Peichl, M., 2018. Partitioning of the net CO2 exchange using an automated chamber system reveals plant phenology as key control of production and respiration fluxes in a boreal peatland. Glob. Chang. Biol. https://doi.org/10.1111/gcb.14292.

Jassey, V.E.J., Signarbieux, C., 2019. Effects of climate warming on Sphagnum photosynthesis in peatlands depend on peat moisture and species-specific anatomical traits. Glob. Chang. Biol. 25, 3859–3870. https://doi.org/10.1111/gcb.14788.

Jassey, V.E.J., Chiapusio, G., Binet, P., Buttler, A., Laggoun-Défarge, F., Delarue, F., Bernard, N., Mitchell, E.A., Toussaint, M.L., Francez, A.J., Gilbert, D., 2013. Above- and belowground linkages in Sphagnum peatland: climate warming affects plant-microbial interactions. Glob. Chang. Biol. 19, 811–823. https://doi.org/10.1111/gcb.12075.

Jassey, V.E.J., Reczuga, M.K., Zielińska, M., Słowińska, S., Robroek, B.J.M., Mariotte, P., Seppey, C.V.W., Lara, E., Barabach, J., Słowiński, M., Bragazza, L., Chojnicki, B.H., Lamentowicz, M., Mitchell, E.A.D., Buttler, A., 2018. Tipping point in plant–fungal interactions under severe drought causes abrupt rise in peatland ecosystem respiration. Glob. Chang. Biol. 24, 972–986. https://doi.org/10.1111/gcb.13928.

Jin, H., Eklundh, L., 2014. A physically based vegetation index for improved monitoring of plant phenology. Remote Sens. Environ. 152, 512–525. https://doi.org/10.1016/j.rse.2014.07.010.

Jones, M.O., Jones, L.A., Kimball, J.S., McDonald, K.C., 2011. Satellite passive microwave remote sensing for monitoring global land surface phenology. Remote Sens. Environ. 115, 1102–1114. https://doi.org/10.1016/j.rse.2010.12.015.

Jurado, E., Flores, J., 2005. Is seed dormancy under environmental control or bound to plant traits? J. Veg. Sci. 16, 559. https://doi.org/10.1658/1100-9233(2005)16[559:isduec]2.0.co;2.

Juszczak, R., Augustin, J., 2013. Exchange of the greenhouse gases methane and nitrous oxide at a temperate pristine fen mire in Central Europe. Wetlands 33 (5), 895–907. https://doi.org/10.1007/s13157-013-0448-3.

Juszczak, R., Humphreys, E., Acosta, M., Michalak-Galczewska, M., Kayzer, D., Olejnik, J., 2013. Ecosystem respiration in a heterogeneous temperate peatland and its sensitivity to peat temperature and water table depth. Plant Soil 366 (1–2), 505–520. https://doi.org/10.1007/s11104-012-1441-y.

Karkauskaite, P., Tagesson, T., Fensholt, R., 2017. Evaluation of the plant phenology index (PPI), NDVI and EVI for start-of-season trend analysis of the northern hemisphere boreal zone. Remote Sens. 9, 485. https://doi.org/10.3390/rs9050485.

Kaštovská, E., Straková, P., Edwards, K., Urbanová, Z., Bárta, J., Mastný, J., Šantrůčková, H., Picek, T., 2018. Cotton-grass and blueberry have opposite effect on peat characteristics and nutrient transformation in peatland. Ecosystems 21, 443–458. https://doi.org/10.1007/s10021-017-0159-3.

Koebsch, F., Sonnentag, O., Järveoja, J., Peltoniemi, M., Alekseychik, P., Aurela, M., Arslan, A.N., Dinsmore, K., Gianelle, D., Helfter, C., Jackowicz-Korczynski, M., Korrensalo, A., Leith, F., Linkosalmi, M., Lohila, A., Lund, M., Maddison, M., Mammarella, I., Mander, Ü., Minkkinen, K., Pickard, A., Pullens, J.W.M., Tuittila, E.S., Nilsson, M.B., Peichl, M., 2020. Refining the role of phenology in regulating gross ecosystem productivity across european peatlands. Glob. Chang. Biol. 26, 876–887. https://doi.org/10.1111/gcb.14905.

Korrensalo, A., Hájek, T., Alekseychik, P., Rinne, J., Vesala, T., Mammarella, I., Tuittila, E., 2016. Species-specific temporal variation in photosynthesis as a moderator of peatland carbon sequestration. Biogeosciences, 1–19 https://doi.org/10.5194/bg-2016-265.

Kuiper, J., Mooji, W., Bragazza, L., Robroek, B.J.M., 2014. Plant functional types define magnitude of drought response in peatland CO2 exchange. Ecology https://doi.org/10.1890/13-0270.1.

Küttim, M., Laine, A.M., Küttim, L., Ilomets, M., Robroek, B.J.M., 2019. Winter climate change increases physiological stress in calcareous fen bryophytes. Sci. Total Environ. 695, 133867. https://doi.org/10.1016/j.scitotenv.2019.133867.

Laiho, R., 2006. Decomposition in peatlands: reconciling seemingly contrasting results on the impacts of lowered water levels. Soil Biol. Biochem. 38, 2011–2024. https://doi.org/10.1016/j.soilbio.2006.02.017.

Laine, A.M., Bubier, J., Riutta, T., Nilsson, M.B., Moore, T.R., Vasander, H., Tuittila, E.S., 2012. Abundance and composition of plant biomass as potential controls for mire net ecosytem CO 2 exchange. Botany 90, 63–74. https://doi.org/10.1139/B11-068.

Lamentowicz, M., Gałka, M., Marcisz, K., Słowinski, M., Kajukało-Drygalska, K., Dayras, M.D., Jassey, V.E.J., 2019. Unveiling tipping points in long-term ecological records from Sphagnum-dominated peatlands. Biol. Lett. 15. https://doi.org/10.1098/rsbl.2019.0043.

Leišová-Svobodová, L., Phillips, J., Martinussen, I., Holubec, V., 2018. Genetic differentiation of Rubus chamaemorus populations in the Czech Republic and Norway after the last glacial period. Ecol. Evol. 8, 5701–5711. https://doi.org/10.1002/ece3.4101.

Li, Q., Gogo, S., Leroy, F., Guimbaud, C., Laggoun-Défarge, F., 2021. Response of peatland CO2 and CH4 fluxes to experimental warming and the carbon balance. Front. Earth Sci. 9, 1–13. https://doi.org/10.3389/feart.2021.631368.

Liu, Q., Piao, S., Janssens, I.A., Fu, Y., Peng, S., Lian, X., Ciais, P., Myneni, R.B., Peñuelas, J., Wang, T., 2018. Extension of the growing season increases vegetation exposure to frost. Nat. Commun. 9. https://doi.org/10.1038/s41467-017-02690-y.

Loisel, J., Yu, Z., 2013. Recent acceleration of carbon accumulation in a boreal peatland, south central Alaska. J. Geophys. Res. Biogeosci. 118, 41–53. https://doi.org/10.1029/2012JG001978.

Łuców, D., Basinska, A., Chojnicki, B., Józefczyk, D., Juszczak, R., Lesny, J., Olejnik, J., Reczuga, M., Samson, M., Silvennoinen, H., Strózecki, M., Urbaniak, M., Zielińska, M., Lamentowicz, M., 2017. The response of vegetation structure to active warming and precipitation reduction of the Sphagnum peatland. Geophys. Res. Abstr. 19, 2017–8001.

Lund, M., Lafleur, P.M., Roulet, N.T., Lindroth, A., Christensen, T.R., Aurela, M., Chojnicki, B.H., Flanagan, L.B., Humphreys, E.R., Laurila, T., Oechel, W.C., Olejnik, J., Rinne, J., Schubert, P., Nilsson, M.B., 2010. Variability in exchange of CO2 across 12 northern peatland and tundra sites. Glob. Chang. Biol. 16, 2436–2448. https://doi.org/10.1111/j.1365-2486.2009.02104.x.

Lyngstad, A., Moen, A., Pedersen, B., 2017. Flowering in the rich fen species Eriophorum latifolium depends on climate and reproduction in the previous year. Wetlands 37, 1–13. https://doi.org/10.1007/s13157-016-0794-z.

Lyons, C.L., Lindo, Z., 2020. Above- and belowground community linkages in boreal peatlands. Plant Ecol. 221, 615–632. https://doi.org/10.1007/s11258-020-01037-w.

Lyons, C.L., Branfireun, B.A., McLaughlin, J., Lindo, Z., 2020. Simulated climate warming increases plant community heterogeneity in two types of boreal peatlands in north–central Canada. J. Veg. Sci. 31, 908–919. https://doi.org/10.1111/jvs.12912.

Mäkiranta, P., Laiho, R., Mehtätalo, L., Straková, P., Sormunen, J., Minkkinen, K., Penttilä, T., Fritze, H., Tuittila, E., 2018. Responses of phenology and biomass production of boreal fens to climate warming under different water-table level regimes. Glob. Chang. Biol. 24, 944–956. https://doi.org/10.1111/gcb.13934.

Malhotra, A., Brice, D.J., Childs, J., Graham, J.D., Hobbie, E.A., Vander Stel, H., Feron, S.C., Hanson, P.J., Iversen, C.M., 2020. Peatland warming strongly increases fine-root growth. Proc. Natl. Acad. Sci. U. S. A. 117, 17627–17634. https://doi.org/10.1073/pnas.2003361117.

Malmer, N., Svensson, B.M., Wallén, B., 1994. Interactions between sphagnum mosses and field layer vascular plants in the development of peat-forming systems. Folia Geobot. Phytotaxon. 29, 483–496. https://doi.org/10.1007/BF02883146.

Malmer, N., Albinsson, C., Svensson, B.M., Wallén, B., 2003. Interferences between Sphagnum and vascular plants: effects on plant community structure and peat formation. Oikos 100, 469–482. https://doi.org/10.1034/j.1600-0706.2003.12170.x.

Malmer, N., Johansson, T., Olsrud, M., Christensen, T.R., 2005. Vegetation, climatic changes and net carbon sequestration in a North-Scandinavian subarctic mire over 30 years. Glob. Chang. Biol. 11, 1895–1909. https://doi.org/10.1111/j.1365-2486.2005.01042.x.

Mao, R., Zhang, X., Song, C., Wang, X., Finnegan, P.M., 2018. Plant functional group controls litter decomposition rate and its temperature sensitivity: an incubation experiment on litters from a boreal peatland in northeast China. Sci. Total Environ. 626, 678–683. https://doi.org/10.1016/j.scitotenv.2018.01.162.

Mauquoy, D., Engelkes, T., Groot, M.H.M., Markesteijn, F., Oudejans, M.G., Van Der Plicht, J., Van Geel, B., 2002a. High-resolution records of late-Holocene climate change and carbon accumulation in two north-west European ombrotrophic peat bogs. Palaeogeogr. Palaeoclimatol. Palaeoecol. https://doi.org/10.1016/S0031-0182(02)00513-8.

Mauquoy, D., Van der Plicht, J., Blauuw, M., 2002b. Evidence from northwest European bogs shows 'Little Ice Age' climatic changes driven by variations in solar activity. Holocene 12, 1–6. https://doi.org/10.1191/0959683602hl514rr.

May, J.L., Hollister, R.D., Betway, K.R., Harris, J.A., Tweedie, C.E., Welker, J.M., Gould, W.A., Oberbauer, S.F., 2020. NDVI changes show warming increases the length of the green season at Tundra communities in Northern Alaska: a fine-scale analysis. Front. Plant Sci. 11, 1–12. https://doi.org/10.3389/fpls.2020.01174.

McPartland, M.Y., Falkowski, M.J., Reinhardt, J.R., Kane, E.S., Kolka, R., Turetsky, M.R., Douglas, T.A., Anderson, J., Edwards, J.D., Palik, B., Montgomery, R.A., 2019a. Characterizing boreal peatland plant composition and species diversity with hyperspectral remote sensing. Remote Sens. 11. https://doi.org/10.3390/rs11141685.

McPartland, M.Y., Kane, E.S., Falkowski, M.J., Kolka, R., Turetsky, M.R., Palik, B., Montgomery, R.A., 2019b. The response of boreal peatland community composition and NDVI to hydrologic change, warming, and elevated carbon dioxide. Glob. Chang. Biol. https://doi.org/10.1111/gcb.14465.

McPartland, M.Y., Montgomery, R.A., Hanson, P.J., Phillips, J.R., Kolka, R., Palik, B., 2020. Vascular plant species response to warming and elevated carbon dioxide in a boreal peatland. Environ. Res. Lett. 15. https://doi.org/10.1088/1748-9326/abc4fb.

Menzel, A., Sparks, T.H., Estrella, N., Koch, E., Aaasa, A., Ahas, R., Alm-Kübler, K., Bissolli, P., Braslavská, O., Briede, A., Chmielewski, F.M., Crepinsek, Z., Curnel, Y., Dahl, Å., Defila, C., Donnelly, A., Filella, Y., Jatczak, K., Måge, F., Mestre, A., Nordli, Ø., Peñuelas, J., Pirinen, P., Remišová, V., Scheifinger, H., Striz, M., Susnik, A., Van Vliet, A.J.H., Wielgolaski, F.E., Zach, S., Zust, A., 2006. European phenological response to climate change matches the warming pattern. Glob. Chang. Biol. 12, 1969–1976. https://doi.org/10.1111/j.1365-2486.2006.01193.x.

Moore, T.R., Bubier, J.L., Frolking, S.E., Lafleur, P.M., Nigel, T., 2002. Plant biomass and production and CO2 exchange in an ombrotrophic bog. J. Ecol. 90, 25–36.

Moore, T.R., Lafleur, P.M., Poon, D., Heumann, B., Seaquist, J.W., Roulet, N.T., 2006. Spring photosynthesis in a cool temperate bog. Glob. Chang. Biol., 2323–2335 https://doi.org/10.1111/j.1365-2486.2006.01247.x.

Moore, T.R., De Young, A., Bubier, J.L., Humphreys, E.R., Lafleur, P.M., Roulet, N.T., 2011. A multi-year record of methane flux at the Mer Bleue Bog, Southern Canada. Ecosystems 14, 646–657. https://doi.org/10.1007/s10021-011-9435-9.

Müller, J., Joos, F., 2021. Committed and projected future changes in global peatlands – continued transient model simulations since the last glacial maximum. Biogeosciences 18, 3657–3687. https://doi.org/10.5194/bg-18-3657-2021.

Nijp, J.J., Limpens, J., Metselaar, K., Peichl, M., Nilsson, M.B., van der Zee, S.E.A.T.M., Berendse, F., 2015. Rain events decrease boreal peatland net CO 2 uptake through reduced light availability. Glob. Chang. Biol. 21, 2309–2320. https://doi.org/10.1111/gcb.12864.

Norby, R.J., Childs, J., Hanson, P.J., Warren, J.M., 2019. Rapid loss of an ecosystem engineer: Sphagnum decline in an experimentally warmed bog. Ecol. Evol. 9, 12571–12585. https://doi.org/10.1002/ece3.5722.

Noyce, G.L., Varner, R.K., Bubier, J.L., Frolking, S., 2014. Effect of Carex rostrata on seasonal and interannual variability in peatland methane emissions. J. Geophys. Res. Biogeosci. 119, 24–34. https://doi.org/10.1002/2013JG002474.

Oke, T.A., Hager, H.A., 2020. Plant community dynamics and carbon sequestration in Sphagnum -dominated peatlands in the era of global change. Glob. Ecol. Biogeogr., 1–11 https://doi.org/10.1111/geb.13152.

Parmesan, C., Yohe, G., 2003. Aglobally coherent fingerprint of climate change impacts across natural systems. Nature, 37–42 https://doi.org/10.1038/nature01286.

Peichl, M., Sonnentag, O., Nilsson, M.B., 2015. Bringing color into the picture: using digital repeat photography to investigate phenology controls of the carbon dioxide exchange in a boreal mire. Ecosystems 18, 115–131. https://doi.org/10.1007/s10021-014-9815-z.

Peichl, M., Gažovič, M., Vermeij, I., De Goede, E., Sonnentag, O., Limpens, J., Nilsson, M.B., 2018. Peatland vegetation composition and phenology drive the seasonal trajectory of maximum gross primary production. Sci. Rep. 8, 1–11. https://doi.org/10.1038/s41598-018-26147-4.

Pellerin, S., Lavoie, C., 2003. Reconstructing the recent dynamics of mires using a multitechnique approach. J. Ecol. 91, 1008–1021. https://doi.org/10.1046/j.1365-2745.2003.00834.x.

Penfield, S., 2017. Seed dormancy and germination. Curr. Biol. 27, R874–R878. https://doi.org/10.1016/j.cub.2017.05.050.

Peñuelas, J., Filella, I., 2001. Phenology: responses to a warming world. Science (80-.). 294, 793–795. https://doi.org/10.1126/science.1066860.

Peñuelas, J., Filella, I., Comas, P., 2002. Changed plant and animal life cycles from 1952 to 2000 in the Mediterranean region. Glob. Chang. Biol. 8, 531–544. https://doi.org/10.1046/j.1365-2486.2002.00489.x.

Peñuelas, J., Gordon, C., Llorens, L., Nielsen, T., Tietema, A., Beier, C., Bruna, P., Emmett, B., Estiarte, M., Gorissen, A., 2004. Nonintrusive field experiments show different plant responses to warming and drought among sites, seasons, and species in a north-south European gradient. Ecosystems 7, 598–612. https://doi.org/10.1007/s10021-004-0179-7.

Radu, D., Duval, T., 2018. Precipitation frequency alters peatland ecosystem structure and CO 2 exchange: contrasting effects on moss, sedge, and shrub communities. Glob. Chang. Biol. https://doi.org/10.1111/gcb.14057.

Rastogi, A., Stróżecki, M., Kalaji, H.M., Łuców, D., Lamentowicz, M., Juszczak, R., 2019. Impact of warming and reduced precipitation on photosynthetic and remote sensing properties of peatland vegetation. Environ. Exp. Bot. 160, 71–80. https://doi.org/10.1016/j.envexpbot.2019.01.005.

Rastogi, A., Antala, M., Gąbka, M., Rosadziński, S., Stróżecki, M., Brestic, M., Juszczak, R., 2020. Impact of warming and reduced precipitation on morphology and chlorophyll concentration in peat mosses (Sphagnum angustifolium and S. fallax). Sci. Rep. 10, 1–9. https://doi.org/10.1038/s41598-020-65032-x.

Riutta, T., Laine, J., Aurela, M., Rinne, J., Vesala, T., Laurila, T., Haapanala, S., Pihlatie, M., Tuittila, E.S., 2007. Spatial variation in plant community functions regulates carbon gas dynamics in a boreal fen ecosystem. TellusSer. B Chem. Phys. Meteorol. 59, 838–852. https://doi.org/10.1111/j.1600-0889.2007.00302.x.

Robroek, B.J.M., Limpens, J., Breeuwer, A., Crushell, P.H., Schouten, M.G.C., 2007a. Interspecific competition between Sphagnum mosses at different water tables. Funct. Ecol. 21, 805–812. https://doi.org/10.1111/j.1365-2435.2007.01269.x.

Robroek, B.J.M., Limpens, J., Breeuwer, A., Schouten, M.G.C., 2007b. Effects of water level and temperature on performance of four Sphagnum mosses. Plant Ecol. 190, 97–107. https://doi.org/10.1007/s11258-006-9193-5.

Robroek, B.J.M., Schouten, M.G.C., Limpens, J., Berendse, F., Poorter, H., 2009. Interactive effects of water table and precipitation on net CO2 assimilation of three co-occurring Sphagnum mosses differing in distribution above the water table. Glob. Chang. Biol. 15, 680–691. https://doi.org/10.1111/j.1365-2486.2008.01724.x.

Robroek, B.J.M., Jassey, V.E.J., Kox, M.A.R., Berendsen, R.L., Mills, R.T.E., Cécillon, L., Puissant, J., Meima-Franke, M., Bakker, P.A.H.M., Bodelier, P.L.E., 2015. Peatland vascular plant functional types affect methane dynamics by altering microbial community structure. J. Ecol. 103, 925–934. https://doi.org/10.1111/1365-2745.12413.

Robroek, B.J.M., Jassey, V.E.J., Beltman, B., Hefting, M.M., 2017a. Diverse fen plant communities enhance carbon-related multifunctionality, but do not mitigate negative effects of drought. R. Soc. Open Sci. 4. https://doi.org/10.1098/rsos.170449.

Robroek, B.J.M., Jassey, V.E.J., Payne, R.J., Martí, M., Bragazza, L., Bleeker, A., Buttler, A., Caporn, S.J.M., Dise, N.B., Kattge, J., Zajac, K., Svensson, B.H., Van Ruijven, J., Verhoeven, J.T.A., 2017b. Taxonomic and functional turnover are decoupled in European peat bogs. Nat. Commun. 8. https://doi.org/10.1038/s41467-017-01350-5.

Rochefort, L., 2000. New frontiers in bryology and lichenology: Sphagnum - a keystone genus in habitat restoration. Bryologist 103, 503–508. https://doi.org/10.1639/0007-2745(2000)103[0503:sakgih]2.0.co;2.

Rooney-Varga, J.N., Giewat, M.W., Duddleston, K.N., Chanton, J.P., Hines, M.E., 2007. Links between archaeal community structure, vegetation type and methanogenic pathway in Alaskan peatlands. FEMS Microbiol. Ecol. 60, 240–251. https://doi.org/10.1111/j.1574-6941.2007.00278.x.

Ruosteenoja, K., Räisänen, J., Venäläinen, A., Kämäräinen, M., 2016. Projections for the duration and degree days of the thermal growing season in Europe derived from CMIP5 model output. Int. J. Climatol. 36, 3039–3055. https://doi.org/10.1002/joc.4535.

Rupp, D., Kane, E.S., Dieleman, C., Keller, J.K., 2019. Plant functional group effects on peat carbon cycling in a boreal rich fen. Biogeochemistry 144, 305–327. https://doi.org/10.1007/s10533-019-00590-5.

Sala, O.E., Chapin, F.S., Armesto, J.J., Berlow, E., Bloomfield, J., Dirzo, R., Huber-Sanwald, E., Huenneke, L.F., Jackson, R.B., Kinzig, A., Leemans, R., Lodge, D.M., Mooney, H.A., Oesterheld, M., Poff, N.L.R., Sykes, M.T., Walker, B.H., Walker, M., Wall, D.H., 2000. Global biodiversity scenarios for the year 2100. Science 287, 1770–1774. https://doi.org/10.1126/science.287.5459.1770.

Schaepman-strub, G., Limpens, J., Bartholomeus, H., Schaepman, M.E., 2008. Towards spatial assessment of carbon sequestration in peatlands: spectroscopy based estimation of fractional cover of three plant functional types. Biogeosci. Discuss. 5, 1293–1317. https://doi.org/10.5194/bgd-5-1293-2008.

Sletvold, N., Ågren, J., 2015. Climate-dependent costs of reproduction: survival and fecundity costs decline with length of the growing season and summer temperature. Ecol. Lett. 18, 357–364. https://doi.org/10.1111/ele.12417.

Sonesson, M., Carlsson, B.Å., Callaghan, T.V., Halling, S., Björn, L.O., Bertgren, M., Johanson, U., 2002. Growth of two peat-forming mosses in subarctic mires: species interactions and effects of simulated climate change. Oikos 99, 151–160. https://doi.org/10.1034/j.1600-0706.2002.990115.x.

Stenström, A., 1999. Sexual reproductive ecology of Carex bigelowii, an arctic-alpine sedge. Ecography (Cop.) 22, 305–313. https://doi.org/10.1111/j.1600-0587.1999.tb00506.x.

Stenström, A., Jónsdóttir, I.S., 1997. Responses of the clonal sedge, Carex bigelowii, to two seasons of simulated climate change. Glob. Chang. Biol. 3, 89–96. https://doi.org/10.1111/j.1365-2486.1997.gcb134.x.

Stenström, A., Jónsdóttir, I.S., 2004. Effects of simulated climate change on phenology and life history traits in Carex bigelowii. Nord. J. Bot. 24, 355–371. https://doi.org/10.1111/j.1756-1051.2004.tb00850.x.

Stenström, A., Olle Jonsson, B., Jónsdóttir, I.S., Fagerström, T., Augner, M., 2001. Genetic variation and clonal diversity in four clonal sedges (Carex) along the Arctic coast of Eurasia. Mol. Ecol. 10, 497–513. https://doi.org/10.1046/j.1365-294X.2001.01238.x.

Straková, P., Anttila, J., Spetz, P., Kitunen, V., Tapanila, T., Laiho, R., 2010. Litter quality and its response to water level drawdown in boreal peatlands at plant species and community level. Plant Soil 335, 501–520. https://doi.org/10.1007/s11104-010-0447-6.

Strakova, P., Niemi, R.M., Freeman, C., Peltoniemi, K., Toberman, H., Heiskanen, I., Fritze, H., Laiho, R., 2011. Litter type affects the activity of aerobic decomposers in a boreal peatland more than site nutrient and water table regimes. Biogeosciences 8, 2741–2755. https://doi.org/10.5194/bg-8-2741-2011.

Strom, L., Mastepanov, M., Christensen, T.R., 2005. Species-specific effects of vascular plants on carbon turnover and methane emissions from wetland. Biogeochemistry 75, 65–82. https://doi.org/10.1007/s.

Sullivan, P.F., Welker, J.M., 2005. Warming chambers stimulate early season growth of an arctic sedge: results of a minirhizotron field study. Oecologia 142, 616–626. https://doi.org/10.1007/s00442-004-1764-3.

Swindles, G.T., Morris, P.J., Mullan, D., Watson, E.J., Turner, T.E., Roland, T.P., Amesbury, M.J., Kokfelt, U., Schoning, K., Pratte, S., Gallego-Sala, A., Charman, D.J., Sanderson, N., Garneau, M., Carrivick, J.L., Woulds, C., Holden, J., Parry, L., Galloway, J.M., 2015. The long-term fate of permafrost peatlands under rapid climate warming. Sci. Rep. 5, 1–6. https://doi.org/10.1038/srep17951.

Tripati, A.K., Roberts, C.D., Eagle, R.A., 2009. Coupling of CO2 and ice sheet stability over major climate transitions of the last 20 million years. Science (80-.) 326, 1394–1397. https://doi.org/10.1126/science.1178296.

Turetsky, M.R., Wieder, R.K., Vitt, D.H., Evans, R.J., Scott, K.D., 2007. The disappearance of relict permafrost in boreal North America: effects on peatland carbon storage and fluxes. Glob. Chang. Biol. 13, 1922–1934. https://doi.org/10.1111/j.1365-2486.2007.01381.x.

Turetsky, M.R., Euskirchen, E., Talbot, J., Frolking, S., Mcguire, A.D., 2012. Tansley review the resilience and functional role of moss in boreal and arctic ecosystems. New Phytol. 49–67.

van Breemen, N., 1995. How Sphagnum bogs down other plants. Trends Ecol. Evol. 10, 270–275. https://doi.org/10.1016/0169-5347(95)90007-1.

Van Geel, B., Buurman, J., Waterbolk, H.T., 1996. Archaeological and palaeoecological indications of an abrupt climate change in the Netherlands, and evidence for climatological teleconnections around 2650 BP. J. Quat. Sci. 11, 451–460. https://doi.org/10.1002/(SICI)1099-1417(199611/12)11:6<451::AID-JQS275>3.0.CO;2-9.

Visser, M.E., Both, C., 2005. Shifts in phenology due to global climate change: the need for a yardstick. Proc. R. Soc. B Biol. Sci. https://doi.org/10.1098/rspb.2005.3356.

Visser, E.J.W., Bogemann, G.M., van der S.H., M., Pierik, R., Blom, C.W.P.M., 2000. Flooding tolerance of Carex species in relation to field distribution and aerenchyma formation. New Phytol. 148, 93–103. https://doi.org/10.1046/j.1469-8137.2000.00742.x.

Walker, T.N., Ward, S.E., Ostle, N.J., Bardgett, R.D., 2015. Contrasting growth responses of dominant peatland plants to warming and vegetation composition. Oecologia 178, 141–151. https://doi.org/10.1007/s00442-015-3254-1.

Ward, S.E., Bardgett, R.D., McNamara, N.P., Ostle, N.J., 2009. Plant functional group identity influences short-term peatland ecosystem carbon flux: evidence from a plant removal experiment. Funct. Ecol. 23, 454–462. https://doi.org/10.1111/j.1365-2435.2008.01521.x.

Ward, S.E., Nicholas, J., Oakley, S., Henrys, P.A., 2013. Warming effects on greenhouse gas fluxes in peatlands are modulated by vegetation composition. Ecol. Lett., 1285–1293 https://doi.org/10.1111/ele.12167.

Wein, R.W., 1973. Eriophorum vaginatum L. J. Ecol. 61, 601. https://doi.org/10.2307/2259047.

Weltzin, J.F., Pastor, J., Harth, C., Bridgham, S.D., Updegraff, K., Chapin, C.T., 2000. Response of bog and fen plant communities to warming and water-table manipulations. Ecology 81, 3464–3478. https://doi.org/10.1890/0012-9658(2000)081[3464:ROBAFP]2.0.CO;2.

Weltzin, J.F., Harth, C., Bridgham, S.D., 2001. Production and microtopography of bog bryophytes: response to warming and water-table manipulations. Oecologia, 557–565 https://doi.org/10.1007/s004420100691.

Weltzin, J.F., Bridgham, S.D., Pastor, J., Chen, J., Harth, C., 2003. Potential effects of warming and drying on peatland plant community composition. Glob. Chang. Biol. 9, 141–151. https://doi.org/10.1046/j.1365-2486.2003.00571.x.

Weston, D.J., Timm, C.M., Walker, A.P., Gu, L., Muchero, W., Schmutz, J., Shaw, A.J., Tuskan, G.A., Warren, J.M., Wullschleger, S.D., 2015. Sphagnum physiology in the context of changing climate: emergent influences of genomics, modelling and host – microbiome interactions on understanding ecosystem function. Plant Cell Environ. 38, 1737–1751. https://doi.org/10.1111/pce.12458.

Whalen, S.C., 2005. Natural wetlands and the atmosphere. Environ. Eng. Sci. 22, 73–94. https://doi.org/10.1089/ees.2005.22.73.

Wiedermann, M.M., Nordin, A., Gunnarsson, U., Nilsson, M.B., Ericson, L., 2007. Global change shifts vegetation and plant-parasite interactions in a boreal mire. Ecology 88, 454–464. https://doi.org/10.1890/05-1823.

Wiedermann, M.M., Kane, E.S., Potvin, L.R., Lilleskov, E.A., 2017. Interactive plant functional group and water table effects on decomposition and extracellular enzyme activity in Sphagnum peatlands. Soil Biol. Biochem. 108, 1–8. https://doi.org/10.1016/j.soilbio.2017.01.008.

Williams, C.J., Yavitt, J.B., 2000. Phenol oxidase activity in peatlands in New York State: response to summer drought and peat type. Wetlands 20. https://doi.org/10.1672/0277-5212(2000)020.

Wilson, D., Alm, J., Riutta, T., Laine, J., Byrne, K.A., Farrell, E.P., Tuittila, E.S., 2007. A high resolution green area index for modelling the seasonal dynamics of CO2 exchange in peatland vascular plant communities. Plant Ecol. 190, 37–51. https://doi.org/10.1007/s11258-006-9189-1.

Wolkovich, E.M., Cook, B.I., Allen, J.M., Crimmins, T.M., Betancourt, J.L., Travers, S.E., Pau, S., Regetz, J., Davies, T.J., Kraft, N.J.B., Ault, T.R., Bolmgren, K., Mazer, S.J., McCabe, G.J., McGill, B.J., Parmesan, C., Salamin, N., Schwartz, M.D., Cleland, E.E., 2012. Warming experiments underpredict plant phenological responses to climate change. Nature 485, 494–497. https://doi.org/10.1038/nature11014.

Xu, J., Morris, P.J., Liu, J., Holden, J., 2018. PEATMAP: refining estimates of global peatland distribution based on a meta-analysis. Catena 160, 134–140. https://doi.org/10.1016/j.catena.2017.09.010.

Yang, Q.N., Li, H.C., Zhao, H.Y., Li, H.K., Bu, Z.J., Wang, S.Z., Chou, C.Y., Liu, Z.P., 2019. Hydroclimate controls of the distribution and abundance of mosses in Hani mire, Northeast China: modern vegetation survey and peat-core analysis. Quat. Int. 528, 30–40. https://doi.org/10.1016/j.quaint.2019.09.026.

Yuan, W., Liu, S., Dong, W., Liang, S., Zhao, S., Chen, J., Xu, W., Li, X., Barr, A., Andrew Black, T., Yan, W., Goulden, M.L., Kulmala, L., Lindroth, A., Margolis, H.A., Matsuura, Y., Moors, E., Van Der Molen, M., Ohta, T., Pilegaard, K., Varlagin, A., Vesala, T., 2014. Differentiating moss from higher plants is critical in studying the carbon cycle of the boreal biome. Nat. Commun. 5. https://doi.org/10.1038/ncomms5270.

Yuan, J., Wang, P., Weiner, J., Bian, H., Tang, Z., Sheng, L., 2017. The effects of soil drying on the growth of a dominant peatland species, Carex lasiocarpa. Wetlands 37, 1135–1143. https://doi.org/10.1007/s13157-017-0946-9.

Zhang, X., Wang, X., Finnegan, P.M., Tan, W., Mao, R., 2019. Effects of litter mixtures on aerobic decomposition rate and its temperature sensitivity in a boreal peatland. Geoderma 354, 113890. https://doi.org/10.1016/j.geoderma.2019.113890.

Zhang, Y., Song, C., Wang, X., Chen, N., Zhang, H., Du, Y., Zhang, Z., Zhu, X., 2022. Warming effects on the flux of CH 4 from peatland mesocosms are regulated by plant species composition: richness and functional types. Sci. Total Environ. 806. https://doi.org/10.1016/j.scitotenv.2021.150831.

Nonphotochemical quenching does not alter the relationship between sun-induced fluorescence and gross primary production under heatwave

Publication No. 2

Antala, M., Juszczak, R., Rastogi, A., (2024). Nonphotochemical quenching does not alter the relationship between sun-induced fluorescence and gross primary production under heatwave. *New Phytologist*. 20312. https://doi.org/10.1111/nph.20312

Correspondence

Nonphotochemical quenching does not alter the relationship between sun-induced fluorescence and gross primary production under heatwave

A comment on Martini *et al*. (2022): 'Heatwave breaks down the linearity between sun-induced fluorescence and gross primary production'

Sun-induced fluorescence (SIF) is a remote sensing signal that has recently received substantial attention due to its origin from plants' photosynthetic apparatus, which makes it more related to photosynthesis than reflectance-based vegetation indices (Mohammed *et al*., 2019). Upon absorption by the light-harvesting complex of photosystems, the energy can be used by four major paths: (1) photochemistry (*p*), which mainly, but not exclusively, results in gross primary production (GPP; or simply photosynthetic assimilation of carbon); (2) light-intensity-dependent heat dissipation, commonly referred to as nonphotochemical quenching (*npq*); (3) light-intensity-independent (or basal) heat dissipation (*d*); and (4) fluorescence (*f*), which is, in natural conditions, termed SIF. These four processes compete for the absorbed energy, and *p* and *npq* together normally constitute *c*. 80% of the energy use (Lazár, 2015). Only 1–2% of absorbed energy is normally emitted as *f*. The widespread notion of using this small proportion of emitted energy for the estimation of photosynthesis originates in the covariance of *f* and *p* that originate from reaction centres (RCs) due to *npq* that decreases the amount of energy reaching RCs, therefore available for further partitioning into *p*, *f* and *d* (Van Der Tol *et al*., 2014; Magney *et al*., 2020). However, the assumption of the proportional impact of *npq* on *f* and *p* and the stable share of *p* being used for GPP is close to the truth only in optimal conditions. The range of environmental stresses affecting plants decreases the SIF vs GPP correlation, and during severe stress, this correlation may cease to exist completely (Wieneke *et al*., 2018). One of the most impactful studies in regard to not only reporting the broken SIF vs GPP correlation during heat stress but also interpreting the plant physiology behind the broken correlation by leaf-level active Chl *f* measurements was published by Martini *et al*. (2022). However, it could not escape our attention, that this study somewhat misinterpreted the results and not very correctly assigned the broken correlation to nonphotochemical quenching (NPQ) of maximal fluorescence saturation. Therefore, we wrote this short commentary to point out overlooked factors from the article of Martini *et al*. (2022), its supplementary materials and raw data (10.5281/zenodo.5773208), and bring an impulse for a different interpretation of this interesting and important dataset.

Heatwave did not break the linearity between SIF and GPP

Despite the title of Martini *et al*. (2022) suggests that the heatwave (HW) which occurred at the beginning of August 2018 caused the broken correlation of SIF and GPP, a look at the time series of the used data suggests that the correlation was also broken in the 'normal', pre-HW, conditions (Fig. 1). Before noon (9:00–12:00 h), SIF and GPP do not correlate as GPP is steadily decreasing from morning till afternoon, but SIF is increasing with increasing photosynthetically active radiation (PAR) and decreasing solar zenith angle (SZA) and peaking at noon. In the afternoon hours (14:00–16:00 h), when SIF decreases following PAR decrease and SZA increase, SIF and GPP may exhibit a positive correlation. During the HW and particularly on 3 and 6 August, SIF did not decrease in the afternoon but kept rising, which drives the negative correlation of SIF and GPP in HW. The positive correlation of pre-HW SIF and GPP is driven solely by differences among days. The within-day correlations are not significant for any of the 8 pre-HW days. The last 3 d in the pre-HW period even show a negative SIF vs GPP trend (Fig. 2). That, and decreasing SIF and GPP (Fig. 1), suggest that at least 31 July and 1 August were not pre-HW, but rather the beginning of HW days.

NPQ did not saturate

Modifications of xanthophylls, known as the xanthophyll cycle, are one of the major components of *npq*. As the xanthophyll pool of plants is not infinite and the other *npq*-related changes in photosynthetic apparatus (for a detailed description, see Ruban, 2016) cannot continue forever, the safe energy dissipation by *npq* may saturate under severe stress and high light intensity (Lazár, 2015; Ruban, 2016). However, despite the claims of Martini *et al*. (2022) about the role of NPQ in energy partitioning and SIF vs GPP correlation modulation making theoretical sense, the presented data do not support them. One of the main points of the publication is the NPQ saturation in the HW. Nevertheless, fig. 4 of Martini *et al*. (2022) does not support this idea when NPQ clearly does not saturate with decreasing GPP and also does not reach the saturation point with increasing VPD. The apparent saturation of SIF and NPQ is, paradoxically, driven by low values of NPQ. We would like to draw attention to the fact that the parameter NPQ is a ratio of the quantum yield of light-dependent heat dissipation (φNPQ) and the sum of the quantum yield of basal

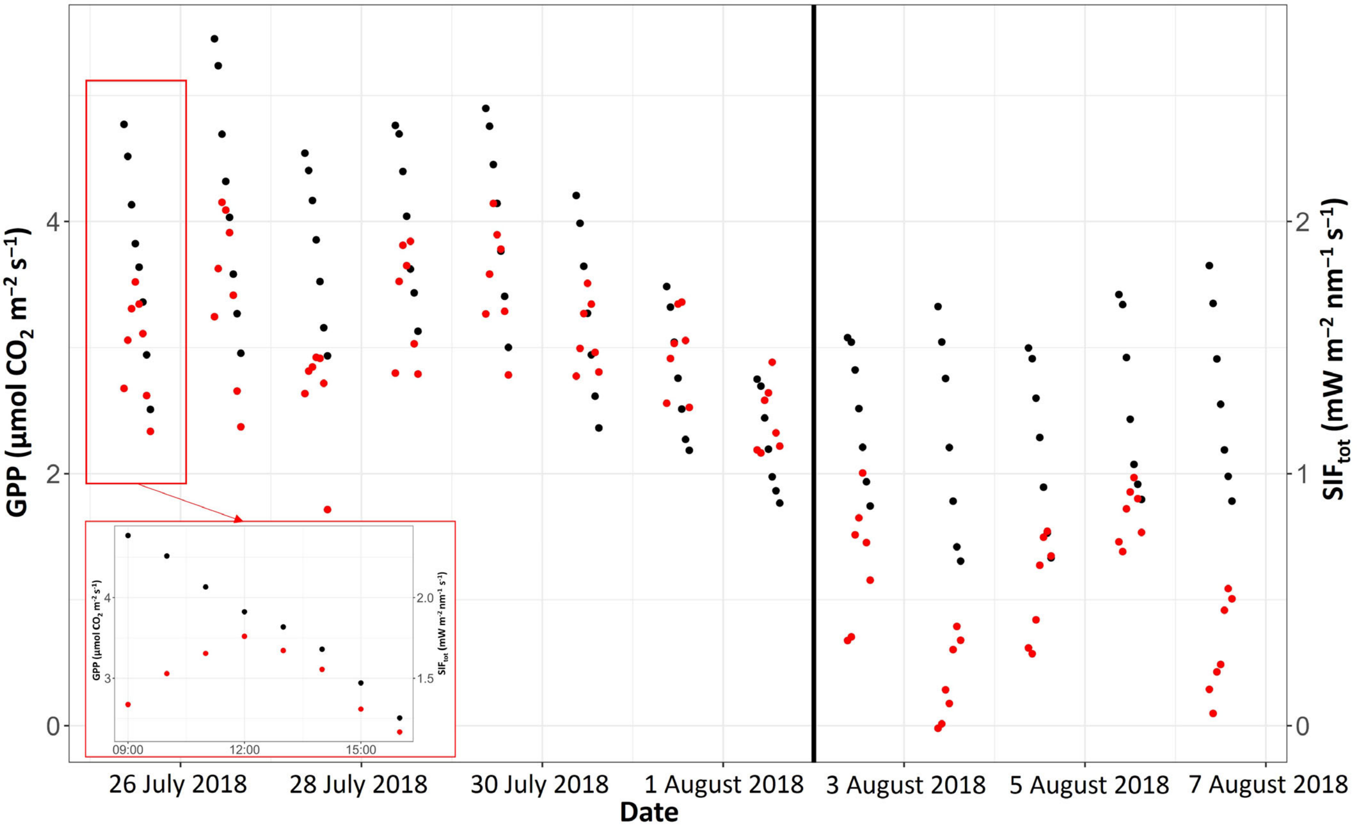

Fig. 1 Time series of total sun-induced fluorescence (SIF$_{tot}$; red points) and gross primary production (GPP; black points). The thick black line separates the pre-heatwave (left) and heatwave (right) periods as identified by Martini *et al*. (2022). The insert depicts a magnified time series of 1 d. The data plotted in the figure is the data used by (Martini *et al*., 2022) and available at 10.5281/zenodo.5773208.

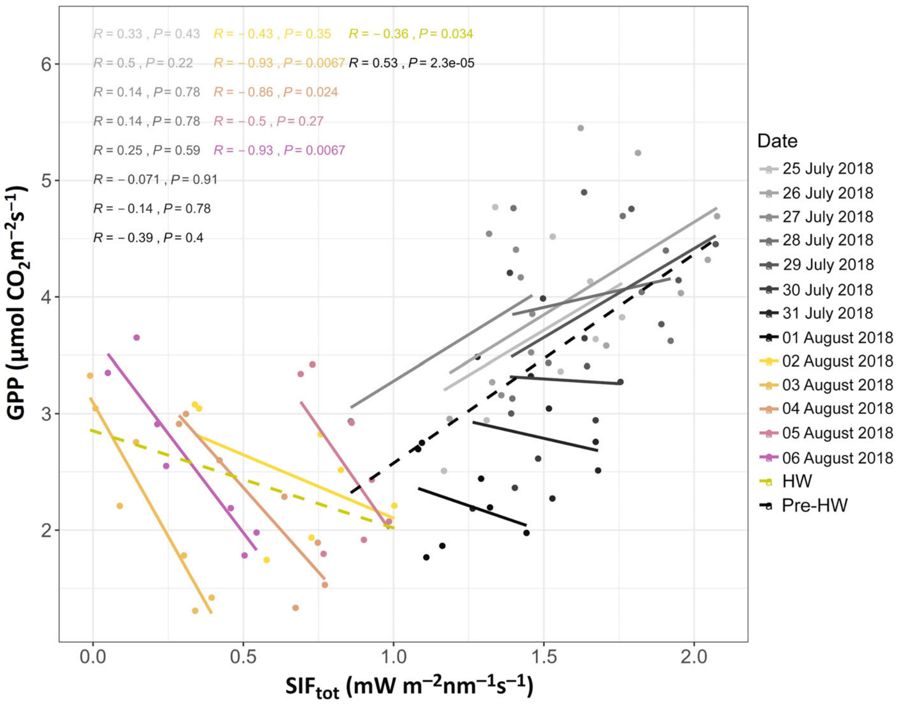

Fig. 2 Spearman correlations of total sun-induced fluorescence (SIF$_{tot}$) and gross primary production (GPP) for pre-heatwave (pre-HW; grey scale) and heatwave (HW; yellow scale) days. The solid lines present daily linear regressions, while the dashed lines depict the linear regressions of pre-HW and HW periods. The data plotted in the figure is the data used by (Martini *et al*., 2022) and available at 10.5281/zenodo.5773208.

heat dissipation and quantum yield of fluorescence (Van Der Tol *et al.*, 2014; Lazár, 2015; Kalaji *et al.*, 2017). That means that NPQ also contains information about the fluorescence emission; therefore, it is not correct to use NPQ as an energy partitioning parameter explaining changes in SIF and GPP. Instead, φNPQ or, as the authors called it, NPQ yield, should be used to explain the use of absorbed energy for different pathways (Lazár, 2015; Kalaji *et al.*, 2017). Correlating φNPQ with a quantum yield of photochemistry further supports no saturation of φNPQ in measured data and suggests that the excess energy was dissipated by *npq* also during HW (data not shown, but available at 10.5281/zenodo.5773208).

Martini *et al.* (2022) further argued that during the HW, there was a change in the energy allocation from NPQ towards SIF. This seems to be very unlikely not only for the reasons stated above but also because of the disproportionally high decrease in SIF described below.

What caused the broken linearity between SIF and GPP?

If NPQ was not the cause of broken linearity between SIF and GPP, then the logical question is: what was causing the decoupling of SIF's and GPP's daily courses?

As mentioned earlier, in normal conditions, SIF and GPP correlate because the SIF intensity and amount of fixed carbon are both regulated by the amount of energy reaching RCs. Hence, they are both dependent on the absorbed PAR, which in turn largely depends on PAR reaching the top of the canopy (Van Der Tol *et al.*, 2014; Magney *et al.*, 2020). However, during heat and drought stress, photosynthesis is not limited by PAR but by water availability, which regulates the stomatas' opening and closure (Farquhar *et al.*, 1980). The limitation of gas exchange between the atmosphere and leaf interior induces a cascade of changes in photosynthetic apparatus activity, including upregulation of alternative electron sinks that can use the energy passed to *p*, causing a situation whereby SIF increases due to energy reaching RCs, but GPP does not increase because of electrons being used for alternative processes (Alric & Johnson, 2017).

The data from Martini *et al.* (2022) and the associated dataset (10.5281/zenodo.5773208) help us to understand the broken linearity of SIF and GPP. While SIF was strongly correlated with PAR, especially in the pre-HW period (Supporting Information Fig. S1B), GPP was not significantly correlated with PAR for any of the analysed days (Fig. S1A). However, GPP was negatively dependent on vapour pressure deficit (VPD, which is largely temperature-dependent) every day in pre-HW and HW periods (Fig. S1C). By contrast, SIF did not correlate significantly with VPD in the pre-HW period but correlated strongly in 3 of the 5 HW days (Fig. S1D). As high VPD is a main driver of stomata closure, these results indicate that stomatal limitation of photosynthesis was the main cause of the broken correlation between SIF and GPP during pre-HW, but stomatal conductance alone cannot explain the reverse relationship during HW (Grossiord *et al.*, 2020). The below-discussed changes in SIF must be taken into account in severe heat conditions.

Fluorescence dramatically decreased with severe heat

One of the strongest effects of HW reported by Martini *et al.* (2022) was a significant decrease in SIF. This decrease is undoubtedly caused by plant physiology; however, as seen in Fig. 1, the SIF retrieval stopped being reliable, as some of the reported values were negative. Negative SIF is a theoretical nonsense as negative emission of photons is impossible and practically had to result from lowering the signal-to-noise ratio to such an extent that even as simple a method as improved Fraunhofer line depth (iFLD) stopped yielding trustworthy results (Alonso *et al.*, 2008). Correcting SIF by the near-infrared reflectance of vegetation (NIRv)-derived fluorescence escape ratio and absorbed PAR yielded even more negative values than top-of-canopy SIF itself. Such results point to our general lack of understanding of top-of-canopy SIF and top-of-canopy SIF-derived parameters during severe stress, such as temperatures above 40°C. Therefore, more attention should be paid to the impact of environmental and plant stress conditions on retrieved SIF reliability, which is an important outcome of the Martini *et al.* (2022) study that did not get enough attention in the publication.

The decrease in SIF in HW was disproportionally larger than the decrease in GPP or increase in NPQ. This would cause a large error in linear regression-based GPP estimation using either instantaneous or mid-day SIF. Moreover, such a large decrease in SIF due to severe stress is not well understood and should be further examined. One possible, although rather speculative, explanation for the observed large decrease in SIF is the temperature dependency of fluorescence emission after crossing the physiological threshold of plants (Kouřil *et al.*, 2004). Kouřil *et al.* (2004) also reported an increase in fluorescence after leaves were heated to 40–45°C, similar to data presented in Fig. 1 and Fig. S1D during HW, especially on 3 and 6 August. Therefore, more consideration should be given to temperature as a factor influencing SIF in future studies performed in extreme heat conditions.

We believe that this Correspondence will induce a new way of thinking about the SIF : GPP : NPQ relationship, the absorbed energy partitioning between photochemical and nonphotochemical processes, the role of stomata in the SIF : GPP relationship and the changes in SIF emission under severe heat or other abiotic and biotic stress conditions.

Acknowledgements

This Correspondence article resulted from the work on projects (nos 2020/37/B/ST10/01213 and 2022/45/N/ST10/01654) financed by the National Science Centre of Poland (NCN).

Competing interests

None declared.

Author contributions

MA, RJ and AR developed the concept. MA prepared the figures and wrote the first draft. RJ and AR reviewed and edited the text.

ORCID

Michal Antala https://orcid.org/0000-0003-1294-9507
Radosław Juszczak https://orcid.org/0000-0002-5212-7383
Anshu Rastogi https://orcid.org/0000-0002-0953-7045

Data availability

These data were derived from the following resources available in the public domain: 10.5281/zenodo.5773208.

Michal Antala*, Radosław Juszczak and Anshu Rastogi*

Laboratory of Bioclimatology, Poznan University of Life Sciences,
Piatkowska 94, 60-649, Poznan, Poland
(*Authors for correspondence: email antala.michal9@gmail.com (AM), anshu.rastogi@up.poznan.pl (AR))

References

Alonso L, Gómez-Chova L, Vila-Francés J, Amorós-López J, Guanter L, Calpe J, Moreno J. 2008. Improved fraunhofer line discrimination method for vegetation fluorescence quantification. *IEEE Geoscience and Remote Sensing Letters* 5: 620–624.

Alric J, Johnson X. 2017. Alternative electron transport pathways in photosynthesis: a confluence of regulation. *Current Opinion in Plant Biology* 37: 78–86.

Farquhar GD, Von Caemmerer S, Berry JA. 1980. A biochemical model of photosynthetic CO_2 assimilation in leaves of C_3 species. *Planta* 149: 78–90.

Grossiord C, Buckley TN, Cernusak LA, Novick KA, Poulter B, Siegwolf RTW, Sperry JS, McDowell NG. 2020. Plant responses to rising vapor pressure deficit. *New Phytologist* 226: 1550–1566.

Kalaji MH, Goltsev VN, Zuk-Golaszewska K, Zivcak M, Brestic M. 2017. *Chlorophyll fluorescence – basics and applicatrions*. Boca Raton, FL, USA: CRC Press.

Kouřil R, Lazár D, Ilík P, Skotnica J, Krchňák P, Nauš J. 2004. High-temperature induced chlorophyll fluorescence rise in plants at 40–50°C: experimental and theoretical approach. *Photosynthesis Research* 81: 49–66.

Lazár D. 2015. Parameters of photosynthetic energy partitioning. *Journal of Plant Physiology* 175: 131–147.

Magney TS, Barnes ML, Yang X. 2020. On the covariation of chlorophyll fluorescence and photosynthesis across scales. *Geophysical Research Letters* 47. doi: 10.1029/2020GL091098.

Martini D, Sakowska K, Wohlfahrt G, Pacheco-Labrador J, van der Tol C, Porcar-Castell A, Magney TS, Carrara A, Colombo R, El-Madany TS *et al.* 2022. Heatwave breaks down the linearity between sun-induced fluorescence and gross primary production. *New Phytologist* 233: 2415–2428.

Mohammed GH, Colombo R, Middleton EM, Rascher U, van der Tol C, Nedbal L, Goulas Y, Pérez-Priego O, Damm A, Meroni M *et al.* 2019. Remote sensing of solar-induced chlorophyll fluorescence (SIF) in vegetation: 50 years of progress. *Remote Sensing of Environment* 231: 111177.

Ruban AV. 2016. Nonphotochemical chlorophyll fluorescence quenching: Mechanism and effectiveness in protecting plants from photodamage. *Plant Physiology* 170: 1903–1916.

Van Der Tol C, Berry JA, Campbell PKE, Rascher U. 2014. Models of fluorescence and photosynthesis for interpreting measurements of solar-induced chlorophyll fluorescence. *Journal of Geophysical Research: Biogeosciences* 119: 2312–2327.

Wieneke S, Burkart A, Cendrero-Mateo MP, Julitta T, Rossini M, Schickling A, Schmidt M, Rascher U. 2018. Linking photosynthesis and sun-induced fluorescence at sub-daily to seasonal scales. *Remote Sensing of Environment* 219: 247–258.

Supporting Information

Additional Supporting Information may be found online in the Supporting Information section at the end of the article.

Fig. S1 Correlation of gross primary production (GPP) and total sun-induced fluorescence (SIF_{tot}) with photosynthetically active radiation and GPP and SIF with vapour pressure deficit.

Key words: gross primary production, heat stress, nonphotochemical quenching, stomatal conductance, sun-induced fluorescence.

Received, 29 May 2024; accepted, 30 October 2024.

Sun-induced fluorescence spectrum as a tool for assessing peatland vegetation productivity in the framework of warming and reduced precipitation experiment

Publication No. 3

Antala, M., Rastogi, A., Cogliati, S., Stróżecki, M., Colombo, R., Juszczak, R. (2024). Sun-induced fluorescence spectrum as a tool for assessing peatland vegetation productivity in the framework of warming and reduced precipitation experiment. *Remote Sensing of Environment*. 301, 113921. https://doi.org/10.1016/j.rse.2023.113921

Remote Sensing of Environment 301 (2024) 113921

Contents lists available at ScienceDirect

Remote Sensing of Environment

journal homepage: www.elsevier.com/locate/rse

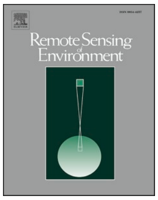

Sun-induced fluorescence spectrum as a tool for assessing peatland vegetation productivity in the framework of warming and reduced precipitation experiment

Michal Antala [a], Anshu Rastogi [a,*], Sergio Cogliati [b], Marcin Stróżecki [a], Roberto Colombo [b], Radosław Juszczak [a,*]

[a] *Laboratory of Bioclimatology, Department of Ecology and Environmental Protection, Faculty of Environmental and Mechanical Engineering, Poznań University of Life Sciences, Piątkowska 94, 60-649 Poznań, Poland*
[b] *Remote Sensing of Environmental Dynamics Lab., DISAT, University of Milano-Bicocca, Piazza della Scienza 1, 20126 Milano, Italy*

ARTICLE INFO

Keywords:
Fen
Peatland
Warming
Reduced precipitation
Climate manipulation
Sun-induced fluorescence
Gross primary production

ABSTRACT

Northern peatlands store a large amount of carbon in the form of partially decomposed organic matter. Because the majority of northern peatlands are located in remote areas, remote sensing serves as a suitable alternative to traditional surveys, enabling to enhance our understanding of peatland vegetation. Among various optical remote sensing signals, sun-induced fluorescence (SIF) is the most directly connected to carbon assimilation by plants, making it a promising early-response indicator for assessing the impact of climate change on natural ecosystems. However, the behavior of SIF throughout the season and the strength of the relationship between SIF and carbon assimilation for peatland vegetation, which consists of peat mosses and vascular plants with diverse anatomy, morphology, physiology, and phenology, have not yet been studied. Therefore, we conducted the first comprehensive assessment of the full spectrum SIF, reflectance, and gross primary production (GPP) for two distinct peatland vegetation communities under control (C), warming (W), and warming with reduced precipitation (WP) conditions throughout an entire season. While we could detect clear differences in SIF and reflectance between the two vegetation communities for original, C, vegetation during the main growing season, these differences diminished when W and WP were applied. The W and WP conditions caused a more pronounced change in plant biomass for vegetation characterized by a higher proportion of peat mosses and low creeping shrubs, which resulted in significant changes in the SIF and reflectance spectrum. Our findings demonstrate that the domination of peatland by vascular plants that is expected due to future warmer conditions causes stronger seasonal variation of SIF, reflectance, and GPP. We observed that far-red SIF and the spectrally integrated full SIF spectrum strongly correlate ($r^2 > 0.85$) with GPP regardless of vegetation community, temperature, and precipitation regime. However, the use of a novel multiple wavelength regression model using ten bands from the full SIF spectrum allowed for higher accuracy in the estimation of GPP compared to the use of single bands or integrated total SIF value. Moreover, such a model has a more stable performance when transferring from one vegetation community to another. Conversely, the correlation strength of traditional vegetation indices like the Normalized Difference Vegetation Index or MERIS Terrestrial Chlorophyll Index depends on the peatland vegetation community. While the SIF:GPP relationship exhibits similar r^2 values for vegetation communities with different ratios of planophile and electrophile leaves, the slope of the linear model depends on this ratio. This study performed at the ground level shows for the first time the importance of full spectrum SIF for the monitoring of a heterogeneous ecosystem like peatland, which will help to better utilize the SIF products obtained through current and future satellite missions.

---

* Corresponding authors.
E-mail addresses: anshu.rastogi@up.poznan.pl (A. Rastogi), sergio.cogliati@unimib.it (S. Cogliati), marcin.strozecki@up.poznan.pl (M. Stróżecki), roberto.colombo@unimib.it (R. Colombo), radoslaw.juszczak@up.poznan.pl (R. Juszczak).

https://doi.org/10.1016/j.rse.2023.113921
Received 26 July 2023; Received in revised form 25 October 2023; Accepted 18 November 2023

1. Introduction

Rapidly changing climate belongs to the biggest concerns of policy-makers of the third millennium, and keeping global climate warming under 2 °C compared to the pre-industrial era (1850-1900) is becoming a serious and challenging goal. Natural ecosystems around the globe have the potential to help with human endeavors, but if they are further affected by adverse activities of people and climate change, they may become another contributor to climate change (Calvin et al., 2023; Cox et al., 2000). One of the most important ecosystems from the carbon storage point of view are peatlands, more particularly northern peatlands (Nichols and Peteet, 2019; Scharlemann et al., 2014), which occupy the boreal region of the northern hemisphere experiencing the fastest rate of climatic changes on the planet (Calvin et al., 2023; Xu et al., 2018).

Peatlands have accumulated large amounts of carbon over time. The carbon is stored in the form of partially decomposed organic matter (peat), thanks to waterlogged, nutrient-poor, low pH conditions and specific vegetation. Peat mosses (*Sphagnum* spp.) are considered the creators of an environment suitable for peat accumulation (Malmer et al., 2003; Nichols and Peteet, 2019; van Breemen, 1995). However, *Sphagnum* spp. is suppressed by vascular plants as a result of climate warming (Bao et al., 2022; Bragazza et al., 2016; Dieleman et al., 2015; Norby et al., 2019). The peatland vegetation is, in general, very heterogeneous and dynamic with relatively high resilience, but once the tolerance threshold is crossed, abrupt changes occur (Lamentowicz et al., 2019). The fate of the carbon stored in peatlands depends on the reaction of vegetation and microbiota to changing conditions that are still not adequately investigated (Antala et al., 2022).

Despite their importance, peatlands are not as well understood as desirable. This is, to a considerable extent, caused by their remoteness and challenging terrain constraining personal observation and data acquisition. Satellite remote sensing appears to be an effective approach for peatland vegetation monitoring. However, before satellite data can be used, the link of spectral properties with physiological properties, the most important being carbon assimilation, also known as gross primary production (GPP), must be examined (Bandopadhyay et al., 2019; McPartland et al., 2019). Ground-based hyperspectral measurements combined with GPP measurements have been successfully used to understand the relationship between carbon assimilation and top-of-canopy (ToC) remote sensing signals for different vegetation types under varying environmental conditions (Martini et al., 2022; Migliavacca et al., 2017; Pierrat et al., 2022; Yang et al., 2015), but such information for peatlands is missing.

Optical remote sensing has been used for decades to acquire information about natural and managed ecosystems. Typically, optical remote sensing uses simple reflectance-based vegetation indices (VIs) based on two-three bands or wavelengths to gain information about overall vegetation “greenness” dependent on the leaf area index and the pigments’ content (i.e., chlorophyll *a*nd carotenoids). The VIs allow only the monitoring of potential photosynthesis based on the amount of green biomass and absorbed photosynthetically active radiation (APAR) by pigments (Cogliati et al., 2015; Siegmann et al., 2021).

Sun-induced fluorescence (SIF) is emitted surplus energy by excited chlorophyll molecules after sunlight has been absorbed. Unlike reflectance, SIF is directly linked to photosynthetic activity because its emission competes with the energy used for photochemistry and heat dissipation (Drusch et al., 2017; Kalaji et al., 2014; Porcar-Castell et al., 2014; Rossini et al., 2015). Consequently, the temporal response of SIF to altered plant physiology is shorter compared to VIs (Damm et al., 2022). However, SIF monitoring became possible only in the last two decades because it is a relatively weak optical signal that requires high-spectral resolution spectrometers and advanced retrieval techniques (Bandopadhyay et al., 2020; Mohammed et al., 2019).

The majority of the SIF retrieval methods, such as variations of Fraunhofer Line Depth (FLD) or Spectral Fitting Method (SFM), retrieve the SIF value at O_2-A and O_2—B absorption bands (Cendrero-Mateo et al., 2019; Meroni et al., 2009). Moreover, due to its relatively easier retrieval, most of the works focus on the O_2-A band SIF, which is in the far-red region of the SIF spectrum. Plants strongly reflect far-red (near infrared) light; hence, far-red SIF is reflected and scattered within the canopy, and its intensity at the ToC depends mainly on vegetation structure (Dechant et al., 2020; Rascher et al., 2021). On the other hand, red SIF is a result of emission primarily by photosystem II (PSII) and is more related to electron transport and carbon assimilation rates. However, red SIF is strongly reabsorbed within the canopy, making its detection and interpretation at the ToC more challenging (Rascher et al., 2021).

Although ToC SIF in O_2 bands is easier to estimate, recent advancements enabled the retrieval of the full SIF and the subsequent possibility to calculate multiple parameters (Cogliati et al., 2019; Cogliati et al., 2015; Verrelst et al., 2015; Zhao et al., 2018). Several different methods for full spectrum SIF estimation were developed, such as the Fluorescence Spectrum Reconstruction (FSR), advanced FSR (aFSR), the Full-spectrum Spectral Fitting (F-SFM), or SpecFit algorithm (Cogliati et al., 2019; Liu et al., 2015; Zhao et al., 2018; Zhao et al., 2014). Thanks to the retrieval of SIF as a continuous spectrum, novel parameters, for example, the SIF at both peaks (in the red and far-red region of the spectrum) or the total SIF (calculated as integral over all wavelengths), can be determined. For instance, the SpecFit algorithm was employed to obtain the full season SIF spectrum dynamics of agricultural crops, pointing to the different behavior of red and far-red peaks during biomass growth (Cogliati et al., 2019). Nevertheless, natural ecosystems differ from agricultural fields by their complexity and the evergreen nature of many species in different habitats. The seasonal changes in the full spectrum of SIF for heterogeneous ecosystems like peatlands remain unexamined. However, to fully utilize the potential of the new generation of satellites like FLuorescence EXplorer (FLEX) being developed by the European Space Agency (ESA), there is a need to understand SIF from all kinds of ecosystems.

The two spectrometers of FLuORescence Imaging Spectrometer (FLORIS), which are planned to be installed aboard the FLEX satellite, will allow the full spectrum SIF retrieval from space with almost global coverage (Cogliati et al., 2015; Drusch et al., 2017). Thanks to its moderate spatial resolution (pixel of 300 m), different ecosystems scattered in the landscape, like peatlands, can be monitored (Drusch et al., 2017). Before the data from FLEX can be used to assess the dynamics of peatland vegetation, ground-based measurements by high-resolution spectrometers need to be performed to allow interpretation of satellite data because the error due to atmospheric and directional effects is magnitudes lower (Cogliati et al., 2015; Harenda et al., 2021).

SIF parameters were used to retrieve different vegetation properties, such as stress response, transpiration, GPP, or biodiversity (Lu et al., 2018; Tagliabue et al., 2020; Wieneke et al., 2018; Xu et al., 2021). Special attention was paid to the link between SIF and GPP because photosynthesis is the most important process for life on Earth, and SIF is a product of the photosynthetic apparatus. A number of studies attempted to estimate global photosynthesis using satellite SIF observations (Bai et al., 2022; Gao et al., 2021; Li et al., 2018; Sun et al., 2018; Zhang et al., 2019b). However, the correlation between SIF and GPP depends on the structure and physiological status of vegetation (Martini et al., 2022; Migliavacca et al., 2017). Hence, we can expect higher uncertainty in the estimation of GPP from SIF with increasing satellites' spatial resolution. To minimize this uncertainty in regional and global carbon assimilation, the relationship between GPP and SIF parameters must be investigated for different ecosystems and under different environmental conditions. In this context, we designed an experiment and assessed the full SIF spectrum, spectral reflectance, and GPP of two different peatland vegetation communities under control, warming, and warming and reduced precipitation conditions over the whole season. The specific goals of our study are: I) to identify the seasonal variation of full SIF spectrum and GPP of two peatland vegetation communities under different temperature and precipitation regimes, and II) to investigate different full spectrum SIF-derived parameters for peatland vegetation monitoring by assessing their relationship with VIs, and GPP.

2. Material and methods

2.1. Site and experimental design description

A detailed description of the experimental sites used for this study is provided in (Górecki et al., 2021). Here, we present a short description of the most important factors for this work.

The experimental sites are localized in Rzecin peatland (52°’45’41” N, 16°18’35″ E, 54 m a.s.l.), western Poland (Fig. 1). The main area of peatland, which covers approximately 86 ha, including around 16 ha of a shallow lake, is overgrown by different vegetation communities (Bandopadhyay et al., 2019). The distribution of vegetation communities follows the hydrological and nutrient gradients. Vegetation of rich fen with more vascular plants and taller shrubs grows closer to the edges, while poor fen vegetation with a higher share of peat mosses is found in the central part of peatland on a floating mat (Bandopadhyay et al., 2019). The floating mat starts 150-200 m from the edge of the peatland. Its formation started around 200 years ago, and it is approximately 70 cm thick (Juszczak et al., 2012; Lamentowicz et al., 2015; Milecka et al., 2017). The average annual precipitation and temperature at Rzecin experimental station were in the last 17 years (2004-2020) 600 mm and 9.0 °C, respectively.

Two experimental sites were established in 2017 in the central part of Rzecin peatland (Fig. 1). The sites are named according to the dominant graminoid species: CL – dominated by *Carex lasiocarpa* Ehrh., and CR – dominated by *Carex rostrata* Stokes (Fig. 2).

CL site is located closer to the edge of the peatland, at the transition between the part underlaid by sediment and the floating mat. Because the surface at the site oscillates only within a few centimeters during the year, the water table depth (WTD) fluctuation is higher than on the CR site, with the maximum during winter and minimum during summer months. The vegetation of the site is dominated by *Carex lasiocarpa* (graminoid), *Vaccinium oxycoccos* L. (a low creeping evergreen shrub), *Sphagnum* spp. (peat moss), and *Equisetum palustre* L. (pteridophyte). These three species and one genus with their litter cover >90 % of experimental plots. Apart from them, *Menyanthes trifoliata* L. (herbaceous species), *Comarum palustre* L. (low creeping deciduous shrub), as well as minor species covering 1 % or less are present in plots. The maximal leaf area index of vascular plants at the CL site in 2021 reached 1.39 (±0.31) $m^2 \cdot m^{-2}$, 2.06 (±0.36) $m^2 \cdot m^{-2}$, and 1.71 (±0.82) $m^2 \cdot m^{-2}$ for control (C), warming (W), and warming and reduced precipitation (WP) plots, respectively (see the description of treatments below).

CR site is located at the floating mat, causing different hydrological conditions than the CL site. The whole surface of the CR site follows the oscillation of water level throughout the year, which causes a relatively more stable WTD. The vegetation of the site is poorer in species. It is dominated by *Vaccinium oxycoccos*, *Sphagnum* spp., and *Carex rostrata*. These two species and a genus with their litter cover >90 % of the plots. *Equisetum palustre* is present in plots as a minor species, and *Menyanthes trifoliata* is present on the site but not in any of the experimental plots. The maximal leaf area index of vascular plants at the CR site reached in the observed year 0.71 (±0.19) $m^2 \cdot m^{-2}$ in C, 0.93 (±0.19) $m^2 \cdot m^{-2}$ in W, and 0.85 (±0.34) $m^2 \cdot m^{-2}$ in WP treatment.

Plots of three different climate treatments in triplicate are present at both experimental sites (Fig. 1). Replicates were chosen in a way that they represent the same vegetation community but also the natural variability within the community. Therefore, each plot within the same treatment has different shares of the present species. Control (C) plots consist of squared collars used for gas exchange measurements with an inside length of 70 cm inserted into the peatland surface without any other manipulation. Warming (W) plots are enclosed by prototyped openable hexagonal open top chambers (OTCs; 2.1 m × 1.6 m base-width, 1.4 m × 1.1 m top-width, and 0.65 m height) made of transparent polycarbonate on aluminum frame (Górecki et al., 2021). Because passive warming by OTCs increases only daylight temperature, infrared heaters of 100 W power were installed above the plots in March 2021. Heaters switch on automatically at nighttime when photosynthetically active radiation (PAR) is lower than 50 $\mu mol \cdot m^{-2} s^{-1}$. Warming and reduced precipitation (WP) plots are enclosed in OTCs exactly like W plots. Additionally, curtains made of water-resistant fabric are installed above WP plots (1.8 m × 1.6 m) to reduce precipitation. The curtains open automatically during the nighttime (PAR < 50 $\mu mol \cdot m^{-2} s^{-1}$) rain events only if the wind speed is $< 3.0\ m \cdot s^{-1}$ and air temperature is above 5.0 °C (the conditions ensure manipulation of only precipitation

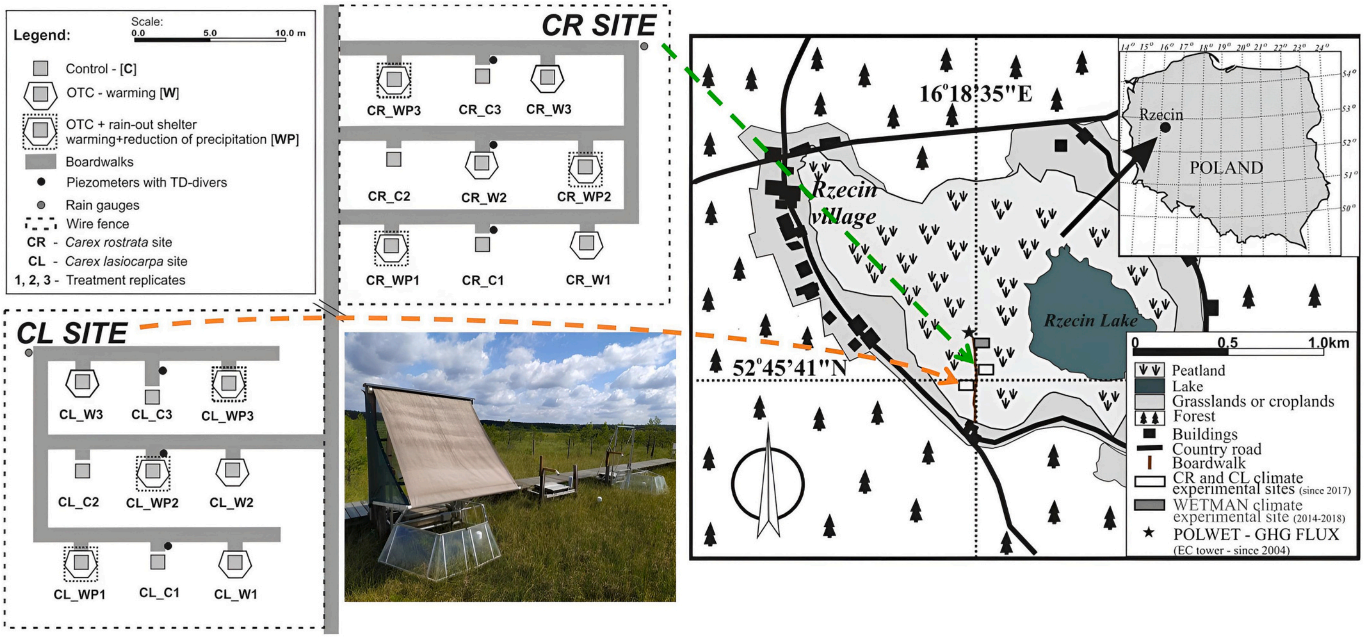

Fig. 1. Experimental design of CL and CR sites and the location of an experimental station in Rzecin peatland (adapted from Górecki et al., 2021, CC BY-NC-ND license).

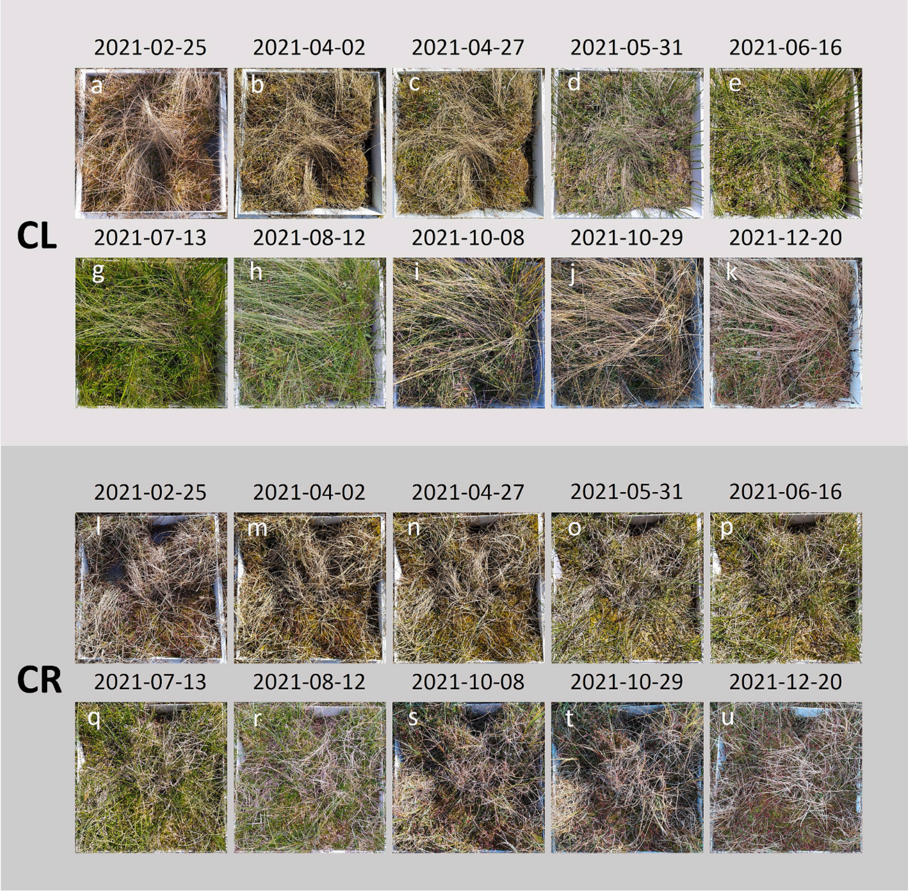

Fig. 2. The representative top-view images of control plots of CL and CR vegetations during the hyperspectral measurements campaigns.

and not light conditions and protect infrastructure from damages by weather). As the curtains cover OTCs only from the top and south directions (Fig. 1), gardening shading mesh was installed from the other three directions to prevent wind-blown rain drops from entering OTCs. The same collars for gas exchange measurements as at C plots were installed in the center of OTCs in W and WP plots (Górecki et al., 2021). As manipulated plots (W and WP) aim to predict the influence of future climatic conditions on peatland, we have used the term "climate manipulation" hereafter.

2.2. Hydrometeorological conditions measurements

Air temperature and relative humidity were measured by radiation-sheltered thermohygrometers HygroVue5 (Campbell Sci., USA) installed 30 cm above the surface, next to the collars marking plots inside of OTCs in the case of W and WP. Thermohygrometers were installed next to the plots of each treatment at each site and connected to datalogger CR1000 (Campbell Sci., USA). Air temperature and humidity were recorded every 30 min during the whole day. The average daily temperature for treatments and sites separately was calculated by averaging 48 reads per plot per day, followed by averaging the daily temperatures obtained from three thermohygrometers of the same treatment per site.

The amount of precipitation was recorded by the heated rain gauges (TPG-124-H-24, A-STER, Poland) installed at each site. The precipitation reduction by curtains at WP plots was calculated based on precipitation amount during the nighttime rain events fulfilling conditions mentioned in the previous subchapter and the registered status of curtains (open, closed).

The depth of the water table level was measured by three TD-divers (Eijkelkamp Soil & Water, the Netherlands) installed at each site in the PVC piezometers permanently fixed to the construction of the wooden platforms that reach the solid bottom of the peatland. Because the surface of the peatland fluctuates during the year together with the water table, the distance between the top edge of piezometers and the surface was measured every 2-3 weeks, and the surface movement in periods between measurements was linearly interpolated. WTD was subsequently calculated as the difference between the distance of the TD-diver to the piezometer's top edge and the surface's distance to the piezometer's top edge. Three measurements of WTD at each site were averaged to get the fluctuation of WTD over the year per site (Górecki et al., 2021).

PAR was measured by BF5 Sunshine Sensor (Delta-T, UK) installed on a tower 3 m above the peatland surface 70 m from CR and 120 m from CL sites. The sensor measures PAR every 30 s of the day. General PAR from BF5 Sunshine Sensor in $\mu mol \cdot m^{-2} \cdot s^{-1}$ was used for GPP modeling. PAR was also calculated from the hyperspectral data in order to check the data quality (see 2.4 Hyperspectral data pre-processing and VIs calculation).

2.3. Hyperspectral irradiance and radiance measurements

Irradiance coming from the Sun and radiance reflected/emitted from the canopy were measured by the Piccolo Doppio (PD) system (MacArthur et al., 2014). The system has a dual field of view with cosine corrected fore optics to capture downwelling irradiance and 25° fore optics to measure upwelling radiance from the canopy. The system consists of two hyperspectral VNIR spectrometers. One spectrometer is FLAME-T-VIS_NIR (Ocean Insight Inc., Dunedin, FL, USA), with a full-width half maximum (FWHM) of 1.3 nm, a sampling interval of approximately 0.33 nm, and a spectral range of 350-1000 nm. The other spectrometer is QEPro-FL (Ocean Insight Inc., Dunedin, FL, USA) with the FWHM of 0.31 nm, a sampling interval of approximately 0.16 nm, and a spectral range of 640-780 nm (Xu et al., 2021). A double bifurcated fiber optic transfers light from the fore optics to the spectrometers; therefore, each spectrometer receives light from the same Earth's surface area.

The hyperspectral measurements were taken on clear sky days from February to December 2021 (Supplement 1) around solar noon. Because of quickly changing weather and partial cloud coverage at midday, measurements were mostly taken before solar noon, when conditions were more stable compared to the afternoon. Three instrumental reads of irradiance and radiance were taken from three points around the center of each plot. Measurements were taken from a solid boardwalk from the north side of plots with a nadir view and the down-looking optics approximately 1.4 m above the peat surface, resulting in the field of view with a diameter of 0.62 m. Both fore optics of PD were mounted on a poll with a bubble level to ensure proper measurements of downwelling irradiance and upwelling radiance. The walls of OTCs were opened for the time of measurements to avoid shadowing and reflection from the frame or polycarbonate (Supplement 2). Integration time for spectrometers was periodically optimized to assure similar signal strength of readouts.

2.4. Hyperspectral data pre-processing and VIs calculation

The irradiance and radiance from both spectrometers of PD were calculated from digital numbers by correcting for instrumental dark-current, taking into account instrument integration time, and using spectral/radiometric calibration coefficients obtained by calibration at the National Institute for Laser, Plasma, and Radiation Physics, Magurele, Romania.

The PAR for every measurement point was calculated by integration of irradiance in the range between 400 and 700 nm. Before the integration, energy for every wavelength was converted from $mW \cdot m^{-2} \cdot sr^{-1} nm^{-1}$ to $\mu mol \cdot m^{-2} \cdot s^{-1}$. Similarly, reflected PAR was calculated as an integral of radiance between 400 and 700 nm. Subsequently, APAR was computed as a difference of PAR and reflected PAR. APAR calculated in this way can also be termed $APAR_{total}$ as PAR absorbed by photosynthetic pigments, and PAR absorbed by non-photosynthetic parts of vegetation are not discriminated (Gitelson and Gamon, 2015). The transmitted radiation was not considered in the APAR calculation for two reasons: a) it is practically impossible to measure transmitted light through mosses, which cover a substantial part of the plots' surface, as there is no space under the mosses; b) instead of soil background for vascular plants, there are other plants (mosses), which either absorb or reflect the light with minimal transmission to the deeper, dead, layer of mosses.

Selected VIs related to biomass and pigments content were calculated using the reflectance spectrum obtained by the FLAME-T-VIS_NIR spectrometer (Table 1). All indices were calculated using one wavelength reflectance formulas except near infra-red (NIR) in Normalized Difference Vegetation Index (NDVI) and Near-Infrared Reflectance of vegetation (NIRv). Average reflectance over the region from 855 to 865 nm was used because of higher noise in NIR from FLAME-T-VIS_NIR after 800 nm.

Table 1
Reflectance-based vegetation indices used in this study: ρ is reflectance at a given wavelength, NDVI is Normalized Difference Vegetation Index, reNDVI is red-edge NDVI, PRI is Photochemical Reflectance Index; NIRv is Near-Infrared Reflectance of vegetation, and MTCI is MERRIS Terrestrial Chlorophyll Index.

VI	Formula	Reference
NDVI	$\frac{(\rho855:\rho865)-\rho670}{(\rho855:\rho865+\rho670}$	(Rouse et al., 1974)
reNDVI	$\frac{\rho750-\rho710}{\rho750+\rho710}$	(Gitelson and Merzlyak, 1994)
PRI	$\frac{\rho570-\rho531}{\rho570+\rho531}$	(Gamon et al., 1992)
NIRv	$(\rho855:\rho865)\frac{(\rho855:\rho865)-\rho670}{(\rho855:\rho865)+\rho670}$	(Badgley et al., 2017)
MTCI	$\frac{\rho754-\rho709}{\rho709+\rho681}$	(Dash and Curran, 2004)

2.5. Sun-induced fluorescence spectrum and related parameters

The Spectrum Fitting (SpecFit) algorithm described in (Cogliati et al., 2019)) was employed to retrieve SIF spectrum as this retrieval method suppose to be used for SIF retrieval from data acquired by expected FLEX mission. As SpecFit code for groud measurements was developed for use with different spectroradiometer system, the code was slightly adapted to process PD data (without altering the core SIF retrieval algorithm). The SIF full spectrum was retrieved from irradiance and radiance spectra measured by QEPro-FL in the spectral window between 670 and 780 nm, which is narrower compared to 640-800 nm measurement window of spectrometer to avoid noise-prone edges of measured spectrum. SpecFit estimates the SIF spectrum by iterative optimization technique based on the comparison between modeled and measured upwelling radiance from the canopy. The SIF full spectrum is modeled by a parametric mathematical function that combines two Lorentzian functions intended to represent the red and far-red peaks. The spectrum is further adjusted by a spectrally variable factor (1-reflectance) that enables to account for canopy reabsorption (red) and multiple scattering (far-red). This factor can be interpreted as a spectrally variable escape probability that helps to model the SIF spectra of the canopy in different conditions. In practice, it offers to reduce the number of free parameters to be estimated in the retrieval. The reflectance is modeled by a piece-wise cubic spline with several knots. The SIF and reflectance are estimated by means of numerical nonlinear optimization to find the best match between modeled and measured radiance spectra. The radiance measured by the QEPro-FL spectrometer of the PD and the one modeled by SpecFit were compared for assessment of the algorithm's performance (Supplement 3B).

SIF in the O_2-A and —B bands, at the peaks of the SIF spectrum in the red and far-red regions, the position of the peaks, and the spectrally integrated value of the full SIF spectrum were subsequently determined. The values of SIF at the peaks of red and far-red regions were determined as the maximal SIF at the region under 690 nm and above 720 nm, respectively. The positions of red and far-red peaks were identified as the wavelength at which the SIF reached the maximal value, and the integrated SIF was calculated as an integral of all SIF values from 670 to 780 nm. SIF yield was calculated for different parameters (e.g. red, far-red, total SIF) as a particular parameter divided by total APAR by canopy calculated from PD's FLAME-T-VIS_NIR spectrometer for every measurement.

Due to the fact that SpecFit is a rather new, lesser-known SIF retrieval algorithm, improved FLD (iFLD) and SFM were utilized as two of the more commonly used retrieval methods for methods comparison (Alonso et al., 2008; Meroni et al., 2010; Meroni and Colombo, 2006). The radiance modeled by SFM and measured by the QEPro-FL spectrometer of the PD were compared to allow the algorithm's performance and to facilitate the comparison with SpecFit (Supplement 3 A).

2.5.1. Multiple wavelength regression for gross primary production modeling

To perform multiple wavelength regression (MWR), bidirectional stepwise linear regression (*ols_step_both_p* function from the *olsrr* package of RStudio) was first used to select the combination of SIF spectrum bands for predicting GPP characterized by the highest significance of correlation and the lowest error (Chatterjee and Hadi, 2012). Subsequently, the multiple linear regression model was built and cross-validated with k-fold cross-validation (*train* function of *caret* package of RStudio) using the selected bands. Because of the rather small number of observations (60), k = 3 was used to obtain representative testing datasets (Chatterjee and Hadi, 2012; Stone, 1974).

2.6. Carbon flux measurements and gross primary production modeling

Carbon dioxide fluxes were measured with the closed dynamic portable chamber system as described in (Acosta et al., 2017) and (Juszczak et al., 2018). The chamber system consisted of the gas analyzer (Li-840, LI-COR Biosciences, USA) installed in the portable box (equipped with pump, air-flow controller, filters, CR-1000 datalogger (Campbell Sci. USA), and batteries), the transparent chamber made from 3-mm thick Plexiglas (Evonik Industries, Darmstadt, Germany) and opaque chamber made from white 3-mm thick PVC to facilitate net ecosystem exchange (NEE) and ecosystem respiration (Reco) fluxes measurements, respectively. The air was circulated between chambers and the gas analyzer through 5 m long Teflon tubes with the constant rate of 0.7 $L \cdot m^{-1}$. The chambers' dimensions were 0.78 × 0.78 × 0.50 m, and their volume was 0.296 m^3. Each chamber was equipped with a shielded HygroVUE™5 temperature and relative humidity sensor (Campbell Sci. the USA), 2 computer fans (1.4 W each) to mix the air in the chamber headspace, and a vent to equilibrate air pressure during measurements (Juszczak et al., 2013; Juszczak et al., 2012). The transparent chamber was equipped additionally with two SKP215 quantum sensors (Skye Instruments, UK) to measure incoming and reflected photosynthetic photon flux density (PPFD). During measurements, chambers were placed on preinstalled 20 cm high white PVC soil frames with outside dimensions 0.75 × 0.75 m inserted 15 cm deep into the peat. Sealing and tightness of the chamber were assured through the elastic rubber installed at the bottom edge of each chamber's walls.

Chamber measurements were taken every 3-5 weeks all year round (overall 10 campaigns in 2021) under sunny and cloudless conditions, and they coincided with hyperspectral measurements. Measurements started early in the morning and were continued till late afternoon for both CL and CR sites on the same days. The maximum closure time was 1.5 min and 2.5 min for NEE and Reco measurements, respectively. Considering the number of plots (9 per site) and the time needed to take the complete round (1 h per site), the measurements at the same plot were taken maximum 2 h after each other. Over the day, 3 (in winter) to 5 (in summer) complete rounds of measurements were taken for each site, resulting in 54 to 90 NEE and Reco flux rates estimations per site.

Flux rates (NEE and Reco) were calculated on the basis of CO_2 concentration change in the chamber headspace during the closure time, as described by Hoffmann et al. (2015). GPP was calculated for each plot as a sum of consecutively measured NEE and Reco (Sakowska et al., 2018). Average around midday (10,00-13:00) GPP flux rates were calculated for each plot based on 2 flux estimations from measurements taken within this time window. To calculate daily GPP, the rectangular hyperbolic light response Michaelis-Menten kinetic model was applied (as described in Hoffmann et al., 2015) based on the calculated site- and treatment-specific GPP rates (all replicates of the same treatments within each site were used) and PAR measured at the time of NEE measurements. The estimated model parameters were then used to calculate GPP based on the PAR measured with 30 min time step. The sum of half-hourly GPP fluxes cumulated over the campaign day was considered as daily GPP. The daily GPP was used for subsequent analysis because the daily carbon assimilation is more important from the ecosystem's carbon budget point of view than the midday value. Considering that the ultimate goal is to use the satellite (FLEX) SIF for monitoring global productivity and that FLEX data will be available as only a single measurement per, in the best case, 16 days, it is important to assess the value of such data for a bigger purpose, the carbon assimilation monitoring. Moreover, the correlation between instantaneous and daily GPP was assessed and was found to be very high, with r^2 0.91 and 0.86 for CL and CR sites, respectively (Supplement 4).

Light Use Efficiency (LUE) was calculated using total APAR by vegetation canopy defined as LUE_{total} in Gitelson and Gamon (2015). As the daily GPP was used for calculation, the average daily APAR was applied to determine LUE as per Eq. 1.

$$\mathrm{LUE} = \frac{daily\ GPP}{daily\ APAR} \tag{1}$$

2.7. Statistical analysis

The normality of distribution for parameters for every treatment on each day and site was checked by the Shapiro-Wilk test, and the equality of variance among treatments was checked by Bartlett's test (Bartlett, 1937; Shapiro and Wilk, 1965). The statistical significance of differences among treatments (C, W, WP) for days and sites separately was tested by one way analysis of variance (ANOVA) followed by Tukey's range test if the assumptions were fulfilled (Girden, 1992; Tukey, 1949). For the days and sites when the assumptions for ANOVA were not fulfilled, the significance of differences was examined by Kruskal-Wallis one-way analysis of variance followed by Dunn's test (Dunn, 1964; Kruskal and Wallis, 1952). All statistical tests were performed with alpha = 0.05. Because some of the collected hyperspectral measurements were of lower quality, they had to be excluded, and the number of observations per day, site, and treatment deviated from 9, which was the basic sample used for testing of statistical significance. All numbers of observations are summarized in Supplement 1.

Parameters of linear regression for GPP and SIF variables were calculated by simple linear regression. The standard error of simple linear regression was calculated as ratio of standard deviation and the square root of the sample size (10 for treatments and 30 for site). Coefficients of determination (r^2) for the relationship among GPP, VIs, and SIF parameters were determined by Pearson's correlation (Altman and Krzywinski, 2015; Wright, 1921). Normalized root mean square error (NRMSE) for relationships with GPP and LUE was calculated as the ratio of RMSE and the mean of the corresponding parameter.

All statistical analysis was carried out in RStudio version 2022.02.0 + 443 (RStudio Inc., Boston, MA, USA).

3. Results

3.1. Hydrometeorological and radiation conditions at the studied site

The average annual temperature in 2021 at C plots of the CL site was 8.0 (±0.1) °C and at the CR site 8.1 (±0.3) °C with minimal to the maximal daily average temperature range of -16.2 °C to 25.7 °C and -16.7 °C to 25.6 °C for CL and CR site, respectively. The seasonal patterns of daily mean temperature for both sites are presented in Fig. 3A. The warming induced by OTCs and infrared heaters resulted in the increase of average annual temperature to 8.4 (±0.4) °C in W and 8.6 (±0.3) °C in WP at CL site, and 8.8 (±0.2) °C in W and 8.8 (±0.3) °C in WP at CR site. The average annual increase of temperature was 0.4 °C and 0.6 °C in W plots and 0.7 °C and 0.7 °C in WP plots at CL and CR sites, respectively. However, the warming effect of OTCs was not uniform over the year. The temperature increase caused by manipulation was higher during the green-up (April-June) and senescence (September-October), lower during the peak of the season (July-August) due to relatively higher cloudiness, and the lowest during the off-season (November-March; Fig. 3A) when the days are short, and less direct irradiance is available for heating up the OTCs.

Annual precipitation in 2021 recorded in Rzecin peatland was 530.3 mm. The precipitation in WP plots was 467.6 mm, which means that the annual precipitation reduction was 11.8 %. Two periods of especially high precipitation reduction occurred during the periods of generally lower precipitation within the growing season. The drought wave occurred between the 18th of July and the 22nd of August, when the rainfall at nonmanipulated plots was 13.3 mm in 36 days. In the same period, the precipitation at WP sites was 8.3 mm, which is a 38 % reduction. The other relatively dry period occurred between 30th August and 11th October, when the precipitation in nonmanipulated plots reached 32.5 mm, but at WP plots, only 12.3 mm, which is a 62.2%

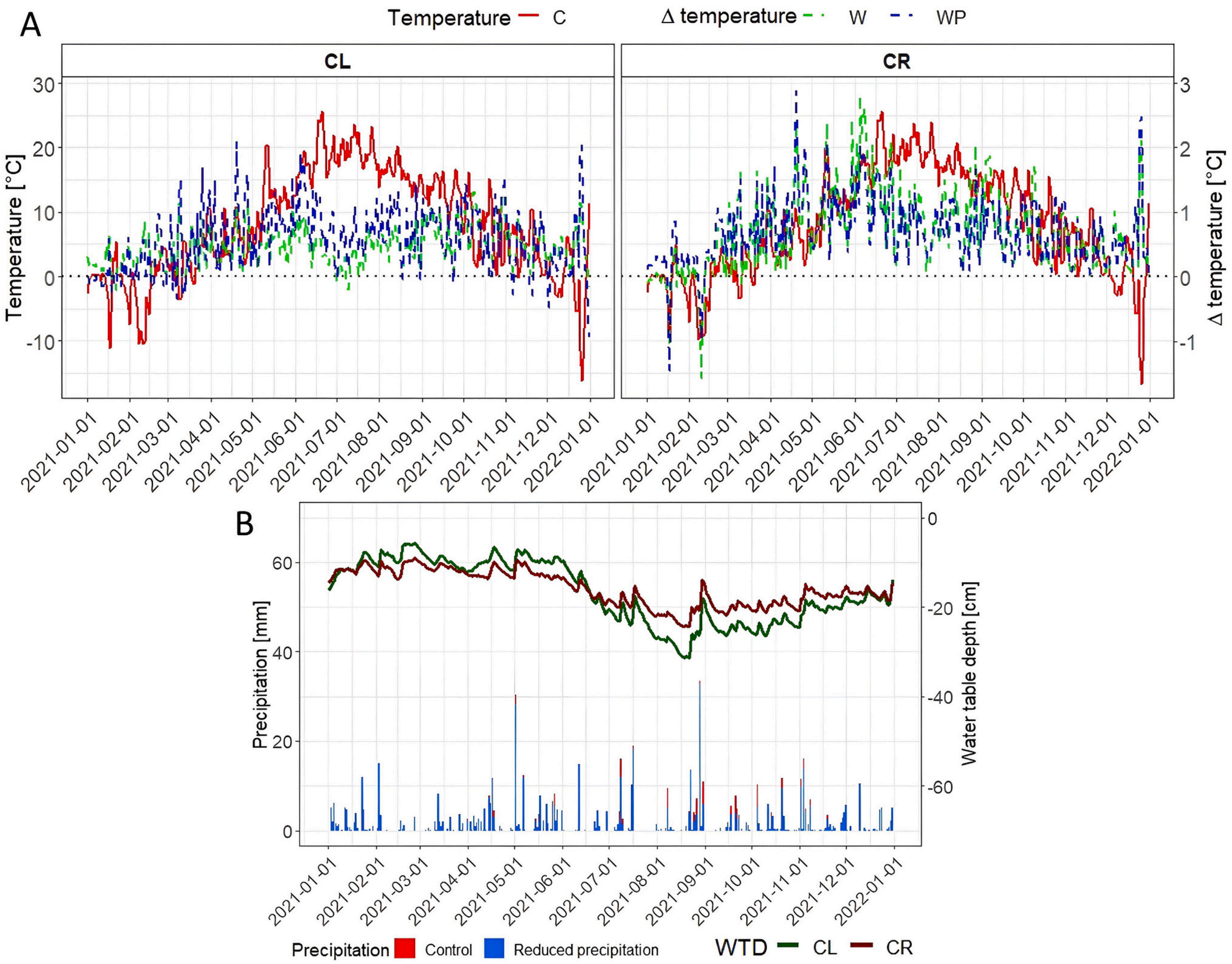

Fig. 3. (A) Average daily temperature (°C) at control (C) plots and the difference in daily average temperature (°C; Δ temperature) in warming (W), and warming and reduced precipitation (WP) plots for CL (left) and CR (right) sites; (B) average daily water table depth (cm) at CL and CR sites and the sum of daily precipitation (mm) for control and WP (reduced precipitation) plots, note: *where the bar for control (red) is not visible, control and reduced precipitation are the same; otherwise, the visible red part itself indicates the actual amount of reduced precipitation*. (For interpretation of the references to colour in this figure legend, the reader is referred to the web version of this article.)

reduction.

Although the average WTD of the two sites during the year was similar, -16.7 cm at CL and -15.8 cm at CR, the sites substantially differed in the fluctuation of WTD. Minimal and maximal daily WTD at the CL site was -31.4 cm and -5.7 cm, respectively, while WTD at the CR site oscillated between -24.4 cm and -9.0 cm.

PAR during the hyperspectral measurements at the beginning and end of the observed period showed a strong seasonality with increasing light intensity from February to the end of April and decreasing from August to December (Supplement 5). During the main vegetation season (May–August), hyperspectral measurements were taken under very similar irradiance. Even though PAR was changing within the day during the time of measurements, there are no differences in light intensity variance or statistically significant differences in PAR among treatments for most of the cases. Two exceptions of this rule occurred at the CR site when measurements on 31st May were taken at W plots under higher PAR than C and WP and on 20th December when PAR was lower for measurements at WP compared to C and W (Supplement 5, 6).

3.2. Seasonal changes in the full sun-induced fluorescence and reflectance spectrum

The changes in the average full spectrum of SIF and reflectance patterns for different treatments (C, W, WP) of both studied vegetations (CL and CR) during the year are presented in Fig. 4. The magnitude of seasonal change in the far-red spectrum region is more pronounced than in the red region of the spectrum (Fig. 4A). The peak in the far-red region was higher than the peak in the red for the whole period of measurements for both vegetation types. Climate manipulation caused a considerable change in the full SIF spectrum at the beginning (Feb-Apr) and the end (October) of the season and in June in the case of CL vegetation, but the SIF of CR vegetation subjected to manipulation was substantially higher than the SIF of C plots from the first campaign at the end of February until the beginning of October.

The characteristic spectral pattern of vegetation reflectance with low reflectance (high absorbance) of the blue and red part of the spectrum was observed for both vegetation communities from the end of May till

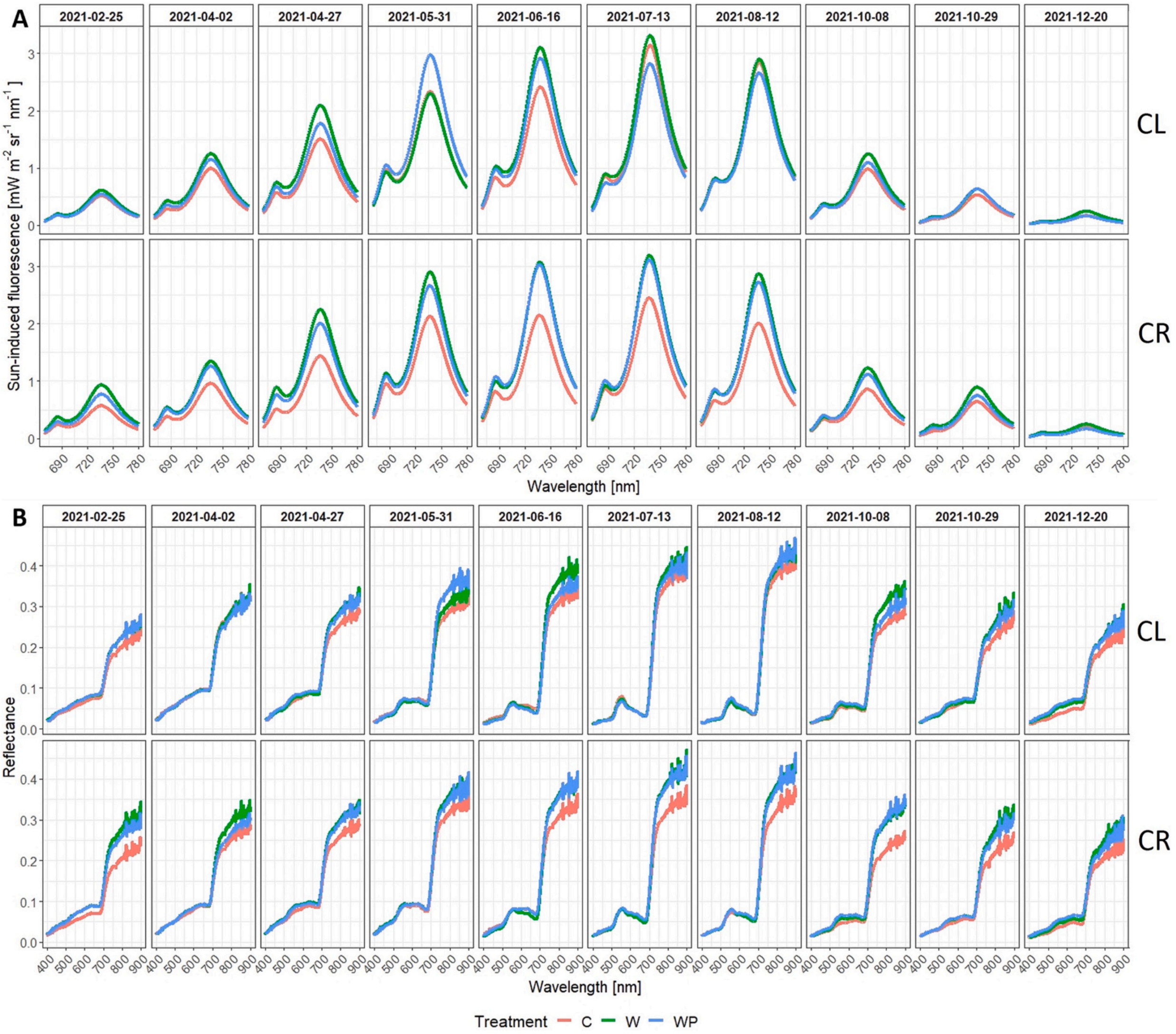

Fig. 4. Seasonal changes in (A) the full spectrum of sun-induced fluorescence ($mW{\cdot}m^{-2}{\cdot}sr^{-1}{\cdot}nm^{-1}$) and (B) reflectance of peatland vegetation communities under climate manipulation, measured around solar noon. Different days are presented in columns, and different sites in rows. C stands for control, W for warming, and WP for warming and reduced precipitation.

the beginning of October (Fig. 4B). The characteristic “red dip” was not present at the beginning and end of the season, when the photosynthetic activity of plants was minimal. The climate manipulation caused more significant changes in the red-edge (RE, 700.5-749.5 nm) and NIR (750-900 nm) region of the spectra than in visible light (VL, 400-700 nm) part of the spectra (Supplement 7 A-C).

Visible light reflectance, which is inversely proportional to the total canopy fraction of APAR (fAPAR), did not show strong seasonal variability for either of the studied vegetation communities (Supplement 7 A). The significantly higher VL reflectance due to manipulation at the CL site was recorded from August till the end of the season for WP and only in December for W. VL reflectance of CR vegetation under WP condition was significantly higher during the February, early October, and December campaigns. W caused significantly higher VL reflectance at the CR site in February but lower in June.

Overall reflectance was more influenced by NIR and RE portions of the spectra than VL part, which was expected because of half order magnitude higher NIR reflectance than VL one (Supplement 7 A-D). NIR reflectance exhibited the most substantial seasonality out of all parts of the spectra. The differences caused by manipulation were very similar for RE, NIR, and overall reflectance. Less significant changes were recorded in CL vegetation compared to CR vegetation. W and WP caused significantly higher RE, NIR, and overall reflectance during the main vegetation season (June-August) but also in February, the end of April, and the beginning of October at the CR site (Supplement 7B—D).

3.3. Effect of climate manipulation and vegetation community composition on sun-induced fluorescence parameters

The SIF full spectrum retrieval allows to assess several different parameters. The values of SIF at the peaks in the red and far-red region of the SIF spectrum and the total integrated SIF are presented in Fig. 5 A-C. All of the parameters presented in Fig. 5 show a seasonal behavior characterized by an increase in the values at the beginning and a decrease at the end of the season. The peak values of far-red and SIF total occurred in July, while red SIF peaked earlier, at the end of May.

Climate manipulation caused more significant changes in red SIF during the first half of the season than during the second half. W of CL vegetation caused significantly higher red SIF emission in April and June, while red SIF of WP plots was significantly higher only in June and significantly lower in July. In the case of CR vegetation, both types of manipulation caused significantly higher red SIF in April and June. W alone significantly increased the red SIF at the CR site at the end of February (Fig. 5A).

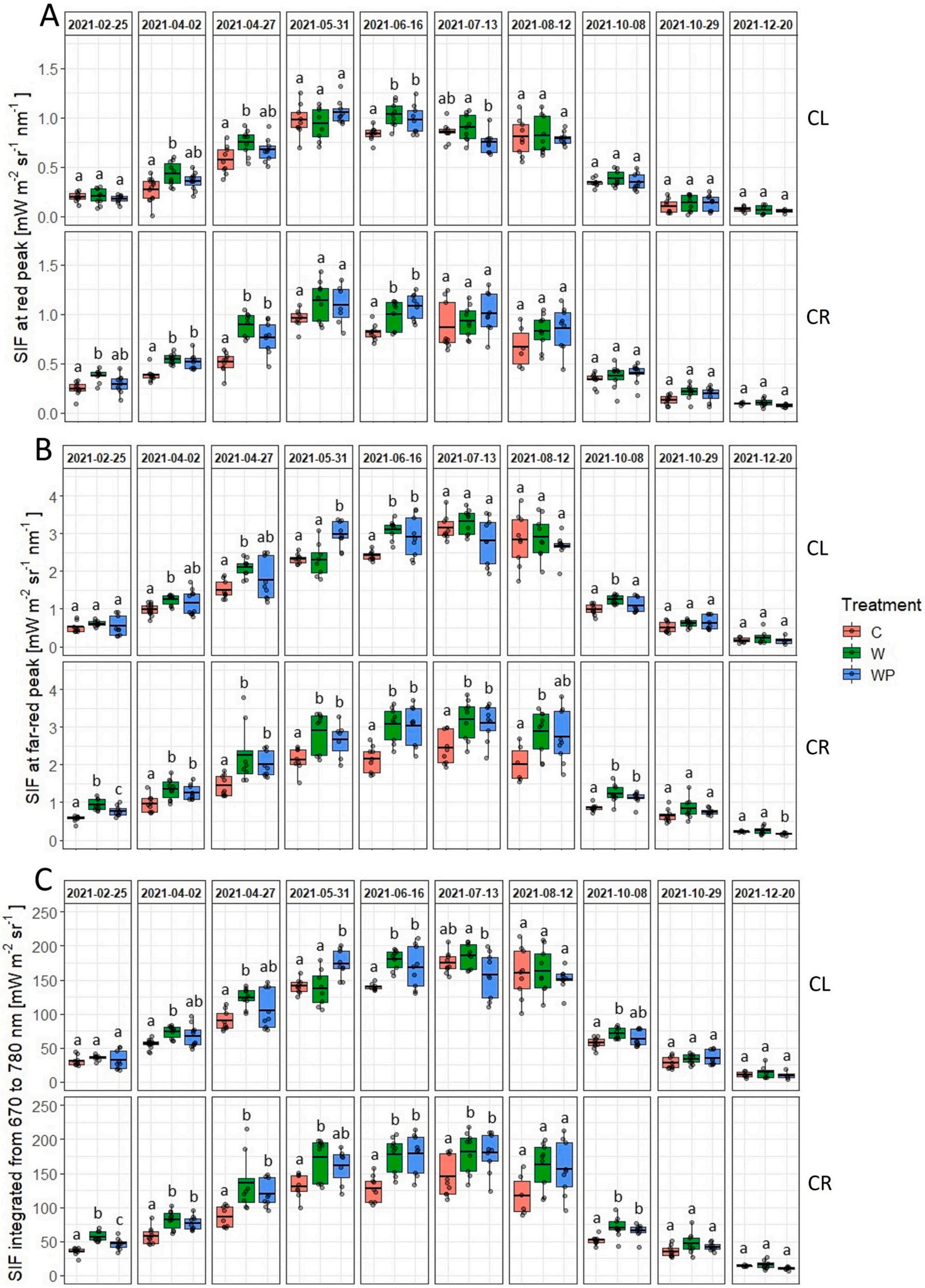

Fig. 5. Seasonal changes in A) sun-induced fluorescence (SIF) at red peak (mW·m^{-2}·sr^{-1}·nm^{-1}), B) SIF at far-red peak (mW·m^{-2}·sr^{-1}·nm^{-1}), and C) integrated full spectrum of SIF between 670 and 780 nm (mW·m^{-2}·sr^{-1}). Different days are presented in columns and different sites in rows, points represent single measurements, different letters within the same day, and site (CL or CR) represent statistically significant differences among treatments (control – C, warming – W, warming and reduced precipitation – WP) at alpha = 0.05. (For interpretation of the references to colour in this figure legend, the reader is referred to the web version of this article.)

The impact of climate manipulation on far-red and total SIF was very similar (Fig. 5B, C). In the case of CL vegetation, both parameters were significantly higher in June for both kinds of manipulation. W alone in April and the beginning of October and WP at the end of May were the cause of a significant increase of far-red and total SIF for CL vegetation. Total SIF in July was significantly lower in WP than in C. W, and WP had a more significant impact on SIF emission in CR vegetation. The total and far-red SIF of manipulated plots was higher from the beginning of measurements in February till the peak in July and then again at the beginning of October. Only far-red SIF of W was significantly higher in August for CR vegetation.

Correcting the red SIF intensity by APAR changed its seasonal pattern from the typical described above to the one with second increase at the end of the year (Supplement 8 A). The seasonality of all three presented SIF parameters was weaker for respective SIF yield than for absolute SIF value, suggesting that the majority of seasonality is driven by changes in PAR and fAPAR. Although changes in the significance of differences among treatments due to division by APAR occurred, they were only minimal, proving that the differences in SIF were not caused by differing light conditions (Fig. 5, Supplement 8).

3.4. *Influence of climate manipulation and vegetation community on gross primary production*

The maximum GPP of CR vegetation at the peak of vegetation season was lower than the GPP of CL vegetation (Fig. 6). Both sites assimilated carbon at similar rates until April and from the end of October onwards. WP plots of both sites and W of the CR site reached the maximum GPP in June, while the GPP of C at both sites and W of the CL site peaked in July. GPP of WP at the CL site was visibly higher than C or W at the end of May and in June. This was due to heterogeneity of vegetation, when annual vascular plants of WP plots started their growth more uniformly, while their spring growth in one C and W plot was slightly postponed compared to the other plots resulting in lower GPP (assessed from vegetation images taken during the campaigns that are not part of this publication). Climate manipulation caused in CR vegetation higher GPP during the green-up in May and June, but the GPP of WP was lower in August (Fig. 6).

3.5. *Correlation of remote sensing metrics with gross primary production*

Comparison of SIF retrieval methods revealed very high correlation of values with r^2 0.96 and 0.89 between SpecFit and iFLD retrieved O_2-A and O_2—B band SIF, respectively, and r^2 0.88 for both O_2 bands between SpecFit and SFM (Supplement 9). SIF retrieval by iFLD and SpecFit resulted in very similar values with a small intercept and slope over 0.9, but SIF retrieved by SFM is characterized by considerably lower values in both O_2 bands compared to SpecFit or iFLD (Supplement 9). While the correlation of GPP and LUE with O_2-A band SIF retrieved by various methods is similar, their correlation with SpecFit retrieved O_2—B band SIF was substantially higher compared with SFM or iFLD retrievals (Fig. 8A). Results of methods comparison, their comparison with GPP, and the radiance spectrum reconstruction by Specfit (Supplement 3B) reinforce the reliability of SpecFit's SIF retrieval.

The correlation of red SIF, far-red SIF, and total SIF with GPP was statistically highly significant ($p < 0.01$) for all treatments and both sites (Fig. 7). The correlation of red, far-red, and total SIF with GPP was stronger and more significant for CR than for CL vegetation (Fig. 7A-C).

The correlation slope between SIF parameters and GPP was lower for CR than CL vegetation for all parameters and all treatments (Table 2). The differences in the slope of correlation among treatments are not significant, but the trend of lower GPP with the same value of far-red and total SIF for manipulated vegetation compared to C was observed (Fig. 7B-D).

The correlation of LUE and SIF yield was weaker than the GPP and SIF correlation for all examined parameters (Supplement 10 A-C). There was no significant correlation of LUE with SIF yield at the red peak for any of the treatments at the CR site (Supplement 10 A). Correcting GPP and SIF by APAR did not reveal new significant differences in correlation among treatments or between vegetations (Table 2, Supplement 11). However, while the correlation of SIF yield parameters and LUE was comparatively much weaker than the SIF:GPP relationship in CR vegetation, it was only moderately weaker in CL vegetation.

Green biomass-related VIs like NDVI, red-edge NDVI (reNDVI), NIRv, and MERIS Terrestrial Chlorophyll Index (MTCI) show high ($\sim$0.8) r^2 for GPP of CL vegetation, but only moderate ($0.52 > r^2 > 0.42$) for GPP of CR with the exception of NIRv that shows high (0.72) r^2 also for GPP of CR vegetation (Supplement 12). Similarly to NDVI, reNDVI, or MTCI, the relationship between PRI and GPP was stronger in CL ($r^2 = 0.52$) than in CR vegetation ($r^2 = 0.34$; Fig. 8). While the red SIF peak position only weakly correlated with other studied variables, the far-red SIF peak position shows a similar relationship with GPP and other SIF parameters like "greenness" VIs (Fig. 8).

APAR measured around mid-day during SIF and reflectance

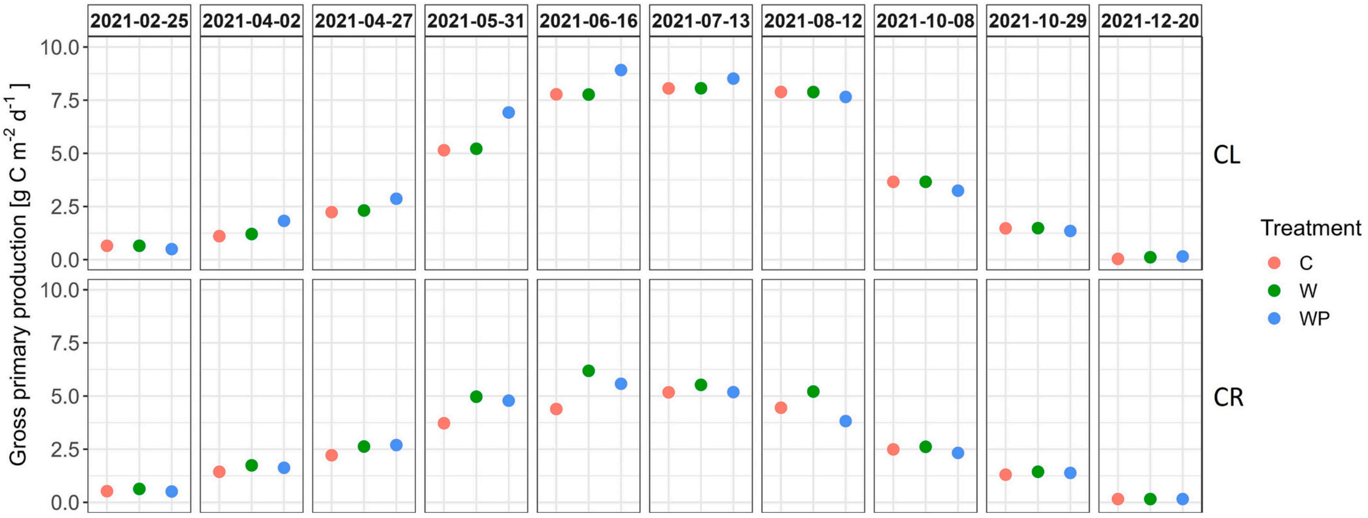

Fig. 6. Seasonal changes in daily gross primary production (g C·m^{-2}·d^{-1}) of peatland vegetation communities in control (C), warming (W), and warming and reduced precipitation (WP) treatments. Different days are presented in columns, and different sites in rows. The points represent GPP for treatment modeled based on the fluxes of all three replicates together.

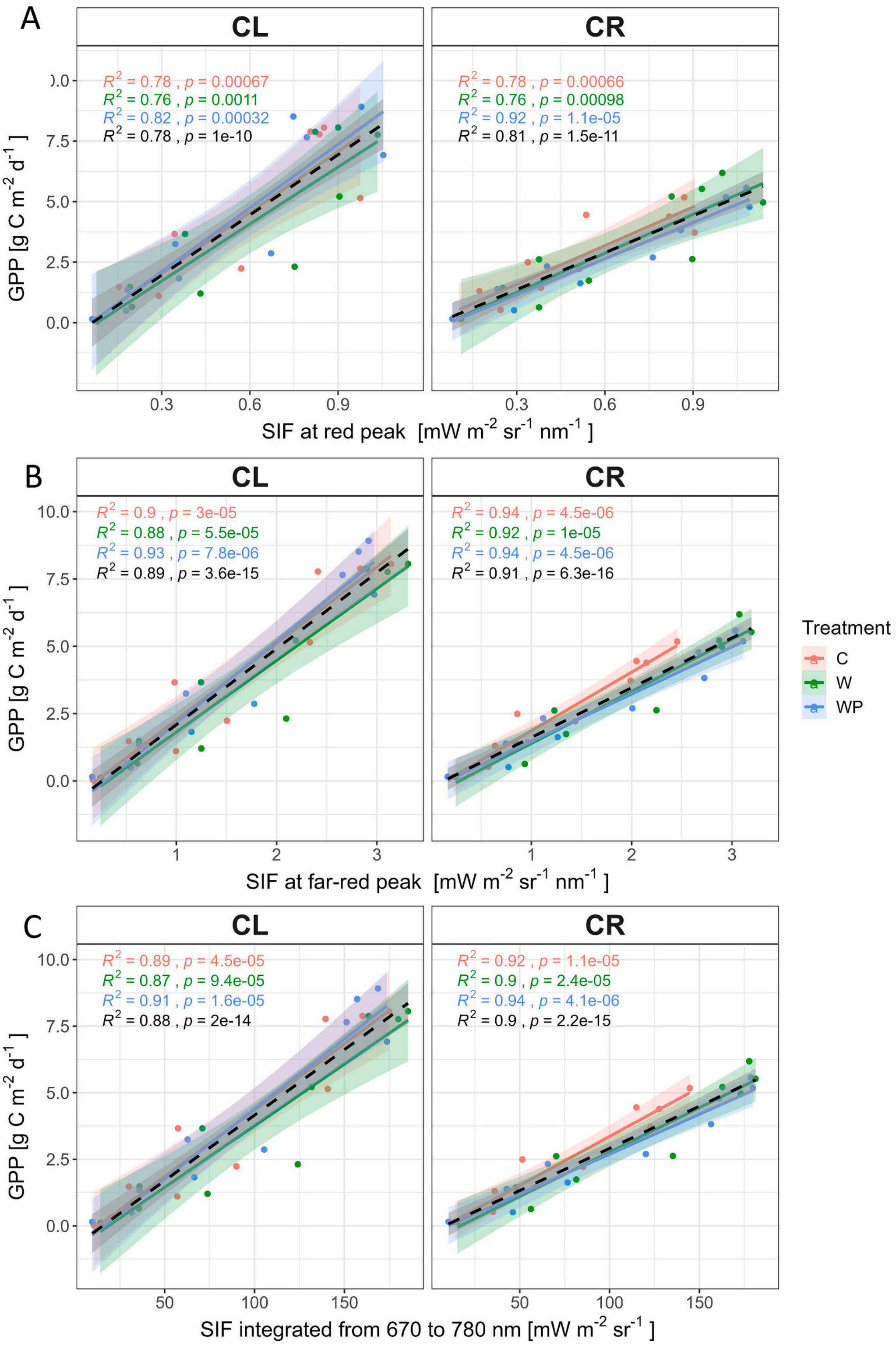

Fig. 7. Correlation of gross primary production (GPP; g C·m^{-2}·d^{-1}) with A) sun-induced fluorescence (SIF) at red peak (mW·m^{-2}·sr^{-1}·nm^{-1}), B) SIF at far-red peak (mW·m^{-2}·sr^{-1}·nm^{-1}), C), and integrated full spectrum of SIF between 670 and 780 nm (mW·m^{-2}·sr^{-1}). Different colors represent different treatments (control – C, warming – W, warming and reduced precipitation – WP), while black dashed lines and black characters represent the general relationship for vegetation community (CL or CR). The hue around the line represents the error of the linear model. n (treatment) = 10, n (site) = 30. (For interpretation of the references to colour in this figure legend, the reader is referred to the web version of this article.)

measurements, and average daily APAR were highly correlated with each other ($r^2 = 0.9$ and 0.92 for CL and CR, respectively; Fig. 8) and the r^2 for APAR to PAR correlation was 1 (data not shown). Around mid-day, APAR was strongly correlated with all SIF intensity parameters ($r^2 > 0.8$), while relatively weakly correlated with VIs ($r^2 < 0.5$). The correlation of APAR with GPP was stronger for CR vegetation than for CL vegetation (Fig. 8).

Table 2

Slope (*S*), intercept (*I*), and root mean square error (*RMSE*; $g\ C\cdot m^{-2}\cdot d^{-1}$) of the linear regression between gross primary production (GPP) and sun-induced fluorescence (SIF) in red peak (SIF R peak), in far-red peak (SIF FR peak), and integrated full spectrum between 670 and 780 nm (SIF integrated) for control (C), warming (W), warming and reduced precipitation (WP), and the whole site in general (Site) for CL and CR vegetation communities.

	C			W			WP			Site		
CL	*S*	*I*	*RMSE*	*S*	*I*	*RMSE*	*S*	I	*RMSE*	*S*	*I*	*RMSE*
GPP:SIF R peak	8.399	-0.488	1.410	7.848	-0.636	1.4803	8.771	-0.524	1.3927	8.298	-0.533	1.4578
GPP:SIF FR peak	2.842	-0.577	0.9616	2.664	-0.848	1.0311	3.030	-0.872	0.8805	2.825	-0.737	1.0118
GPP:SIF integrated	0.050	-0.640	1.0127	0.046	-0.867	1.0122	0.052	-0.858	0.9617	0.049	-0.760	1.0759
GPP:multiband SIF	0.947	0.174	0.4312	1.009	-0.073	0.1432	1.039	-0.141	0.3118	0.998	-0.007	0.3408
CR												
GPP:SIF R peak	5.103	-0.029	0.7140	5.255	-0.256	1.0247	4.880	-0.259	0.5449	4.996	-0.114	0.8071
GPP:SIF FR peak	2.137	-0.285	0.4555	1.934	-0.543	0.5776	1.751	-0.277	0.4648	1.845	-0.237	0.5785
GPP:SIF integrated	0.036	-0.255	0.4965	0.033	-0.545	0.6448	0.030	-0.296	0.4633	0.032	-0.252	0.6019
GPP:multiband SIF	-0.198	1.250	0.5386	-0.051	0.987	0.4305	-0.029	0.928	0.3611	0.061	0.981	0.4493

3.5.1. *Sun-induced fluorescence-based multiple wavelength regression*

Results of bidirectional stepwise linear regression show that out of 696 bands of full spectrum SIF, the combination of 10 bands presented in Table 3 enables to reach the highest correlation and the lowest error (assessed as RMSE). Although the last 3 of the selected bands have a small impact on the correlation of GPP and the calculated GPP from MWR (the difference in r^2 between the use of 7 and 10 bands is only 0.01), they are important for model accuracy (RMSE decreased from 0.5497 to 0.4818). The majority of the selected bands is from the far-red region of the spectrum, and only one band is from the red region (Table 3, Supplement 13).

Comparing the single band or total SIF with the MWR based on 10 bands of SIF, correlation with GPP improved for both sites and all treatments (Figs. 7 and 9). The RMSE of the model for CL vegetation improved considerably for all of the treatments. Although RMSE values of MWR for manipulation treatments and the site, in general, were lower also for the CR site, RMSE for CR C plots was higher compared to far-red and total SIF.

4. Discussion

The studies of full SIF spectrum are, up to date, scarce, and this is the first investigation of the whole season full SIF spectrum variation in a natural ecosystem of evergreen type. In this article, we evaluated the impact of climate manipulation on reflectance, SIF, GPP, and their relationships for two peatland vegetation communities.

4.1. *Dynamics of hydrometeorological conditions*

The average annual temperature measured in C plots in 2021 was 1.0 °C lower than the average of the previous 17 years. The year 2021 is in Poland, considered a year with normal temperature compared to the long-term average (1991-2020; (Miętus, 2021)). However, lake region of Poland, where the experimental site is located, has warmed up by approximately 2.0 °C since 1951, already exceeding the global target of 2.0 °C compared to the pre-industrial era, which stresses the importance of climate manipulation study in the area (Miętus, 2021).

The increase in annual temperature due to climate manipulation was higher in the CR site than CL site. This effect is due to different amounts of vascular plants' biomass in OTCs at sites. More plant biomass of CL vegetation mitigates the warming effect by higher transpiration rates than in CR canopies. The effect of vegetation on temperature increase in OTCs was observed in a number of studies before (Dabros et al., 2010; Górecki et al., 2021; Welshofer et al., 2018).

Because of, on average, a higher water table and sparser cover of vascular plants at the CR site, W, and WP conditions resulted in the same annual temperature increase. However, in the case of CL vegetation, where WTD is deeper during the growing season (Fig. 3B), the warming effect in WP plots was stronger than in W plots. This effect was expected as reduced precipitation decreases the wetness of the surface layer of peat and the moisture availability for peat mosses. The drier mosses have a lower capacity to cool down by evaporation, and their temperature rises, which causes an increase in the air temperature, too (Blok et al., 2011). In addition, *Vaccinium oxycoccos* has a shallow root system, and a drier peat surface layer decreases the amount of available water (Jacquemart, 1997). Consequently, the leaf cooling by transpiration is lower, and their surface temperature increases.

The annual precipitation in 2021 was 69.8 mm lower than the long-term (2004-2020) average in the studied area, although the year is considered normal in regard to annual precipitation (Miętus, 2021). The nighttime precipitation reduction resulted in only an 11.8% annual reduction, but it considerably impacted rainfall during the summer period, when drought waves occurred (Fig. 3B). The predicted changes in precipitation do not show a high reduction in terms of annual rainfall but rather an increase in precipitation extremes. Our climate manipulation is, therefore, fitting well with the latest predictions about the future with more pronounced droughts (Calvin et al., 2023).

Varying fluctuation in WTD impacts peatlands in multiple ways. More pronounced fluctuation results in a higher decomposition rate and release of mineral nutrients, which in turn increase the growth of vascular plants (Blodau and Moore, 2003; Breeuwer et al., 2009; Górecki et al., 2021; Malmer et al., 2003). This effect is visible in our two sites, where the CL site with stronger WTD oscillation hosts more vascular plants by biomass and species richness than the CR site with lower WTD changes (Fig. 3B).

The intensity of solar irradiance is changing during the year, which is also shown in our measurements by Piccolo Doppio (Supplement 5). Although there is an increase and decrease in PAR at the beginning and end of the season, respectively, little change among campaigns during the peak of the season was observed. This was caused by a deviation of data acquisition time around the mid-day and offers a perfect opportunity to compare the SIF in the peak season period as the differences in SIF intensity are caused only by vegetation and solar zenith angle and not by different illumination intensities. Due to diurnal changes in solar irradiance, it was impossible to measure all 18 experimental plots with the same illumination. However, the measurements were done within 1.5 h around the noon, and no differences in light intensity variance or statistically significant differences in PAR among treatments were found for most of the cases, with two exceptions at the CR site mentioned in section 3.1 of the results (Supplement 5, 6).

4.2. *Dynamics of SIF during the season*

Cogliati et al. (2019) identified in their work three different patterns of the SIF spectrum during the season for the field of forage. At the beginning of the season, when the vegetation cover was low, the intensity of red peak SIF was higher than the intensity of far-red peak SIF. With the growth of plants, the two peaks show similar magnitudes, and later on, far-red SIF dominated the spectrum. In our work, we did not observe a SIF spectrum with the red SIF intensity higher than the far-red

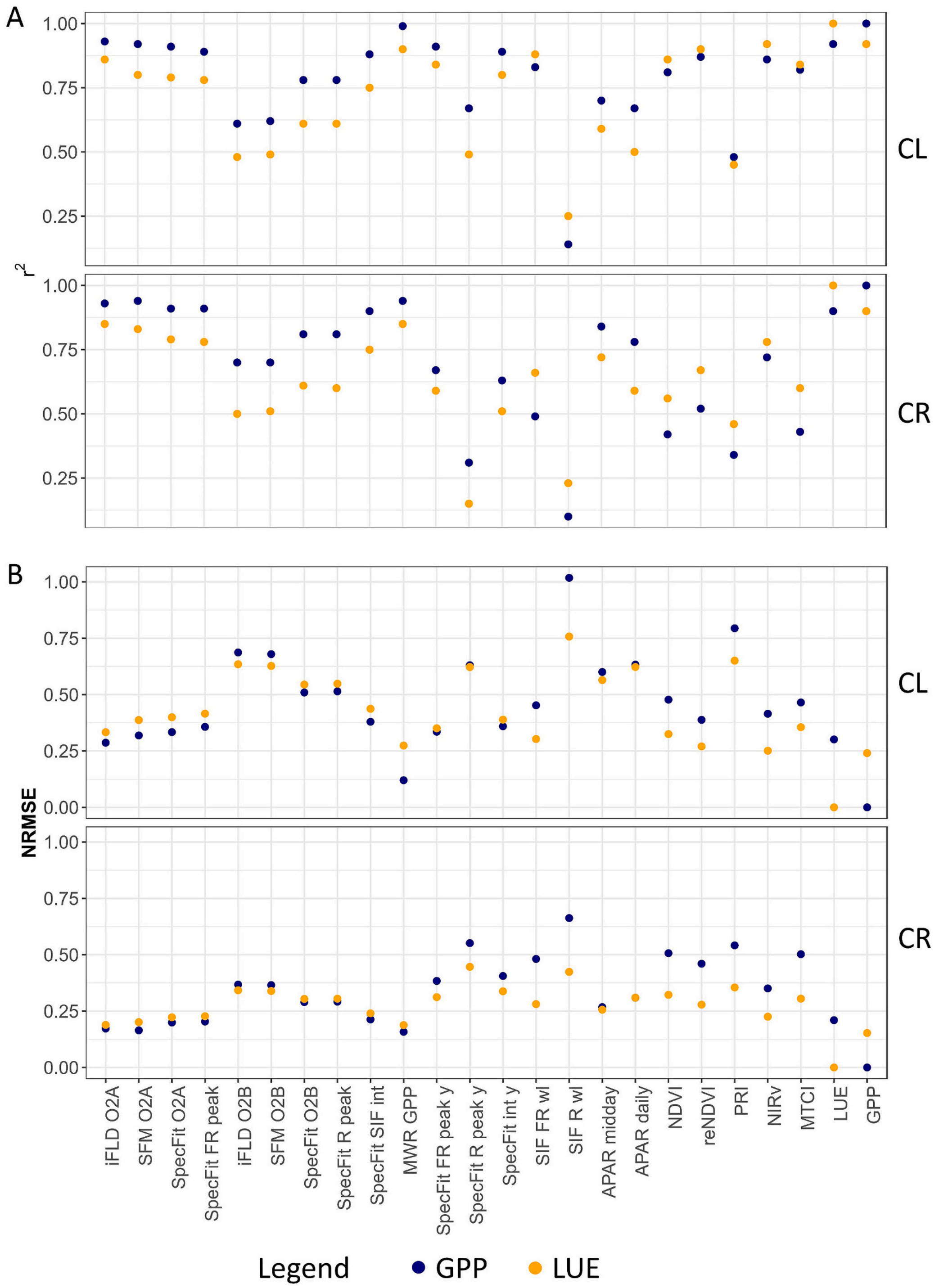

Fig. 8. (A) Coefficients of determination (r^2) for Pearson's correlations and (B) normalized root mean square error (NRMSE) of linear regression between gross primary production (GPP; blue) or light use efficiency (LUE; yellow) and among sun-induced fluorescence (SIF) at O_2-A band retrieved by iFLD (iFLD_O2A), SIF at O_2-A band retrieved by SFM (SFM_O2A), SIF at O_2-A band retrieved by SpecFit (SpecFit_O2A), SIF at far-red peak retrieved by SpecFit (SpecFit_FR_peak), SIF at O_2—B band retrieved by iFLD (iFLD_O2B), SIF at O_2—B band retrieved by SFM (SFM_O2B), SIF at O_2—B band retrieved by SpecFit (SpecFit_O2B), SIF at red peak retrieved by SpecFit (SpecFit_R_peak), integrated full spectrum SIF between 670 and 780 nm (SpecFit_SIF_int), gross primary production modeled by multiple-wavelength regression (MWR_GPP), SIF by SPecFit yield at far-red peak (SIF_FR_peak_y), SIF by SPecFit yield at red peak (SIF_R_peak_y), SIF by SPecFit yield integrated between 670 and 780 nm (SIF_int_y), the position of the far-red peak of SIF spectrum by SPecFit (SIF_FR_wl), the position of the red peak of SIF spectrum by SPecFit (SIF_R_wl), around mid-day absorbed photosynthetically active radiation measured at the time of spectral measurements (APAR_midday), average daily APAR (APAR_daily), Normalized Difference Vegetation Index (NDVI), red-edge NDVI (reNDVI), Phytochemical Reflectance Index (PRI), Near-Infrared Reflectance of vegetation (NIRv), MERRIS Terrestrial Chlorophyll Index (MTCI), light use efficiency (LUE) and GPP. All measurement days and all nine plots for every site are considered regardless of treatment. (For interpretation of the references to colour in this figure legend, the reader is referred to the web version of this article.)

Table 3
The wavelengths of the SIF spectrum used for the multiple wavelength regression ordered by importance based on stepwise linear regression with r^2 and root mean square error (RMSE; g C·m^{-2}·d^{-1}) of gross primary production prediction for each quantity of bands.

Number of bands	1	2	3	4	5	6	7	8	9	10
Wavelength	778.9	722.8	669.9	741.3	772.9	736.2	724.7	757.8	750	743.8
r^2	0.836	0.911	0.931	0.947	0.954	0.959	0.963	0.966	0.970	0.973
RMSE	1.0935	0.8123	0.7223	0.6377	0.5978	0.5699	0.5497	0.5260	0.5057	0.4818

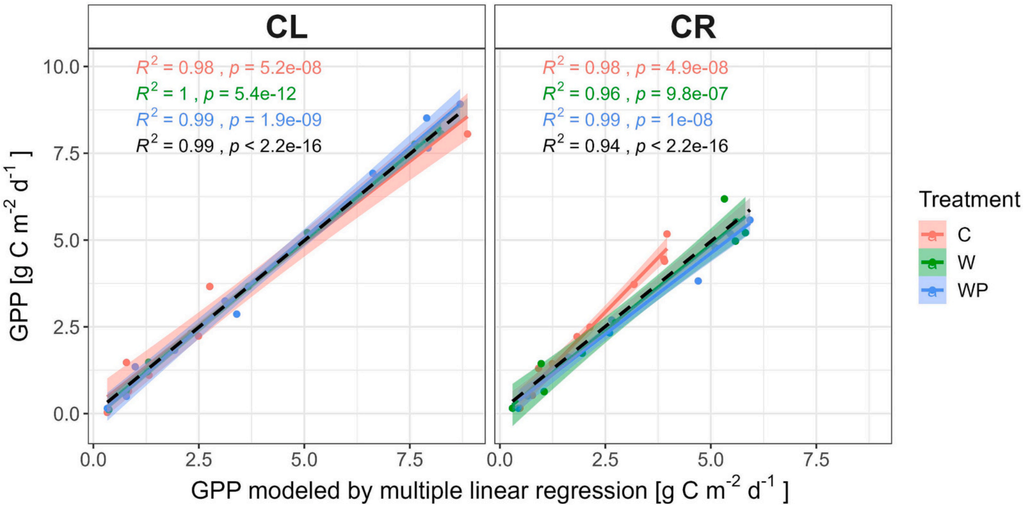

Fig. 9. Correlation of gross primary production (GPP; g C·m^{-2}·d^{-1}) with GPP (GPP; g C·m^{-2}·d^{-1}) modeled by multiple wavelength regression based on selected sun-induced fluorescence bands. Different colors represent different treatments (control – C, warming – W, warming and reduced precipitation – WP), while black dashed lines and black characters represent the general relationship for vegetation community (CL or CR). The hue around the line represents the standard error of the linear model. n (treatment) = 10, n (site) = 30.

SIF intensity (Fig. 3). This is because, in the canopy of peatland vegetation, there are plants with green leaves absorbing the majority of PAR at any time of the year (Fig. 2, Supplement 7 A), and red fluorescence is always reabsorbed, keeping the red peak SIF observed at ToC always at low values. Our results are similar to those obtained from needles of Scotch pine (*Pinus sylvestris* L.), which suggests that the seasonal pattern of the full SIF spectrum for evergreen ecosystems evolves similarly (Zhang et al., 2019a).

The two peaks of the SIF spectrum reached their maximum values at different times of the year. While the red peak culminated in May, when the maximum growth of vegetation occurs, the far-red SIF peak reached the maximum in July with the maximal plant biomass (Fig. 2g, q, 5A, B). Such results are expected at the ToC level as the reabsorption of red SIF within the canopy gets stronger with the increase of chlorophyll content and does not allow for more red light to escape. ToC intensity of far-red SIF, which is rather scattered than reabsorbed, increases with the increased green biomass, as more green biomass means more SIF emission per area (Porcar-Castell et al., 2021; Rascher et al., 2021). As the far-red peak is in evergreen ecosystems always dominant, the total SIF pattern over the year is mostly determined by it (Fig. 3; Zhang et al., 2019a). This is in contrast to agricultural crops and may decrease the value of total SIF for such ecosystems' observation (Cogliati et al., 2019). The observed increase in SIF intensity due to climate manipulation (Fig. 5A-C) was caused by the change in the biomass of vascular plants and the earlier start of photosynthetic activity in warmer conditions (Antala et al., 2022). The significant impact of W and WP on red and far-red SIF of peatland vegetation during the spring green-up proves the sooner start of photosynthetic activity (Fig. 5A, B). Temperature increase caused more considerable changes in CR vegetation than in CL vegetation, as visible at far-red SIF, RE, and NIR reflectance (Fig. 5B, Supplement 7B—C). The cover of vascular plants in CR vegetation is sparser than in CL vegetation (Fig. 2); therefore, the same absolute increase in biomass results in a higher relative increase (Rastogi et al., 2022). It is important to keep in mind that the changes in vegetation on studied sites are not the result of one but four years of manipulation. Also, the temperature is not the only factor influencing the growth of plants. Peatlands are nutrient, mostly nitrogen and phosphorus, -limited ecosystems. When the maximal biomass possible due to nutrient abundance is reached, plants' growth ceases (Salmon et al., 2021). This seems to be a case of CL vegetation, where the peak values of SIF parameters are similar for all treatments (Fig. 5). However, at the beginning of the season, when the nutrient availability is the highest, increased temperature enhances the development of plants (Koebsch et al., 2020), as in the case of CL vegetation in June (Fig. 5B, C). Nevertheless, SIF provides only indirect evidence, and the analysis of available nutrients in the peat should be performed to validate the hypothesis about the effect of nutrients on the measured signals in CL vegetation. Far-red SIF, RE, and NIR reflectance of CR vegetation under manipulation were significantly higher for almost the whole vegetation season, which leads us to the conclusion that climate warming causes significant structural changes in this peatland vegetation community that is characterized by a lower abundance of graminoids and a higher abundance of *Sphagnum* spp. and *Ericaceae* shrubs.

4.3. Relationship between optical remote sensing parameters and GPP

The correlation between SIF and GPP was examined in various ecosystems at different scales (Dechant et al., 2020; Liu et al., 2019; Martini et al., 2022; Migliavacca et al., 2017; Pierrat et al., 2022; Xu et al., 2021), but is underexplored for peatlands. We investigated the relationship of different parameters derived from the SIF full spectrum with the GPP of two peatland vegetation communities under C, W, and WP conditions.

Although red SIF at the photosystem level is considered a better proxy of GPP than far-red SIF (Liu et al., 2020), the correlation of red SIF with GPP at ToC-level in the seasonal course is weaker (Figs. 7, 8) compared to far-red SIF. The cause of the weaker correlation lies in strong reabsorption by green vegetation. Reabsorption of red SIF prevents the proportional increase together with GPP as vegetation grows. On the contrary, the intensity of far-red SIF that is mainly scattered within the canopy increases with GPP and growing vegetation (Goulas et al., 2017).

Far-red SIF is a good proxy of APAR, which largely determines also carbon assimilation rate (Magney et al., 2019; Wieneke et al., 2018). Therefore, it is not a surprise that the most widely used SIF parameter is the intensity of SIF in the far-red region band, typically in the O_2-A band (Mohammed et al., 2019). In our work, we used the SIF at the far-red peak instead because it provides a better idea about the far-red SIF intensity and is well correlated with SIF in the O_2-A band (Cogliati et al., 2019). Based on our results, far-red SIF is the best correlated remote sensing-based signal with GPP of peatland vegetation, with a very strong correlation characterized by the r^2 equal to 0.88 and 0.91 (far-red SIF peak) for CL and CR vegetation, respectively (Fig. 8). Similarly, a very strong correlation between SIF and GPP at a seasonal scale was found for deciduous and evergreen forests and agricultural fields (Goulas et al., 2017; Pierrat et al., 2022; Yang et al., 2015). However, the correlation decreases with the finer temporal resolution because of the stronger contribution of light intensity and plant physiology (Pierrat et al., 2022). The relationship between SIF and GPP shifts from non-linear to linear when the temporal resolution is lower because of the stronger effect of APAR and the lower effect of plant physiology (Li et al., 2020; Pierrat et al., 2022; Wieneke et al., 2018). That is the reason for the observed linearity of correlation in this and many other studies examining the SIF: GPP relationship over a longer time period (Goulas et al., 2017; Migliavacca et al., 2017; Pierrat et al., 2022). When the data is forced to a non-linear model, the correlation decreases, and the error increases compared to linear regression (data not shown).

Total SIF is, in the case of an evergreen ecosystem, determined mostly by the far-red peak (Zhang et al., 2019a). Therefore, the correlation of total SIF and GPP is very similar to far-red SIF:GPP correlation (Fig. 7B, C, 8) and the use of total SIF for estimation of peatland vegetation GPP, and likely the GPP of all evergreen ecosystems, seems to not bring advantage over the use of far-red peak SIF intensity in the statistical model. Moreover, SIF at the O_2A band was found to be the best correlating studied parameter with GPP, suggesting that for statistical modeling of peatland GPP, full SIF spectrum is not necessary and simpler retrieval methods, such as iFLD or SFM, can be used (Fig. 8). However, total SIF is necessary for the mechanistic linkage of SIF with photosynthesis and the assessment of carbon assimilation through mechanistic modeling (Gu et al., 2019; Liu et al., 2022). Even if the use of a mechanistic light-response model, as suggested by Gu et al. (2019), is, at the moment, not possible for complex peatland vegetation due to the lack of knowledge about different steps in the process of photosynthesis for specific peatland plants like peat mosses, the work like this improve our understanding of using SIF for peatland photosynthesis monitoring.

As already demonstrated by previous studies, using multiple bands from the whole SIF spectrum improves the correlation and the predictive power of the statistical model for GPP compared to single-band models (Liu et al., 2019; Verrelst et al., 2016b). However, those studies considered only 6-7 SIF parameters, while in our study, we retrieved the full SIF spectrum with hundreds of bands (696). Similarly to hyperspectral reflectance, hyperspectral SIF contains too many bands for the statistical model because of too many possible combinations and very similar information carried by multiple bands. Therefore, the number of bands reduction to only those carrying important information is necessary (Verrelst et al., 2016a). We found out that the use of 10 bands from across the SIF spectrum in MWR provides the most accurate GPP estimation with similar results irrespective of site (RMSE 0.3408 and 0.4493 for CL and CR, respectively). These results differ from the use of a single SIF parameter in the ordinary linear regression model, where the error was almost two times higher for the CL site for all three tested SIF parameters (Table 2). As mentioned above, several bands of hyperspectral reflectance, or SIF, carry very similar information. Based on our tests, changing the band by ±10 bands (which is ±1.5 nm in the spectrum) compared to the band indicated in Table 3 yields the model without considerable change in performance (data not shown). Therefore, the bands presented in Table 3 represent portions of SIF spectra as wide as 3 nm with the center around the indicated wavelength rather than the exact bands. This is important information considering that 2 out of 3 most important bands are at the very edges of the retrieved spectrum and shows that if one retrieves the full spectrum with a slightly narrower window, the MWR approach will still be a valuable tool for GPP estimation.

Our results from two peatland vegetation communities are similar to those from the deciduous forest by Liu et al. (2019) or SCOPE simulations by Verrelst et al. (2016b), which indicated the best results using a combination of red, far-red, and water vapor (around 720 nm) bands. Our stepwise linear regression results show that the 3 most important parts of SIF spectra are indeed in the right shoulder of the far-red peak, water vapor band region, and left shoulder of the red peak, in the mentioned order. The addition of another band from the water vapor band region, 2 bands from around the far-red peak, and 4 bands from the right shoulder of the far-red peak further improved the model accuracy (Table 3). This strong far-red portion of SIF domination is probably caused by the evergreen nature of the peatland ecosystem, where far-red peak always dominates the SIF spectrum, and may be different for annual crops that exhibited different behavior (Cogliati et al., 2019). However, the low presence of bands from the red peak and valley between peaks portion of SIF spectra could be partially caused by inherited lower accuracy of SpecFit retrieval in these regions when LAI and leaf chlorophyll content are low, which was the case of our vegetation at the beginning and the end of the year (first and last two campaigns; Cogliati et al., 2019).

Based on our results, traditional green biomass-related VIs, like NDVI, reNDVI, or MTCI, correlate well with GPP in the case of CL vegetation but not in CR vegetation. However, a relatively newer VI, NIRv, correlates well with GPP and even better with a more physiologically-related parameter, LUE, for both vegetation communities (Fig. 8). A good correlation of NIRv with SIF and GPP for different vegetation communities is in concordance with previous research (Badgley et al., 2017; Dechant et al., 2020; Zeng et al., 2019). However, Maguire et al. (2021) found a weak correlation between SIF and NIRv for northern peatlands when measured one time and not over the whole season, suggesting that more data need to be acquired for a better mechanistic understanding of this relationship. Other presented indices seem to be not sensitive enough to smaller changes in green biomass to show a strong correlation with GPP. Therefore, the use of SIF instead of reflectance-based VIs for peatland vegetation productivity brings more consistent results, as also found in the study of boreal forest by Pierrat et al. (2022).

Exclusion of APAR effect on SIF:GPP correlation resulted in a comparatively weaker relationship in the case of CR vegetation than in CL vegetation, as visible at the decrease of r^2 from 0.81, 0.91, and 0.90 to 0.15, 0.59, and 0.51 for red, far-red and total SIF:GPP and SIF yield:LUE, respectively in CR compared to decrease from 0.77, 0.88, and 0.87 to 0.49, 0.83, and 0.80 for red, far-red and total SIF:GPP and SIF yield:LUE, respectively in CL (Fig. 8). Mid-day APAR showed a very strong correlation with SIF intensity parameters for both vegetation communities. The very strong correlation of APAR with GPP and substantial decrease in correlation described above for CR vegetation suggest that the seasonal relationship of SIF and GPP for this vegetation community is almost exclusively driven by changes in light intensity with little contribution by vegetation, which is different from CL vegetation (Fig. 8). A closer examination of treatments at the CR site separately (discussed more below) revealed that the original, C, plots exhibit the weakest correlations of SIF yield with LUE, most likely due to the lowest share of vascular plants (Supplement 10). This finding suggests that a high enough biomass of vascular plants is necessary for vegetation to have a significant effect on SIF:GPP relationship on a seasonal scale.

Far-red SIF peak position, which most probably depends on the reabsorption in the red-edge region and, ultimately, vegetation architecture, shows a relationship with GPP and other SIF parameters similar to NDVI, reNDVI, and MTCI that depend on the same vegetation properties. The shift of far-red peak position to longer wavelengths with increasing green biomass is in concordance with the results of Zhao et al. (2020), who found a similar trend at the leaf level with increasing chlorophyll content. Interestingly, the far-red SIF peak position correlates better with LUE than with GPP in both vegetation communities, indicating that chlorophyll content rather than light intensity causes changes in the far-red SIF peak position (Fig. 8). However, Zhao et al. (2020) reported a significant impact of PAR on the SIF peaks position. The possible explanation for these different findings is different spatial and temporal scales. While PAR has an effect on SIF peak positions when the same leaf is measured within hours, its effect seems to be low at the canopy level over the season timespan.

Climate manipulation's impact on the correlation of GPP with SIF parameters was unsubstantial. The warming of <1.0 °C on an annual average does not cause a strong enough physiological response to impact the relationship of light and dark reactions of photosynthesis like a short-term high increase in temperature does (Martini et al., 2022). Despite the climate manipulation caused changes in the intensity of SIF, these were mostly followed by increased carbon assimilation, which suggests that the climate-induced changes in peatland vegetation photosynthesis are mediated by the green biomass of vascular plants (Figs. 5, 6, 7). Absolute SIF intensity and absolute GPP on a seasonal scale are driven mainly by APAR, which fluctuates during the year due to incoming PAR and the growth of plants. Therefore, SIF yield and LUE are usually calculated to retrieve more vegetation physiology-related information and reveal the effect of stress (Li et al., 2020; Xu et al., 2021). Red SIF yield:LUE correlation for both vegetation as well as far-red and total SIF yield:LUE correlations for CL vegetation and manipulated plots of CR vegetation showed, similarly to SIF:GPP correlations, no significant differences among treatments (Fig. 7A-C, Supplement 10 A-C). We can only hypothesize that the difference in far-red and total SIF:LUE relationship between C and manipulated plots at the CR site, as well as the weaker correlation of C compared to manipulated plots, is caused by higher (higher than in CL vegetation and higher than in manipulated plots) share of *Sphagnum* spp. mosses in C plots. More elaborated conclusions can be drawn only after a more detailed investigation of SIF, GPP, SIF yield, and LUE seasonal patterns for peat mosses that remain unexplored. ToC SIF in the far-red region can be further adjusted for within-canopy scattering and reabsorption (Yang et al., 2020; Zeng et al., 2019). However, our results did not show any advantage of such correction for the understanding of the differences between sites and among treatments (data not shown).

SIF emission is nearly Lambertian, meaning that SIF is emitted in all directions at the same intensity (Rascher et al., 2021). However, with a higher share of plants with erectophile leaf orientation, like *Carex* spp., in vegetation canopy, the scattering and reabsorption are higher (Knyazikhin et al., 2013). This results in similar SIF intensity at the ToC for plots of CR site with lower leaf biomass but more leaves with planophile orientation and CL vegetation with higher leaf biomass but more leaves with erectophile orientation (Figs. 2, 5). Contrary to SIF, canopy-level carbon assimilation is a simple sum of single leaves' carbon assimilation (Dechant et al., 2020). Therefore, the GPP of CL vegetation is higher than that of CR vegetation, especially during the main vegetation season (summer, Fig. 5). The abovementioned phenomena are the reason for the different slopes of the SIF parameters and GPP correlations for two studied peatland vegetations when a steeper slope is generally observed for CL vegetation (Table 2, Fig. 7). Similar results of the varying slope of SIF:GPP correlation with the changing vegetation composition from planophile to erectophile was reported for Mediterranean savannah vegetation (Migliavacca et al., 2017). SIF yield:LUE correlations exhibited a similar difference in the slope of the linear model between the two examined vegetation communities (Supplement 11).

5. Conclusions and future perspectives

We examined, for the first time, the temporal evolution of the full SIF spectrum, hyperspectral reflectance, and carbon assimilation for the peatland ecosystem, which was, in addition, under climate manipulation. Our results suggest that in this natural ecosystem with an evergreen nature, the intensity of SIF in the far-red region is always higher than in the red region, which differs from agricultural fields of annual crops. The climate manipulation caused significant changes in the SIF and reflectance spectrum, especially for CR vegetation, which is characterized by a higher share of low creeping shrubs and peat mosses and more pronounced changes in plant biomass due to higher temperature. We showed that the domination of peatland by vascular plants that is expected due to future warmer conditions causes stronger seasonal variation of SIF, reflectance, and GPP.

Based on our results, SIF in the far-red region (peak or O_2A band retrieved by different methods) is the most suitable SIF parameter for the assessment of peatland's GPP by a statistical, linear, model. Far-red SIF is especially useful for peatland vegetation GPP monitoring when the share of erectophile vascular plants is low, as in the case of the CR site in this study. However, when the vascular plants' share is too low, such a relationship is driven mostly by APAR, which largely depends on the green biomass amount. Although ToC far-red SIF is very well correlated with the GPP of peatland vegetation on a seasonal scale, red SIF may provide better information about the actual state of the photosynthetic apparatus, especially if an accurate correction for reabsorption is developed. Full spectrum SIF can be in the future used for GPP calculation directly, using a mechanistic approach connecting light and dark phases of photosynthesis.

The strong correlation of far-red SIF and GPP stayed unchanged under W and WP conditions. The differences between the two studied vegetation communities caused by different hydrology were more prominent than the impact of climate manipulation treatments. It is important to mention that because of the campaign-based measurements and the need for merging plots of the same treatment for modeling GPP, we were limited in the correlation of SIF parameters and GPP only to the seasonal scale. The possible short-term changes in the SIF: GPP relationship for peatland vegetation due to stress caused by heat or drought waves remain to be investigated. We demonstrated that the use of the MWR model trained on SIF bands chosen by stepwise linear regression allows for higher accuracy in the estimation of GPP compared to the use of single bands or integrated total SIF value. Moreover, such a model has a more stable performance when transferring from one vegetation community to another. However, there is a need for more data across various ecosystems to evaluate and optimize the MWR as a universal statistical model for the estimation of GPP from FLEX satellite data.

CRediT authorship contribution statement

Michal Antala: Conceptualization, Data curation, Formal analysis, Investigation, Methodology, Writing – original draft. **Anshu Rastogi:** Conceptualization, Funding acquisition, Project administration, Supervision, Formal analysis, Investigation, Resources, Visualization, Writing – review & editing. **Sergio Cogliati:** Conceptualization, Supervision, Methodology, Software, Writing – review & editing. **Marcin Stróżecki:** Supervision, Investigation, Methodology, Writing – review & editing. **Roberto Colombo:** Writing – review & editing. **Radosław Juszczak:** Conceptualization, Funding acquisition, Project administration, Resources, Supervision, Visualization, Writing – review & editing.

Declaration of Competing Interest

Anshu Rastogi reports financial support was provided by National Science Centre Poland. Michal Antala reports financial support was provided by European Cooperation in Science and Technology. Radoslaw Juszczak reports financial support was provided by National Science Centre Poland. If there are other authors, they declare that they have no known competing financial interests or personal relationships that could have appeared to influence the work reported in this paper.

Data availability

Data will be made available on request.

Acknowledgement

The authors would like to thank Mar Albert Saíz and Maria del Pilar Cendrero Mateo for their help with the data analysis.

This research was supported by the National Science Centre of Poland (NCN) within grants No. 2016/21/B/ST10/02271 and 2020/37/B/ST10/01213, Polish National Agency for Academic Exchange (NAWA) within the Bekker Programme grant No. PPN/BEK/2019/1/00090, and the Action CA17134 SENSECO (Optical synergies for spatiotemporal sensing of scalable ecophysiological traits) funded by COST (European Cooperation in Science and Technology, www.cost.eu). The publication was financed within the framework of the Polish Ministry of Science and Higher Education's Program: "Regional Excellence Initiative" in the years 2019-2023 with grant No. 005/RID/2018/19.

Appendix A. Supplementary data

Supplementary data to this article can be found online at https://doi.org/10.1016/j.rse.2023.113921.

References

Acosta, M., Juszczak, R., Chojnicki, B., Pavelka, M., Havránková, K., Lesny, J., Krupková, L., Urbaniak, M., Machačová, K., Olejnik, J., 2017. CO2 fluxes from different vegetation communities on a peatland ecosystem. Wetlands 37, 423–435. https://doi.org/10.1007/s13157-017-0878-4.

Alonso, L., Gómez-Chova, L., Vila-Francés, J., Amorós-López, J., Guanter, L., Calpe, J., Moreno, J., 2008. Improved fraunhofer line discrimination method for vegetation fluorescence quantification. IEEE Geosci. Remote Sens. Lett. 5, 620–624. https://doi.org/10.1109/LGRS.2008.2001180.

Altman, N., Krzywinski, M., 2015. Points of significance: simple linear regression. Nat. Methods 12, 999–1000. https://doi.org/10.1038/nmeth.3627.

Antala, M., Juszczak, R., van der Tol, C., Rastogi, A., 2022. Impact of climate change-induced alterations in peatland vegetation phenology and composition on carbon balance. Sci. Total Environ. 827, 154294 https://doi.org/10.1016/j.scitotenv.2022.154294.

Badgley, G., Field, C.B., Berry, J.A., 2017. Canopy near-infrared reflectance and terrestrial photosynthesis. Sci. Adv. 3, 1–6. https://doi.org/10.1126/sciadv.1602244.

Bai, J., Zhang, H., Sun, R., Li, X., Xiao, J., Wang, Y., 2022. Estimation of global GPP from GOME-2 and OCO-2 SIF by considering the dynamic variations of GPP-SIF relationship. Agric. For. Meteorol. 326, 109180 https://doi.org/10.1016/j.agrformet.2022.109180.

Bandopadhyay, S., Rastogi, A., Rascher, U., Rademske, P., Schickling, A., Cogliati, S., Julitta, T., Arthur, A. Mac, Hueni, A., Tomelleri, E., Celesti, M., Burkart, A., Strózecki, M., Sakowska, K., Gabka, M., Rosadziński, S., Sojka, M., Iordache, M.D., Reusen, I., Van Der Tol, C., Damm, A., Schuettemeyer, D., Juszczak, R., 2019. Hyplant-derived Sun-induced fluorescence-a new opportunity to disentangle complex vegetation signals from diverse vegetation types. Remote Sens. (Basel) 11. https://doi.org/10.3390/rs11141691.

Bandopadhyay, S., Rastogi, A., Juszczak, R., 2020. Review of top-of-canopy sun-induced fluorescence (SIF) studies from ground, uav, airborne to spaceborne observations. Sensors (Switzerland) 20. https://doi.org/10.3390/s20041144.

Bao, T., Jia, G., Xu, X., 2022. Warming enhances dominance of vascular plants over cryptogams across northern wetlands. Glob. Chang. Biol. 28, 4097–4109. https://doi.org/10.1111/gcb.16182.

Bartlett, M.S., 1937. Properties of sufficiency and statistical tests. Proc. R. Soc. Lond. A Math. Phys. Sci. 160, 268–282. https://doi.org/10.2307/96803.

Blodau, C., Moore, T.R., 2003. Experimental response of peatland carbon dynamics to a water table fluctuation. Aquat. Sci. 65, 47–62. https://doi.org/10.1007/s000270300004.

Blok, D., Heijmans, M.M.P.D., Schaepman-Strub, G., van Ruijven, J., Parmentier, F.J.W., Maximov, T.C., Berendse, F., 2011. The cooling capacity of mosses: controls on water and energy fluxes in a Siberian tundra site. Ecosystems 14, 1055–1065. https://doi.org/10.1007/s10021-011-9463-5.

Bragazza, L., Buttler, A., Robroek, B.J.M., 2016. Persistent high temperature and low precipitation reduce peat carbon accumulation. Glob. Chang. Biol. 22, 4114–4123. https://doi.org/10.1111/gcb.13319.

Breeuwer, A., Robroek, B.J.M., Limpens, J., Heijmans, M.M.P.D., Schouten, M.G.C., Berendse, F., 2009. Decreased summer water table depth affects peatland vegetation. Basic Appl Ecol 10, 330–339. https://doi.org/10.1016/j.baae.2008.05.005.

Calvin, K., Dasgupta, D., Krinner, G., Mukherji, A., Thorne, P.W., Trisos, C., Romero, J., Aldunce, P., Barrett, K., Blanco, G., Cheung, W.W.L., Connors, S., Denton, F., Diongue-Niang, A., Dodman, D., Garschagen, M., Geden, O., Hayward, B., Jones, C., Jotzo, F., Krug, T., Lasco, R., Lee, Y.-Y., Masson-Delmotte, V., Meinshausen, M., Mintenbeck, K., Mokssit, A., Otto, F.E.L., Pathak, M., Pirani, A., Poloczanska, E., Pörtner, H.-O., Revi, A., Roberts, D.C., Roy, J., Ruane, A.C., Skea, J., Shukla, P.R., Slade, R., Slangen, A., Sokona, Y., Sörensson, A.A., Tignor, M., van Vuuren, D., Wei, Y.-M., Winkler, H., Zhai, P., Zommers, Z., Hourcade, J.-C., Johnson, F.X., Pachauri, S., Simpson, N.P., Singh, C., Thomas, A., Totin, E., Alegría, A., Armour, K., Bednar-Friedl, B., Blok, K., Cissé, G., Dentener, F., Eriksen, S., Fischer, E., Garner, G., Guivarch, C., Haasnoot, M., Hansen, G., Hauser, M., Hawkins, E., Hermans, T., Kopp, R., Leprince-Ringuet, N., Lewis, J., Ley, D., Ludden, C., Niamir, L., Nicholls, Z., Some, S., Szopa, S., Trewin, B., van der Wijst, K.-I., Winter, G., Witting, M., Birt, A., Ha, M., 2023. Climate change 2023: synthesis report. In: Contribution of Working Groups I, II and III to the Sixth Assessment Report of the Intergovernmental Panel on Climate Change. https://doi.org/10.59327/IPCC/AR6-9789291691647.

Cendrero-Mateo, M.P., Wieneke, S., Damm, A., Alonso, L., Pinto, F., Moreno, J., Guanter, L., Celesti, M., Rossini, M., Sabater, N., Cogliati, S., Julitta, T., Rascher, U., Goulas, Y., Aasen, H., Pacheco-Labrador, J., Arthur, A. Mac, 2019. Sun-induced chlorophyll fluorescence III: benchmarking retrieval methods and sensor characteristics for proximal sensing. Remote Sens. (Basel) 11. https://doi.org/10.3390/rs11080921.

Chatterjee, S., Hadi, A.S. (Eds.), 2012. Regression Analysis by Example, 5th ed. Wiley. https://doi.org/10.1080/02664763.2013.817041.

Cogliati, S., Verhoef, W., Kraft, S., Sabater, N., Alonso, L., Vicent, J., Moreno, J., Drusch, M., Colombo, R., 2015. Retrieval of sun-induced fluorescence using advanced spectral fitting methods. Remote Sens. Environ. 169, 344–357. https://doi.org/10.1016/j.rse.2015.08.022.

Cogliati, S., Celesti, M., Cesana, I., Miglietta, F., Genesio, L., Julitta, T., Schuettemeyer, D., Drusch, M., Rascher, U., Jurado, P., Colombo, R., 2019. A spectral fitting algorithm to retrieve the fluorescence spectrum from canopy radiance. Remote Sens. (Basel) 11. https://doi.org/10.3390/rs11161840.

Cox, P.M., Betts, R.A., Jones, C.D., Spall, S.A., Totterdell, I.J., 2000. Acceleration of global warming due to carbon-cycle feedbacks in a coupled climate model. Nature 408, 184–187. https://doi.org/10.1038/35041539.

Dabros, A., Fyles, J.W., Strachan, I.B., 2010. Effects of open-top chambers on physical properties of air and soil at post- disturbance sites in northwestern Quebec. Plant and Soil 333, 203–218. https://doi.org/10.1007/s11104-010-0336-z.

Damm, A., Cogliati, S., Colombo, R., Fritsche, L., Genangeli, A., Genesio, L., Hanus, J., Peressotti, A., Rademske, P., Rascher, U., Schuettemeyer, D., Siegmann, B., Sturm, J., Miglietta, F., 2022. Response times of remote sensing measured sun-induced chlorophyll fluorescence, surface temperature and vegetation indices to evolving soil water limitation in a crop canopy. Remote Sens. Environ. 273, 112957 https://doi.org/10.1016/j.rse.2022.112957.

Dash, J., Curran, P.J., 2004. The MERIS terrestrial chlorophyll index. Int. J. Remote Sens. 25, 5403–5413. https://doi.org/10.1080/0143116042000274015.

Dechant, B., Ryu, Y., Badgley, G., Zeng, Y., Berry, J.A., Zhang, Y., Goulas, Y., Li, Z., Zhang, Q., Kang, M., Li, J., Moya, I., 2020. Canopy structure explains the relationship between photosynthesis and sun-induced chlorophyll fluorescence in crops. Remote Sens. Environ. 241 https://doi.org/10.1016/j.rse.2020.111733.

Dieleman, C.M., Branfireun, B.A., Mclaughlin, J.W., Lindo, Z., 2015. Climate change drives a shift in peatland ecosystem plant community: implications for ecosystem function and stability. Glob. Chang. Biol. 21, 388–395. https://doi.org/10.1111/gcb.12643.

Drusch, M., Moreno, J., Del Bello, U., Franco, R., Goulas, Y., Huth, A., Kraft, S., Middleton, E.M., Miglietta, F., Mohammed, G., Nedbal, L., Rascher, U., Schüttemeyer, D., Verhoef, W., 2017. Concept — ESA ' s Earth Explorer 8. IEEE Trans. Geosci. Remote Sens. 55, 1273–1284.

Dunn, O.J., 1964. Multiple comparisons using rank sums. Technometrics 6, 241–252.

Gamon, J.A., Peñuelas, J., Field, C.B., 1992. A narrow-waveband spectral index that tracks diurnal changes in photosynthetic efficiency. Remote Sens. Environ. 41, 35–44. https://doi.org/10.1016/0034-4257(92)90059-S.

Gao, H., Liu, S., Lu, W., Smith, A.R., Valbuena, R., Yan, W., Wang, Z., Xiao, L., Peng, X., Li, Q., Feng, Y., McDonald, M., Pagella, T., Liao, J., Wu, Z., Zhang, G., 2021. Global analysis of the relationship between reconstructed solar-induced chlorophyll fluorescence (Sif) and gross primary production (gpp). Remote Sens. (Basel) 13. https://doi.org/10.3390/rs13142824.

Girden, E.R., 1992. ANOVA : Repeated Measures, Sage University Paper series on Quantitative Applications in the Social Sciences, series no. 07-084. Sage Publications, Inc., Newbury Park, CA.

Gitelson, A.A., Gamon, J.A., 2015. The need for a common basis for defining light-use efficiency: implications for productivity estimation. Remote Sens. Environ. 156, 196–201. https://doi.org/10.1016/j.rse.2014.09.017.

Gitelson, A., Merzlyak, M.N., 1994. Quantitative estimation of chlorophyll-a using reflectance spectra: experiments with autumn chestnut and maple leaves.

J. Photochem. Photobiol. B 22, 247–252. https://doi.org/10.1016/1011-1344(93)06963-4.

Górecki, K., Rastogi, A., Stróżecki, M., Gąbka, M., Lamentowicz, M., Łuców, D., Kayzer, D., Juszczak, R., 2021. Water table depth, experimental warming, and reduced precipitation impact on litter decomposition in a temperate Sphagnum-peatland. Sci. Total Environ. 771 https://doi.org/10.1016/j.scitotenv.2021.145452.

Goulas, Y., Fournier, A., Daumard, F., Champagne, S., Ounis, A., Marloie, O., Moya, I., 2017. Gross primary production of a wheat canopy relates stronger to far red than to red solar-induced chlorophyll fluorescence. Remote Sens. (Basel) 9, 97. https://doi.org/10.3390/rs9010097.

Gu, L., Han, J., Wood, J.D., Chang, C.Y.Y., Sun, Y., 2019. Sun-induced Chl fluorescence and its importance for biophysical modeling of photosynthesis based on light reactions. New Phytol. 223, 1179–1191. https://doi.org/10.1111/nph.15796.

Harenda, K.M., Samson, M., Juszczak, R., Markowicz, K.M., Stachlewska, I.S., Kleniewska, M., Macarthur, A., Schüttemeyer, D., Chojnicki, B.H., 2021. Impact of atmospheric optical properties on net ecosystem productivity of peatland in Poland. Remote Sens. (Basel) 13, 1–22. https://doi.org/10.3390/rs13112124.

Hoffmann, M., Jurisch, N., Albiac Borraz, E., Hagemann, U., Drösler, M., Sommer, M., Augustin, J., 2015. Automated modeling of ecosystem CO2 fluxes based on periodic closed chamber measurements: a standardized conceptual and practical approach. Agric. For. Meteorol. 200, 30–45. https://doi.org/10.1016/j.agrformet.2014.09.005.

Jacquemart, A.-L., 1997. Vaccinium Oxycoccos L. (Oxycoccus Palustris Pers.) and *Vaccinium Microcarpum* (Turcz. ex Rupr.) Schmalh. (Oxycoccus Microcarpus Turcz. ex Rupr.). J. Ecol. 85, 381. https://doi.org/10.2307/2960511.

Juszczak, R., Acosta, M., Olejnik, J., 2012. Comparison of daytime and nighttime ecosystem respiration measured by the closed chamber technique on a temperate mire in Poland. Pol. J. Environ. Stud. 21, 643–658.

Juszczak, R., Humphreys, E., Acosta, M., Michalak-Galczewska, M., Kayzer, D., Olejnik, J., 2013. Ecosystem respiration in a heterogeneous temperate peatland and its sensitivity to peat temperature and water table depth. Plant and Soil 366, 505–520. https://doi.org/10.1007/s11104-012-1441-y.

Juszczak, R., Uździcka, B., Stróżecki, M., Sakowska, K., 2018. Improving remote estimation of winter crops gross ecosystem production by inclusion of leaf area index in a spectral model. PeerJ 2018. https://doi.org/10.7717/peerj.5613.

Kalaji, H.M., Schansker, G., Ladle, R.J., Goltsev, V., Bosa, K., Allakhverdiev, S.I., Brestic, M., Bussotti, F., Calatayud, A., Dąbrowski, P., Elsheery, N.I., Ferroni, L., Guidi, L., Hogewoning, S.W., Jajoo, A., Misra, A.N., Nebauer, S.G., Pancaldi, S., Penella, C., Poli, D., Pollastrini, M., Romanowska-Duda, Z.B., Rutkowska, B., Serôdio, J., Suresh, K., Szulc, W., Tambussi, E., Yanniccari, M., Zivcak, M., 2014. Frequently asked questions about in vivo chlorophyll fluorescence: practical issues. Photosynth. Res. 122, 121–158. https://doi.org/10.1007/s11120-014-0024-6.

Knyazikhin, Y., Schull, M.A., Stenberg, P., Mõttus, M., Rautiainen, M., Yang, Y., Marshak, A., Carmona, P.L., Kaufmann, R.K., Lewis, P., Disney, M.I., Vanderbilt, V., Davis, A.B., Baret, F., Jacquemoud, S., Lyapustin, A., Myneni, R.B., 2013. Hyperspectral remote sensing of foliar nitrogen content. Proc. Natl. Acad. Sci. U. S. A. 110, 1–8. https://doi.org/10.1073/pnas.1210196109.

Koebsch, F., Sonnentag, O., Järveoja, J., Peltoniemi, M., Alekseychik, P., Aurela, M., Arslan, A.N., Dinsmore, K., Gianelle, D., Helfter, C., Jackowicz-Korczynski, M., Korrensalo, A., Leith, F., Linkosalmi, M., Lohila, A., Lund, M., Maddison, M., Mammarella, I., Mander, Ü., Minkkinen, K., Pickard, A., Pullens, J.W.M., Tuittila, E., Nilsson, M.B., Peichl, M., 2020. Refining the role of phenology in regulating gross ecosystem productivity across European peatlands. Glob. Chang. Biol. 0–3 https://doi.org/10.1111/gcb.14905.

Kruskal, W.H., Wallis, W.A., 1952. Use of ranks in one-criterion variance analysis. J. Am. Stat. Assoc. 47, 583–621. https://doi.org/10.1080/01621459.1952.10483441.

Lamentowicz, M., Mueller, M., Gałka, M., Barabach, J., Milecka, K., Goslar, T., Binkowski, M., 2015. Reconstructing human impact on peatland development during the past 200 years in CE Europe through biotic proxies and X-ray tomography. Quat. Int. 357, 282–294. https://doi.org/10.1016/j.quaint.2014.07.045.

Lamentowicz, M., Gałka, M., Marcisz, K., Słowinski, M., Kajukało-Drygalska, K., Dayras, M.D., Jassey, V.E.J., 2019. Unveiling tipping points in long-term ecological records from Sphagnum-dominated peatlands. Biol. Lett. 15 https://doi.org/10.1098/rsbl.2019.0043.

Li, X., Xiao, J., He, B., Altaf Arain, M., Beringer, J., Desai, A.R., Emmel, C., Hollinger, D.Y., Krasnova, A., Mammarella, I., Noe, S.M., Ortiz, P.S., Rey-Sanchez, A.C., Rocha, A.V., Varlagin, A., 2018. Solar-induced chlorophyll fluorescence is strongly correlated with terrestrial photosynthesis for a wide variety of biomes: first global analysis based on OCO-2 and flux tower observations. Glob. Chang. Biol. 24, 3990–4008. https://doi.org/10.1111/gcb.14297.

Li, Z., Zhang, Q., Li, J., Yang, X., Wu, Y., Zhang, Z., Wang, S., Wang, H., Zhang, Y., 2020. Solar-induced chlorophyll fluorescence and its link to canopy photosynthesis in maize from continuous ground measurements. Remote Sens. Environ. 236 https://doi.org/10.1016/j.rse.2019.111420.

Liu, X., Liu, L., Zhang, S., Zhou, X., 2015. New spectral fitting method for full-spectrum solar-induced chlorophyll fluorescence retrieval based on principal components analysis. Remote Sens. (Basel) 7, 10626–10645. https://doi.org/10.3390/rs70810626.

Liu, Z., Lu, X., An, S., Heskel, M., Yang, H., Tang, J., 2019. Advantage of multi-band solar-induced chlorophyll fluorescence to derive canopy photosynthesis in a temperate forest. Agric. For. Meteorol. 279, 107691 https://doi.org/10.1016/j.agrformet.2019.107691.

Liu, X., Liu, L., Hu, J., Guo, J., Du, S., 2020. Improving the potential of red SIF for estimating GPP by downscaling from the canopy level to the photosystem level. Agric. For. Meteorol. 281, 107846 https://doi.org/10.1016/j.agrformet.2019.107846.

Liu, Z., Zhao, F., Liu, X., Yu, Q., Wang, Y., Peng, X., Cai, H., Lu, X., 2022. Direct estimation of photosynthetic CO2 assimilation from solar-induced chlorophyll fluorescence (SIF). Remote Sens. Environ. 271, 112893 https://doi.org/10.1016/j.rse.2022.112893.

Lu, X., Liu, Z., An, S., Miralles, D.G., Maes, W., Liu, Y., Tang, J., 2018. Potential of solar-induced chlorophyll fluorescence to estimate transpiration in a temperate forest. Agric. For. Meteorol. 252, 75–87. https://doi.org/10.1016/j.agrformet.2018.01.017.

MacArthur, A., Robinson, I., Rossini, M., Davis, N., MacDonald, K., 2014. Edinburgh Research Explorer A dual-field-of-view spectrometer system for reflectance and fluorescence measurements (Piccolo Doppio) and correction of etaloning Citation for published version: A DUAL-FIELD-OF-VIEW SPECTROMETER SYSTEM FOR REFLECTANCE AND FL. Proceedings of the Fifth International Workshop on Remote Sensing of Vegetation Fluorescence, 22-24 APRIL 2014, PARIS (FRANCE), pp. 1–8.

Magney, T.S., Frankenberg, C., Köhler, P., North, G., Davis, T.S., Dold, C., Dutta, D., Fisher, J.B., Grossmann, K., Harrington, A., Hatfield, J., Stutz, J., Sun, Y., Porcar-Castell, A., 2019. Disentangling changes in the spectral shape of chlorophyll fluorescence: implications for remote sensing of photosynthesis. Eur. J. Vasc. Endovasc. Surg. 124, 1491–1507. https://doi.org/10.1029/2019JG005029.

Maguire, A.J., Eitel, J.U.H., Magney, T.S., Frankenberg, C., Köhler, P., Orcutt, E.L., Parazoo, N.C., Pavlick, R., Pierrat, Z.A., 2021. Spatial covariation between solar-induced fluorescence and vegetation indices from Arctic-Boreal landscapes. Environ. Res. Lett. 16 https://doi.org/10.1088/1748-9326/ac188a.

Malmer, N., Albinsson, C., Svensson, B.M., Wallén, B., 2003. Interferences between Sphagnum and vascular plants: effects on plant community structure and peat formation. Oikos 100, 469–482. https://doi.org/10.1034/j.1600-0706.2003.12170.x.

Martini, D., Sakowska, K., Wohlfahrt, G., Pacheco-Labrador, J., van der Tol, C., Porcar-Castell, A., Magney, T.S., Carrara, A., Colombo, R., El-Madany, T.S., Gonzalez-Cascon, R., Martín, M.P., Julitta, T., Moreno, G., Rascher, U., Reichstein, M., Rossini, M., Migliavacca, M., 2022. Heatwave breaks down the linearity between sun-induced fluorescence and gross primary production. New Phytol. 233, 2415–2428. https://doi.org/10.1111/nph.17920.

McPartland, M.Y., Falkowski, M.J., Reinhardt, J.R., Kane, E.S., Kolka, R., Turetsky, M.R., Douglas, T.A., Anderson, J., Edwards, J.D., Palik, B., Montgomery, R.A., 2019. Characterizing boreal peatland plant composition and species diversity with hyperspectral remote sensing. Remote Sens. (Basel) 11. https://doi.org/10.3390/rs11141685.

Meroni, M., Colombo, R., 2006. Leaf level detection of solar induced chlorophyll fluorescence by means of a subnanometer resolution spectroradiometer. Remote Sens. Environ. 103, 438–448. https://doi.org/10.1016/j.rse.2006.03.016.

Meroni, M., Rossini, M., Guanter, L., Alonso, L., Rascher, U., Colombo, R., Moreno, J., 2009. Remote sensing of solar-induced chlorophyll fluorescence: review of methods and applications. Remote Sens. Environ. 113, 2037–2051. https://doi.org/10.1016/j.rse.2009.05.003.

Meroni, M., Busetto, L., Colombo, R., Guanter, L., Moreno, J., Verhoef, W., 2010. Performance of spectral fitting methods for vegetation fluorescence quantification. Remote Sens. Environ. 114, 363–374. https://doi.org/10.1016/j.rse.2009.09.010.

Miętus, M., 2021. Climate of Poland 2021. Polish Climate Monitoring Bulletin.

Migliavacca, M., Perez-Priego, O., Rossini, M., El-Madany, T.S., Moreno, G., van der Tol, C., Rascher, U., Berninger, A., Bessenbacher, V., Burkart, A., Carrara, A., Fava, F., Guan, J.H., Hammer, T.W., Henkel, K., Juarez-Alcalde, E., Julitta, T., Kolle, O., Martín, M.P., Musavi, T., Pacheco-Labrador, J., Pérez-Burgueño, A., Wutzler, T., Zaehle, S., Reichstein, M., 2017. Plant functional traits and canopy structure control the relationship between photosynthetic CO2 uptake and far-red sun-induced fluorescence in a Mediterranean grassland under different nutrient availability. New Phytol. 214, 1078–1091. https://doi.org/10.1111/nph.14437.

Milecka, K., Kowalewski, G., Fiałkiewicz-Kozieł, B., Gałka, M., Lamentowicz, M., Chojnicki, B.H., Goslar, T., Barabach, J., 2017. Hydrological changes in the Rzecin peatland (Puszcza Notecka, Poland) induced by anthropogenic factors: implications for mire development and carbon sequestration. Holocene 27, 651–664. https://doi.org/10.1177/0959683616670468.

Mohammed, G.H., Colombo, R., Middleton, E.M., Rascher, U., van der Tol, C., Nedbal, L., Goulas, Y., Pérez-Priego, O., Damm, A., Meroni, M., Joiner, J., Cogliati, S., Verhoef, W., Malenovský, Z., Gastellu-Etchegorry, J.P., Miller, J.R., Guanter, L., Moreno, J., Moya, I., Berry, J.A., Frankenberg, C., Zarco-Tejada, P.J., 2019. Remote sensing of solar-induced chlorophyll fluorescence (SIF) in vegetation: 50 years of progress. Remote Sens. Environ. 231, 111177 https://doi.org/10.1016/j.rse.2019.04.030.

Nichols, J.E., Peteet, D.M., 2019. Rapid expansion of northern peatlands and doubled estimate of carbon storage. Nat. Geosci. 12, 917–921. https://doi.org/10.1038/s41561-019-0454-z.

Norby, R.J., Childs, J., Hanson, P.J., Warren, J.M., 2019. Rapid loss of an ecosystem engineer: Sphagnum decline in an experimentally warmed bog. Ecol. Evol. 9, 12571–12585. https://doi.org/10.1002/ece3.5722.

Pierrat, Z., Magney, T., Parazoo, N.C., Grossmann, K., Bowling, D.R., Seibt, U., Johnson, B., Helgason, W., Barr, A., Bortnik, J., Norton, A., Maguire, A., Frankenberg, C., Stutz, J., 2022. Diurnal and seasonal dynamics of solar-induced chlorophyll fluorescence, vegetation indices, and gross primary productivity in the boreal Forest. Eur. J. Vasc. Endovasc. Surg. 127 https://doi.org/10.1029/2021JG006588.

Porcar-Castell, A., Tyystjärvi, E., Atherton, J., Van Der Tol, C., Flexas, J., Pfündel, E.E., Moreno, J., Frankenberg, C., Berry, J.A., 2014. Linking chlorophyll a fluorescence to photosynthesis for remote sensing applications: mechanisms and challenges. J. Exp. Bot. 65, 4065–4095. https://doi.org/10.1093/jxb/eru191.

Porcar-Castell, A., Malenovský, Z., Magney, T., Van Wittenberghe, S., Fernández-Marín, B., Maignan, F., Zhang, Y., Maseyk, K., Atherton, J., Albert, L.P., Robson, T. M., Zhao, F., Garcia-Plazaola, J.I., Ensminger, I., Rajewicz, P.A., Grebe, S., Tikkanen, M., Kellner, J.R., Ihalainen, J.A., Rascher, U., Logan, B., 2021. Chlorophyll a fluorescence illuminates a path connecting plant molecular biology to Earth-system science. Nat Plants 7, 998–1009. https://doi.org/10.1038/s41477-021-00980-4.

Rascher, U., Acebron, K., Bendig, J., Krämer, J., Krieger, V., Quiros-Vargas, J., Siegmann, B., Muller, O., 2021. Measuring and understanding the dynamics of solar-induced fluorescence (Sif) and its relation to photochemical and non-photochemical energy dissipation – scaling leaf level regulation to canopy and ecosystem remote sensing. International Geoscience and Remote Sensing Symposium (IGARSS) 203–206. https://doi.org/10.1109/IGARSS47720.2021.9554870.

Rastogi, A., Antala, M., Prikaziuk, E., Yang, P., van der Tol, C., Juszczak, R., 2022. Exploring the potential of SCOPE model for detection of leaf area index and Sun-induced fluorescence of peatland canopy. Remote Sens. (Basel) 14, 4010. https://doi.org/10.3390/rs14164010.

Rossini, M., Nedbal, L., Guanter, L., Ač, A., Alonso, L., Burkart, A., Cogliati, S., Colombo, R., Damm, A., Drusch, M., Hanus, J., Janoutova, R., Julitta, T., Kokkalis, P., Moreno, J., Novotny, J., Panigada, C., Pinto, F., Schickling, A., Schüttemeyer, D., Zemek, F., Rascher, U., 2015. Red and far red Sun-induced chlorophyll fluorescence as a measure of plant photosynthesis. Geophys. Res. Lett. 42, 1632–1639. https://doi.org/10.1002/2014GL062943.

Rouse, J.W., Haas, R.H., Schell, J.A., Deering, D.W., 1974. Monitoring vegetation systems in the great plains with ERTS. In: Freden, S.C., Mercanti, E.P., Becker, M. (Eds.), Third Earth Resources Technology Satellite–1 Symposium. Volume I: Technical Presentations. NASA, Washington D.C., pp. 309–317. https://doi.org/10.1021/jf60203a024

Sakowska, K., Alberti, G., Genesio, L., Peressotti, A., Delle Vedove, G., Gianelle, D., Colombo, R., Rodeghiero, M., Panigada, C., Juszczak, R., Celesti, M., Rossini, M., Haworth, M., Campbell, B.W., Mevy, J.P., Vescovo, L., Cendrero-Mateo, M.P., Rascher, U., Miglietta, F., 2018. Leaf and canopy photosynthesis of a chlorophyll deficient soybean mutant. Plant Cell Environ. 41, 1427–1437. https://doi.org/10.1111/pce.13180.

Salmon, V.G., Brice, D.J., Bridgham, S., Childs, J., Graham, J., Griffiths, N.A., Hofmockel, K., Iversen, C.M., Jicha, T.M., Kolka, R.K., Kostka, J.E., Malhotra, A., Norby, R.J., Phillips, J.R., Ricciuto, D., Schadt, C.W., Sebestyen, S.D., Shi, X., Walker, A.P., Warren, J.M., Weston, D.J., Yang, X., Hanson, P.J., 2021. Nitrogen and phosphorus cycling in an ombrotrophic peatland: a benchmark for assessing change. Plant and Soil 466, 649–674. https://doi.org/10.1007/s11104-021-05065-x.

Scharlemann, J.P.W., Tanner, E.V.J., Hiederer, R., Kapos, V., 2014. Global soil carbon: understanding and managing the largest terrestrial carbon pool. Carbon Manag 5, 81–91. https://doi.org/10.4155/cmt.13.77.

Shapiro, S.S., Wilk, M.B., 1965. An analysis of variance test for normality (complete samples). Biometrika 52, 591–611.

Siegmann, B., Cendrero-Mateo, M.P., Cogliati, S., Damm, A., Gamon, J., Herrera, D., Jedmowski, C., Junker-Frohn, L.V., Kraska, T., Muller, O., Rademske, P., van der Tol, C., Quiros-Vargas, J., Yang, P., Rascher, U., 2021. Downscaling of far-red solar-induced chlorophyll fluorescence of different crops from canopy to leaf level using a diurnal data set acquired by the airborne imaging spectrometer HyPlant. Remote Sens. Environ. 264, 112609 https://doi.org/10.1016/j.rse.2021.112609.

Stone, M., 1974. Cross-Validatory choice and assessment of statistical predictions. J. R. Stat. Soc. B. Methodol. 36, 111–133. https://doi.org/10.1111/j.2517-6161.1974.tb00994.x.

Sun, Y., Frankenberg, C., Jung, M., Joiner, J., Guanter, L., Köhler, P., Magney, T., 2018. Overview of solar-induced chlorophyll fluorescence (SIF) from the orbiting carbon Observatory-2: retrieval, cross-mission comparison, and global monitoring for GPP. Remote Sens. Environ. 209, 808–823. https://doi.org/10.1016/j.rse.2018.02.016.

Tagliabue, G., Panigada, C., Celesti, M., Cogliati, S., Colombo, R., Migliavacca, M., Rascher, U., Rocchini, D., Schüttemeyer, D., Rossini, M., 2020. Sun–induced fluorescence heterogeneity as a measure of functional diversity. Remote Sens. Environ. 247, 111934 https://doi.org/10.1016/j.rse.2020.111934.

Tukey, J.W., 1949. Comparing individual means in the analysis of variance. Biometrics 5, 99–114.

van Breemen, N., 1995. How Sphagnum bogs down other plants. Trends Ecol. Evol. 10, 270–275. https://doi.org/10.1016/0169-5347(95)90007-1.

Verrelst, J., Rivera, J.P., van der Tol, C., Magnani, F., Mohammed, G., Moreno, J., 2015. Global sensitivity analysis of the SCOPE model: what drives simulated canopy-leaving sun-induced fluorescence? Remote Sens. Environ. 166, 8–21. https://doi.org/10.1016/j.rse.2015.06.002.

Verrelst, J., Rivera, J.P., Gitelson, A., Delegido, J., Moreno, J., Camps-Valls, G., 2016a. Spectral band selection for vegetation properties retrieval using Gaussian processes regression. Int. J. Appl. Earth Obs. Geoinf. 52, 554–567. https://doi.org/10.1016/j.jag.2016.07.016.

Verrelst, J., van der Tol, C., Magnani, F., Sabater, N., Rivera, J.P., Mohammed, G., Moreno, J., 2016b. Evaluating the predictive power of sun-induced chlorophyll fluorescence to estimate net photosynthesis of vegetation canopies: a SCOPE modeling study. Remote Sens. Environ. 176, 139–151. https://doi.org/10.1016/j.rse.2016.01.018.

Welshofer, K.B., Zarnetske, P.L., Lany, N.K., Thompson, L.A.E., 2018. Open-top chambers for temperature manipulation in taller-stature plant communities. Methods Ecol. Evol. 9, 254–259. https://doi.org/10.1111/2041-210X.12863.

Wieneke, S., Burkart, A., Cendrero-Mateo, M.P., Julitta, T., Rossini, M., Schickling, A., Schmidt, M., Rascher, U., 2018. Linking photosynthesis and sun-induced fluorescence at sub-daily to seasonal scales. Remote Sens. Environ. 219, 247–258. https://doi.org/10.1016/j.rse.2018.10.019.

Wright, S., 1921. Correlation and causation. J. Agric. Res. 20, 557–585.

Xu, J., Morris, P.J., Liu, J., Holden, J., 2018. PEATMAP: refining estimates of global peatland distribution based on a meta-analysis. Catena (Amst) 160, 134–140. https://doi.org/10.1016/j.catena.2017.09.010.

Xu, S., Atherton, J., Riikonen, A., Zhang, C., Oivukkamäki, J., MacArthur, A., Honkavaara, E., Hakala, T., Koivumäki, N., Liu, Z., Porcar-Castell, A., 2021. Structural and photosynthetic dynamics mediate the response of SIF to water stress in a potato crop. Remote Sens. Environ. 263 https://doi.org/10.1016/j.rse.2021.112555.

Yang, X., Tang, J., Mustard, J.F., Lee, J.E., Rossini, M., Joiner, J., Munger, J.W., Kornfeld, A., Richardson, A.D., 2015. Solar-induced chlorophyll fluorescence that correlates with canopy photosynthesis on diurnal and seasonal scales in a temperate deciduous forest. Geophys. Res. Lett. 42, 2977–2987. https://doi.org/10.1002/2015GL063201.

Yang, P., van der Tol, C., Campbell, P.K.E., Middleton, E.M., 2020. Fluorescence Correction Vegetation Index (FCVI): a physically based reflectance index to separate physiological and non-physiological information in far-red sun-induced chlorophyll fluorescence. Remote Sens. Environ. 240, 111676 https://doi.org/10.1016/j.rse.2020.111676.

Zeng, Y., Badgley, G., Dechant, B., Ryu, Y., Chen, M., Berry, J.A., 2019. A practical approach for estimating the escape ratio of near-infrared solar-induced chlorophyll fluorescence. Remote Sens. Environ. 232, 111209 https://doi.org/10.1016/j.rse.2019.05.028.

Zhang, C., Atherton, J., Peñuelas, J., Filella, I., Kolari, P., Aalto, J., Ruhanen, H., Bäck, J., Porcar-Castell, A., 2019a. Do all chlorophyll fluorescence emission wavelengths capture the spring recovery of photosynthesis in boreal evergreen foliage? Plant Cell Environ. 42, 3264–3279. https://doi.org/10.1111/pce.13620.

Zhang, Z., Chen, J.M., Guanter, L., He, L., Zhang, Y., 2019b. From canopy-leaving to total canopy far-red fluorescence emission for remote sensing of photosynthesis: first results from TROPOMI. Geophys. Res. Lett. 46, 12030–12040. https://doi.org/10.1029/2019GL084832.

Zhao, F., Guo, Y., Verhoef, W., Gu, X., Liu, L., Yang, G., 2014. A method to reconstruct the solar-induced canopy fluorescence spectrum from hyperspectral measurements. Remote Sens. (Basel) 6, 10171–10192. https://doi.org/10.3390/rs61010171.

Zhao, F., Li, R., Verhoef, W., Cogliati, S., Liu, X., Huang, Y., Guo, Y., Huang, J., 2018. Reconstruction of the full spectrum of solar-induced chlorophyll fluorescence: Intercomparison study for a novel method. Remote Sens. Environ. 219, 233–246. https://doi.org/10.1016/j.rse.2018.10.021.

Zhao, F., Yuan, J., Huang, Y., Magney, T.S., Porcar-Castell, A., 2020. Preliminary study of wavelength positions of leaf fluorescence peaks with experimental data. In: IGARSS 2020 - 2020 IEEE International Geoscience and Remote Sensing Symposium. IEEE, pp. 4838–4841. https://doi.org/10.1109/IGARSS39084.2020.9324344.

Photosynthetic Responses of Peat Moss (*Sphagnum* spp.) and Bog Cranberry (*Vaccinium oxycoccos* L.) to Spring Warming

Publication No. 4

Antala, M., Abdelmajeed, A.Y.A., Stróżecki, M., Krzesiński, W., Juszczak, R., Rastogi, A. (2024). Photosynthetic Responses of Peat Moss (*Sphagnum* spp.) and Bog Cranberry (*Vaccinium oxycoccos* L.) to Spring Warming. *Plants* 13 (22), 3246. https://doi.org/10.3390/plants13223246

plants

Article

Photosynthetic Responses of Peat Moss (*Sphagnum* spp.) and Bog Cranberry (*Vaccinium oxycoccos* L.) to Spring Warming

Michal Antala [1,*], Abdallah Yussuf Ali Abdelmajeed [1], Marcin Stróżecki [1], Włodzimierz Krzesiński [2], Radosław Juszczak [1] and Anshu Rastogi [1,*]

[1] Laboratory of Bioclimatology, Department of Ecology and Environmental Protection, Poznan University of Life Sciences, 60-649 Poznan, Poland; abdallah.abdelmajeed@up.poznan.pl (A.Y.A.A.); marcin.strozecki@up.poznan.pl (M.S.); radoslaw.juszczak@up.poznan.pl (R.J.)

[2] Department of Vegetable Crops, Poznan University of Life Sciences, 60-995 Poznan, Poland; wlodzimierz.krzesinski@up.poznan.pl

* Correspondence: antala.michal9@gmail.com (M.A.); anshu.rastogi@up.poznan.pl (A.R.)

Abstract: The rising global temperature makes understanding the impact of warming on plant physiology in critical ecosystems essential, as changes in plant physiology can either help mitigate or intensify climate change. The northern peatlands belong to the most important parts of the global carbon cycle. Therefore, knowledge of the ongoing and future climate change impacts on peatland vegetation photosynthesis is crucial for further refinement of peatland or global carbon cycle and vegetation models. As peat moss (*Sphagnum* spp.) and bog cranberry (*Vaccinium oxycoccos* L.) represent some of the most common plant functional groups of peatland vegetation, we examined the impact of experimental warming on the status of their photosynthetic apparatus during the early vegetation season. We also studied the differences in the winter to early spring transition of peat moss and bog cranberry photosynthetic activity. We have shown that peat moss starts photosynthetic activity earlier because it relies on light-dependent energy dissipation through the winter. However, bog cranberry needs a period of warmer temperature to reach full activity due to the sustained, non-regulated, heat dissipation during winter, as suggested by the doubling of photosystem II efficiency and 36% decrease in sustained heat dissipation between the mid-March and beginning of May. The experimental warming further enhanced the performance of photosystem II, indicated by a significant increase in the photosystem II performance index on an absorption basis due to warming. Therefore, our results suggest that bog cranberry can benefit more from early spring warming, as its activity is sped up more compared to peat moss. This will probably result in faster shrub encroachment of the peatlands in the warmer future. The vegetation and carbon models should take into account the results of this research to predict the peatland functions under changing climate conditions.

Keywords: bog cranberry; peat moss; climate change; peatland; photosynthesis

Citation: Antala, M.; Abdelmajeed, A.Y.A.; Stróżecki, M.; Krzesiński, W.; Juszczak, R.; Rastogi, A. Photosynthetic Responses of Peat Moss (*Sphagnum* spp.) and Bog Cranberry (*Vaccinium oxycoccos* L.) to Spring Warming. *Plants* **2024**, *13*, 3246. https://doi.org/10.3390/plants13223246

Received: 7 November 2024
Revised: 15 November 2024
Accepted: 18 November 2024
Published: 19 November 2024

1. Introduction

Due to anthropogenic activities, the climate is changing faster than humankind could ever experience. The temperatures in the recent decades continue to rise at an unprecedented pace [1,2]. The period from June 2023 to May 2024 was the warmest year ever recorded for the globe, as May was already the 12th month in a row that was the warmest month from the beginning of records [3]. Because the climate projections show a further increase in the temperature over the next few years, it is crucial to understand the impact of the warming on the plants' physiology in critical ecosystems that may mitigate or accelerate climate change [1].

Northern peatlands are a specific ecosystem that plays an essential role in the global carbon cycle, which is disproportionally larger than their global coverage [4]. They are mostly found in the high latitudes of the northern hemisphere, where the temperature rises the fastest [1,5]. Carbon storage, which depends mainly on a low decomposition rate due to anoxic, low-pH conditions, is the most important function of peatlands. However, the assimilation of carbon by vegetation is not a negligible portion of the carbon cycle, as the final carbon balance is the difference between assimilation and release [4,6]. If the vegetation season starts earlier, the amount of assimilated carbon and the probability that the peatlands will remain the carbon sink increase [7,8].

The northern peatland vegetation comprises mainly mosses, graminoids, and ericoid shrubs [9]. Peat moss (*Sphagnum* spp.) and ericoid shrubs like bog cranberry (*Vaccinium oxycoccos* L.) can be characterized as evergreens, which means they start to be photosynthetically active as soon as the conditions in spring become favorable, without the need to grow leaf first [10,11]. Mosses and shrubs found in peatlands are constantly competing for the available light and nutrients. The recent warming and associated drying of peatlands led to the increased abundance of shrubs on account of mosses due to the evolutionary advantage they possess, such as roots or thick cuticula [10,12,13]. Climate change causes substantial changes in the peatland vegetation composition and its carbon assimilation [6]. Drying of peatlands alters the photosynthetic activity of their vegetation, with vascular plants being the main driver of the changes [14]. The production of peatland shrubs increases with higher temperatures and lower wetness, while moss production decreases with drying [15]. It has been shown that the increased temperature during the summer influences the photosynthetic potential of peatland vegetation negatively, with a stronger effect on peat moss than on bog cranberry [16]. However, it is unclear how different plant functional groups (PFGs) react to the increase in spring temperature and what mechanisms are behind the specific reactions of PFGs' photosynthetic apparatus.

The physiological conditions of various components of photosystem II (PSII), elements of the electron transport chain, and the coordination between light-dependent and light-independent biochemical processes can be assessed through the analysis of fast chlorophyll fluorescence transient curves [17]. Although chlorophyll *a* fluorescence transient is mostly studied to reveal the negative impacts of different stressors on photosynthesis, we employed this technique to reveal the changes in the status of photosynthetic machinery in peatland plants during the spring warm-up [18]. In addition to naturally increasing temperature, we examined the effect of artificial increases in temperature in situ to simulate the future warmer climate. We performed this experiment aiming to clarify the impact of spring warming on the photosynthetic apparatus capacity of bog cranberry and peat moss because such knowledge is important for further refinement of peatland or global carbon cycle and vegetation models.

2. Results

2.1. Thermal Conditions of Experimental Plots

Due to cloudy conditions and high precipitation causing the water level to rise above the peatland's surface, the W conditions had a considerable effect on the near-surface air temperature only from the last week of February onwards (Figure 1). Nigh-time heating mitigated the frost events when the minimal temperature of the coldest night in March (8 March—4 days before the first measurements) was 1.2 °C higher in W plots compared to C. The mean daily temperature one week before measurements was 1.2 °C, 0.9 °C, 0.8 °C, and 1.7 °C higher in W than C for the first, second, third, and fourth measurements, respectively. The cumulative difference in daily mean temperature between W and C rose from effectively 0 on 3 February to 21.6 °C the day before the first measurement and then to 29.3 °C, 44.0 °C, and 67.4 °C the day before the second, third, and fourth measurements, respectively.

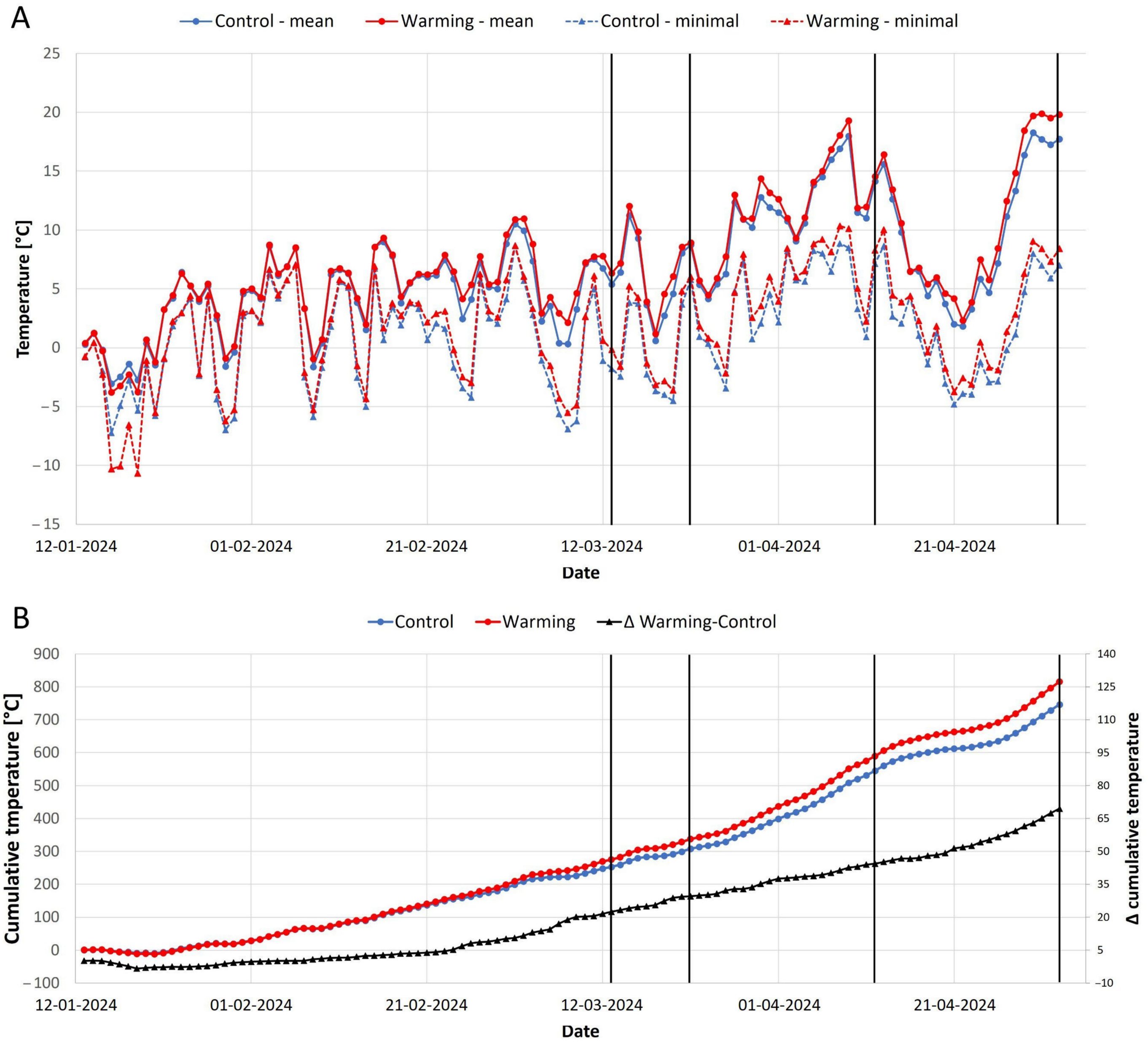

Figure 1. Mean and minimal daily air temperature (**A**), cumulative mean daily air temperature, and the difference (Δ) in cumulative temperatures (**B**) of warming and control plots measured 30 cm above the peatland surface in the period of 2 months before the first measurements until the last measurements. The thick black horizontal lines indicate the days of measurements (from left to right: 13 March, 22 March, 12 April, 3 May).

2.2. Energy Partitioning at Photosystem II (PSII)

The significant differences in energy partitioning at PSII caused by warming were recorded only on the 13 March and the 3 May (Figure 2). While the actual quantum yield of photosystem II photochemistry (ϕPSII) was significantly increased by W conditions only on the 3 May for peat moss, the quantum yield of light-induced energy dissipation (ϕNPQ) was significantly higher for both PFGs on the 13 March and only for peat moss on the 3 May (Figure 2A,B). W induced a significantly lower quantum yield of light-independent energy dissipation (ϕNO) and significantly higher non-photochemical quenching of maximum fluorescence (NPQ) for both PFGs on the 13 March and the 3 May (Figure 2C,D).

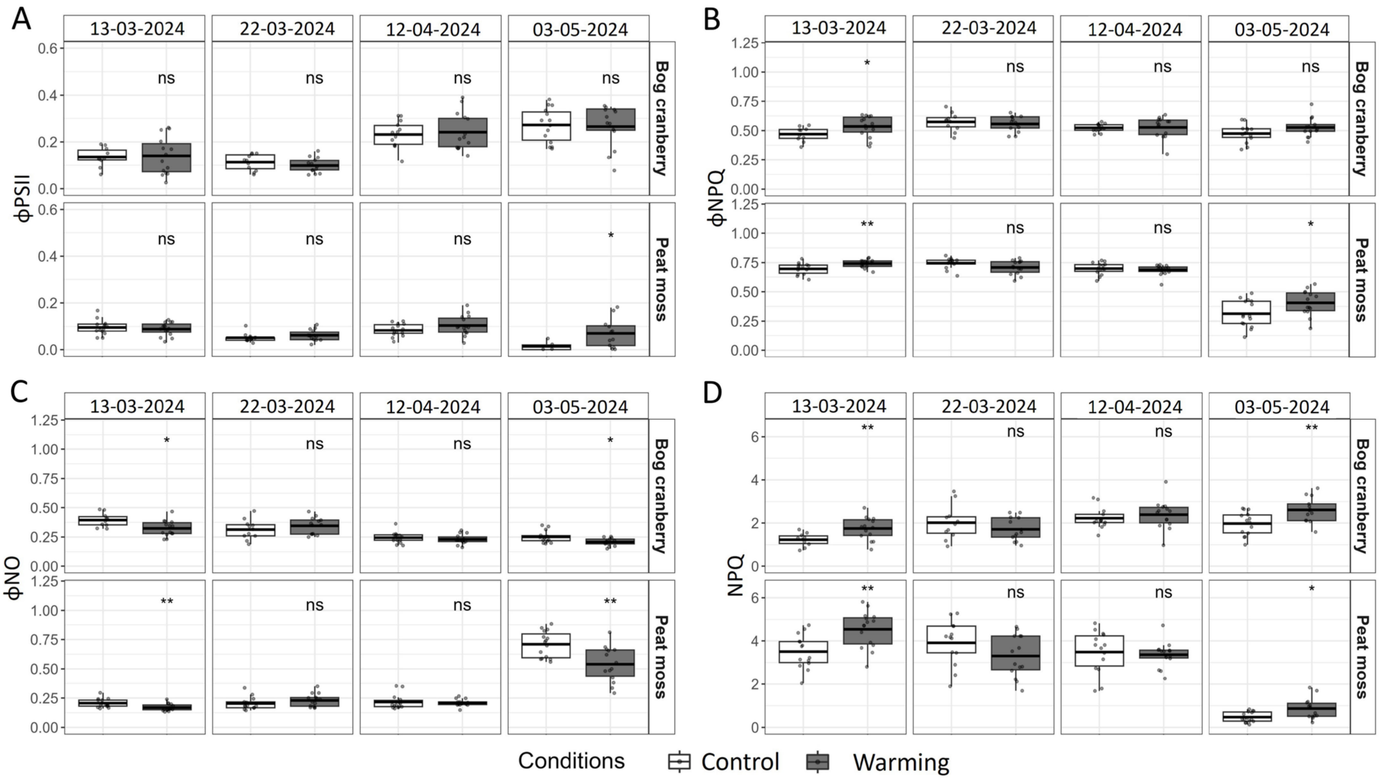

Figure 2. The actual quantum yield of photosystem II photochemistry (ϕPSII; (**A**)), the quantum yield of light-induced energy dissipation (ϕNPQ; (**B**)), the quantum yield of light-independent energy dissipation (ϕNO, (**C**)), and non-photochemical quenching of maximum fluorescence (NPQ; (**D**)) measured at 300 µmol m^{-2} s^{-1} from bog cranberry and peat moss subjected to control and warming conditions. The thick line in the boxplot represents the mean, while the points represent single measurements. The signs denote the significance of the difference between control and warming for each plant functional group and date separately, where "ns" is non-significant, * is <0.05, ** is <0.01.

ϕPSII of bog cranberry was increasing as the season progressed, with a 70% increase on the 12 April and doubling on the 3 May compared to the 13 March. Conversely, the decrease in ϕPSII to effective 0 on the 3 May was observed for peat moss. While bog cranberry used only 40% more of the trapped light for photochemistry than peat moss on the 13 March, this difference increased to 180% on the 12 April. The results from the 3 May could not be compared due to the almost 0 value of ϕPSII for peat moss (Figure 2A). While ϕNPQ of bog cranberry remained stable across all four measurements, it significantly dropped on the 3 May for peat moss. During the first three measurement days, peat moss dissipated around 50% more energy by ϕNPQ than bog cranberry (Figure 2B). ϕNO of bog cranberry was steadily decreasing with the progressing vegetation season when it was 20%, 38%, and 36% lower during the second, third, and fourth measurements, respectively, compared to the first measurement. Peat moss dissipated a remarkably stable fraction of the absorbed energy as ϕNO for the first three measurements. However, we recorded over a 3-fold increase in ϕNO for the measurement on the 3 May compared to the other measurements (Figure 2C). NPQ of bog cranberry increased by 64% between the first and second measurements and by 10 from the second to the third measurement, but it decreased by 11% from the third to the fourth measurement. At the same time, NPQ of peat moss increased only by 12% between the first two measurements and then decreased by 11% and by 84% between the second and third and the third and fourth measurements, respectively (Figure 2D).

2.3. The Fluorescence Transient Kinetics

The typical polyphasic fluorescence transient curves were recorded for bog cranberry in all measurement days and for peat moss in the first three measurements. However, the O-J-I-P curve of peat moss on the 3 May was altered when the change from J to I step was minimal, and the fluorescence intensity quickly dropped after reaching maximum, even to the values lower than minimal fluorescence (F_o; Figure 3A). The double normalization of fluorescence transient by maximal fluorescence (F_m) and F_o (calculated as $(F_t - F_o)/(F_m - F_o)$) revealed the differences, especially in the O-J step of the transient (Figure 3B). The further comparison of warming-induced differences in relative fluorescence for different steps of the O-J-I-P transient revealed the PFG-specific and date-dependent responses (Figure 4).

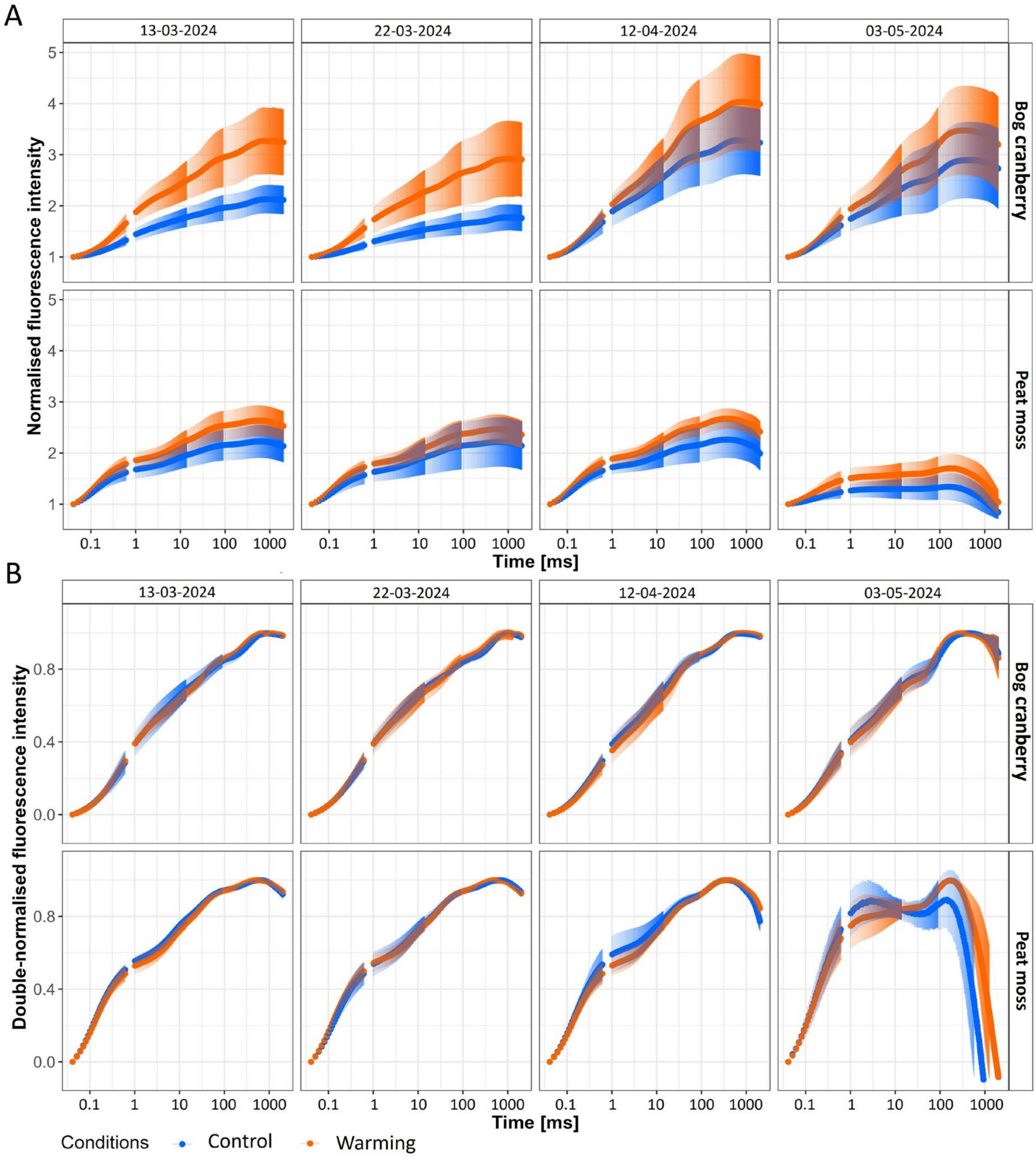

Figure 3. Fast chlorophyll *a* fluorescence transient curves normalized by minimal fluorescence (F_t/F_o; (**A**)) and double normalized by minimal and maximal fluorescence $(F_t - F_o)/(F_m - F_o$; (**B**)) for bog cranberry and peat moss (in rows) growing under control and warming conditions measured during different days (in columns). The points represent the mean, and the bars represent the standard deviation, *n* = 15.

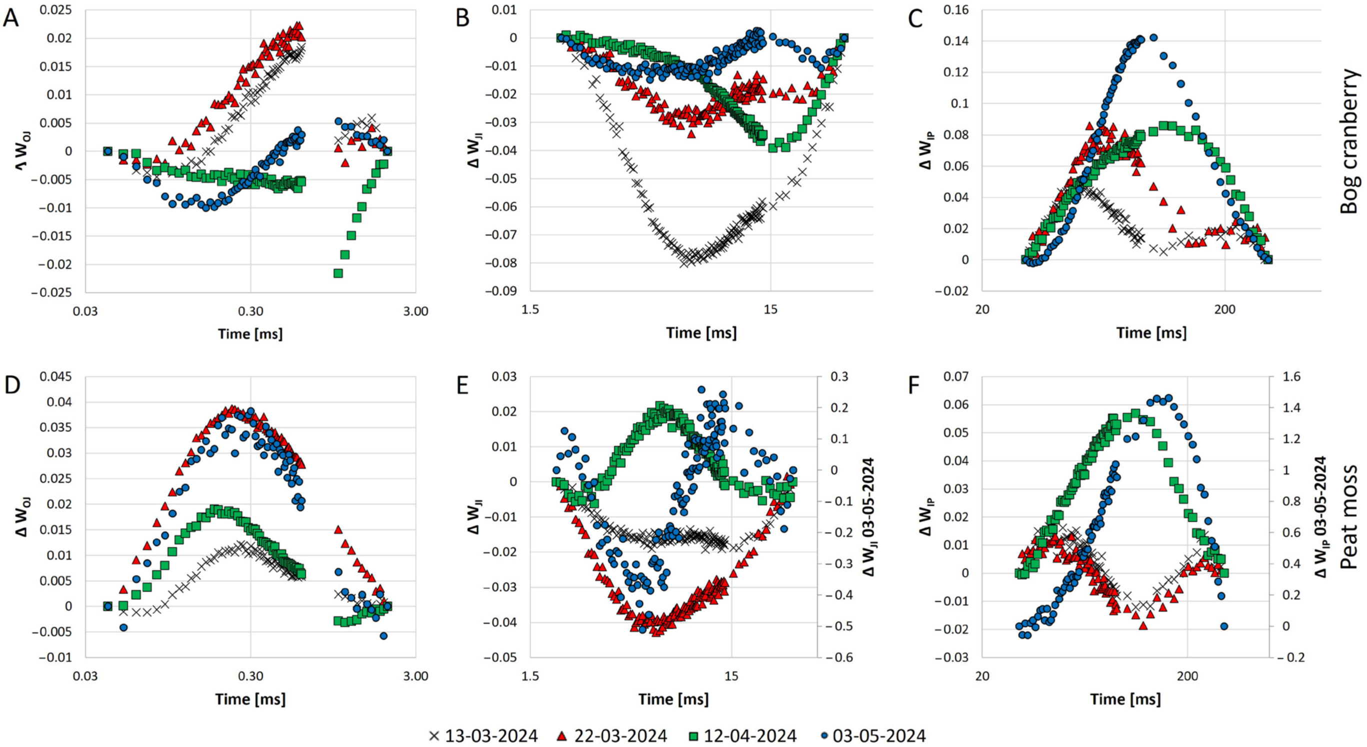

Figure 4. The warming-induced change (calculated as variable fluorescence (V_t) warming—V_t control) in the ratio of variable fluorescence to the amplitude of $F_J - F_o$ (ΔW_{OJ}; (**A**)), $F_I - F_J$ (ΔW_{JI}; (**B**)), and $F_P - F_I$ (ΔW_{IP}; (**C**)) for bog cranberry, and the ratio of V_t to the amplitude of $F_J - F_o$ (ΔW_{OJ}; (**D**)), $F_I - F_J$ (ΔW_{JI}; (**E**)), and $F_P - F_I$ (ΔW_{IP}; (**F**)) for peat moss. Note that there is a secondary axis at panels E and F for 3 May 2024 due to the different magnitudes of the change. The points represent the mean of all measurements for a given plant functional group and day, *n* = 15.

A positive K band occurring between 0.2 ms and 0.3 ms was observed for bog cranberry on the 3 May and for peat moss during all the measurements (Figure 4A,D). While W caused a positive change in the ratio of variable fluorescence of the O-J step (W_{OJ}) for peat moss in all the measurement dates, the change was positive only during the first two measurements, followed by a negative change for the other two measurements in the case of bog cranberry. The apparent sudden changes in the difference of W_{OJ} observed between 0.6 ms and 1 ms are probably so prominent due to the large gap in the time series caused by the manufacturer's equipment settings (Figure 4A,D). The negative difference with variable peak position and the highest prominence on the 13 March was observed for the W_{JI} of bog cranberry for all measurements. However, the warming-induced difference in W_{JI} for peat moss was negative during the March measurements, positive on the 12 April, and then sinusoid on the 3 May, with the first negative trend between 3.1 ms and 9.3 ms and followed by a positive trend until 30 ms (Figure 4B,E). The difference in W_{IP} (ΔW_{IP}) caused by W was characterized by a positive trend with a progressive peak shift to a later time and an increasing magnitude of the difference with the season advancement. Negative change in ΔW_{IP} for peat moss was found in March, while positive change was observed on the 12 April and the 3 May (Figure 4C,E).

Several parameters assessing the electron transport and the status of the reaction centers (RCs) were calculated from the fast chlorophyll *a* transient to facilitate statistical analysis. The general trend for bog cranberry suggests decreasing or diminishing warming-induced differences with progressing vegetation season (Figures 3 and 5). Relative variable fluorescence at step J, relative variable fluorescence at step I, normalized area above O-J curve, energy flux trapped by one active RC at time 0 (TRo/RC), rate of electron transport by one active RC at time 0 (ETo/RC), efficiency of electron transport beyond plastoquinone

(Ψo), and approximated initial slope of the fluorescence transient (Mo) of bog cranberry were not significantly altered by increased temperature in any of the measurement days. The significantly higher maximum fluorescence normalized by minimum fluorescence (F_m/F_o), causing also higher maximum efficiency of the water diffusion reaction on the donor side of photosystem II (F_v/F_o), persisted throughout the observed period. Nevertheless, the difference was decreasing from 47% on the 13 March to 16% on the 3 May for F_m/F_o and from 86% to 25% for F_v/F_o (Figure 5A–D). Additionally, W significantly increased the maximum quantum yield of photosystem II photochemistry (ϕPo) and photosystem II performance index on an absorption basis (PI ABS) while decreasing the normalized area above the O-J-I-P curve, number of plastoquinone reductions from time 0 to time of reaching maximum fluorescence (N), absorption flux per one active RC at time 0 (ABS/RC), energy flux not intercepted by reaction center at time 0 (DIo/RC), and quantum yield of energy dissipation at time 0 (ϕDo) of bog cranberry during the March measurements (Figure 3A,B). ϕPo and PI ABS were significantly increased, and ABS/RC, DIo/RC, and ϕDo were decreased by higher temperature also on the 12 April (Figure 5C). On the 3 May, only the normalized area above the O-J-I-P curve and N were significantly lower in leaves of bog cranberries growing in W plots compared to C (Figure 5D).

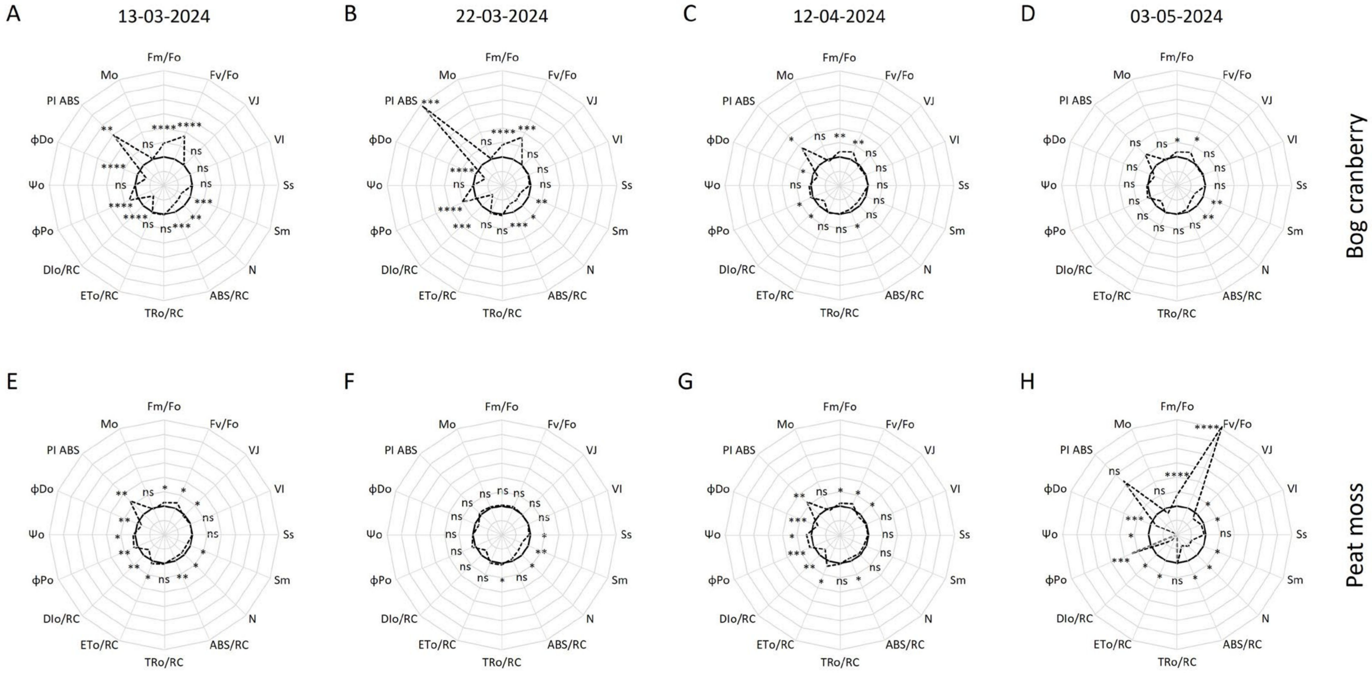

Figure 5. Spider plots presenting the parameters calculated from the chlorophyll *a* fluorescence transient normalized by the respective control for bog cranberry (**A**–**D**) and peat moss (**E**–**H**) on 13 March (**A**,**E**), 22 March (**B**,**F**), 12 April (**C**,**G**), and 3 May (**D**,**H**); the full line indicates the control, while the dashed line indicates warming. The signs denote the significance of the difference between control and warming for each plant functional group and date separately, where "ns" is non-significant, * is <0.05, ** is <0.01, *** is < 0.001, and **** is <0.0001. The distance between concentric circles is 0.5, while the control, thick full line is at value 1. The displayed parameters are: maximum fluorescence normalized by minimum fluorescence (F_m/F_o), maximum efficiency of the water diffusion reaction on the donor side of photosystem II (F_v/F_o), relative variable fluorescence at the step J (V_J), relative variable fluorescence at step I (V_I), the normalized area above O-J curve (Ss), the normalized area above the O-J-I-P curve (Sm), number of plastoquinone reductions from time 0 to time of reaching maximum fluorescence (N), absorption flux per one active reaction center at time 0 (ABS/RC), energy flux trapped by one active reaction center at time 0 (TRo/RC), rate of electron transport by one active reaction center at time 0 (ETo/RC), energy flux not intercepted by reaction center at time 0 (DIo/RC),

the maximum quantum yield of photosystem II photochemistry (ϕPo), efficiency of electron transport beyond plastoquinone (Ψo), quantum yield of energy dissipation at time 0 (ϕDo), photosystem II performance index on an absorption basis (PI ABS), and approximated initial slope of the fluorescence transient (Mo).

Unlike for bog cranberry, there was no chlorophyll *a* fluorescence transient-derived parameter that was significantly altered by W in all campaigns. W induced similar changes in the photosynthetic apparatus of peat moss on the 13 March as it did for bog cranberry when F_m/F_o, F_v/F_m, ETo/RC, ϕPo, Ψo, and PI ABS increased, and relative variable fluorescence at step J, the normalized area above the O-J-I-P curve, N, ABS/RC, DIo/RC, and ϕDo decreased as a result of higher temperature (Figure 5E). Only a decrease in the normalized areas above the O-J and the O-J-I-P curves and N and an increase in TRo/RC for peat moss growing under W conditions were significant compared to C on the 22 March (Figure 5F). W caused again more significant alterations in peat moss photosynthetic apparatus in April and May. Relative variable fluorescence at step J, F_m/F_o, F_v/F_o, ABS/RC, ETo/RC, DIo/RC, ϕPo, Ψo, and ϕDo were significantly changed by increased temperature in both of the last two measurement days, while PI ABS of moss from W plots was significantly higher only on the 12 April, and relative variable fluorescence at step I, the normalized area above the O-J-I-P curve, and N were significantly lower only on the 3 May (Figure 5G,H).

3. Discussion

The beginning of 2024 was unusual in terms of temperature, with every month from January to May being the warmest on record [3]. The 9 February was the last day when the average daily temperature in the studied peatland was below 0 °C (Figure 1A). This could be marked as the beginning of the vegetation season for the evergreen plants in 2024.

The low temperature and high light intensity during winter and early spring could damage the photosynthetic apparatus of evergreen plants. Therefore, the decreasing photosynthetic efficiency and structural changes on PSII protect the plants from damage to photosystems in winter. This decrease is a reversible change, and the photosynthetic efficiency is restored in the spring when temperature rises [18–21]. The increasing ϕPSII of bog cranberry from the 22 March to the 12 April confirms that the season of photosynthetic activity for this shrub started in the late March to early April period. However, the remarkable stability of peat moss ϕPSII shows that its season started already before the 13 March. That may be because the peat moss is photosynthetically active when the temperature is above 0 °C, and it continues the growth over the wintertime, which suggests no permanent downregulation of PSII as in the case of vascular plants [22,23]. Indeed, we found that for the first three measurements gathered during the March–April period, peat mosses dissipated the majority of the excess energy by light-dependent heat dissipation connected with the changes in pH gradient and the xanthophyll cycle (Figure 2). This indicates that peat mosses are able to quickly react on even shorter periods of favorable conditions during winter by increased rates of photochemistry [24]. Therefore, peat mosses are a major contributor to the peatland vegetation carbon uptake during the beginning of vegetation season, before ϕNO of shrubs relaxes due to long enough periods of temperatures above the threshold [25]. Nevertheless, the situation changed during the measurements on the 3 May, when we observed a drop of ϕPSII to almost 0 and a dramatic increase in ϕNO, suggesting that the peat moss switched from photosynthetic activity to sustained energy dissipation (Figure 2). Conversely, the low ϕPSII of bog cranberry was maintained in March by higher ϕNO, which decreased with time and also by increased temperature during the first and last measurements, while the ϕPSII was increasing. At the same time, ϕNPQ remained almost constant. These changes in the absorbed energy partitioning on PSII show that bog cranberries rely on more sustained, light-independent energy dissipation upregulation during cold months, which provides more constant protection of photosynthetic machinery that relaxes slower compared to the strategy employed by peat moss [20,26]. Our findings are seemingly in dispute with the previous research suggesting that the shrubs of the *Vaccinium* genus maintain photosynthetic activity during the winter without downregulation [19,27]. However, those studies were performed on shrubs overwintering under the snow cover that protects them from excessive light or provides insulation from frost. On the contrary, the peatland site used for this study is snow-free for most of the winter, and the plants are exposed to adverse environmental conditions.

Although higher values of NPQ are generally connected to stress conditions, this is not the case in our study, as the NPQ does not increase as a result of increased ϕNPQ but due to decreasing ϕNO [28]. Interestingly, when the peat moss seems to become stressed on the 3 May, the NPQ value decreases from above 3 to below 1 (Figure 2D). Experimental W induced changes in the energy dissipation pathways during the first and last measurements. Further analysis revealed that the days when significant differences in energy partitioning occurred were the days preceded by a week when W plots were, on average, more than 1 °C warmer compared to C. It seems that the lower difference was not enough to influence the major energy distribution processes, but, as discussed below, several other processes were significantly impacted.

The fluorescence transient curve of evergreens undergoes changes in shape during the spring warm-up. The curve has a low magnitude and misses a clear I step in winter, and it achieves its typical O-J-I-P shape as the temperature rises and the physiological activity of plants starts [21]. As our measurements started at the beginning of the meteorological spring, we observed the typical O-J-I-P shape of the curve from the beginning of our measurements for both PFGs. However, the transient curve of C bog cranberries in March was rather flat and became its typical contours only in April. Moreover, the 1.5-fold bigger magnitude of the W plots bog cranberry's curve in March compared to the C plants during the same measurements that was reached by C plants only in April suggests the earlier onset of the photosynthetic activity in W plots (Figure 3A). Similarly to previous work [16], we found that the chlorophyll *a* fluorescence transient of peat moss rises less prominently than the fluorescence of the peatland vascular plants, particularly the bog cranberry (Figure 3A). The fast rise of the fluorescence from the O to J step for peat moss on the 3 May resembles the O-J-I-P curves of plants treated by the electron transport inhibitors. The transient curves of mosses grown in both C and W conditions point to disrupted electron flow beyond plastoquinone's Q_A binding site [29]. The appearance of the positive K band in peat moss and the negative K band in bog cranberry in May points to the temperature-influenced changes in the electron transport and oxygen-evolving complex (Figure 4) [30]. However, the absence of the K step in the fluorescence transient curve indicates no severe stress on the plants [31]. On the contrary, the significantly higher F_v/F_o for plants under W conditions is indicative of increased activity of the oxygen-evolving complex (Figure 5). The warming-induced changes in the oxygen evolution are also visible from the differences in the W_{JI} observer for both PFGs (Figure 4B) [32].

W significantly decreased the functional size of the PSII antenna in bog cranberries, as suggested by ABS/RC [33]. The difference was the most pronounced in the early spring and then decreased and even disappeared as the season progressed. This could be because the lower air temperature of the C plots in early spring did not allow for all the RCs of PSII to be active. However, with increasing temperature, as the season progressed, it became warm enough to activate all the RCs, and the photosynthetic apparatus of cranberries reached very similar status for C and W in May (Figure 5D). The increased ϕPo of bog cranberry in W plots during the March and April measurements was due to the faster conversion of PSII RCs from the heat sinks back to the active state. This is apparent as Mo, representing the net rate of the RCs' closure, TRo/RC or ETo/RC were not altered, but the DIo/RC of W plants decreased significantly, which indicates lower non-photochemical energy dissipation [34,35]. The progressive and temperature-dependent increase in ϕPo found in this work is in concordance with the previous study of evergreen plants by others [21]. Similarly to bog cranberry, W decreased the size of the peat moss PSII antenna and increased the ϕPo and DIo/RC. However, it also caused changes in the electron transport rate, as suggested by relative variable fluorescence at step J, ETo/RC, and Ψo [28]. The peat moss exhibited more complex behavior than the bog cranberry, as there was not one trend of decreasing differences between W and C during the spring. In fact, the differences between temperature regimes disappeared on the 22 March but started to become larger again in April and May (Figure 5E–H).

The uniform relative variable fluorescence at step J values between W and C bog cranberries indicated no change in the plastoquinone pool size, which means that the electrons could be transferred to the dark reaction sites without obstructions in both temperature regimes [33,36]. However, despite the single plastoquinone's Q_A binding site reduction rate being unchanged by W as visible from the normalized area above the O-J curve, the number of turnovers (as suggested by the normalized area above the O-J-I-P curve and N) per single RC decreased due to the abovementioned increase in the number of active PSII RCs [28]. The absence of differences in relative variable fluorescence at step I suggests that the pool size of photosystem I acceptors remained stable irrespective of treatment or date for bog cranberry on all days and the peat moss during the first three measurements. However, the increase in relative variable fluorescence at step I for peat moss C compared to the other values of relative variable fluorescence at step I recorded for peat moss could be interpreted as an increased photosystem I acceptor pool. Despite the size of the photosystem I acceptor pool not changing due to the W, the reduction rate of the photosystem I end electron acceptors was altered, as indicated by the difference in the W_{IP} dynamics (Figure 4C,F) [29,34]. The reduction rate of bog cranberries photosystem I acceptors was increased by W in all of the measurement days, while W enhanced the photosystem I reduction rate in peat moss during the April and May measurements but decreased it negligibly in March (Figure 4C,F).

The warming-induced increase in PI ABS of bog cranberry reflects mainly the decreasing size of the PSII antenna, as the electron trapping efficiency and their transport beyond plastoquinone's Q_A binding site were not significantly altered. However, PI ABS of peat moss was increased by W due to the synergistic effect of antenna size decrease and improved electron trapping and transport [37]. It is not surprising that PI ABS was the parameter with the most pronounced warming-induced changes, as it is the most sensitive parameter representing the overall status of the photosynthetic apparatus, which is considerably temperature-dependent [17,21,30]. Despite the visible relative difference in PI ABS of moss on the 3 May, the difference was insignificant as the values of the index approached 0. That underscores the apparent poor status of peat moss photosynthetic apparatus during the last measurements (Figure 5H). The unusual values of chlorophyll *a* fluorescence recorded on the 3 May for peat moss could be explained by the higher temperature, which caused drying of the moss surface during the dark adaptation in the clip; therefore, causing the stress similar to the application of the electron transport inhibitors. However, this theory needs to be verified by future, well-designed experiments. Should it be true, the specific clips for mosses need to be designed to obtain reliable data.

4. Material and Methods

4.1. Study Site

The data were collected at the experimental station localized in Rzecin peatland (52°45′41″ N, 16°18′35″ E, 54 m a.s.l.), western Poland, where the warming and reduced precipitation experiment was established in 2017 (Figure 6). A detailed description of the site is provided by [38,39]. The plots of control (C) and warming (W) conditions of the CR (dominant graminoid is beaked sedge; *Carex rostra* Stokes) site were used for this study (Figure 6). The vegetation in the experimental plots is natural and consists of bog cranberry, peat mosses, beaked sedge, and swamp horsetail (*Equisetum fluviatile* L.), with only cranberries and mosses being of evergreen nature. The peat moss layer is dominated by the species *Sphagnum angustifolium* (Warnst.) C.E.O. Jensen, *S. fallax* (Klinggr.) Klinggr., and *S. teres* (Schimp.) Ångstr. The species are present in the plots in variable ratios representing the natural variability of the vegetation and have been present on site for at least 3 decades [40,41].

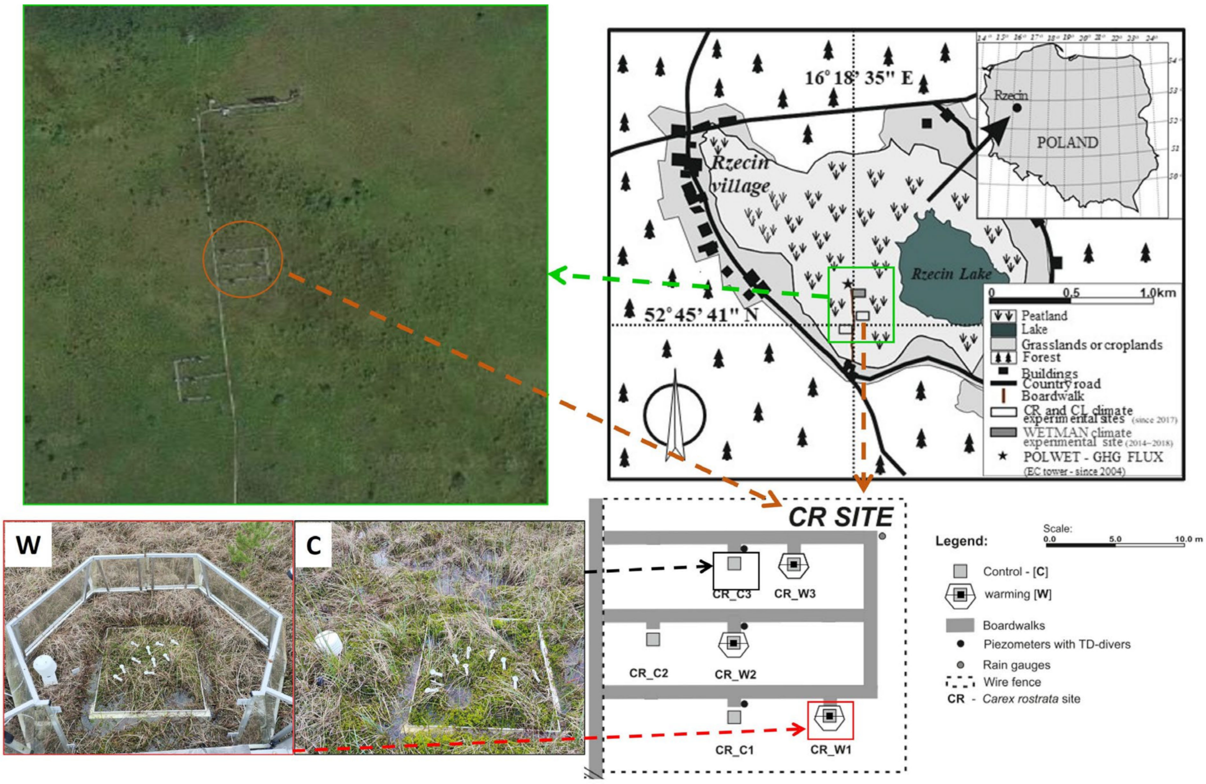

Figure 6. The location of Rzecin peatland in Poland and the location and experimental design of the CR site and its plots used for this study. Panels denoted W and C present representative warming and control plots, respectively, during the dark adaptation of bog cranberry leaves. Please note that the infrared heater was removed from the warming plot during the measurement as it is working only during the night-time (part of the figure was adapted from Górecki et al. [38], CC BY-NC-ND license).

C plots are exposed to ambient conditions, while the increased temperature of W plots is reached passively by open-top chambers (OTCs) during the daytime and actively by a 100 W infrared heater during the night. All the plots are randomly distributed within the experimental site in triplicate. The air temperature was measured next to every plot 30 cm above the surface by HygroVue5 thermohygrometers (Campbell Sci., Logan, UT, USA) and recorded every half an hour on a datalogger CR1000 (Campbell Sci., Logan, UT, USA) [38,39].

Due to the higher-than-usual precipitation of 381 mm in the period between 1 September 2023 and 29 February 2024, the hollows of the site were underwater, and around 70% of the surface was above water level.

4.2. *Chlorophyll a Fluorescence Measurements*

Fast chlorophyll *a* fluorescence kinetics and the pulse–amplitude modulated fluorescence measurements were performed by FluorPen FP 110/D (Photon System Instruments, Drasov, Czech Republic) with detachable dark adaptation clips. The measurements were performed 4 times during the meteorological spring of 2024: on the 13 and 22 March, the 12 April, and the 3 May under cloudy conditions. The fluorescence of bog cranberry was measured on the adaxial side of the leaves of different plants in the plot. Measurements of peat moss fluorescence were derived from the freshly detached capitula's top surface. As the peat moss species occurring in the plots are closely related, they were treated as a genus, *Sphagnum* spp., without further classification into species. After 25 min of dark adaptation, 5 samples of each PFG in the plot were measured by the OJIP protocol, and 5 samples were analyzed by the NPQ3 protocol provided by the manufacturer. The OJIP protocol is a 2-s-lasting fast chlorophyll *a* fluorescence kinetics measurement, while NPQ3 is pulse–amplitude modulated fluorescence measurement under artificial actinic light that takes 200 s and comprises 10 pulses. The measurement light was set to 85%, while the actinic light for the NPQ3 protocol was 300 µmol m^{-2} s^{-1}. The wavelength of the used light was 455 nm. Parameters calculated from the measured fluorescence values are summarized in Table 1.

Table 1. Summary of chlorophyll *a* fluorescence-derived parameters with their abbreviations and the measurement protocols used for their calculation. The nomenclature follows Kalaji et al. (2017) and Strasser et al. (2000) [28,35].

Abbreviation	Name of Parameter	Measurement Protocol
F_o	Minimal fluorescence	OJIP and NPQ3
F_m	Maximal fluorescence	OJIP and NPQ3
ϕPo	Maximum quantum yield of photosystem II photochemistry	OJIP and NPQ3
ϕPSII	Actual quantum yield of photosystem II photochemistry (at 300 µmol m^{-2} s^{-1})	NPQ3
ϕNPQ	Quantum yield of light-induced energy dissipation (at 300 µmol m^{-2} s^{-1})	NPQ3
ϕNO	Quantum yield of light-independent energy dissipation (at 300 µmol m^{-2} s^{-1})	NPQ3
NPQ	Non-photochemical quenching of maximum fluorescence (at 300 µmol m^{-2} s^{-1})	NPQ3
ϕDo	Quantum yield of energy dissipation at time 0	OJIP
F_m/F_o	Maximum fluorescence normalized by minimum fluorescence	OJIP
F_v/F_o	Maximum efficiency of the water diffusion reaction on the donor side of photosystem II	OJIP
V_J	Relative variable fluorescence at step J	OJIP
V_I	Relative variable fluorescence at step I	OJIP
Ψo	Efficiency of electron transport beyond plastoquinone	OJIP
ABS/RC	Absorption flux per one active reaction center at time 0	OJIP
TRo/RC	Energy flux trapped by one active reaction center at time 0	OJIP
ETo/RC	Rate of electron transport by one active reaction center at time 0	OJIP
DIo/RC	Energy flux not intercepted by reaction center at time 0	OJIP
Sm	Normalized area above the O-J-I-P curve	OJIP
Ss	Normalized area above O-J curve	OJIP
Mo	Approximated initial slope of the fluorescence transient	OJIP
N	Number of plastoquinone reductions from time 0 to time of reaching maximum fluorescence	OJIP
PI ABS	Photosystem II performance index on an absorption basis	OJIP

4.3. Statistical Analysis

The data were visually screened for incorrect measurements in Microsoft Excel (Microsoft Corporation, Redmond, WA, USA). The measurements with stable low fluorescence, indicating measurements of closed darkening clips, were removed before the statistical analysis. The significance of differences between C and W conditions was analyzed by Student's *t*-test for every PFG and date separately. All the measurements of the same PFG on the same day from all 3 plots were analyzed together. The analysis was carried out in RStudio version 2023.12.1+402 (RStudio Inc., Boston, MA, USA). As many of the cranberry leaves are smaller than the area of the darkening clip opening, only values normalized by F_o were analyzed and presented in the publication.

5. Conclusions

The unusually warm spring of 2024 shifted the vegetation phenology of plants. However, the experimental warming of the peatland ecosystem in situ proved that further shifts are possible in the near future for peat moss and bog cranberry. We showed that different PFGs (mosses and shrubs) rely on different strategies of photosynthetic apparatus protection during winter, which is demonstrated by higher ϕNO and lower ϕNPQ of bog cranberries compared to peat moss in very early spring. This indicates that peat mosses are able to quickly react on even shorter periods of favorable conditions during winter by increased rates of photochemistry, while bog cranberries utilize the strategy of more constant protection of photosynthetic machinery that relaxes comparatively slower. The switch from the inactive winter status to spring photosynthetic activity is faster if the air temperature is higher. The process of photosynthesis activation in bog cranberries is accompanied by the activation of RCs, decreased heat dissipation, and increased overall efficiency of PSII, all of which were found to be temperature-dependent.

The results of this study help to understand the observed shrub encroachment of peatlands with elevated temperatures. A stronger positive effect of warming on bog cranberry than on peat moss during the spring found in this study and a stronger negative effect of summer warming reported previously show that the photosynthetic apparatus of cranberries is much better equipped for the future with higher temperatures.

Our findings contribute to the understanding of the morphological and physiological advantages of the ericaceous shrubs over the peat moss that allow them to take over bigger and bigger portions of the peatlands as the world warms up. The future vegetation and carbon models should take this information into account to accurately predict the peatland functions under a changing climate.

Author Contributions: M.A.: conceptualization, data curation, formal analysis, investigation, methodology, visualization, and writing—original draft. A.Y.A.A.: investigation and writing—review and editing. M.S.: investigation, supervision, and writing—review and editing. W.K.: resources and writing—review and editing. R.J.: conceptualization, resources, funding acquisition, project administration, supervision, and writing—review and editing. A.R.: conceptualization, funding acquisition, project administration, supervision, formal analysis, resources, and writing—review and editing. All authors have read and agreed to the published version of the manuscript.

Funding: This study was supported by the projects funded by the National Science Centre of Poland (NCN) (Grant No. 2020/37/B/ST10/01213 and No. 2016/21/B/ST10/02271).

Data Availability Statement: The data presented in this study are available on request from the corresponding author.

Conflicts of Interest: The authors declare that they have no known competing financial interests or personal relationships that could have appeared to influence the work reported in this paper.

References

1. Calvin, K.; Dasgupta, D.; Krinner, G.; Mukherji, A.; Thorne, P.W.; Trisos, C.; Romero, J.; Aldunce, P.; Barrett, K.; Blanco, G.; et al. *Climate Change 2023: Synthesis Report. Contribution of Working Groups I, II and III to the Sixth Assessment Report of the Intergovernmental Panel on Climate Change*; Arias, P., Bustamante, M., Elgizouli, I., Flato, G., Howden, M., Méndez-Vallejo, C., Pereira, J.J., Pichs-Madruga, R., Rose, S.K., Saheb, Y., et al., Eds.; Intergovernmental Panel on Climate Change (IPCC): Geneva, Switzerland, 2023.
2. Tripati, A.K.; Roberts, C.D.; Eagle, R.A. Coupling of CO_2 and Ice Sheet Stability over Major Climate Transitions of the Last 20 Million Years. *Science* **2009**, *326*, 1394–1397. [CrossRef] [PubMed]
3. NOAA. National Centers for Environmental Information, Monthly Global Climate Report for May 2024. Available online: https://www.ncei.noaa.gov/access/monitoring/monthly-report/global/202405 (accessed on 1 September 2024).
4. Qiu, C.; Zhu, D.; Ciais, P.; Guenet, B.; Peng, S. The Role of Northern Peatlands in the Global Carbon Cycle for the 21st Century. *Glob. Ecol. Biogeogr.* **2020**, *29*, 956–973. [CrossRef]
5. Xu, J.; Morris, P.J.; Liu, J.; Holden, J. PEATMAP: Refining Estimates of Global Peatland Distribution Based on a Meta-Analysis. *Catena* **2018**, *160*, 134–140. [CrossRef]
6. Antala, M.; Juszczak, R.; van der Tol, C.; Rastogi, A. Impact of Climate Change-Induced Alterations in Peatland Vegetation Phenology and Composition on Carbon Balance. *Sci. Total Environ.* **2022**, *827*, 154294. [CrossRef]

7. Gallego-Sala, A.V.; Charman, D.J.; Brewer, S.; Page, S.E.; Prentice, I.C.; Friedlingstein, P.; Moreton, S.; Amesbury, M.J.; Beilman, D.W.; Björck, S.; et al. Latitudinal Limits to the Predicted Increase of the Peatland Carbon Sink with Warming. *Nat. Clim. Change* **2018**, *8*, 907–913. [CrossRef]
8. Lund, M.; Lafleur, P.M.; Roulet, N.T.; Lindroth, A.; Christensen, T.R.; Aurela, M.; Chojnicki, B.H.; Flanagan, L.B.; Humphreys, E.R.; Laurila, T.; et al. Variability in Exchange of CO_2 across 12 Northern Peatland and Tundra Sites. *Glob. Change Biol.* **2010**, *16*, 2436–2448. [CrossRef]
9. Ward, S.E.; Bardgett, R.D.; McNamara, N.P.; Ostle, N.J. Plant Functional Group Identity Influences Short-Term Peatland Ecosystem Carbon Flux: Evidence from a Plant Removal Experiment. *Funct. Ecol.* **2009**, *23*, 454–462. [CrossRef]
10. Buttler, A.; Robroek, B.J.M.; Laggoun-Défarge, F.; Jassey, V.E.J.; Pochelon, C.; Bernard, G.; Delarue, F.; Gogo, S.; Mariotte, P.; Mitchell, E.A.D.; et al. Experimental Warming Interacts with Soil Moisture to Discriminate Plant Responses in an Ombrotrophic Peatland. *J. Veg. Sci.* **2015**, *26*, 964–974. [CrossRef]
11. Chiapusio, G.; Binet, P.; Bertheau, C.; Priault, P. Sphagnum Physiological Responses to Elevated Temperature, Nitrogen, CO_2 and Low Moisture in Laboratory and in Situ Microhabitats: A Review. *Aquat. Ecol.* **2021**, *56*, 429–445. [CrossRef]
12. Weston, D.J.; Timm, C.M.; Walker, A.P.; Gu, L.; Muchero, W.; Schmutz, J.; Shaw, A.J.; Tuskan, G.A.; Warren, J.M.; Wullschleger, S.D. Sphagnum Physiology in the Context of Changing Climate: Emergent Influences of Genomics, Modelling and Host–Microbiome Interactions on Understanding Ecosystem Function. *Plant Cell Environ.* **2015**, *38*, 1737–1751. [CrossRef]
13. Fewster, R.E.; Morris, P.J.; Swindles, G.T.; Ivanovic, R.F.; Treat, C.C.; Jones, M.C. Holocene Vegetation Dynamics of Circum-Arctic Permafrost Peatlands. *Quat. Sci. Rev.* **2023**, *307*, 108055. [CrossRef]
14. Kokkonen, N.; Laine, A.M.; Männistö, E.; Mehtätalo, L.; Korrensalo, A.; Tuittila, E.-S. Two Mechanisms Drive Changes in Boreal Peatland Photosynthesis Following Long-Term Water Level Drawdown: Species Turnover and Altered Photosynthetic Capacity. *Ecosystems* **2022**, *25*, 1601–1618. [CrossRef]
15. Weltzin, J.F.; Pastor, J.; Harth, C.; Bridgham, S.D.; Updegraff, K.; Chapin, C.T. Response of bog and fen plant communities to warming and water-table manipulations. *Ecology* **2000**, *81*, 3464–3478. [CrossRef]
16. Rastogi, A.; Stróżecki, M.; Kalaji, H.M.; Łuców, D.; Lamentowicz, M.; Juszczak, R. Impact of Warming and Reduced Precipitation on Photosynthetic and Remote Sensing Properties of Peatland Vegetation. *Environ. Exp. Bot.* **2019**, *160*, 71–80. [CrossRef]
17. Strasser, R.J.; Tsimilli-Michael, M.; Srivastava, A. Analysis of the Chlorophyll a Fluorescence Transient. In *Advances in Photosynthesis and Respiration. Chlorophyll a Fluorescence: A Signature of Photosynthesis*; Papageorgiou, G., Govindjee, Eds.; Springer: Dordrecht, The Netherlands, 2004; pp. 321–362.
18. Kalaji, H.M.; Jajoo, A.; Oukarroum, A.; Brestic, M.; Zivcak, M.; Samborska, I.A.; Cetner, M.D.; Łukasik, I.; Goltsev, V.; Ladle, R.J.; et al. The Use of Chlorophyll Fluorescence Kinetics Analysis to Study the Performance of Photosynthetic Machinery in Plants. In *Emerging Technologies and Management of Crop Stress Tolerance*; Elsevier Inc.: Amsterdam, The Netherlands, 2014; Volume 2, pp. 347–384, ISBN 9780128010877.
19. Lundell, R.; Saarinen, T.; Åström, H.; Hänninen, H. The Boreal Dwarf Shrub Vaccinium Vitis-Idaea Retains Its Capacity for Photosynthesis through the Winter. *Botany* **2008**, *86*, 491–500. [CrossRef]
20. Gilmore, A.M.; Ball, M.C. Protection and Storage of Chlorophyll in Overwintering Evergreens. *Proc. Natl. Acad. Sci. USA* **2000**, *97*, 11098–11101. [CrossRef]
21. Lehner, G.; Lütz, C. Photosynthetic Functions of Cembran Pines and Dwarf Pines during Winter at Timberline as Regulated by Different Temperatures, Snowcover and Light. *J. Plant Physiol.* **2003**, *160*, 153–166. [CrossRef]
22. Campbell, C.; Rydin, H. The Effects of Winter Stress on Sphagnum Species with Contrasting Macro- and Microdistributions. *J. Bryol.* **2019**, *41*, 205–217. [CrossRef]
23. Küttim, M.; Küttim, L.; Ilomets, M.; Laine, A.M. Controls of Sphagnum Growth and the Role of Winter. *Ecol. Res.* **2020**, *35*, 219–234. [CrossRef]
24. Bassi, R.; Dall'osto, L. Dissipation of Light Energy Absorbed in Excess: The Molecular Mechanisms. *Annu. Rev. Plant Biol.* **2021**, *72*, 47–76. [CrossRef]
25. Peichl, M.; Sonnentag, O.; Nilsson, M.B. Bringing Color into the Picture: Using Digital Repeat Photography to Investigate Phenology Controls of the Carbon Dioxide Exchange in a Boreal Mire. *Ecosystems* **2015**, *18*, 115–131. [CrossRef]
26. Liu, M.; Wang, Y.; Zhang, H.; Hao, Y.; Wu, H.; Shen, H.; Zhang, P. Mechanisms of Photoprotection in Overwintering Evergreen Conifers: Sustained Quenching of Chlorophyll Fluorescence. *Plant Physiol. Biochem.* **2024**, *210*, 108638. [CrossRef] [PubMed]
27. Saarinen, T.; Lundell, R.; Hänninen, H. Recovery of Photosynthetic Capacity in Vaccinium Vitis-Idaea during Mild Spells in Winter. *Plant Ecol.* **2011**, *212*, 1429–1440. [CrossRef]
28. Kalaji, M.H.; Goltsev, V.N.; Zuk-Golaszewska, K.; Zivcak, M.; Brestic, M. *Chlorophyll Fluorescence—Basics and Applicatrions*; CRC Press: Boca Raton, FL, USA, 2017.
29. Guo, Y.; Lu, Y.; Goltsev, V.; Strasser, R.J.; Kalaji, H.M.; Wang, H.; Wang, X.; Chen, S.; Qiang, S. Comparative Effect of Tenuazonic Acid, Diuron, Bentazone, Dibromothymoquinone and Methyl Viologen on the Kinetics of Chl a Fluorescence Rise OJIP and the MR820 Signal. *Plant Physiol. Biochem.* **2020**, *156*, 39–48. [CrossRef] [PubMed]
30. Yang, Q.; Guo, Y.; Wang, H.; Luo, Z.; Chen, Y.; Jiang, M.; Lu, H.; Valverde, B.E.; Qiang, S.; Strasser, R.J.; et al. Action of the Fungal Compound Citrinin, a Bioherbicide Candidate, on Photosystem II. *Pest. Manag. Sci.* **2024**, *80*, 133–148. [CrossRef]
31. Bednaříková, M.; Folgar-Cameán, Y.; Kučerová, Z.; Lazár, D.; Špundová, M.; Hájek, J.; Barták, M. Analysis of K-and l-Band Appearance in Ojips in Antarctic Lichens in Low and High Temperature. *Photosynthetica* **2020**, *58*, 646–656. [CrossRef]

32. Shomali, A.; Aliniaeifard, S.; Bakhtiarizadeh, M.R.; Lotfi, M.; Mohammadian, M.; Vafaei Sadi, M.S.; Rastogi, A. Artificial Neural Network (ANN)-Based Algorithms for High Light Stress Phenotyping of Tomato Genotypes Using Chlorophyll Fluorescence Features. *Plant Physiol. Biochem.* **2023**, *201*, 107893. [CrossRef]
33. Ferroni, L.; Živčak, M.; Kovar, M.; Colpo, A.; Pancaldi, S.; Allakhverdiev, S.I.; Brestič, M. Fast Chlorophyll a Fluorescence Induction (OJIP) Phenotyping of Chlorophyll-Deficient Wheat Suggests That an Enlarged Acceptor Pool Size of Photosystem I Helps Compensate for a Deregulated Photosynthetic Electron Flow. *J. Photochem. Photobiol. B* **2022**, *234*, 112549. [CrossRef]
34. Chen, S.; Yang, J.; Zhang, M.; Strasser, R.J.; Qiang, S. Classification and Characteristics of Heat Tolerance in Ageratina Adenophora Populations Using Fast Chlorophyll a Fluorescence Rise O-J-I-P. *Environ. Exp. Bot.* **2016**, *122*, 126–140. [CrossRef]
35. Strasser, R.J.; Srivastava, A.; Tsimilli-Michael, M. The Fluorescence Transient as a Tool to Characterize and Screen Photosynthetic Samples. In *Probing Photosynthesis: Mechanism, Regulation and Adaptation*; Yunus, M., Pathre, U., Mohanty, P., Eds.; CRC Press: Boca Raton, FL, USA, 2000; pp. 445–483.
36. Baghbani, F.; Lotfi, R.; Moharramnejad, S.; Bandehagh, A.; Roostaei, M.; Rastogi, A.; Kalaji, H.M. Impact of Fusarium Verticillioides on Chlorophyll Fluorescence Parameters of Two Maize Lines. *Eur. J. Plant Pathol.* **2019**, *154*, 337–346. [CrossRef]
37. Lotfi, R.; Abbasi, A.; Kalaji, H.M.; Eskandari, I.; Sedghieh, V.; Khorsandi, H.; Sadeghian, N.; Yadav, S.; Rastogi, A. The Role of Potassium on Drought Resistance of Winter Wheat Cultivars under Cold Dryland Conditions: Probed by Chlorophyll a Fluorescence. *Plant Physiol. Biochem.* **2022**, *182*, 45–54. [CrossRef] [PubMed]
38. Górecki, K.; Rastogi, A.; Stróżecki, M.; Gąbka, M.; Lamentowicz, M.; Łuców, D.; Kayzer, D.; Juszczak, R. Water Table Depth, Experimental Warming, and Reduced Precipitation Impact on Litter Decomposition in a Temperate Sphagnum-Peatland. *Sci. Total Environ.* **2021**, *771*, 145452. [CrossRef] [PubMed]
39. Antala, M.; Rastogi, A.; Cogliati, S.; Stróżecki, M.; Colombo, R.; Juszczak, R. Sun-Induced Fluorescence Spectrum as a Tool for Assessing Peatland Vegetation Productivity in the Framework of Warming and Reduced Precipitation Experiment. *Remote Sens. Environ.* **2024**, *301*, 113921. [CrossRef]
40. Lamentowicz, M.; Mueller, M.; Gałka, M.; Barabach, J.; Milecka, K.; Goslar, T.; Binkowski, M. Reconstructing Human Impact on Peatland Development During the Past 200 Years in CE Europe Through Biotic Proxies and X-ray Tomography. *Quat. Int.* **2015**, *357*, 282–294. [CrossRef]
41. Milecka, K.; Kowalewski, G.; Fiałkiewicz-Kozieł, B.; Gałka, M.; Lamentowicz, M.; Chojnicki, B.H.; Goslar, T.; Barabach, J. Hydrological Changes in the Rzecin Peatland (Puszcza Notecka, Poland) Induced by Anthropogenic Factors: Implications for Mire Development and Carbon Sequestration. *Holocene* **2017**, *27*, 651–664. [CrossRef]

Declarations of co-authors, supervisors and author

Ing. Michal Antala
Laboratory of Bioclimatology,
Department of Ecology and Environmental Protection,
Faculty of Environmental and Mechanical Engineering,
Poznań University of Life Sciences,
Piątkowska 94,
60-649 Poznań,
Poland

Declaration on co-authorship

I hereby declare that in work Antala, M., Juszczak, R., van der Tol, Ch., Rastogi, A. (2022), Impact of climate change-induced alterations in peatland vegetation phenology and composition on carbon balance. *Science of the Total Environment*, 827, 154294 my individual contribution to its preparation consisted of conceptualization, formal analysis, investigation and preparation of the first draft, including the search for relevant literature and figure and tables preparation.

Date ..19.11.2024...

Antala
....
signature

Prof. Radosław Juszczak
Laboratory of Bioclimatology,
Department of Ecology and Environmental Protection,
Faculty of Environmental and Mechanical Engineering,
Poznań University of Life Sciences,
Piątkowska 94,
60-649 Poznań,
Poland

Declaration on co-authorship

I hereby declare that in work Antala, M., Juszczak, R., van der Tol, Ch., Rastogi, A. (2022), Impact of climate change-induced alterations in peatland vegetation phenology and composition on carbon balance. *Science of the Total Environment*, 827, 154294 my individual contribution to its preparation consisted of funding acquisition and reviewing and editing the manuscript.

Date ..19.11.2024...

....
signature

Dr.ir. Christiaan van der Tol
Faculty of Geo-Information Science and Earth Observation (ITC),
University of Twente,
7500 AE Enschede,
the Netherlands

Declaration on co-authorship

I hereby declare that in work Antala, M., Juszczak, R., van der Tol, Ch., Rastogi, A. (2022), Impact of climate change-induced alterations in peatland vegetation phenology and composition on carbon balance. *Science of the Total Environment*, 827, 154294 my individual contribution to its preparation consisted of reviewing and editing the manuscript.

Date 29.11.2024

signature

Prof. UPP dr hab. Anshu Rastogi
Laboratory of Bioclimatology,
Department of Ecology and Environmental Protection,
Faculty of Environmental and Mechanical Engineering,
Poznań University of Life Sciences,
Piątkowska 94,
60-649 Poznań,
Poland

Declaration on co-authorship

I hereby declare that in work Antala, M., Juszczak, R., van der Tol, Ch., Rastogi, A. (2022), Impact of climate change-induced alterations in peatland vegetation phenology and composition on carbon balance. *Science of the Total Environment*, 827, 154294 my individual contribution to its preparation consisted of supervision of the PhD. student, conceptualization, formal analysis, investigation, funding acquisition, reviewing and editing the manuscript.

Date ..19.11.2024...

Anshu Rastogi
....
signature

Ing. Michal Antala
Laboratory of Bioclimatology,
Department of Ecology and Environmental Protection,
Faculty of Environmental and Mechanical Engineering,
Poznań University of Life Sciences,
Piątkowska 94,
60-649 Poznań,
Poland

Declaration on co-authorship

I hereby declare that in work Antala, M., Rastogi, A., Cogliati, S., Stróżecki, M., Colombo, R. Juszczak, R. (2024), Sun-induced fluorescence spectrum as a tool for assessing peatland vegetation productivity in the framework of warming and reduced precipitation experiment. *Remote Sensing of Environment*, 301, 113921 my individual contribution to its preparation consisted of conceptualization, spectral data collection, processing and analysis, flux and hydrometeorological data analysis and preparation of the first draft, including the figures and tables preparation.

Date ..19.11.2024...

.......................Antala.......................
signature

Prof. UPP dr hab. Anshu Rastogi
Laboratory of Bioclimatology,
Department of Ecology and Environmental Protection,
Faculty of Environmental and Mechanical Engineering,
Poznań University of Life Sciences,
Piątkowska 94,
60-649 Poznań,
Poland

Declaration on co-authorship

I hereby declare that in work Antala, M., Rastogi, A., Cogliati, S., Stróżecki, M., Colombo, R. Juszczak, R. (2024), Sun-induced fluorescence spectrum as a tool for assessing peatland vegetation productivity in the framework of warming and reduced precipitation experiment. *Remote Sensing of Environment*, 301, 113921 my individual contribution to its preparation consisted of supervision of PhD. student, conceptualization, funding and resources acquisition, project administration, formal analysis, investigation, reviewing and editing the manuscript.

Date ..19.11.2024...

Anshu Rastogi
....
signature

Prof. assoc. Sergio Cogliati
Department of Earth and Environmental Sciences,
University of Milano-Bicocca,
Piazza della Scienza 1,
20126 Milano,
Italy

Declaration on co-authorship

I hereby declare that in work Antala, M., Rastogi, A., Cogliati, S., Stróżecki, M., Colombo, R. Juszczak, R. (2024), Sun-induced fluorescence spectrum as a tool for assessing peatland vegetation productivity in the framework of warming and reduced precipitation experiment. *Remote Sensing of Environment*, 301, 113921 my individual contribution to its preparation consisted of supervision of PhD. student, conceptualization, methodology, software development, reviewing and editing the manuscript.

Date ..19.11.2024...

Sergio Cogliati
....
signature

Dr inż. Marcin Stróżecki
Laboratory of Bioclimatology,
Department of Ecology and Environmental Protection,
Faculty of Environmental and Mechanical Engineering,
Poznań University of Life Sciences,
Piątkowska 94,
60-649 Poznań,
Poland

Declaration on co-authorship

I hereby declare that in work Antala, M., Rastogi, A., Cogliati, S., Stróżecki, M., Colombo, R. Juszczak, R. (2024), Sun-induced fluorescence spectrum as a tool for assessing peatland vegetation productivity in the framework of warming and reduced precipitation experiment. *Remote Sensing of Environment*, 301, 113921 my individual contribution to its preparation consisted of supervision of PhD. student, flux and hydrometeorological data collection and processing, reviewing and editing the manuscript.

Date ..19.11.2024...

....
signature

Prof. Roberto Colombo
Department of Earth and Environmental Sciences,
University of Milano-Bicocca,
Piazza della Scienza 1,
20126 Milano,
Italy

Declaration on co-authorship

I hereby declare that in work Antala, M., Rastogi, A., Cogliati, S., Stróżecki, M., Colombo, R. Juszczak, R. (2024), Sun-induced fluorescence spectrum as a tool for assessing peatland vegetation productivity in the framework of warming and reduced precipitation experiment. *Remote Sensing of Environment*, 301, 113921 my individual contribution to its preparation consisted of reviewing and editing the manuscript.

Date ..19.11.2024...

Roberto Colombo
....
signature

Prof. Radosław Juszczak
Laboratory of Bioclimatology,
Department of Ecology and Environmental Protection,
Faculty of Environmental and Mechanical Engineering,
Poznań University of Life Sciences,
Piątkowska 94,
60-649 Poznań,
Poland

Declaration on co-authorship

I hereby declare that in work Antala, M., Rastogi, A., Cogliati, S., Stróżecki, M., Colombo, R. Juszczak, R. (2024), Sun-induced fluorescence spectrum as a tool for assessing peatland vegetation productivity in the framework of warming and reduced precipitation experiment. *Remote Sensing of Environment*, 301, 113921 my individual contribution to its preparation consisted of supervision of PhD. student, conceptualization, funding and resources acquisition, project administration, reviewing and editing the manuscript.

Date ..19.11.2024...

....
signature

Ing. Michal Antala
Laboratory of Bioclimatology,
Department of Ecology and Environmental Protection,
Faculty of Environmental and Mechanical Engineering,
Poznań University of Life Sciences,
Piątkowska 94,
60-649 Poznań,
Poland

Declaration on co-authorship

I hereby declare that in work Antala, M., Juszczak, R., Rastogi, A., (2024). Nonphotochemical quenching does not alter the relationship between sun-induced fluorescence and gross primary production under heatwave. *New Phytologist*. 20312, my individual contribution to its preparation consisted of conceptualization, and preparation of the first draft, including the preparation of the figures.

Date ..29.11.2024...

Antala
....
signature

Prof. Radosław Juszczak
Laboratory of Bioclimatology,
Department of Ecology and Environmental Protection,
Faculty of Environmental and Mechanical Engineering,
Poznań University of Life Sciences,
Piątkowska 94,
60-649 Poznań,
Poland

Declaration on co-authorship

I hereby declare that in work Antala, M., Juszczak, R., Rastogi, A., (2024). Nonphotochemical quenching does not alter the relationship between sun-induced fluorescence and gross primary production under heatwave. *New Phytologist*. 20312 my individual contribution to its preparation consisted of conceptualization, reviewing and editing the manuscript.

Date ..29.11.2024...

....
signature

Prof. UPP dr hab. Anshu Rastogi
Laboratory of Bioclimatology,
Department of Ecology and Environmental Protection,
Faculty of Environmental and Mechanical Engineering,
Poznań University of Life Sciences,
Piątkowska 94,
60-649 Poznań,
Poland

Declaration on co-authorship

I hereby declare that in work Antala, M., Juszczak, R., Rastogi, A., (2024). Nonphotochemical quenching does not alter the relationship between sun-induced fluorescence and gross primary production under heatwave. *New Phytologist.* 20312 my individual contribution to its preparation consisted of conceptualization, reviewing and editing the manuscript.

Date ..29.11.2024...

Anshu Rastogi
....
signature

Ing. Michal Antala
Laboratory of Bioclimatology,
Department of Ecology and Environmental Protection,
Faculty of Environmental and Mechanical Engineering,
Poznań University of Life Sciences,
Piątkowska 94,
60-649 Poznań,
Poland

Declaration on co-authorship

I hereby declare that in work Antala, M., Abdelmajeed, A.Y.A., Stróżecki, M., Krzesiński, W., Juszczak, R., Rastogi, A. (2024). Photosynthetic Responses of Peat Moss (*Sphagnum* spp.) and Bog Cranberry (*Vaccinium oxycoccos* L.) to Spring Warming. *Plants* 13 (22), 3246 my individual contribution to its preparation consisted of conceptualization, fluorescence data collection, processing and analysis, meteorological data analysis and preparation of the first draft, including the figures and table preparation.

Date ..19.11.2024...

Antala
....
signature

Mgr. Abdallah Yussuf Ali Abdelmajeed
Laboratory of Bioclimatology,
Department of Ecology and Environmental Protection,
Faculty of Environmental and Mechanical Engineering,
Poznań University of Life Sciences,
Piątkowska 94,
60-649 Poznań,
Poland

Declaration on co-authorship

I hereby declare that in work Antala, M., Abdelmajeed, A.Y.A., Stróżecki, M., Krzesiński, W., Juszczak, R., Rastogi, A. (2024). Photosynthetic Responses of Peat Moss (*Sphagnum* spp.) and Bog Cranberry (*Vaccinium oxycoccos* L.) to Spring Warming. *Plants* 13 (22), 3246 my individual contribution to its preparation consisted of fluorescence data collection, reviewing and editing the manuscript.

Date ..19.11.2024...

....
signature

Dr inż. Marcin Stróżecki
Laboratory of Bioclimatology,
Department of Ecology and Environmental Protection,
Faculty of Environmental and Mechanical Engineering,
Poznań University of Life Sciences,
Piątkowska 94,
60-649 Poznań,
Poland

Declaration on co-authorship

I hereby declare that in work Antala, M., Abdelmajeed, A.Y.A., Stróżecki, M., Krzesiński, W., Juszczak, R., Rastogi, A. (2024). Photosynthetic Responses of Peat Moss (*Sphagnum* spp.) and Bog Cranberry (*Vaccinium oxycoccos* L.) to Spring Warming. *Plants* 13 (22), 3246 my individual contribution to its preparation consisted of supervision of PhD. student, meteorological data collection and processing, reviewing and editing the manuscript.

Date ..19.11.2024...

....
signature

Prof. UPP dr hab. Włodzimierz Krzesiński
Department of Vegetable Crops,
Faculty of Agriculture, Horticulture and Biotechnology,
Poznań University of Life Sciences,
Jana Henryka Dąbrowskiego 159,
60-995 Poznań,
Poland

Declaration on co-authorship

I hereby declare that in work Antala, M., Abdelmajeed, A.Y.A., Stróżecki, M., Krzesiński, W., Juszczak, R., Rastogi, A. (2024). Photosynthetic Responses of Peat Moss (*Sphagnum* spp.) and Bog Cranberry (*Vaccinium oxycoccos* L.) to Spring Warming. *Plants* 13 (22), 3246 my individual contribution to its preparation consisted of resources acquisition, reviewing and editing the manuscript.

Date ..19.11.2024... ....

signature

Prof. Radosław Juszczak
Laboratory of Bioclimatology,
Department of Ecology and Environmental Protection,
Faculty of Environmental and Mechanical Engineering,
Poznań University of Life Sciences,
Piątkowska 94,
60-649 Poznań,
Poland

Declaration on co-authorship

I hereby declare that in work Antala, M., Abdelmajeed, A.Y.A., Stróżecki, M., Krzesiński, W., Juszczak, R., Rastogi, A. (2024). Photosynthetic Responses of Peat Moss (*Sphagnum* spp.) and Bog Cranberry (*Vaccinium oxycoccos* L.) to Spring Warming. *Plants* 13 (22), 3246 my individual contribution to its preparation consisted of supervision of PhD. student, conceptualization, funding and resources acquisition, project administration, reviewing and editing the manuscript.

Date ..19.11.2024...

....
signature

Prof. UPP dr hab. Anshu Rastogi
Laboratory of Bioclimatology,
Department of Ecology and Environmental Protection,
Faculty of Environmental and Mechanical Engineering,
Poznań University of Life Sciences,
Piątkowska 94,
60-649 Poznań,
Poland

Declaration on co-authorship

I hereby declare that in work Antala, M., Abdelmajeed, A.Y.A., Stróżecki, M., Krzesiński, W., Juszczak, R., Rastogi, A. (2024). Photosynthetic Responses of Peat Moss (*Sphagnum* spp.) and Bog Cranberry (*Vaccinium oxycoccos* L.) to Spring Warming. *Plants* 13 (22), 3246 my individual contribution to its preparation consisted of supervision of PhD. student, conceptualization, funding and resources acquisition, project administration, formal analysis, reviewing and editing the manuscript.

Date ..19.11.2024...

Anshu Rastogi
....
signature

Scientific supervisor:
Prof. UPP dr hab. Anshu Rastogi
Laboratory of Bioclimatology
Poznan University of Life Sciences

Auxiliary supervisor:
Dr inż. Marcin Stróżecki
Laboratory of Bioclimatology
Poznan University of Life Sciences

Declaration of supervisors of the doctoral dissertation

We hereby declare that this doctoral dissertation entitled "Assessment of peatland vegetation physiology under manipulated environmental conditions by leaf and canopy level chlorophyll fluorescence measurements" has been prepared under our supervision, and we hereby state that it meets the requirements for its submission in the degree conferral procedure.

Date ...04.12.2024.........

Signature of the scientific supervisor of the doctoral dissertation

Anshu Rastogi
....

Signature of the auxiliary supervisor of the doctoral dissertation

....

……Michal Antala………

First name and surname of the PhD student

Declaration of the author of the doctoral dissertation

I hereby declare that the submitted Doctoral dissertation entitled "Assessment of peatland vegetation physiology under manipulated environmental conditions by leaf and canopy level chlorophyll fluorescence measurements" has been written by me personally, i.e.

- I have not commissioned the preparation of this dissertation or its part,
- I have not copied the dissertation or its part from other studies and works, which topic is related to my work,
- consultations I have asked for covered only the necessary aspects and were limited to the minimum,
- all the elements of the dissertation, which have been used for its realisation (citations, figures, tables, programmes, etc.), of which I am not an author, have been appropriately marked specifying the source of their origin,
- the dissertation has not been used in any other PhD degree conferral procedure.

I hereby declare that this version of the doctoral dissertation is an identical copy of the attached electronic version.

I am aware that submission of a false declaration will result in excluding me from further stages of the doctoral degree conferral procedure or revoking the decision on the conferral of the doctoral degree and initiation of disciplinary proceedings.

Date ...04.12.2024.........

Antala

....

signature of the dissertation author